

1181-30199

FR-14615
VOLUME II
15 MARCH 1981

ORBIT TRANSFER VEHICLE (OTV) ADVANCED EXPANDER CYCLE ENGINE POINT DESIGN STUDY

FINAL TECHNICAL REPORT

Contract NAS8-33567

**Prepared for
National Aeronautics and Space Administration
George C. Marshall Space Flight Center
Marshall Space Flight Center, Alabama 35812**

THIS DOCUMENT CONTAINS INFORMATION ON CARBON/CARBON MATERIALS AND TECHNOLOGY, WHICH IS SUBJECT TO EXPORT CONTROL REQUIREMENTS OF THE DEPARTMENT OF STATE INTERNATIONAL TRAFFIC AND ARMS REGULATIONS. ADDITIONAL INFORMATION IS GIVEN IN THE DEPARTMENT OF STATE MUNITIONS CONTROL NEWSLETTER, NO. 35, APRIL 1977.



**UNITED
TECHNOLOGIES
PRATT & WHITNEY
AIRCRAFT**

REPRODUCED BY
NATIONAL TECHNICAL
INFORMATION SERVICE
U.S. DEPARTMENT OF COMMERCE
SPRINGFIELD, VA. 22161

FOREWORD

This technical report presents the results of the Orbit Transfer Vehicle (OTV) Advanced Expander Cycle Engine Study. The study was conducted by the Pratt & Whitney Aircraft Group, Government Products Division of the United Technologies Corporation for the National Aeronautics and Space Administration's George C. Marshall Space Flight Center under Contract NAS8-33567.

The results of the study are contained in the following three volumes which are submitted in accordance with the data requirements of Contract NAS8-33567.

Volume I — Executive Summary
Volume II — Final Technical Report
Volume III — Engine Data Summary

This study was initiated in December 1979 with the technical effort completed in eleven months. The study effort was conducted under the direction of the George C. Marshall Space Flight Center's Science and Engineering Organization with Mr. Dale H. Blount as Contracting Officer's Representative. The effort at P&WA/GPD was carried out under the direction of James R. Brown, Program Manager.

The following individuals have provided significant contributions in the preparation of this report.

C.D. Limerick — Systems Performance Analysis
D.E. Galler — Engine Cycle Analysis
J.W. Park — Transient Analysis
J.R. Zant — Transient Modeling
D.B. Roy — Thermal Analysis
R.G. Jaeger — Stress and LCF Analysis
G.W. Moore — Injector Design
P.G. DeIvernois — Pump Design
C. Twardochleb — Turbine Design
J. Namisniak — Engine Layout
A.M. Palgon — Component Integration

TABLE OF CONTENTS

| <i>Section</i> | | <i>Page</i> |
|----------------|---|-------------|
| 1 | INTRODUCTION..... | 1 |
| 2 | ENGINE OPERATING CHARACTERISTICS..... | 6 |
| | 2.1 Introduction..... | 6 |
| | 2.2 Engine System..... | 6 |
| 3 | MAJOR COMPONENT ANALYTICAL DESIGN..... | 64 |
| | 3.1 Thrust Chamber/Nozzle Assembly Design Analysis..... | 64 |
| | 3.2 Hydrogen Regenerator Design Analysis..... | 74 |
| | 3.3 Gaseous Oxygen Heat Exchangers..... | 76 |
| | 3.4 Turbopumps..... | 76 |
| 4 | COMPONENT MECHANICAL DESIGN..... | 98 |
| | 4.1 Thrust Chamber/Nozzle Assembly..... | 98 |
| | 4.2 Heat Exchangers..... | 103 |
| | 4.3 Turbopumps..... | 104 |
| | 4.4 Engine Control Valves..... | 117 |
| | 4.5 Engine Weight..... | 122 |
| 5 | CONCLUSIONS AND RECOMMENDATIONS..... | 125 |
| | 5.1 General..... | 125 |
| | 5.2 Turbomachinery..... | 125 |
| | 5.3 Thrust Chambers..... | 125 |
| | 5.4 Materials..... | 126 |
| | 5.5 Performance..... | 126 |

LIST OF ILLUSTRATIONS

| <i>Figure</i> | | <i>Page</i> |
|---------------|--|-------------|
| 1-1 | Advanced Expander Cycle Engine Point Design Study Schedule..... | 4 |
| 1-2 | Study Flow Diagram..... | 5 |
| 2-1 | Advanced Expander Engine Cycle..... | 6 |
| 2-2 | Engine Propellant Flow Schematic..... | 9 |
| 2-3 | Value Sequence for a Typical Firing..... | 10 |
| 2-4 | Advanced Expander Engine Propellant Flow Schematic at Full Thrust (MR = 6.0)..... | 11 |
| 2-5 | Advanced Expander Engine Propellant Flow at Pumped Idle (MR = 6.0).. | 12 |
| 2-6 | Advanced Expander Engine Propellant Flow at Tank Head Idle (MR = 4.0) | 12 |
| 2-7 | Estimated Effect of Inlet Mixture Ratio on Vacuum Specific Impulse at Full Thrust..... | 13 |
| 2-8 | Estimated Effect of Inlet Mixture Ratio on Vacuum Thrust at Full Thrust Setting..... | 13 |
| 2-9 | Oxidizer Rich Chamber Ignition..... | 15 |
| 2-10 | Torch Igniter Lights Long Before Chamber Reaches Ignitable Region..... | 16 |
| 2-11 | Chamber Characteristics During Ignition..... | 17 |
| 2-12 | Fuel System Pressures During Ignition..... | 18 |
| 2-13 | Fuel System Temperatures During Ignition..... | 19 |
| 2-14 | Fuel System Flows During Ignition..... | 20 |
| 2-15 | Oxidizer System Pressures During Ignition..... | 21 |
| 2-16 | Oxidizer System Temperatures During Ignition..... | 22 |
| 2-17 | Oxidizer System Flows During Ignition..... | 23 |
| 2-18 | Chamber Ignition Characteristics if Pumps Are Already Conditioned..... | 24 |
| 2-19 | Ignition With Pumps Already Conditioned..... | 25 |
| 2-20 | Fuel Pump Cooldown During Tank Head Idle..... | 26 |
| 2-21 | Oxidizer Pump Cooldown During Tank Head Idle..... | 27 |

ILLUSTRATIONS (Continued)

| <i>Figure</i> | | <i>Page</i> |
|---------------|---|-------------|
| 2-22 | Boiling Increases Heat Transfer Causing Oxidizer Flow to Dip..... | 28 |
| 2-23 | Thrust During Tank Head Idle..... | 29 |
| 2-24 | Injector Flows and Chamber Mixture Ratio During Tank Head Idle..... | 30 |
| 2-25 | Igniter Flows and Mixture Ratio During Tank Head Idle..... | 31 |
| 2-26 | Fuel System Pressures During Tank Head Idle..... | 32 |
| 2-27 | Fuel System Temperatures During Tank Head Idle..... | 33 |
| 2-28 | Oxidizer System Pressures During Tank Head Idle..... | 34 |
| 2-29 | Oxidizer System Temperatures During Tank Head Idle..... | 35 |
| 2-30 | Propellant Consumption During Tank Head Idle..... | 36 |
| 2-31C | Valve Actuation for Transition from Full Thrust to Pumped Idle..... | 39 |
| 2-33 | Thrust Characteristics During Transients..... | 41 |
| 2-34 | Chamber Pressure Characteristics During Transients..... | 42 |
| 2-35 | Main Fuel Pump Speed Characteristics During Transients..... | 43 |
| 2-37 | Fuel Pump Suction Characteristics During Transients..... | 45 |
| 2-40 | Injector Pressure Differentials Sufficient for Stable Combustion..... | 48 |
| 2-41 | Pump Flows During Transients..... | 49 |
| 2-42 | Fuel System Pressures During Transients..... | 50 |
| 2-43 | Fuel System Temperatures During Transients..... | 51 |
| 2-44 | Fuel System Flows During Transients..... | 52 |
| 2-45 | Oxidizer System Pressures During Transients..... | 53 |
| 2-46 | Oxidizer System Temperatures During Transients..... | 54 |
| 2-47 | Oxidizer Flow During Transients..... | 55 |
| 2-48 | Turbine Efficiencies During Transients..... | 56 |
| 2-49 | Fuel Pump Efficiencies During Transients..... | 57 |
| 2-50 | Oxidizer Pump Efficiencies During Transients..... | 58 |

ILLUSTRATIONS (Continued)

| <i>Figure</i> | | <i>Page</i> |
|---------------|---|-------------|
| 2-51 | Propellant Consumption During Transients..... | 59 |
| 2-52 | Transient Impulse (Integral of Thrust vs Time)..... | 60 |
| 2-53 | Heat Exchanger Transient Metal Temperatures..... | 61 |
| 2-54 | Influence of Closing the Oxidizer Solenoid Valve on Vehicle Mixture Ratio During Deceleration from Full Thrust to Pumped Idle..... | 63 |
| 3-2 | Combustion Chamber Wall Detail..... | 66 |
| 3-3 | Combustion Chamber Coolant Passage Depth and Mach No..... | 67 |
| 3-4 | Combustion Chamber Hot Wall Temperature and Wall Thickness..... | 68 |
| 3-5 | Primary Nozzle Schematic..... | 68 |
| 3-6 | OTV Engine Thrust Chamber and Primary Nozzle Hot Wall Metal Tem- perature Prediction..... | 69 |
| 3-8 | Efficiency at Design Point as a Function of Injector Configuration..... | 72 |
| 3-10 | Igniter Assembly..... | 74 |
| 3-11 | Single Pass Hydrogen Regenerator..... | 75 |
| 3-12 | GO Vortex Prevaporizer..... | 77 |
| 3-13 | Gaseous Oxygen (GOX) Heat Exchanger..... | 78 |
| 3-14 | Fuel Pump 1st Stage Impeller Head Coefficient..... | 79 |
| 3-15 | Fuel Pump 1st Stage Impeller Efficiency..... | 80 |
| 3-16 | Fuel pump 2nd Stage Impeller Head Coefficient..... | 80 |
| 3-17 | Fuel Pump 2nd Stage Impeller Efficiency..... | 81 |
| 3-18 | Pump Design Parameters Optimized from Test Data..... | 82 |
| 3-19 | Theoretical Pump Suction Capability (N_s)..... | 84 |
| 3-20 | Main Fuel Pump..... | 87 |
| 3-21 | Main Oxidizer Pump..... | 89 |
| 3-22 | Fuel LSI Pump..... | 91 |
| 3-23 | Oxidizer LSI Pump..... | 93 |

ILLUSTRATIONS (Continued)

| <i>Figure</i> | | <i>Page</i> |
|---------------|---|-------------|
| 3-24 | OTV Fuel Turbine Parametric Sizing Study..... | 94 |
| 3-25 | OTV Expander Cycle Fuel Turbine Elevation..... | 95 |
| 3-26 | OTV Oxidizer Parametric Turbine Sizing Study..... | 96 |
| 3-27 | OTV Expander Cycle Oxidizer Turbine Elevation..... | 97 |
| 3-28 | Oxidizer Turbine Elevation..... | 98 |
| 4-1 | Thrust Chamber/Injector/Nozzle Assembly..... | 100 |
| 4-2 | Advanced Expander Cycle Engine Injector..... | 101 |
| 4-3 | Advanced Expander Cycle Engine Igniter Assembly..... | 101 |
| 4-4 | Combustion Chamber Assembly..... | 103 |
| 4-5 | Nozzle Translation System..... | 104 |
| 4-6 | Turbopump Assembly..... | 105 |
| 4-7 | OTV Pumps Critical Speed Analysis..... | 108 |
| 4-8 | Oxidizer Pump Dynamic Bearing Loads..... | 109 |
| 4-9 | OTV Fuel Pump Dynamic Bearing Loads..... | 110 |
| 4-10 | Fuel LSI Roller Bearing Characteristics..... | 111 |
| 4-11 | Fuel LSI Ball Bearing Characteristics..... | 112 |
| 4-12 | LOX Pump Ball Bearing Characteristics..... | 113 |
| 4-13 | LOX Pump Roller Bearing Characteristics..... | 114 |
| 4-14 | LOX LSI Roller Bearing Characteristics..... | 115 |
| 4-15 | LOX LSI Ball Bearing Characteristics..... | 116 |
| 4-16 | Engine Valve Location Schematic..... | 118 |
| 4-17 | Fuel and Oxidizer Propellant Pressurization Valves..... | 119 |
| 4-18 | Oxidizer Flow Control Valve..... | 119 |
| 4-19 | Fuel and Oxidizer Propellant Inlet Shut-Off Valves..... | 120 |
| 4-20 | Main Fuel Shut-Off Valve..... | 120 |

ILLUSTRATIONS (Continued)

| <i>Figure</i> | | <i>Page</i> |
|---------------|-----------------------------|-------------|
| 4-21 | Gaseous Oxidizer Valve..... | 121 |
| 4-22 | Main Fuel Valve..... | 123 |
| 4-23 | Solenoid Valves..... | 124 |

LIST OF TABLES

| <i>Table</i> | | <i>Page</i> |
|--------------|---|-------------|
| 2-1 | Engine Steady-State Design Point Operation..... | 11 |
| 3-1 | Thrust Chamber and Primary Nozzle H ₂ Coolant Conditions at Selected Design Points..... | 67 |
| 3-2 | OTV Impeller Radial Loads..... | 83 |
| 3-3 | OTV Main Fuel Pump Design..... | 85 |
| 3-4 | OTV Main Oxidizer Pump Design..... | 88 |
| 3-5 | OTV Fuel LSI Design..... | 90 |
| 3-6 | OTV Oxidizer LSI Design..... | 92 |
| 3-7 | Advanced Expander Cycle Engine Fuel Turbine Operating Conditions at Design Point..... | 95 |
| 3-8 | Advanced Expander Cycle Engine Oxidizer Turbine Operating Conditions at Design Point..... | 97 |
| 4-1 | Turbopump Materials..... | 107 |
| 4-2 | Turbomachinery Rotor Weights and Operating Speeds..... | 107 |
| 4-3 | Bearings Summary — Conditions Resulting in 100 hr Fatigue Life..... | 117 |
| 4-4 | Comparison of the Centrifugal Effect of Steel and Si ₃ N ₄ on Bearing Life at 3.0×10^6 DN..... | 117 |
| 4-5 | Estimated Weights — Advanced Expander Cycle Engine Components..... | 124 |

SECTION I

INTRODUCTION

The objective of the Orbit Transfer Vehicle (OTV) Advanced Expander Point Design Study was to generate the system design of a performance-optimized, advanced LOX/hydrogen expander cycle space engine. This engine is intended to be used in an Orbital Transfer Vehicle with an IOC date in the late 1980's.

The engine requirements that are emphasized by the OTV application include: high specific impulse within a restricted installed length constraint, long life, multiple starts, different thrust levels and man-rated reliability. Development and operational experience with the expander cycle RL10 engine, combined with our experimental work on high-pressure staged combustion rocket engines, led us to the conclusion that for upper stage space engine applications, selection of the expander power cycle would result in an engine that would be significantly cheaper to develop. Design studies on advanced engines for Shuttle upper stage applications, that we carried out in the early 1970's, showed that the potential difference in specific impulse between advanced expander and staged combustion cycle space engines was less than 1%. This potential difference was too low, in our opinion, to justify the considerably greater development cost and risk of the staged combustion engine in this size.

In 1973, under NAS8-28989, "Design Study of RL10 Derivatives," we designed the RL10 Category IV engine, a "clean sheet" update of the RL10 design concept, using the same expander cycle, but optimized specifically for the Space Tug. The engine requirements for the Full Capability Space Tug, and those for the OTV, as specified in Section 2.0 of the Scope of Work (Engine Requirements), are very similar and are compared in the following:

| 2.0 OTV ENGINE REQUIREMENTS (FROM SOW) | RL10 CATEGORY IV |
|---|--------------------------------------|
| 2.1 Expander Cycle, with LH_2 and LO_2 | Same |
| 2.2 Engine Thrust 15K lb at MR 6.0:1 | Same |
| 2.3 Installed Length (two-position nozzle retracted) ≤ 60 in. | 57 in. |
| 2.4 1980 State of the Art | 1973 State of the Art |
| 2.5 MR Range of 6:1 to 7:1 | MR Range 5.5 to 6.5:1 |
| 2.6 Fuel NPSH 15 ft | Fuel NPSH 0 ft |
| Oxygen NPSH 2 ft | Oxygen NPSH 0 ft |
| 2.7 Life ≥ 300 firings/10 hr | Same |
| 2.8 Chamber pressure spikes $< \pm 5\%$ | Not specified |
| 2.9 2-position contoured bell nozzle | Same |
| 2.10 Gimbal range +15 deg pitch -6 deg pitch ± 6 deg yaw | ± 4 deg pitch ± 4 deg yaw |
| 2.11 Engine provides H_2 and O_2 autogeneous pressurization | Same |
| 2.12 Man-rated, provides abort return | Not specified |
| 2.13 Meet Orbiter Safety Requirements | Same |
| 2.14 Low Thrust Operation at $\approx 1\text{K}$ lb | Maneuver thrust at 3.75K lb |

The impact of the differences in engine requirements, such as different inlet conditions, gimbal angles and mixture ratio range and low thrust level is comparatively minor. An issue that will have to be addressed in conjunction with the Vehicle System Contractors is how the engine can assist in providing abort return of the vehicle.

The study objective calls for a performance-optimized engine system design. For a typical OTV mission, engine specific impulse has a far greater performance impact than engine weight (+1 sec Isp would justify >40-lb increase in engine inert weight), so that the emphasis was on maximizing specific impulse. Since engine cycle, propellants, nozzle concept installed length, and mixture ratio are all specified, this is done primarily through increasing chamber pressure and hence nozzle ratio.

A 15,000-lb thrust Advanced Expander Cycle Engine that has been optimized to meet the study objective, is compared with the RL10 Category IV (1973) engine in the following:

| | <i>RL10 Category IV (1973)</i> | <i>Advanced Expander Cycle Engine</i> |
|------------------|------------------------------------|---|
| Thrust | 15,000 lb | 15,000 lb |
| Installed Length | 57 in. | 60 in. |
| Chamber Pressure | 915 psia | 1500 psia |
| Area Ratio | 401:1 | 640:1 |
| ILC at 6.0 MR | 470 sec | 482 sec |
| Weight | 424 lb | 427 lb |
| Life | 300 firings/10 hr | 300 firings/10 hr |
| Operation | | |
| Full Thrust | Saturated Propellants | Low NPSH (2 ft 0, 15 ft H ₂) |
| Low Thrust | Saturated Propellants | Saturated Propellants |
| Conditioning | Tank Head Idle | Tank Head Idle |
| Technology | 1973 | 1980 |

The most significant difference between these two engines is that the specific impulse of the Advanced Expander Cycle Engine has been increased to 482 sec. This 12-sec increase in specific impulse over the RL10 Category IV engine is due to a combination of factors which include: increased installation length (57 to 60 in.), updated performance prediction, use of the "preheat" expander power cycle, improved technology turbopumps with higher efficiencies, and reduced power margin.

Increasing the installed length of the 57-in. RL10 Category IV engine to 60 in. allows area ratio to be raised to approximately 433:1, increasing Specific Impulse by 1 sec.

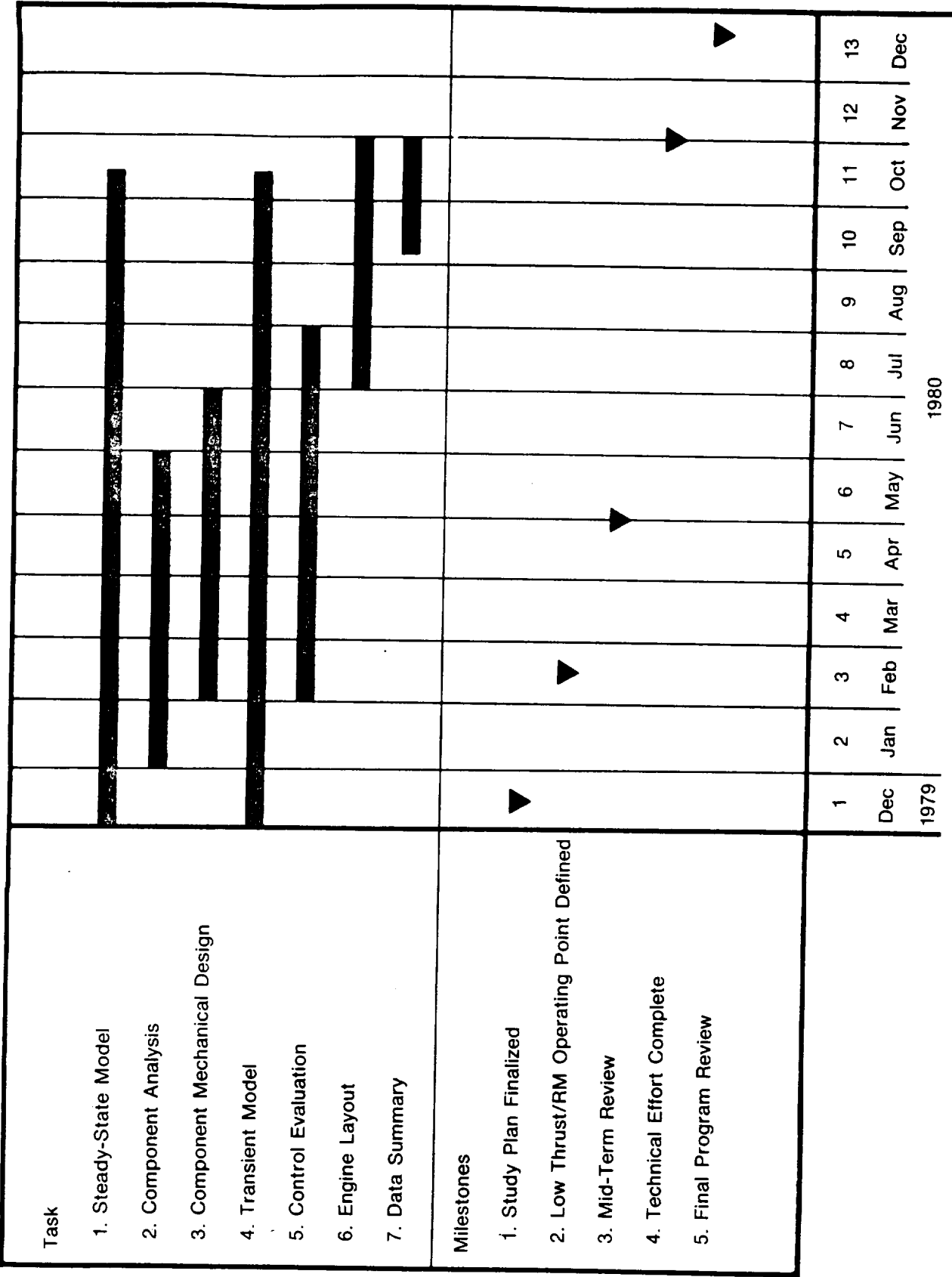
Testing carried out subsequent to 1973 on engines with very high-area-ratio nozzles (i.e., RL10 with $\epsilon = 205$, ASE with $\epsilon = 175$ and 400) showed that the achieved performance was higher than that predicted by the current JANNAF methods by as much as 1.3%.

The chamber pressure of a power-limited expander cycle may be increased by preheating the chamber coolant with the turbine discharge flow, thereby raising turbine inlet temperature, and hence, increasing turbine power. This "preheat" expander power cycle was investigated on an improved version of the RL10 Category IV, the "RL10 Category IV*." Chamber pressure is increased by over 30% to approximately 1200 psia, giving an increase in specific impulse of approximately 1%.

Further increases in chamber pressure have been obtained by increasing turbopump efficiently through increasing speeds and by reducing turbine bypass flow. These higher speeds may require a considerable effort in the design of the fuel turbopump to prevent its operation at or below critical speed. Reducing turbine bypass flow from 5.7 to 3% reduces performance degradation margin, which may be undesirable on a long life engine. The effect of these changes is to allow chamber pressure to be increased by slightly less than 30% to 1,500 psia, giving an increase in specific impulse of approximately ½ %.

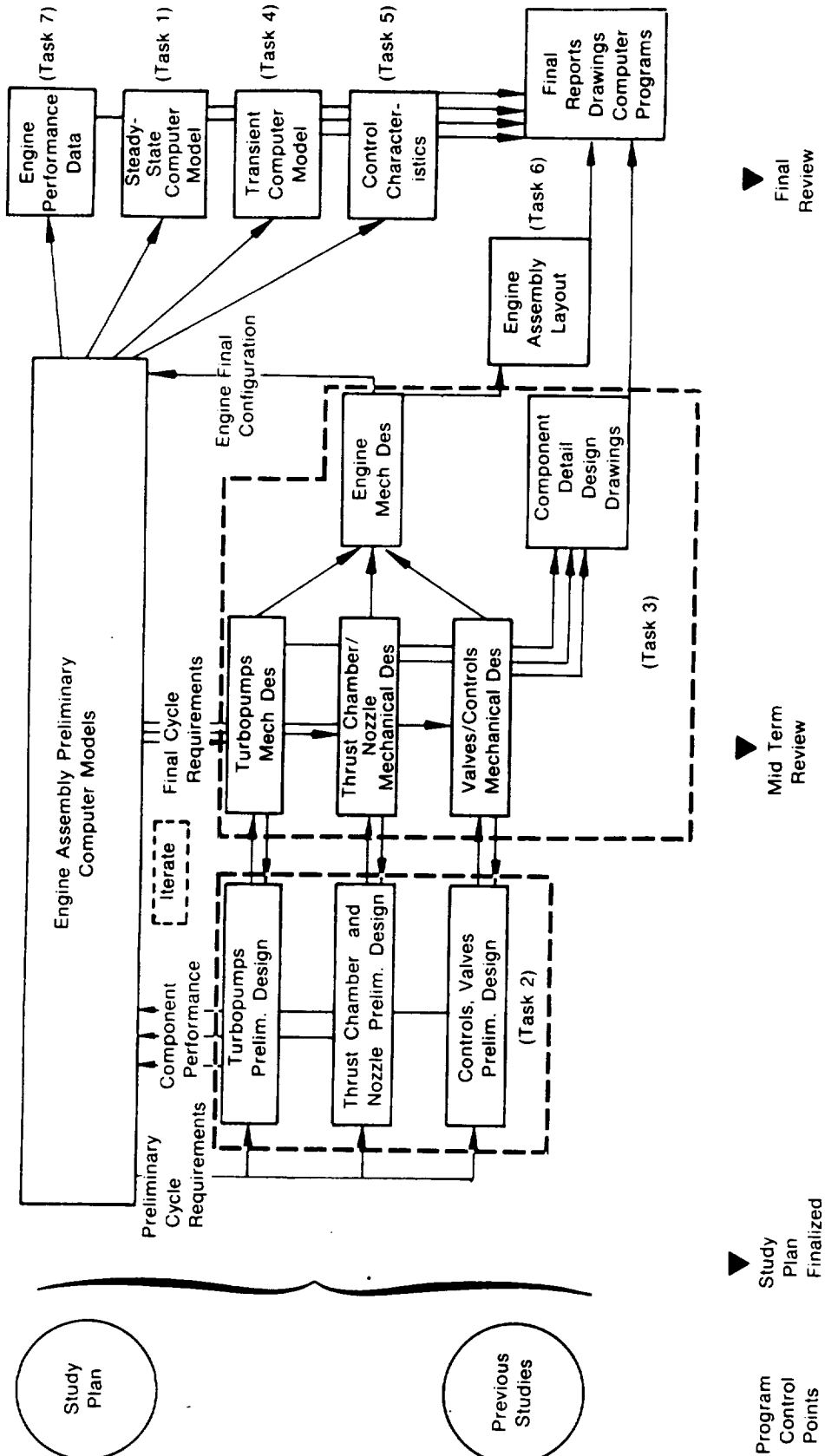
Once the chamber pressure of an OTV engine is increased over 1,200 psia, the rate of increase in specific impulse with further increases in chamber pressure is quite low (approximately 1.3 sec/100 psia), and is decreasing, whereas the difficulty resulting from obtaining these further increases is high, and is increasing. It was not the purpose of this study to optimize performance gain vs development risk; rather, by maximizing performance in a point design of adequate depth, the key performance "driver" elements in an advanced expander cycle engine may be identified, thereby enabling the new technology requirements to be defined.

The schedule followed by P&WA during the performance of this study is shown in Figure 1-1. The interaction of the various design tasks is shown in Figure 1-2 and the results are detailed in the following section of this report.



FD 212851

Figure 1-1. Advanced Expander Cycle Engine Point Design Study Schedule



FD 168955

Figure 1-2. Study Flow Diagram

SECTION 2

ENGINE OPERATING CHARACTERISTICS

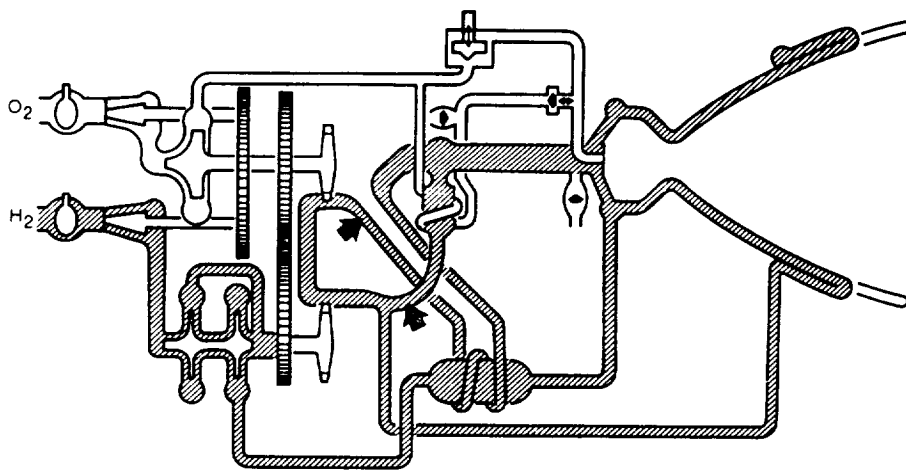
2.1 INTRODUCTION

The design of the Advanced Expander Cycle Engine (AECE) that resulted from this study program conforms to the configuration requirements and operating conditions specified by the contract Scope of Work. The starting point for this study was the preliminary advanced expander cycle optimization task conducted in 1979 under Contract NAS8-33444. (See Pratt & Whitney Report FR-13168, Orbit Transfer Vehicle Engine Study).

2.2 ENGINE SYSTEM

2.2.1 Engine Steady-State Operation

A simplified propellant flow schematic of the 15,000 lb thrust AECE is presented in Figure 2-1. A brief description of the propellant paths at the engine design point (100% thrust and $MR = 6.0$) follows. Fuel (hydrogen) enters the engine through a ball-type inlet shutoff valve mounted on the inlet of a low-pressure pump (boost pump) that is gear-driven from the main oxidizer turbopump shaft. The low-pressure pump operates at a rotational speed of 45,100 rpm with a 15 ft NPSH capability. From the low-pressure pump, fuel enters the first of two back-to-back shrouded impeller centrifugal stages. The impellers are mounted on a shaft driven by a single-stage, low reaction, full admission turbine. The high-pressure pump operates at the nominal speed of 147,100 rpm. Approximately 5.8% of the fuel is used as a thrust-piston balancing flow for the high-pressure pump. This flow is taken off at the second-stage discharge, circulated to the thrust piston, and then injected back into the propellant flowpath at the high-pressure pump interstage.



FD 197567

Figure 2-1. Advanced Expander Engine Cycle

The fuel moves from the high-pressure pump discharge and enters the hydrogen-hydrogen regenerator which utilizes energy from the turbine discharge flow to preheat the chamber coolant. The regenerator is a cross-flow heat exchanger which increases the temperature to approximately 350°R, providing the fuel in a gaseous state for cooling the

thrust chamber. The chamber regenerative coolant enters an inlet manifold located at the injector face plane and flows into and through the nontubular (copper alloy liner and electroformed nickel shell) combustion chamber downstream past the throat to an area ratio of approximately 6. There the coolant enters the tubular nozzle section and flows down half of the tubes to an area ratio of 210:1 where a turnaround manifold routes it back (counter to the combustion gas flow) through the remaining tubes. At an area ratio of approximately 60:1 where the double pass construction starts, the flow is collected in a manifold and is withdrawn.

At the jacket discharge, the fuel flow is split, with about 3% of the flow bypassed around the turbines. This flow passes through the GOX heat exchanger providing the heat transfer for gaseous oxygen tank pressurization capability, if required. The remaining 97% of the flow is routed through the turbines to provide the power to drive the turbopumps, and then through the hot side of the hydrogen-hydrogen regenerator. After leaving the regenerator, the turbine bypass flow re-enters the main stream and hydrogen tank pressurization flow is removed through the tank pressurization valve, if required. The flow is then injected into the thrust chamber.

Oxidizer (oxygen) enters the engine through an inlet valve similar to the fuel-side inlet valve. A low-pressure oxidizer pump, geared from the main oxidizer turbopump and operating at a shaft speed of 9,750 rpm, provides the engine with a 2 ft. NPSH capability. The discharge from the low-pressure pump enters a single-stage, shrouded, centrifugal-type, high-pressure pump driven at a speed of 66,100 rpm by a single-stage, low reaction, full admission turbine. Oxidizer tank pressurization, if required, is taken off downstream of the pump through a heat exchanger where it is vaporized by hot fuel, and, is routed through the oxidizer tank pressurization valve to the vehicle tank. The remainder of the flow continues to the oxidizer control valve, which is preset to give the desired mixture ratio. From the control valve, the flow enters the injector manifold and is injected into the combustion chamber.

A hydrogen-oxygen torch igniter is used to light the main combustion chamber. Fuel for the igniter is tapped off immediately downstream of the turbines, and gaseous oxidizer is supplied from the tank pressurization GOX heat exchanger.

During pumped idle operation, thrust is set at approximately 10% of the rated level. This is accomplished by bypassing 54% of the total fuel flow around the turbine. The increased turbine bypass flow also serves the purpose of providing the energy to the oxygen which is diverted around the oxidizer control valve to a heat exchanger. This delivers gaseous oxygen to the injector, resulting in greater combustion stability at the reduced pressure levels. At tank head idle, which is utilized for pump cooldown and propellant settling, the pumps and turbines do not rotate. The fuel flow bleeds down through the pumps, regenerator, and jacket where it enters the turbine bypass leg. Here the flow splits with approximately 10% being routed to the hot side of the regenerator to provide energy to the cold side, keeping vapor at the jacket inlet. The remaining flow goes through the heat exchangers, vaporizing the oxidizer flow. This results in a thrust level of approximately 70 lb.

Simple open-loop control of the engine assures stability. Stable control operation at the three thrust levels is achieved by time sequencing five solenoid valves which pressurize main valve cavities to establish the proper valve positions at each thrust setting. Ground mixture ratio adjustment at each of the three thrust settings is provided.

Two of the valves have pressure feedback during the transition between thrust settings, yet the valve positions are hard against a stop during steady-state operation. Should loss of electrical power or helium pressure occur, all valves will move to their fail-safe position and a safe engine shutdown will result.

The engine is transitioned from one thrust setting to another utilizing vehicle electrical signals. Two check valves are used for tank pressurization. A schematic showing the location of each valve is provided in Figure 2-2. The 5 solenoid valves respond to the electrical signals by opening the appropriate valve cavity to a pressure source, either helium, hydrogen, or oxygen depending upon the application. These solenoid valves vent the valve cavities overboard when deactivated. Figure 2-3 shows typical operation and responding action by the engine control system.

Propellant shut-off is achieved using inlet shut-off valves which are low leakage cryogenic valves and are helium-actuated open during all phases of engine operation.

The main fuel shut-off valve is a low-pressure loss valve which is closed during the tank head idle mode of operation (zero speed). This valve is helium-actuated open during other phases of operation. Shutdown is achieved by closing the main fuel shut-off valve as well as the main fuel control valve to starve the combustion chamber of fuel and cause flame-out.

The oxidizer flow control valve is closed during the tank head idle and pumped idle modes. It opens during the transition between pumped idle and full thrust when the oxidizer pump pressure rise is above 465 psid. Ground adjustment of mixture ratio between 6.0 and 7.0 is provided at the full thrust setting.

The gaseous oxidizer (GO.) valve provides two functions. The first function is to allow mixture ratio to change from 4.0 at tank head idle to 6.0 at pumped idle. The second function is to change the phase at the oxidizer injector from gas to liquid as the engine accelerates from pumped idle to full thrust. Ground adjustment of mixture ratio at tank head idle and pumped idle is provided.

The main fuel control valve has three functions. One function is to vent fuel overboard during shutdown, a second function is to direct flow to the fuel regenerator hot side during tank head idle, and the third function is to set turbine bypass flow during the three thrust settings. Ground adjustment of this valve at each of the three thrust levels is accomplished by adjusting the needle valve at the full thrust level and the stop positions of the valve at the tank head idle and pumped idle thrust levels.

Steady-state operating characteristics for the Advance Expander Cycle engine are shown in Table 2-1 and in the cycle propellant flow schematics presented in Figures 2-4 through 2-6. Off-design full-thrust specific impulse and thrust characteristics are presented in Figures 2-7 and 2-8 respectively.

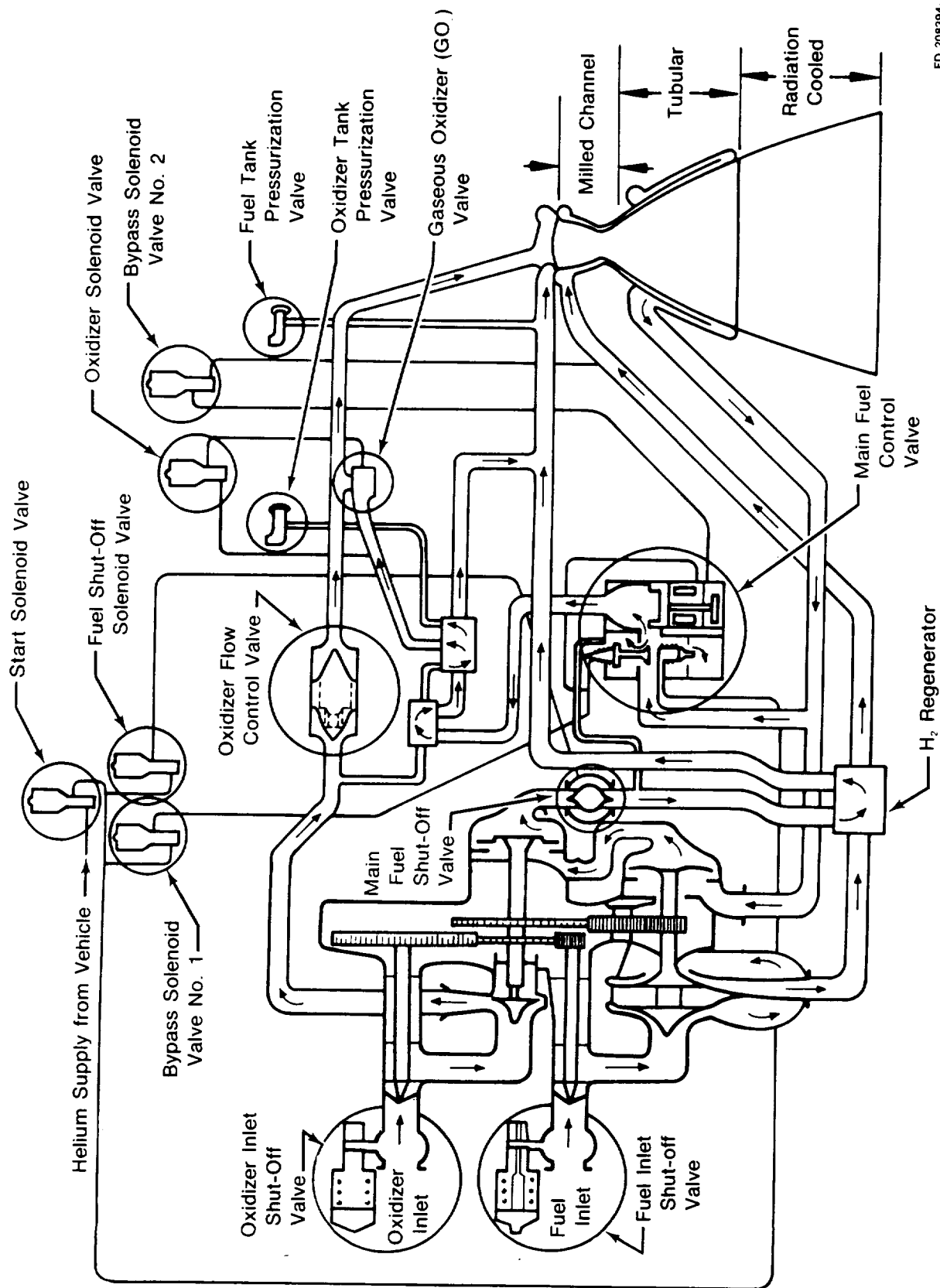
2.2.2 Engine Transient Operating Characteristics

2.2.2.1 Ignition

Ignition occurs during the first 0.25 sec of the tank head idle transient. The tank head idle mode is used to condition the pumps prior to rotation.

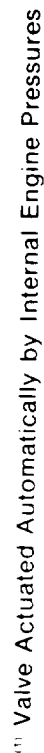
The start solenoid valve and the bypass solenoid valve No. 1 are energized causing the fuel and oxidizer inlet shut-off valves, the turbine bypass, and the fuel regenerator poppet to open and causing the fuel vent poppet to close. Spark to the torch igniter is initiated immediately and terminated once the torch lights (about 0.2 sec).

Chamber ignition is approached from the oxidizer rich side, Figure 2-9. The oxidizer side fills more rapidly than the fuel because of its reduced volume which allows simultaneous opening of the fuel and oxidizer inlet shut-off valves. A torch igniter is used to provide the ignition energy.



FD 208394

Figure 2-2. Engine Propellant Flow Schematic

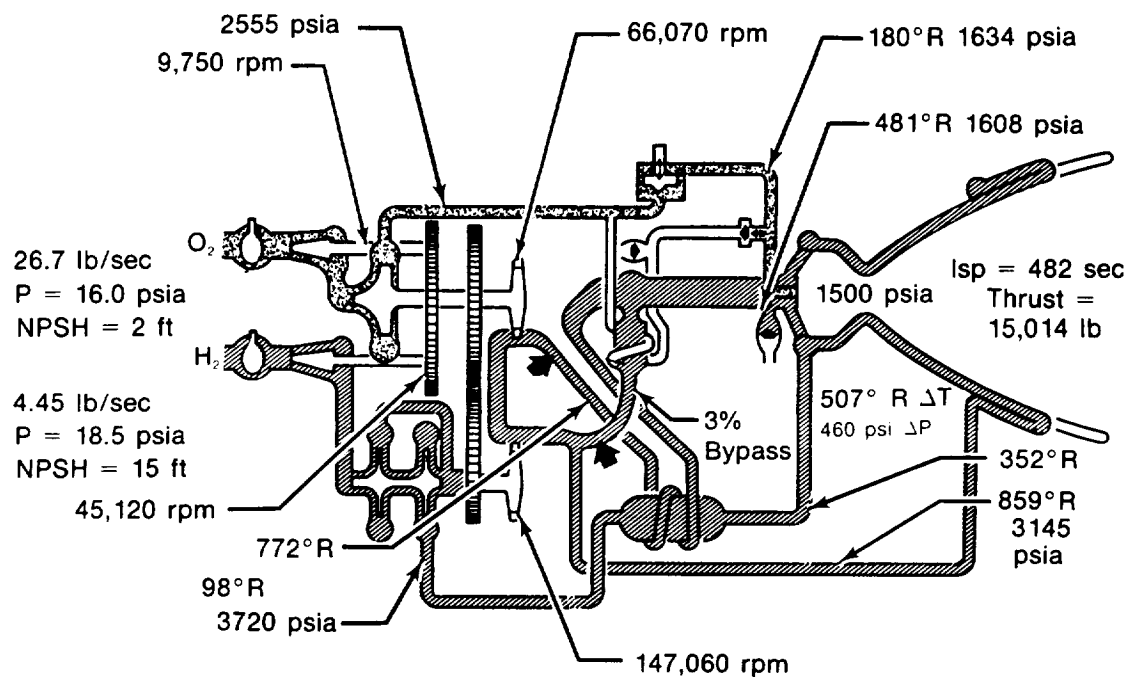


FD 208395A

Figure 2-3. Value Sequence for a Typical Firing

TABLE 2-1. ENGINE STEADY-STATE DESIGN POINT OPERATION

| | |
|---|---------|
| Operating | |
| Full Thrust | |
| Thrust (vac), lb | 15,000 |
| Mixture Ratio | 6.0 |
| Chamber Pressure, psia | 1500. |
| Specific Impulse, sec | 482.2 |
| Required Inlet Conditions | |
| Fuel-NPSH, ft | 15 |
| Temperature°R | 37.8 |
| Oxidizer-NPSH, ft | 2 |
| Temperature°R | 162.7 |
| Engine Life (Time Between Overhauls) | |
| Firings/hr | ≥300/10 |
| Pumped Idle | |
| Thrust (vac), lb | 1500. |
| Mixture Ratio | 6.0 |
| Specific Impulse, sec | 455.4 |
| Tank Head Idle | |
| Thrust (vac), lb | 72. |
| Mixture Ratio | 4.0 |
| Specific Impulse, sec | 449.8 |



FD 197567C

Figure 2-4. Advanced Expander Engine Propellant Flow Schematic at Full Thrust (MR = 6.0)



0 rpm

581°R

9.3 psia

612°R

12.3 psia

0.13 lb/sec

$P = 15.6$ psia

O_2

H_2

0.03 lb/sec

$P = 18.2$ psia

8.1 psia

$I_{sp} = 450$ sec

Thrust = 72

823°R ΔT

4.1 psi ΔP

96% Bypass

70°R

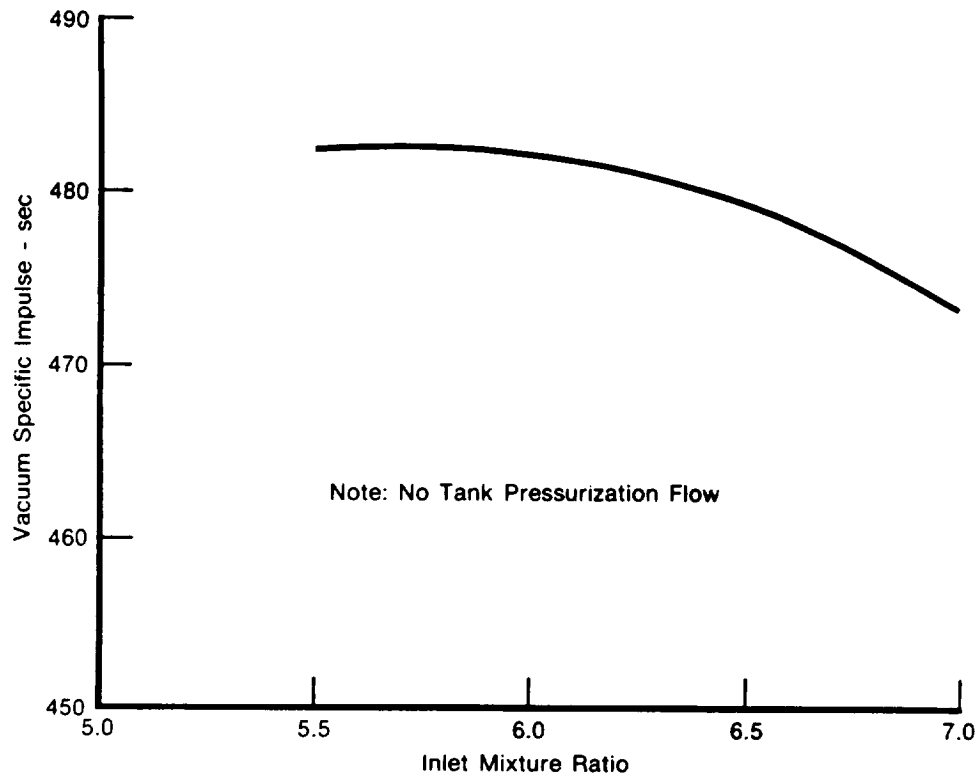
16.1 psia

893°R

14.1 psia

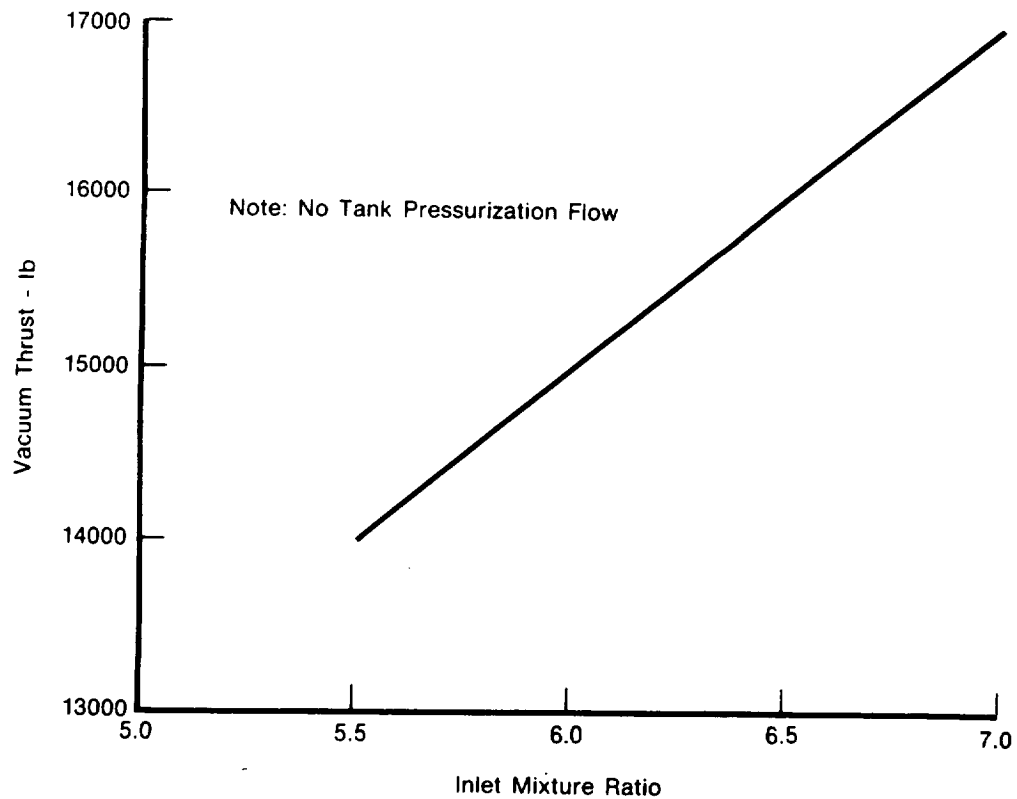
0 rpm

FD 197567A



FD 212852

Figure 2-7. Estimated Effect of Inlet Mixture Ratio on Vacuum Specific Impulse at Full Thrust



FD 212853

Figure 2-8. Estimated Effect of Inlet Mixture Ratio on Vacuum Thrust at Full Thrust Setting

Two ignition transients are presented in this report. One transient shows the ignition characteristics when the pumps are initially at 500°R. In the other transient, the pumps are at tank temperature levels; a relight following a short coast situation. With the pump metal temperatures initially at 500°R, the torch will light at about 0.07 sec when its mixture ratio drops below 20, followed by main chamber ignition at 0.2 sec when its mixture ratio drops below 20. Figures 2-9 and 2-10 show graphically the ignition and main chamber ignition. Figures 2-11 through 2-17 present fuel and oxidizer system pressures, temperatures, flows, etc. during the first 1.0 sec of firing. Ignition characteristics with the pumps already conditioned are presented in Figures 2-18 and 2-19. The torch lights at 0.05 sec followed by main chamber ignition at 0.12 sec.

2.2.2.2 Pump Conditioning

Pump conditioning is implemented utilizing the tank head idle mode where the fuel bypasses the turbine and the pumps do not rotate. About 2 min are required to condition the pump housings and impellers from an initial temperature of 500°R to the temperature level of the propellants in the tank during which time 4 lb of fuel and 16 lb of oxygen consumed. This represents less than 1 sec of full thrust consumption with a specific impulse penalty of only 7%. Figures 2-20 through 2-30 show engine characteristics during conditioning.

2.2.2.3 Tank Head Idle to Pumped Idle

Once the pump housings and impellers are cooled to tank temperatures during the tank head idle mode, the engine may be transitioned to the pumped idle thrust setting. Figure 2-31A presents the valve sequencing for this transition. The bypass solenoid valve No. 1 is closed, bypass solenoid valve No. 2 is opened, and the fuel shutoff solenoid valve is opened. Closing the bypass solenoid valve No. 1 closes the turbine bypass valve and closes the bleed valve supplying flow to the regenerator hot side. With the main fuel shut-off valve open and the turbine bypass valve closed, all the fuel is directed through the turbine producing the maximum available torque for break-away. Opening bypass solenoid valve No. 2 allows the bypass valve to open to its pumped idle setting as valve inlet pressure (speed) increases. Also as speed increases, the gaseous oxidizer valve opens further to adjust mixture ratio from 4 at tank head idle to 6 at pumped idle. The engine characteristics during this transient are shown as the first 8 sec of Figures 2-32 through 2-53.

2.2.2.4 Pumped Idle to Full Thrust

The transition from the pumped idle thrust setting of 1500 lb to the full thrust setting of 15,000 lb is initiated by closing the bypass solenoid valve 2 and opening the oxidizer solenoid valve (see Figure 2-31-B). Closing the bypass solenoid valve, vents the turbine bypass valve cavity causing the bypass valve to close. Opening the oxidizer solenoid valve allows the gaseous oxidizer valve to close as valve inlet pressure increases. The oxidizer flow control valve will open when the overall oxidizer pump pressure rise is greater than 465 psid. The opening of the oxidizer flow control valve occurs just prior to the gaseous oxidizer valve closure. The pressure level for the switch from gaseous oxidizer at the injector to liquid is chosen so that the injector pressure differential ($\Delta P/P$) is sufficient to assure combustion stability. These transient characteristics are shown between 10 and 18 sec of Figures 2-32 through 2-53.

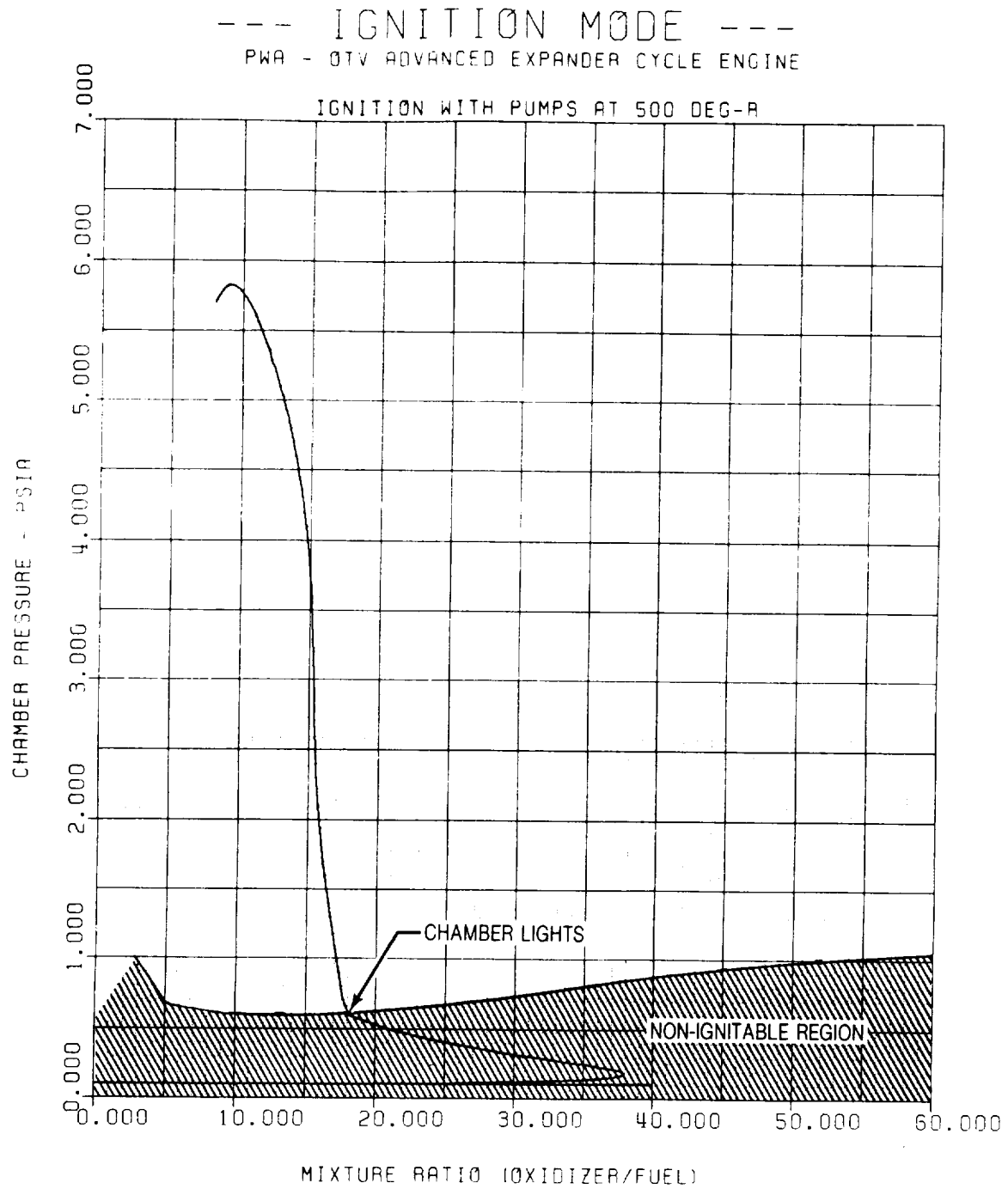


Figure 2-9. Oxidizer Rich Chamber Ignition

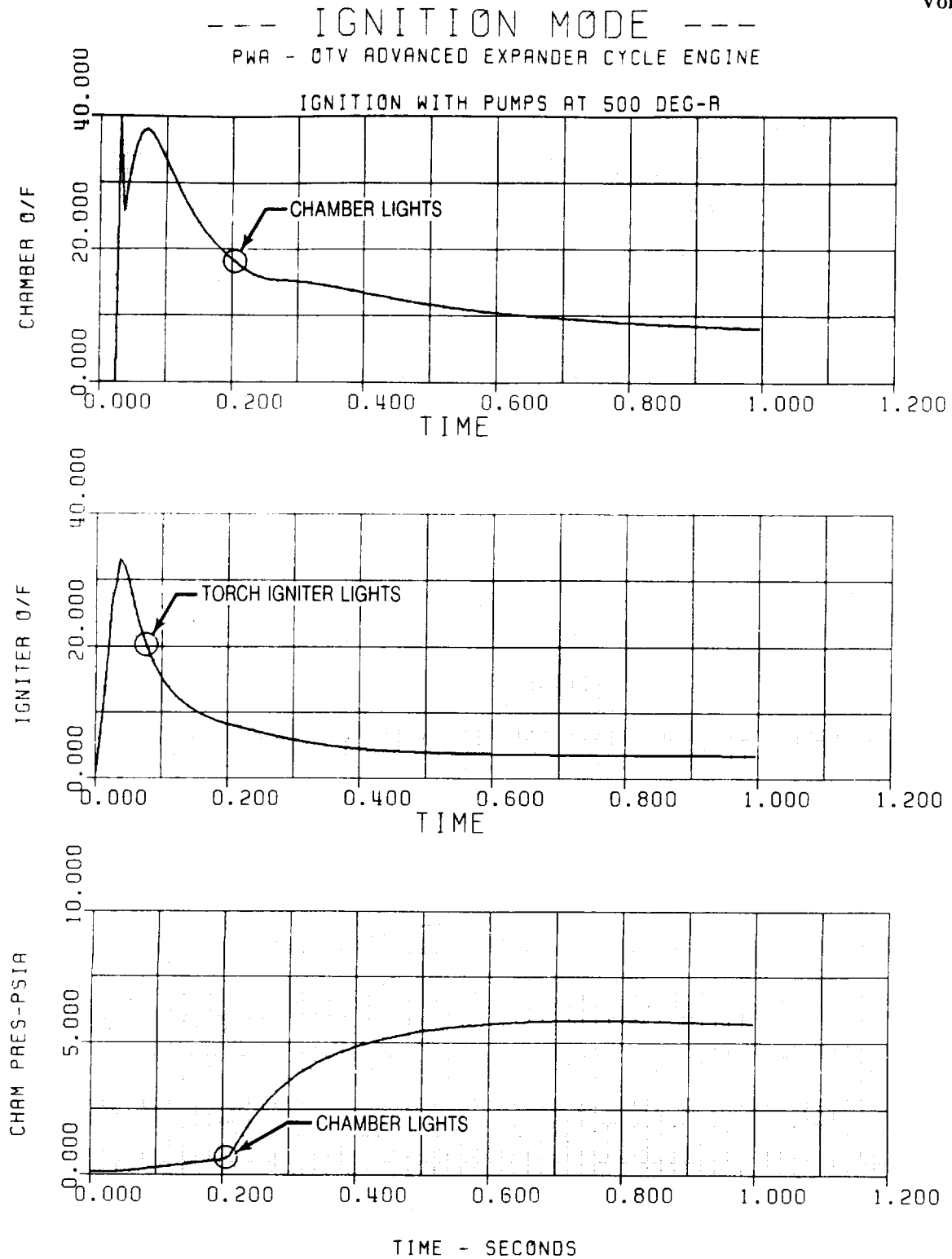


Figure 2-10. Torch Igniter Lights Long Before Chamber Reaches Ignitable Region

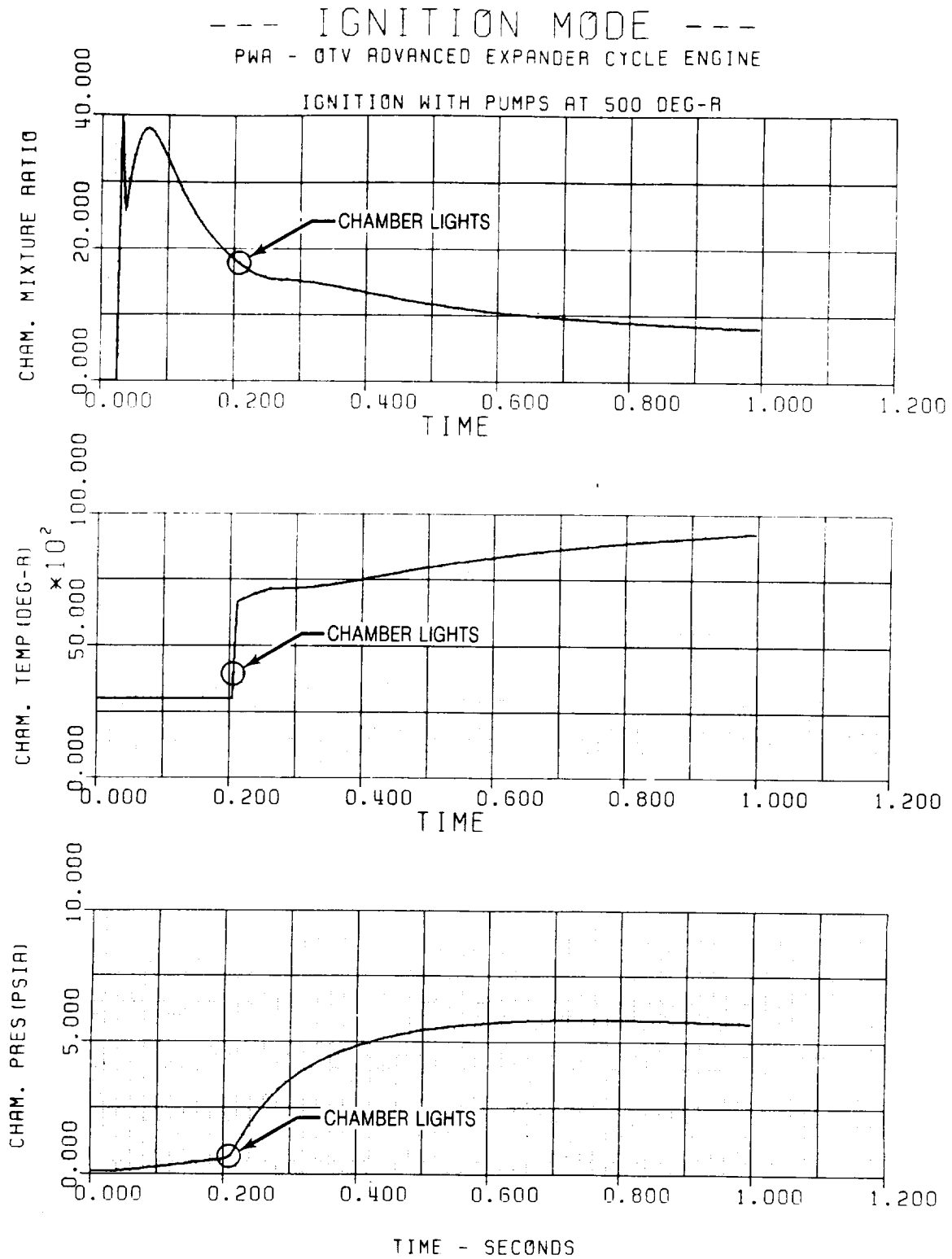


Figure 2-11. Chamber Characteristics During Ignition

--- IGNITION MODE ---
PWA - OTV ADVANCED EXPANDER CYCLE ENGINE

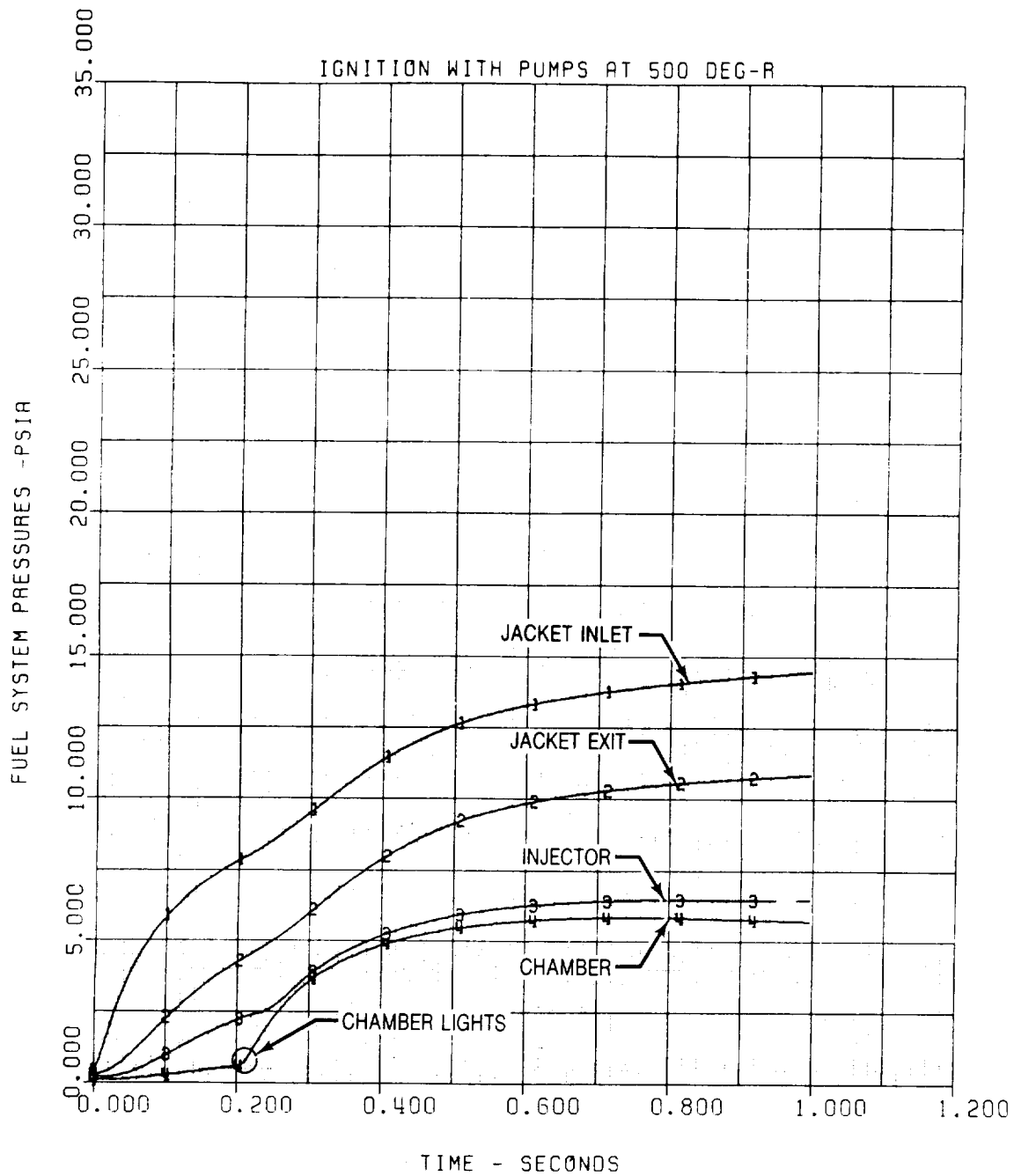


Figure 2-12. Fuel System Pressures During Ignition

--- IGNITION MODE ---
PWA - OTV ADVANCED EXPANDER CYCLE ENGINE

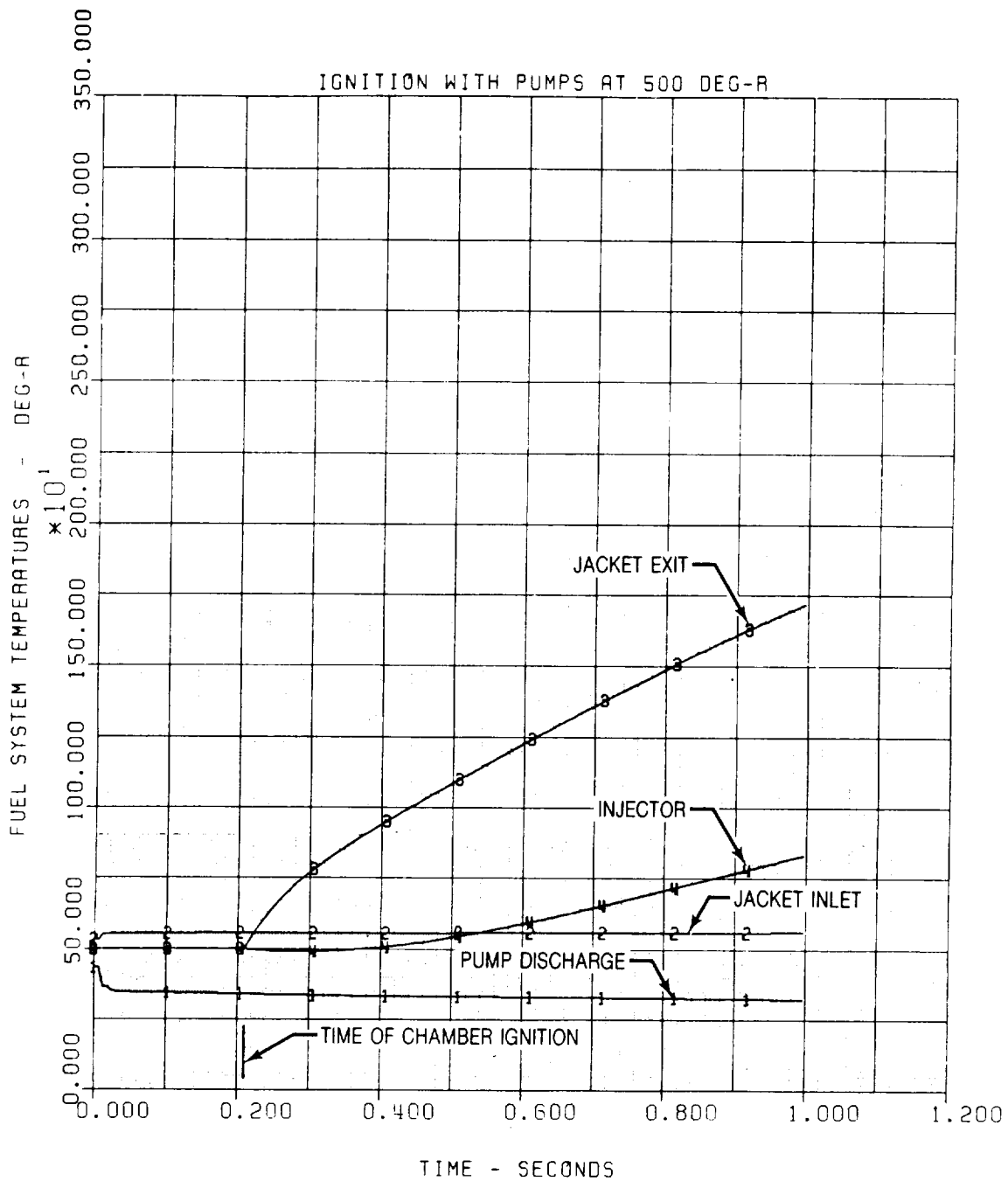


Figure 2-13. Fuel System Temperatures During Ignition

--- IGNITION MODE ---
PWA - OTV ADVANCED EXPANDER CYCLE ENGINE

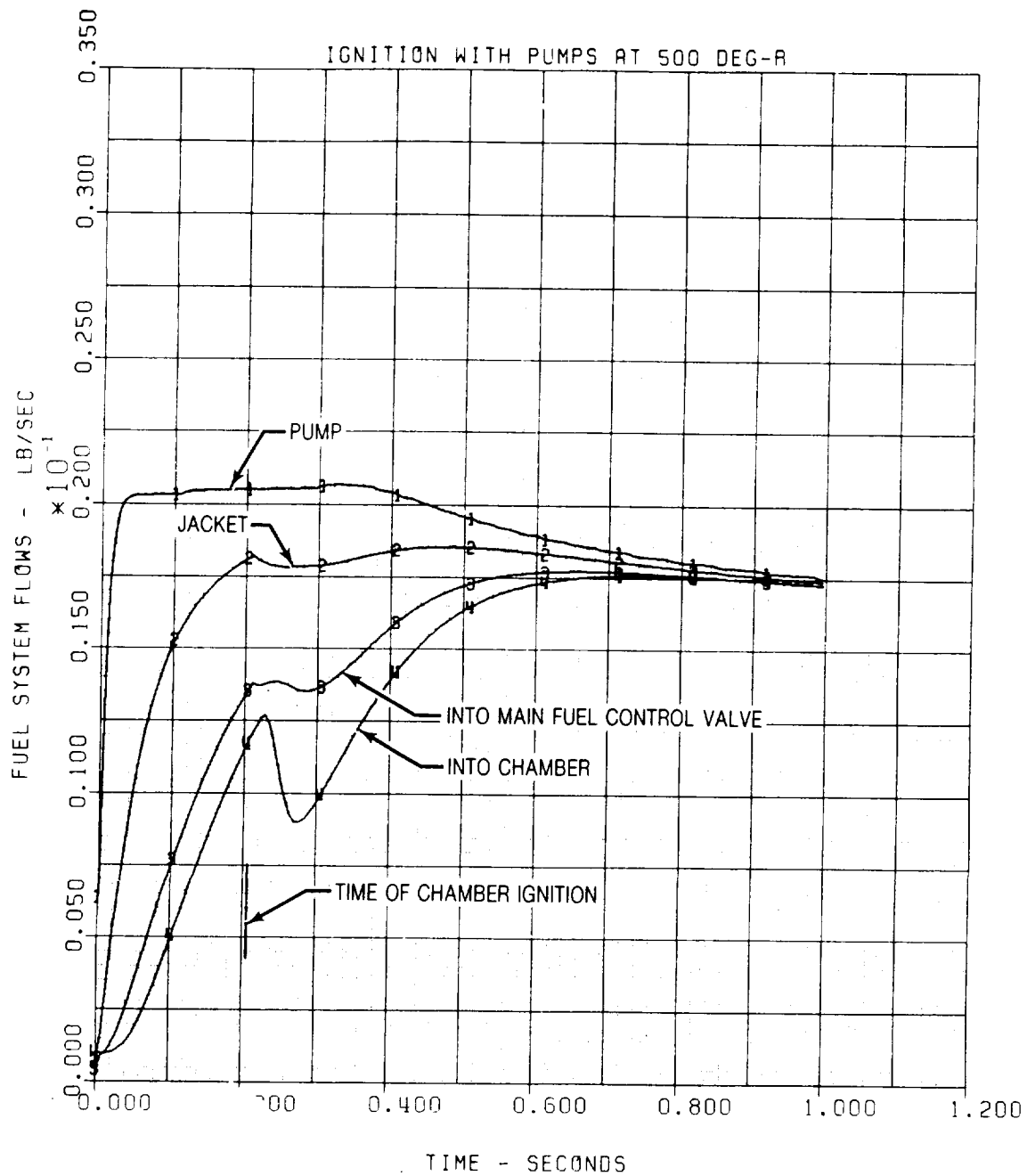


Figure 2-14. Fuel System Flows During Ignition

--- IGNITION MODE ---

PWA - OTV ADVANCED EXPANDER CYCLE ENGINE

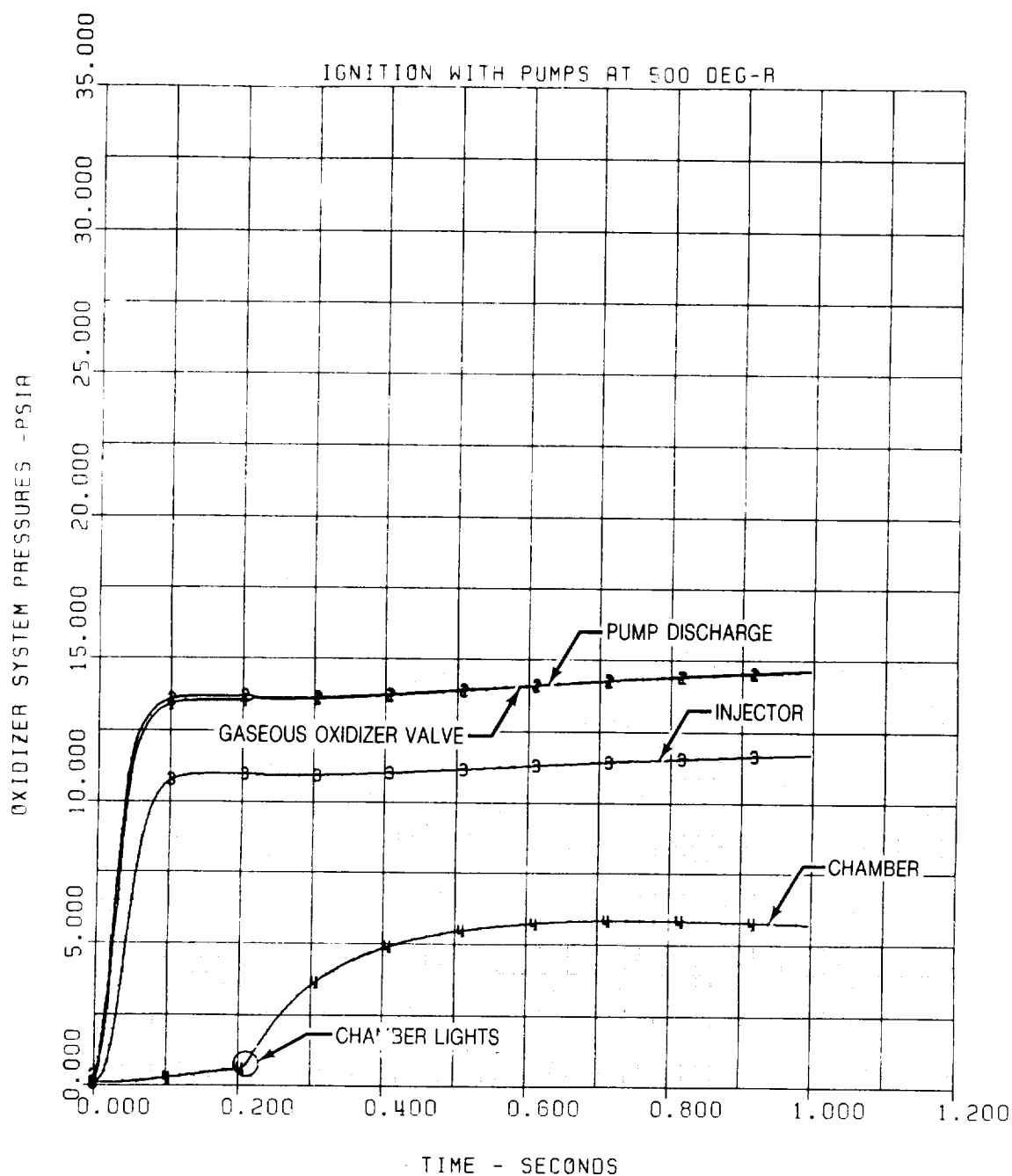


Figure 2-15. Oxidizer System Pressures During Ignition

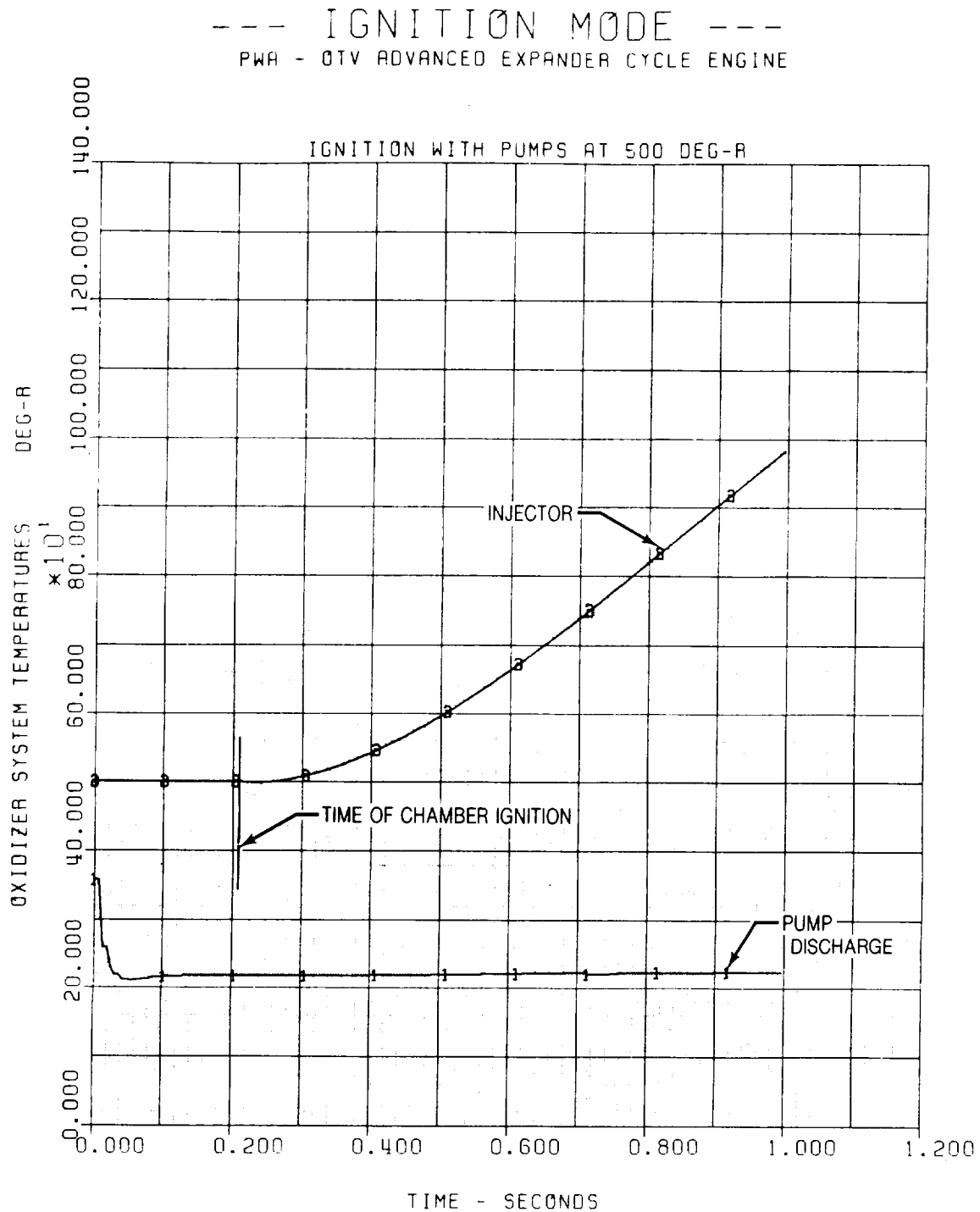


Figure 2-16. Oxidizer System Temperatures During Ignition

--- IGNITION MODE ---
PWA - QTV ADVANCED EXPANDER CYCLE ENGINE

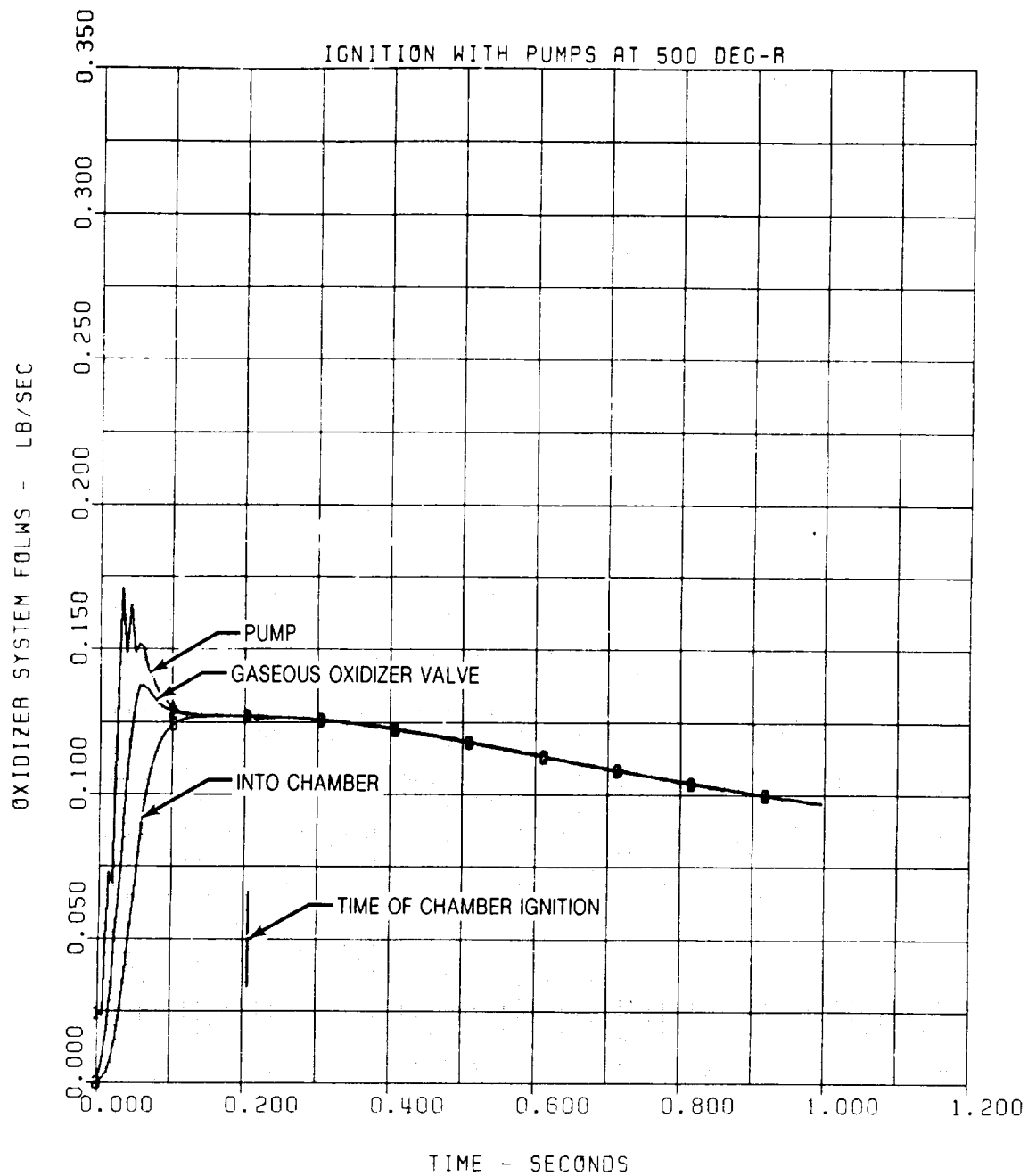
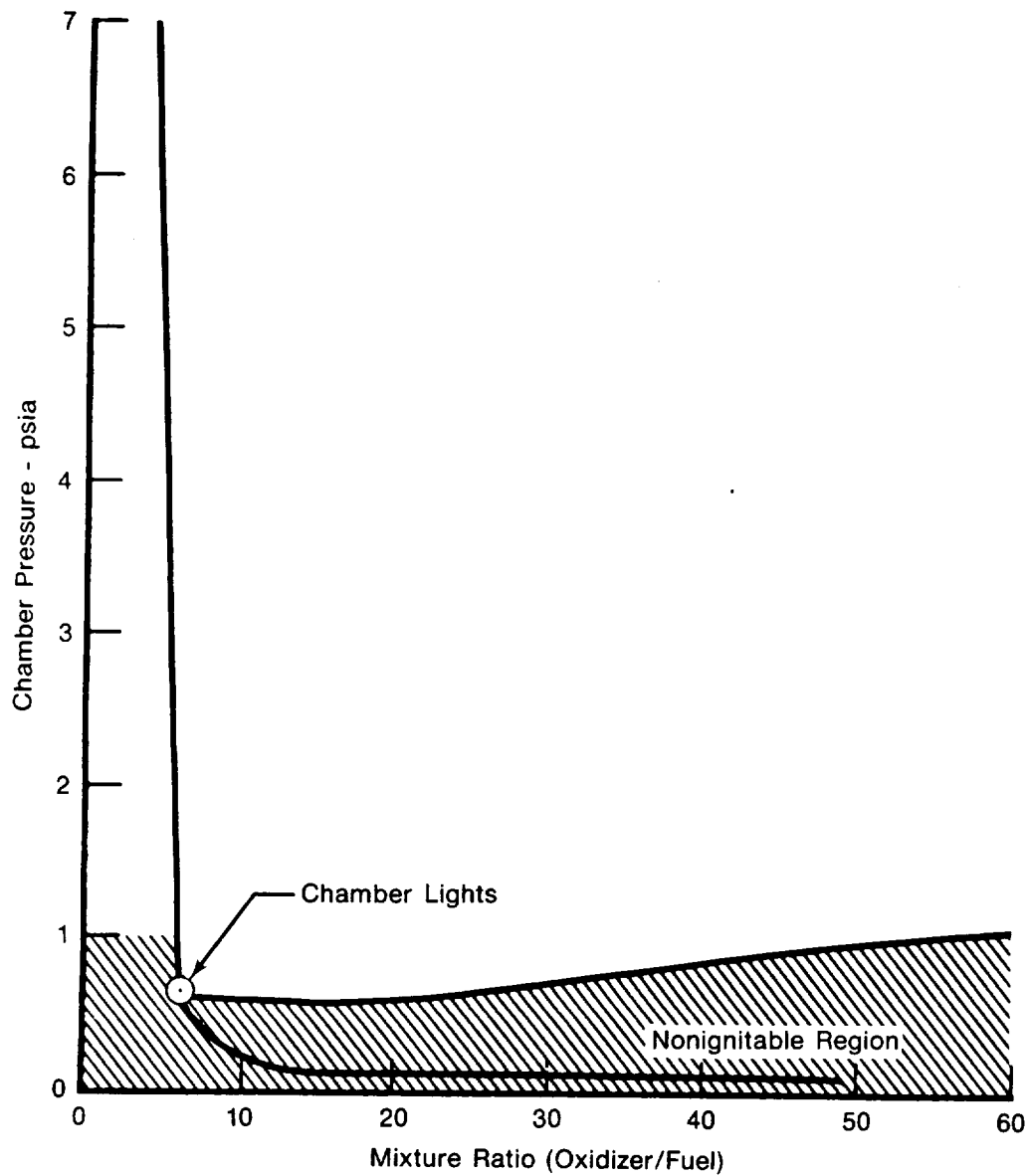
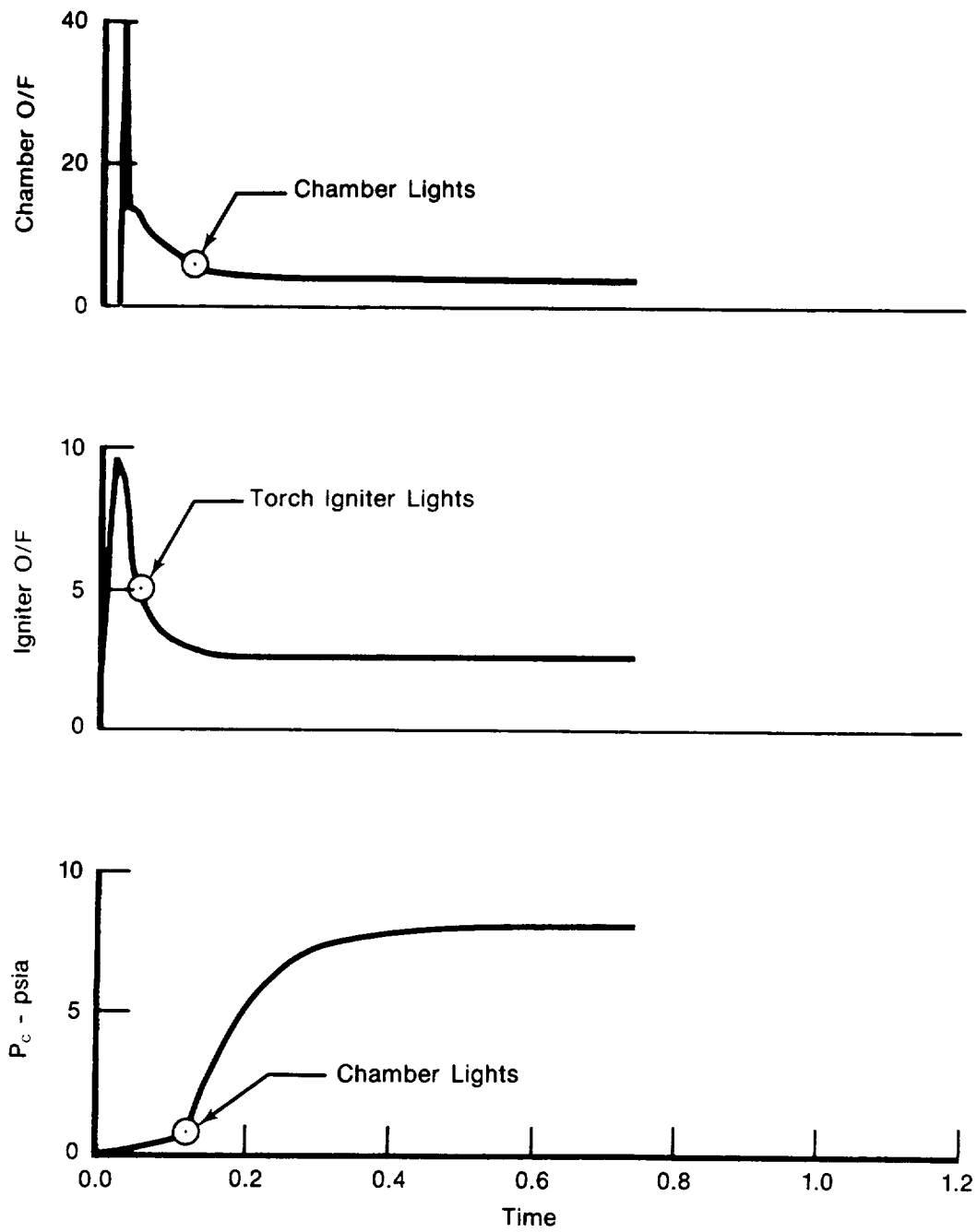


Figure 2-17. Oxidizer System Flows During Ignition



FD 213092

Figure 2-18. Chamber Ignition Characteristics if Pumps Are Already Conditioned



FD 213093

Figure 2-19. Ignition With Pumps Already Conditioned

--- COOLDOWN MODE ---
PWA - OTV ADVANCED EXPANDER CYCLE ENGINE

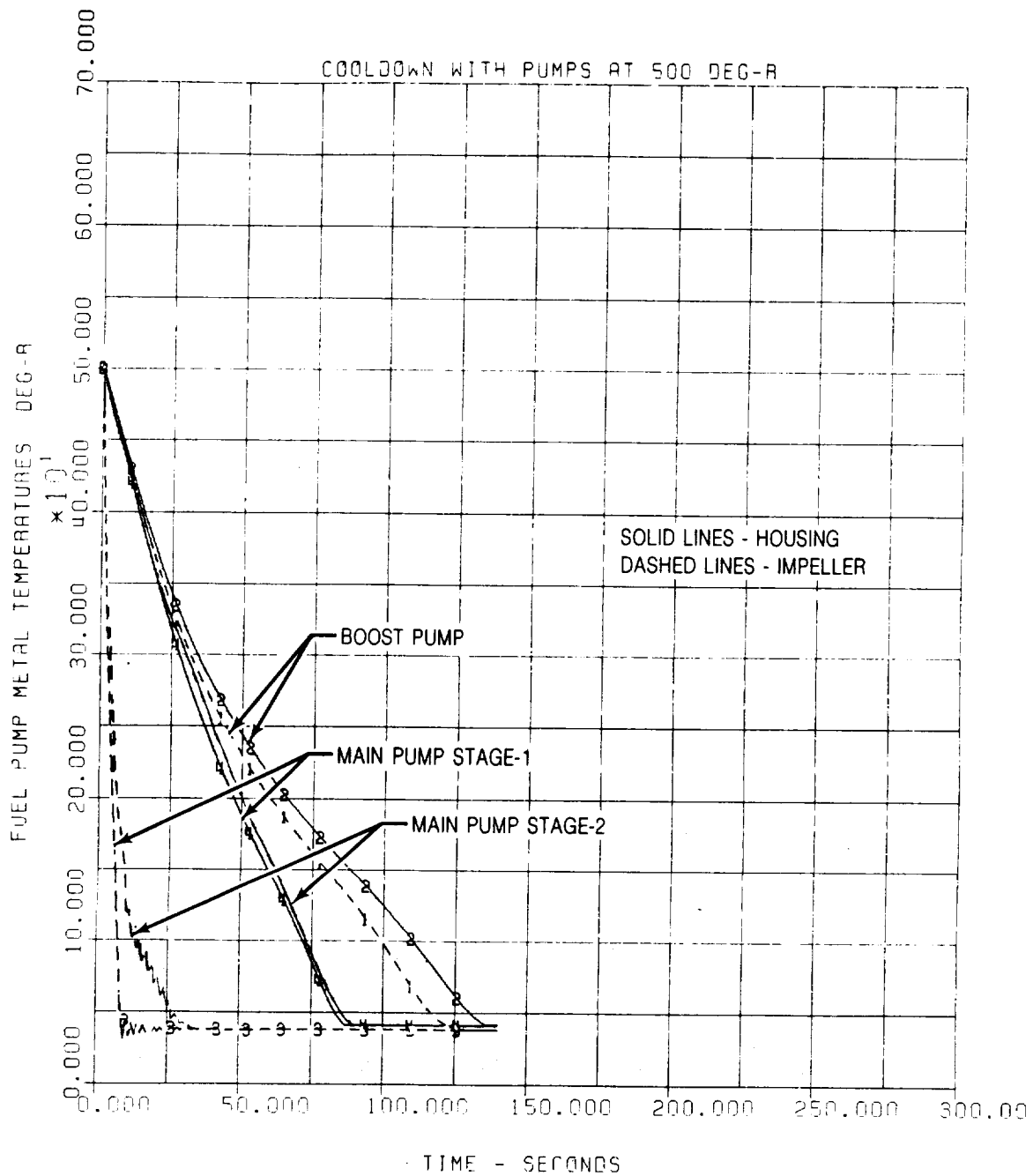


Figure 2-20. Fuel Pump Cooldown During Tank Head Idle

--- COOLDOWN MODE ---
PWA - QTV ADVANCED EXPANDER CYCLE ENGINE

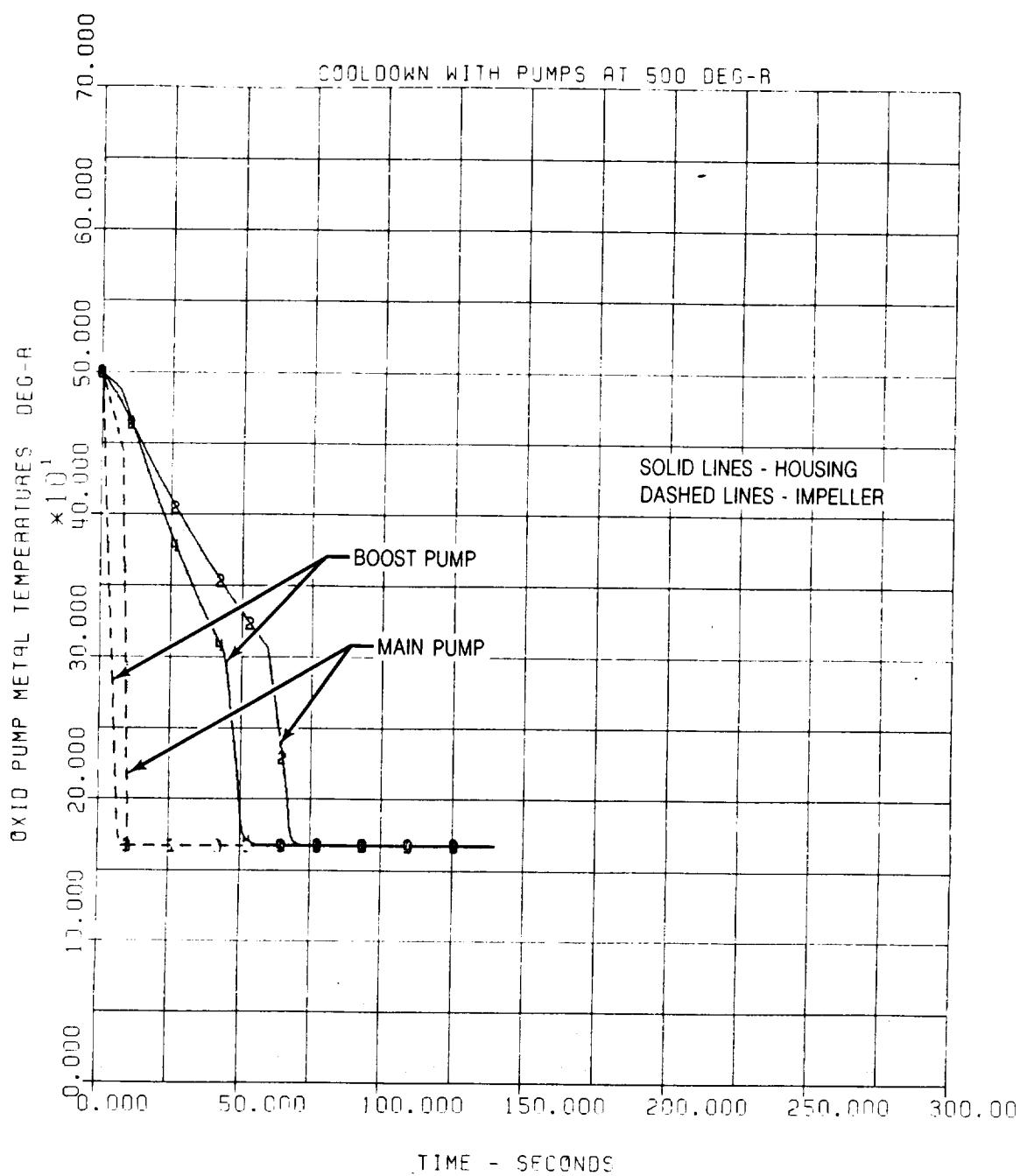


Figure 2-21. Oxidizer Pump Cooldown During Tank Head Idle

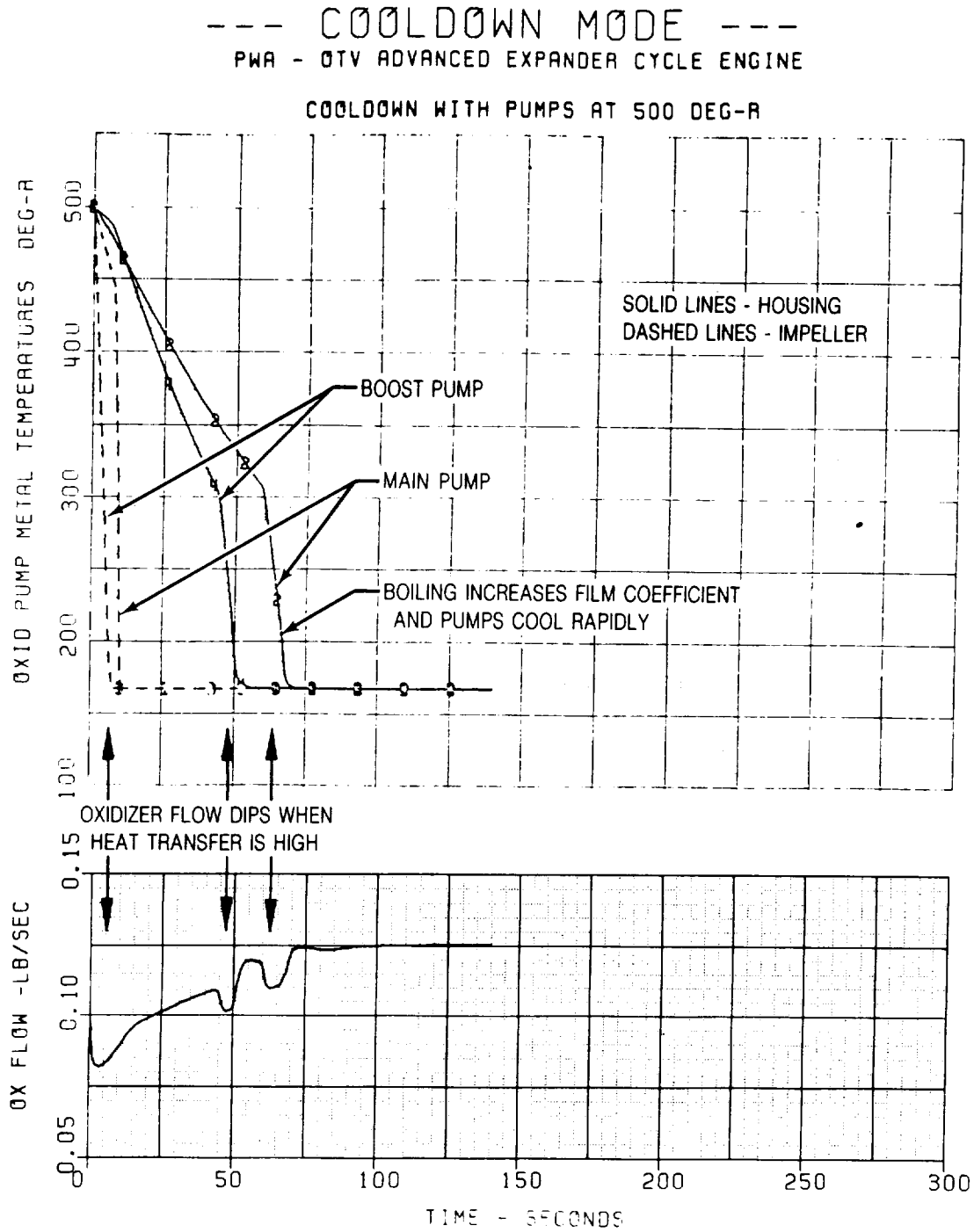


Figure 2-22. Boiling Increases Heat Transfer Causing Oxidizer Flow to Dip

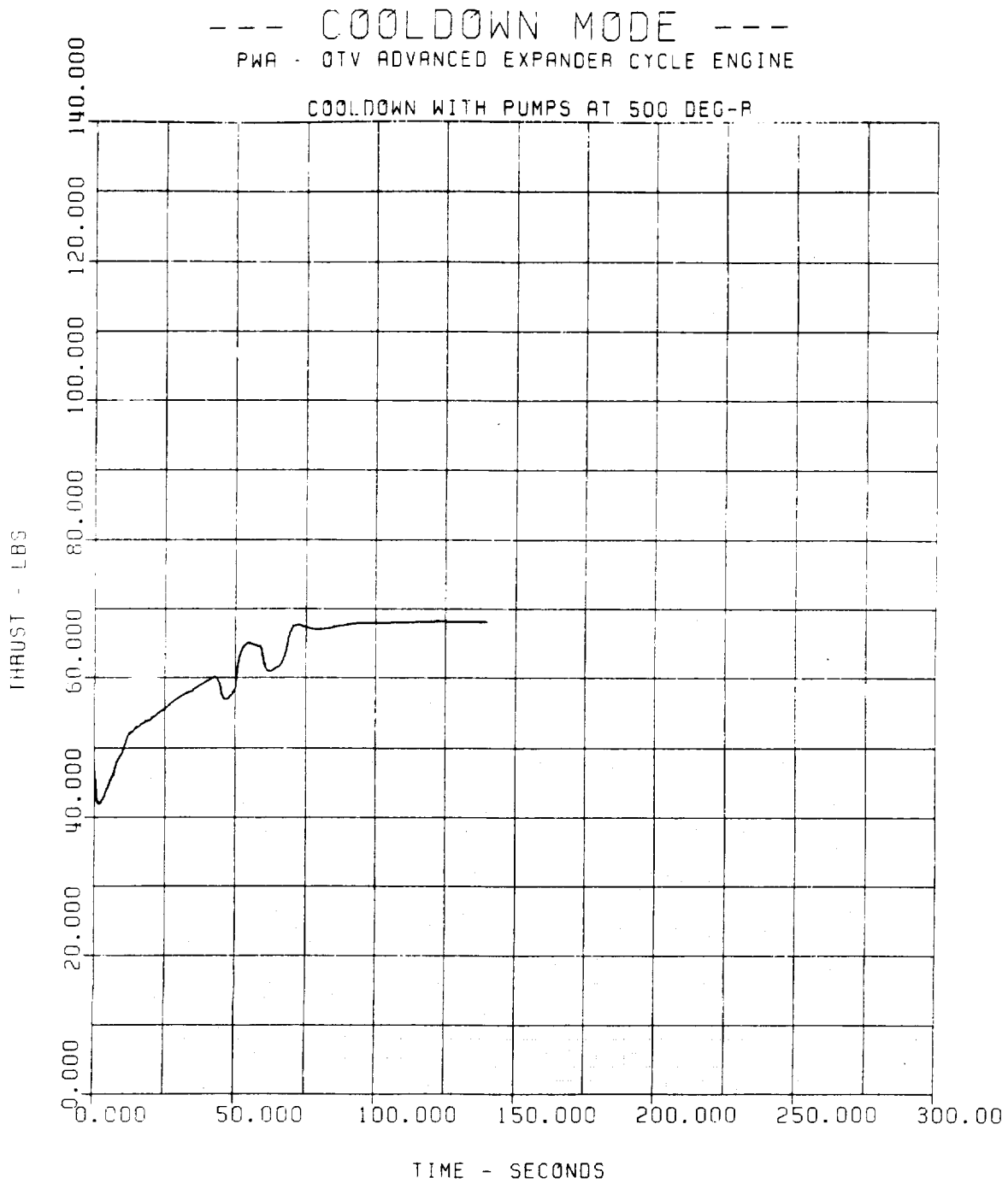


Figure 2-23. Thrust During Tank Head Idle

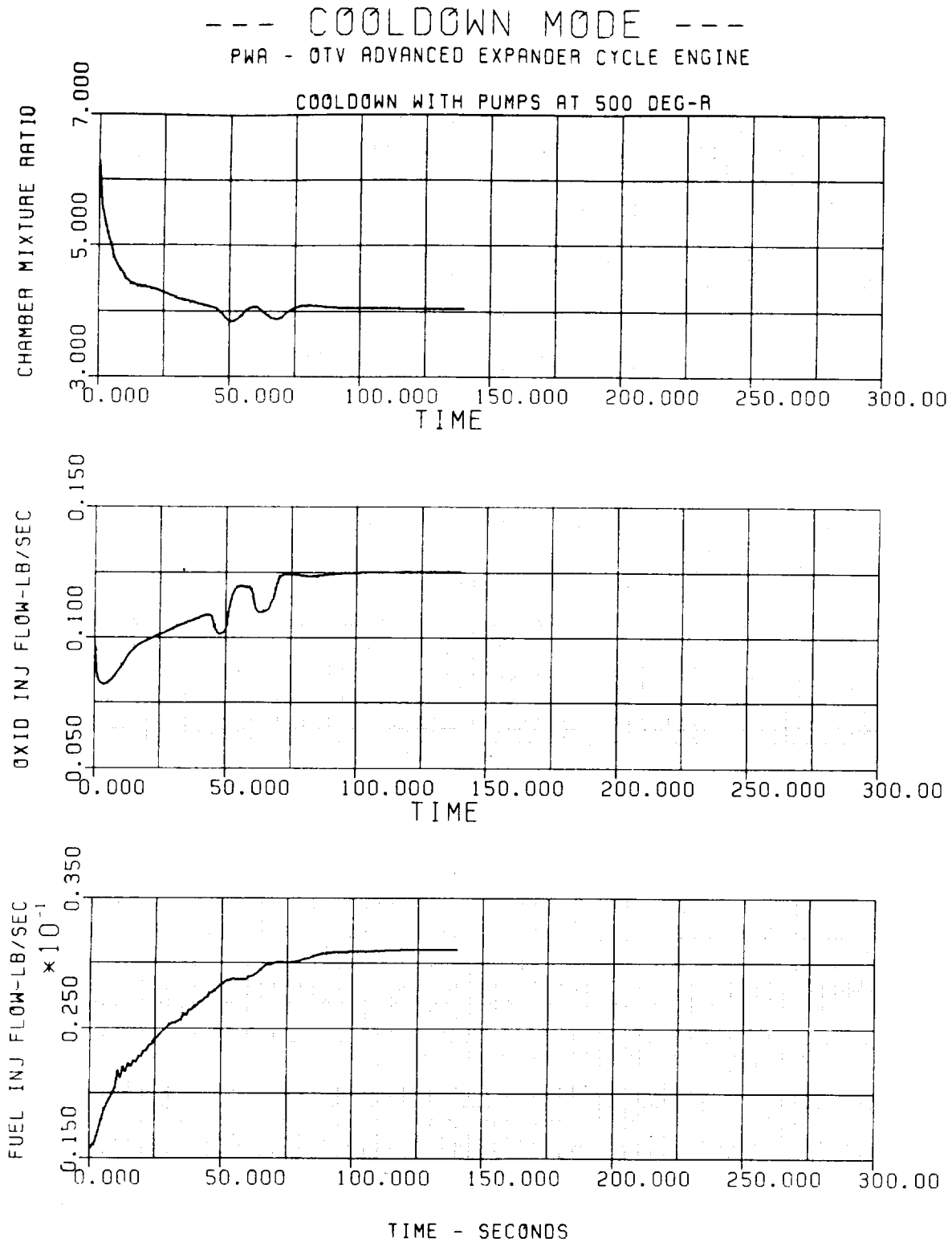


Figure 2-24. Injector Flows and Chamber Mixture Ratio During Tank Head Idle

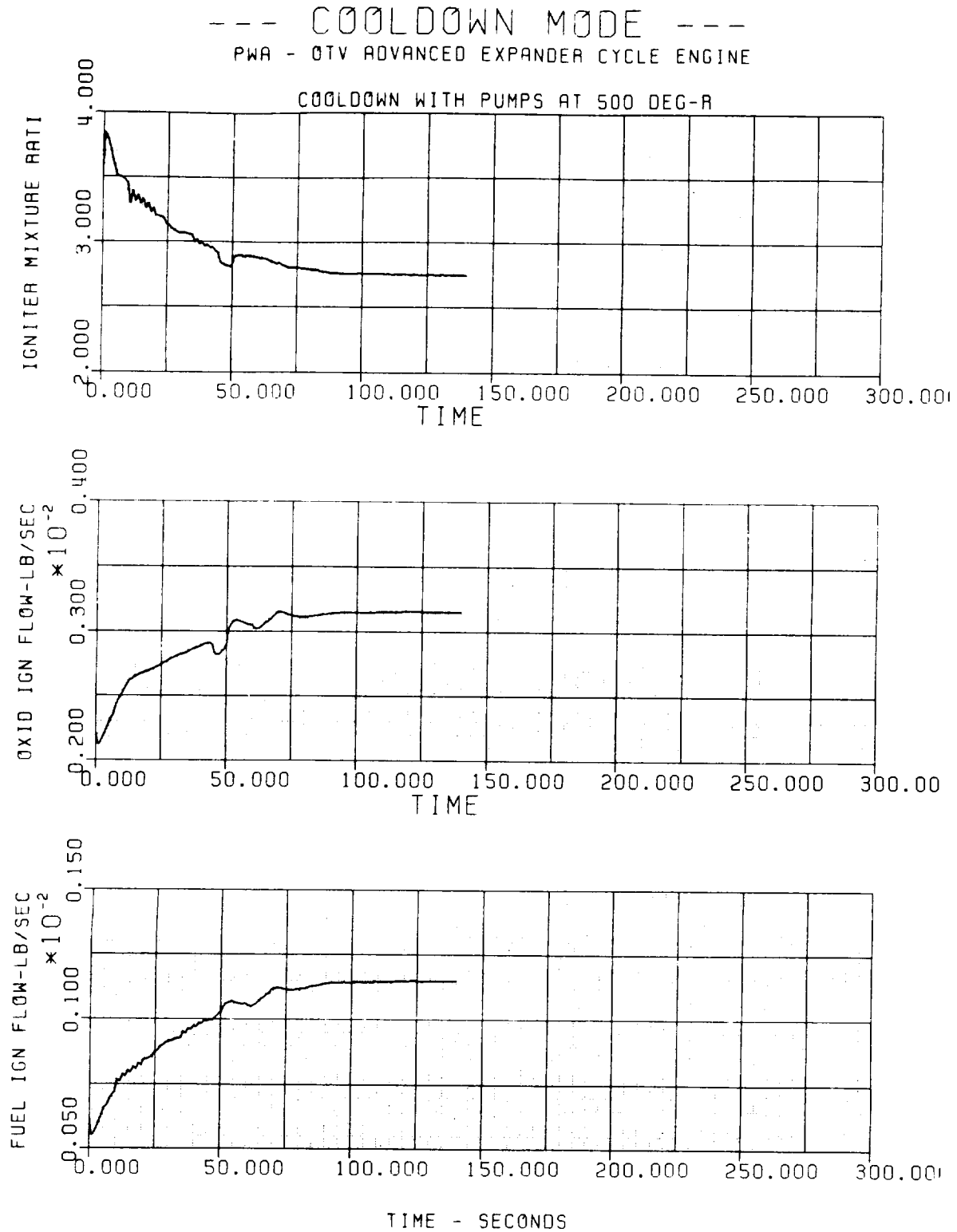


Figure 2-25. Igniter Flows and Mixture Ratio During Tank Head Idle

--- COOLDOWN MODE ---

PWA - QTV ADVANCED EXPANDER CYCLE ENGINE

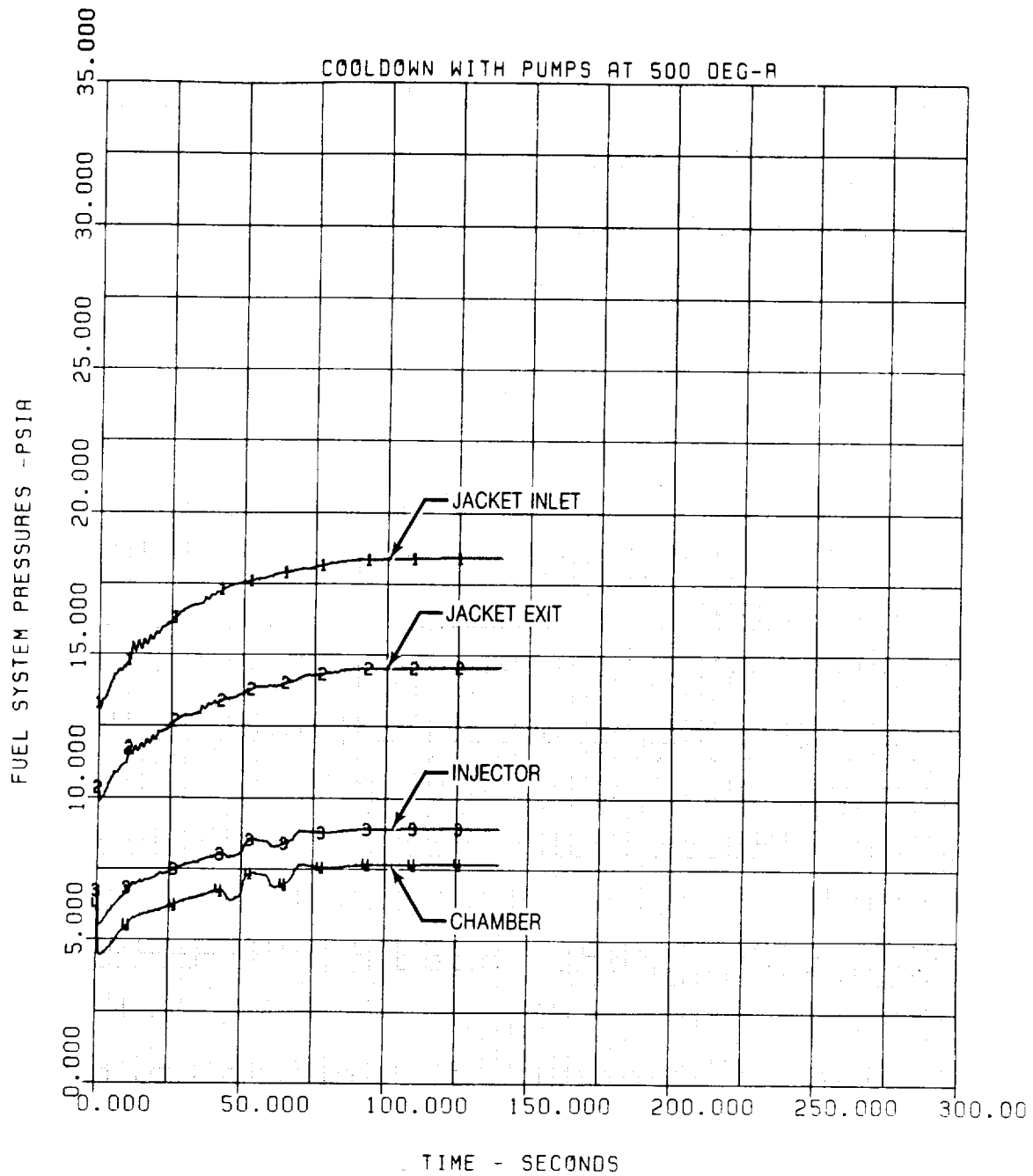


Figure 2-26. Fuel System Pressures During Tank Head Idle

--- COOLDOWN MODE ---
PWA - OTV ADVANCED EXPANDER CYCLE ENGINE

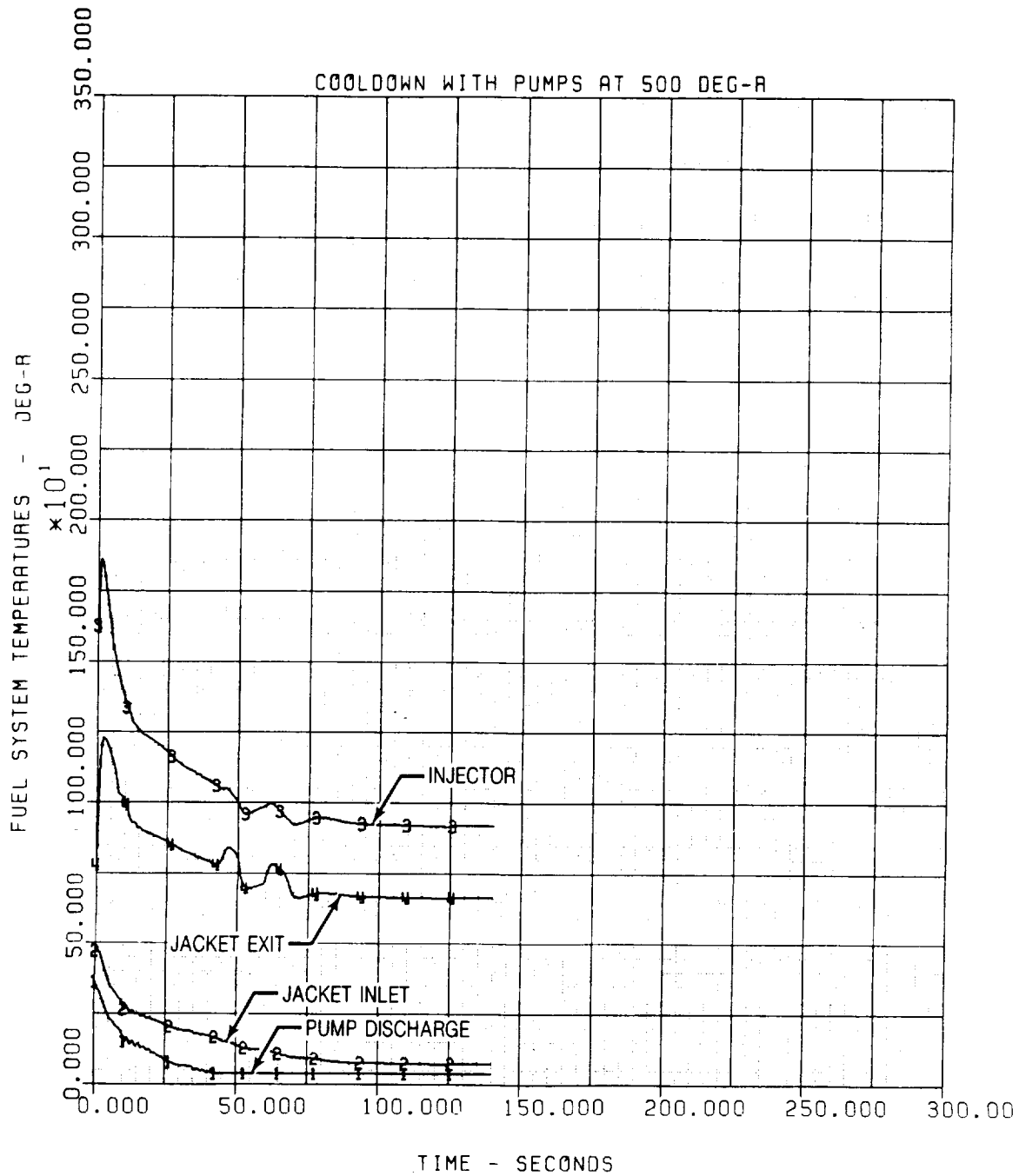


Figure 2-27. Fuel System Temperatures During Tank Head Idle

--- COOLDOWN MODE ---
PWA - QTV ADVANCED EXPANDER CYCLE ENGINE

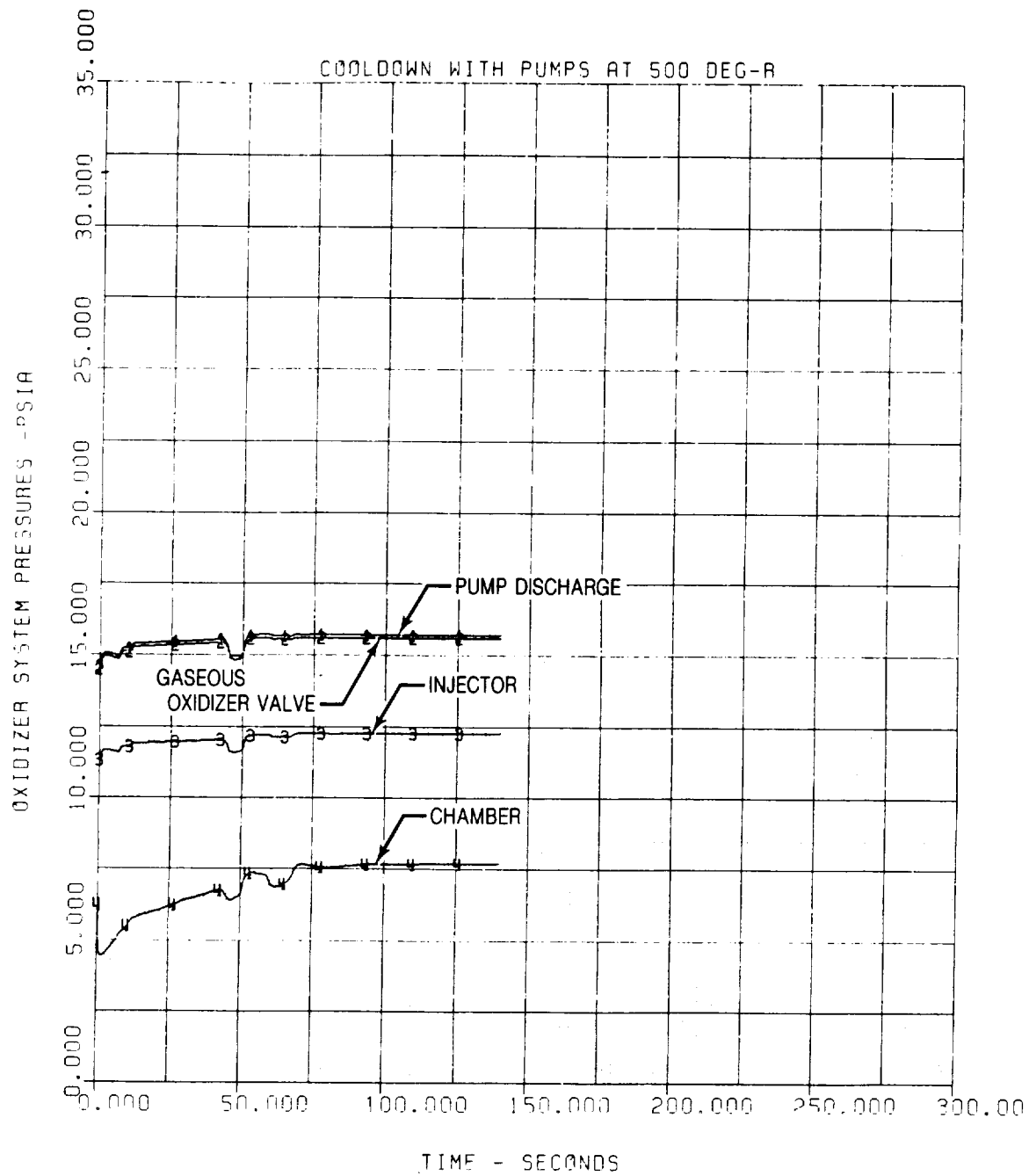


Figure 2-28. Oxidizer System Pressures During Tank Head Idle

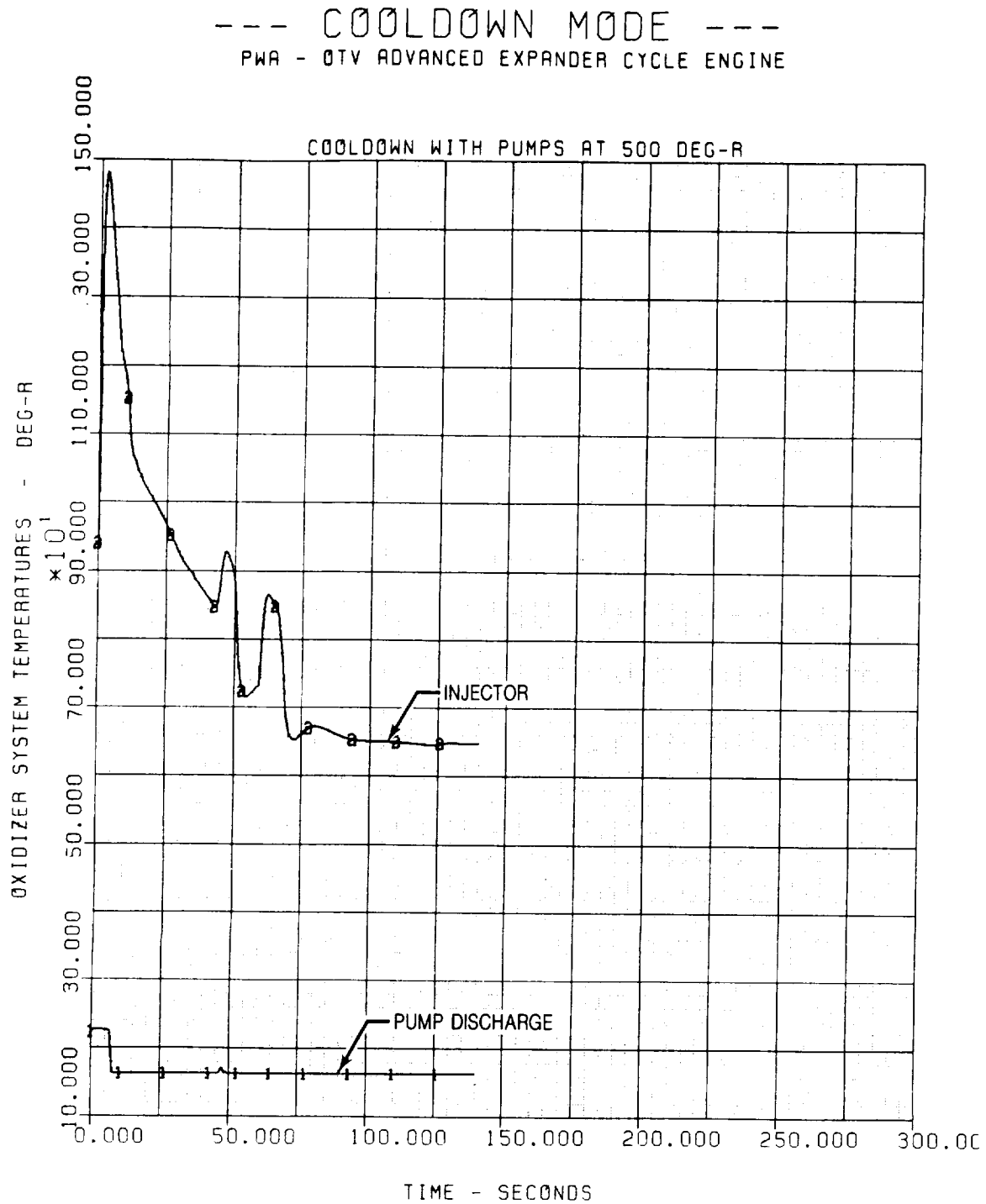


Figure 2-29. Oxidizer System Temperatures During Tank Head Idle

--- COOLDOWN MODE ---

PWA - OTV ADVANCED EXPANDER CYCLE ENGINE

COOLDOWN WITH PUMPS AT 500 DEG-R

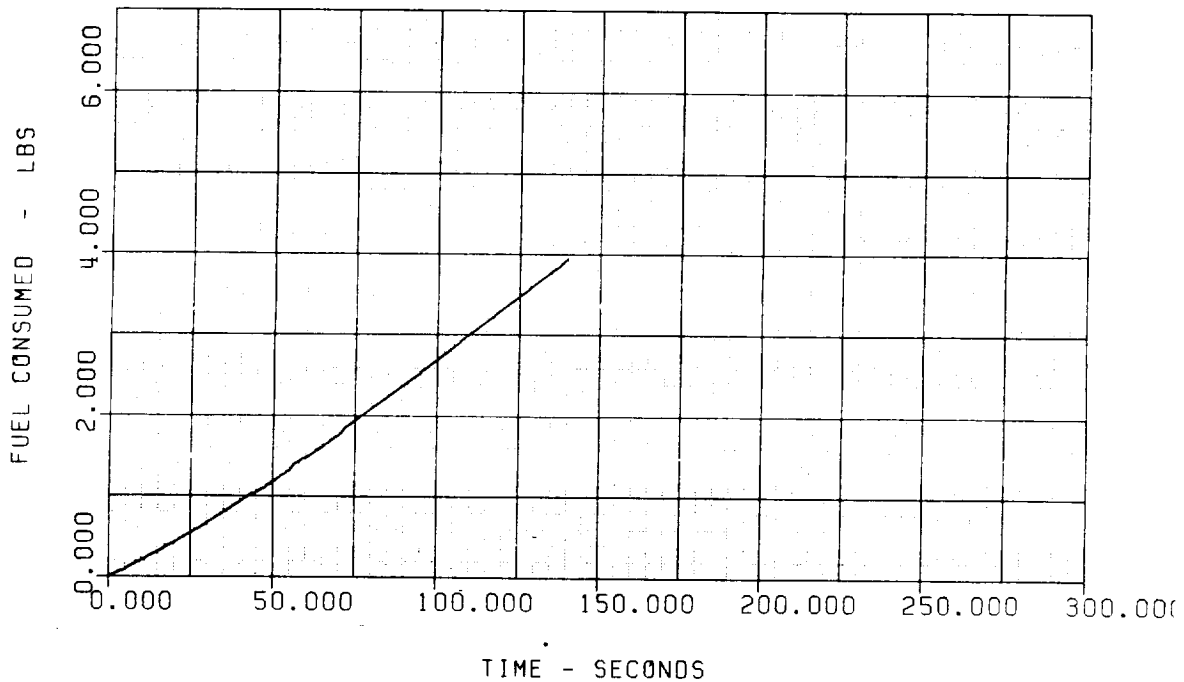
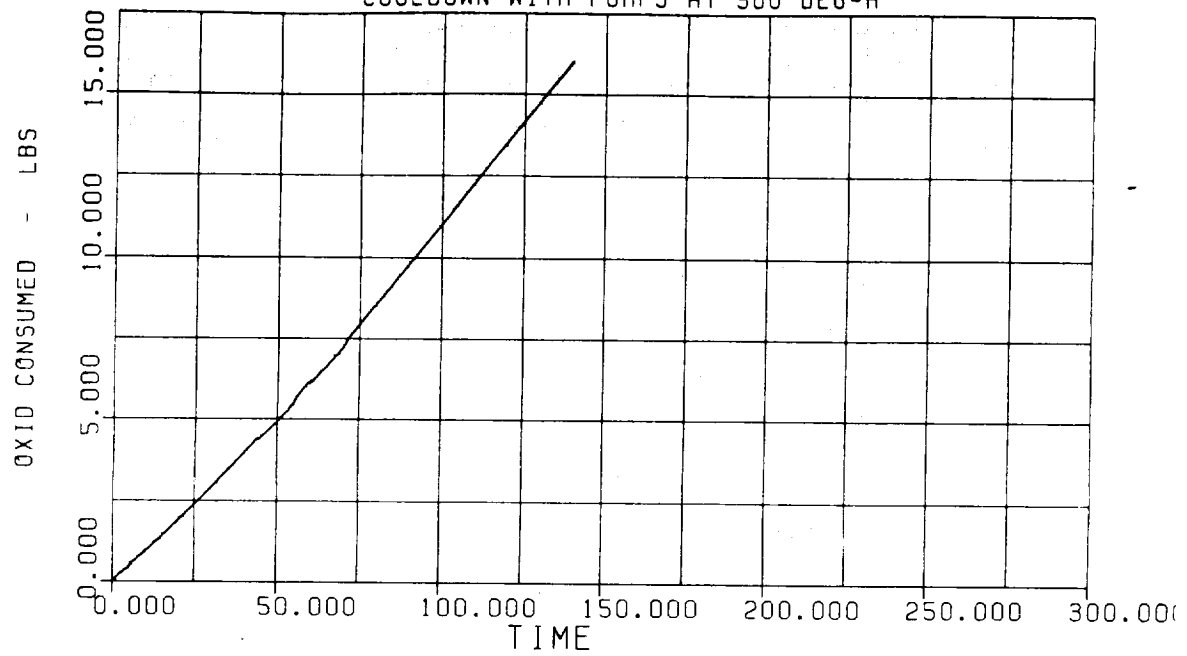
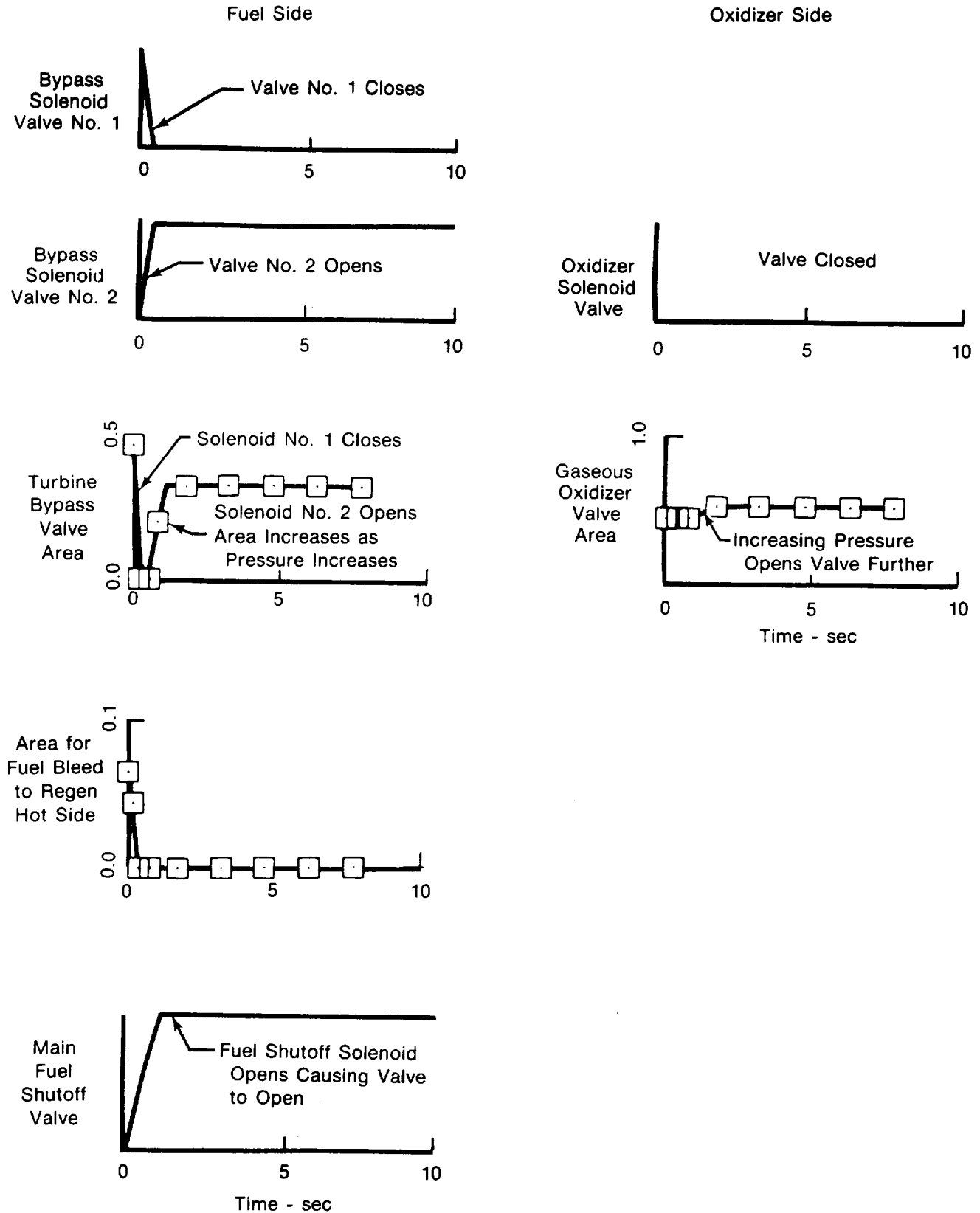


Figure 2-30. Propellant Consumption During Tank Head Idle



FD 213089

Figure 2-31A. Valve Actuation for Transition from Tank Head Idle to Pumped Idle

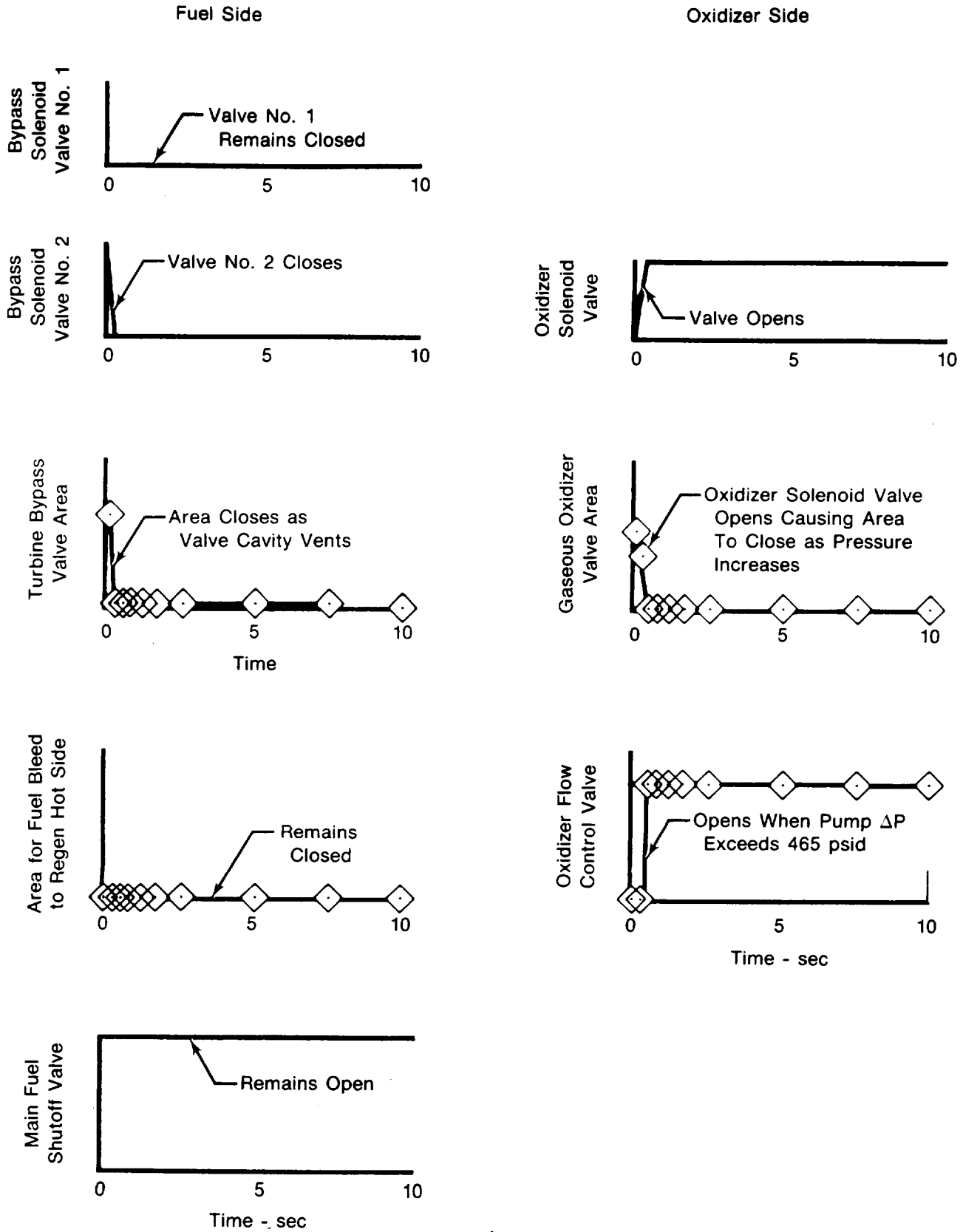
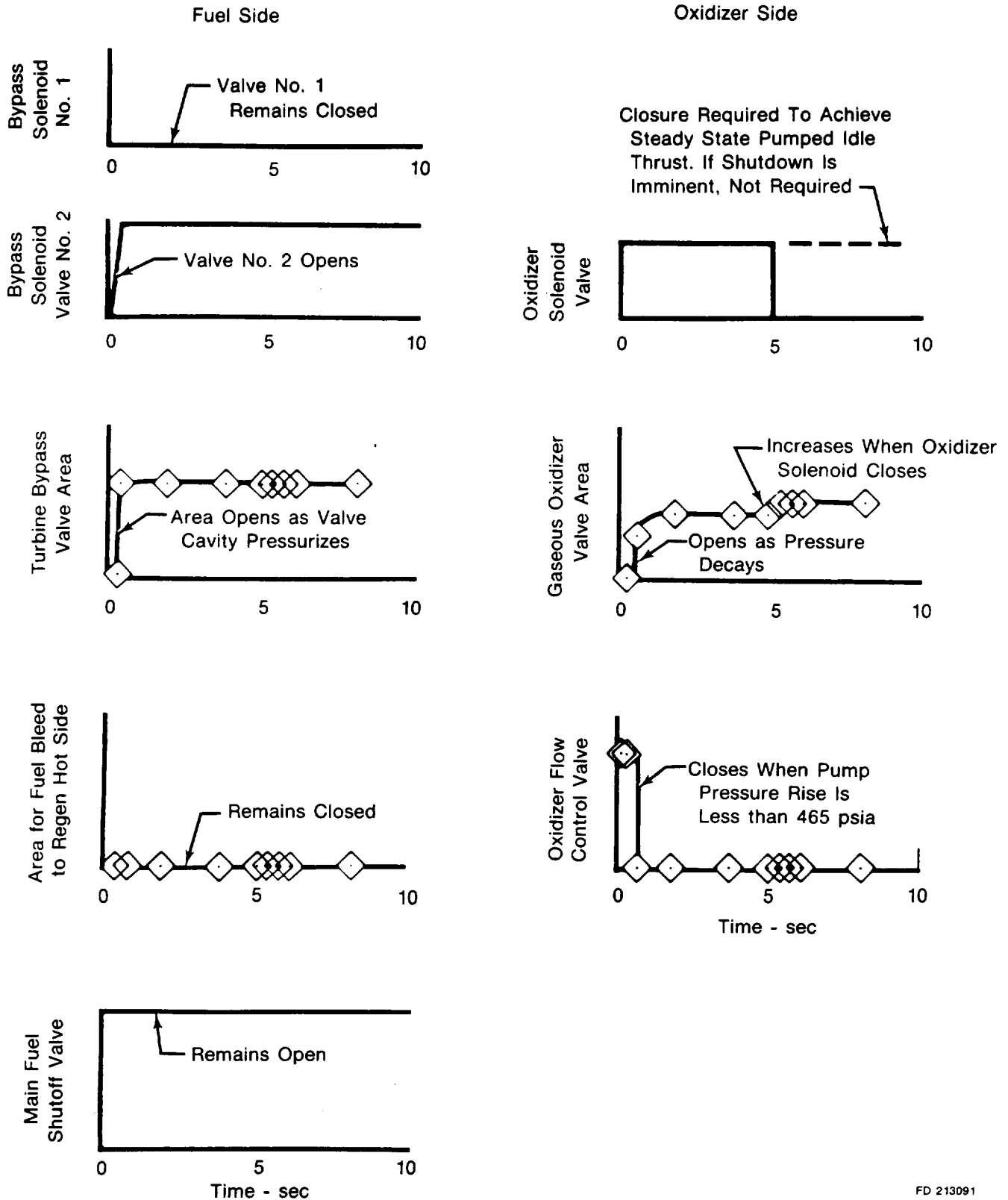


Figure 2-31B. Valve Actuation for Transition from Pumped Idle to Full Thrust



FD 213091

Figure 2-31C. Valve Actuation for Transition from Full Thrust to Pumped Idle

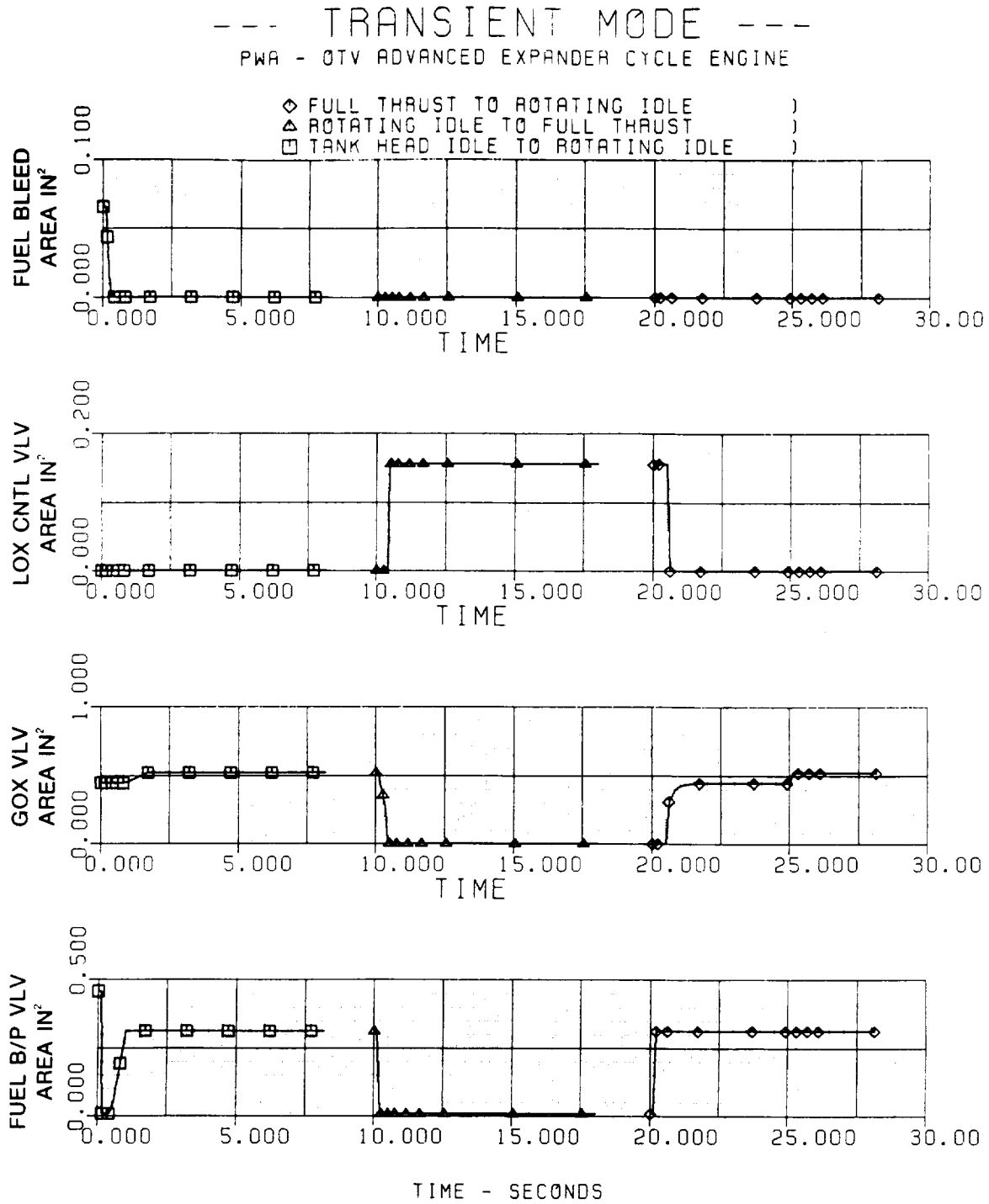


Figure 2-32. Valve Sequence During Transients

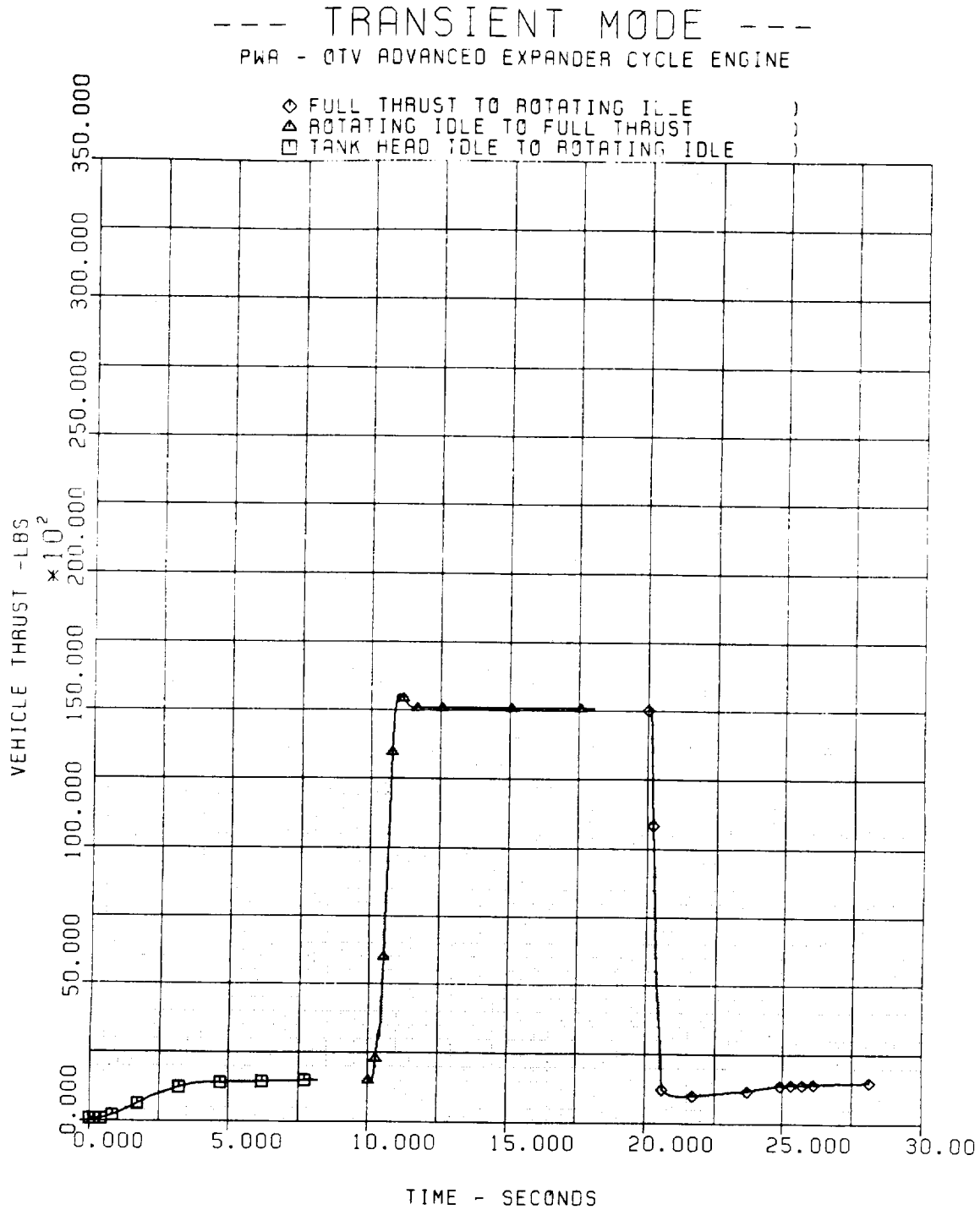


Figure 2-33. Thrust Characteristics During Transients

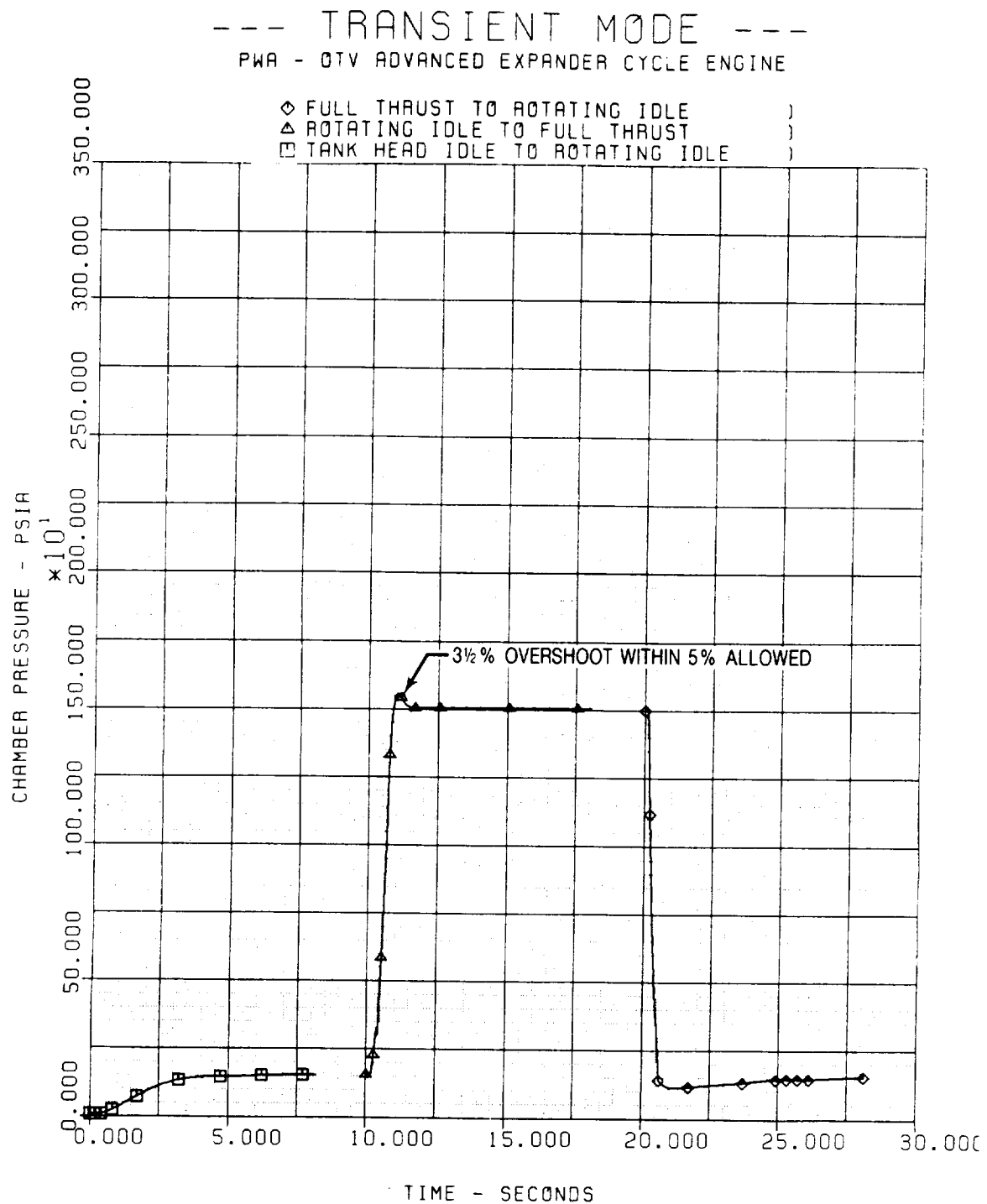


Figure 2-34. Chamber Pressure Characteristics During Transients

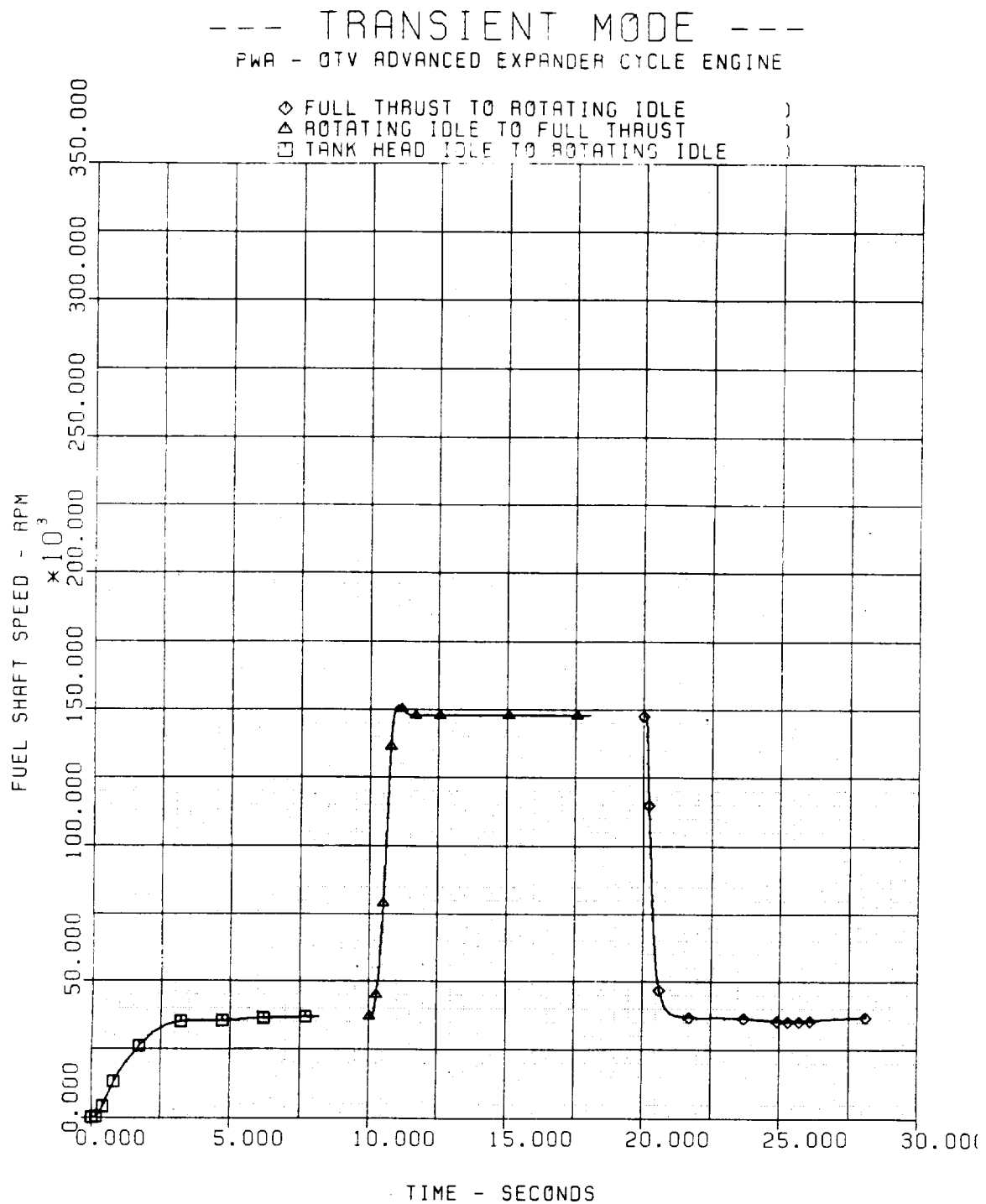


Figure 2-35. Main Fuel Pump Speed Characteristics During Transients

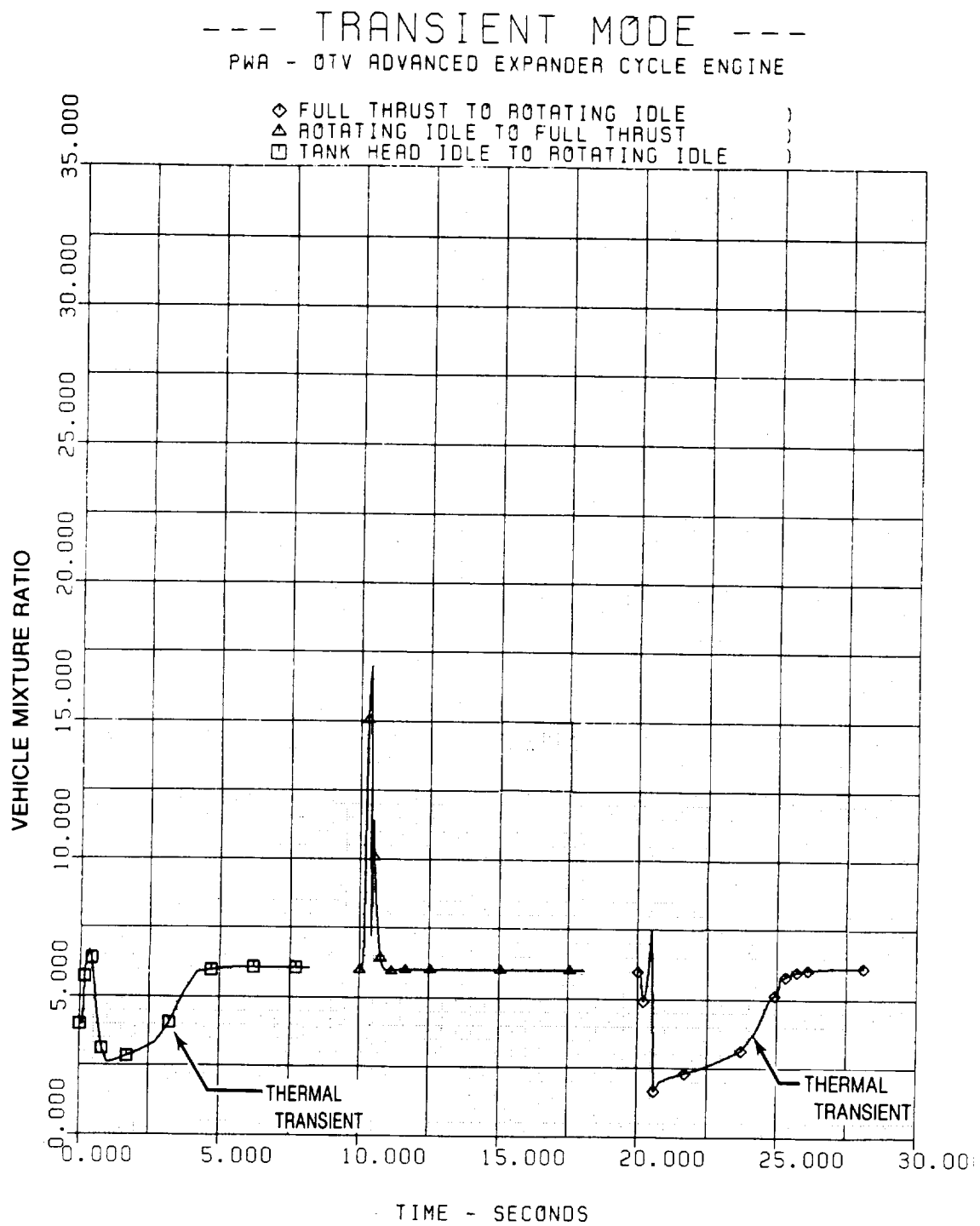


Figure 2-36. Mixture Ratio Characteristics During Transients

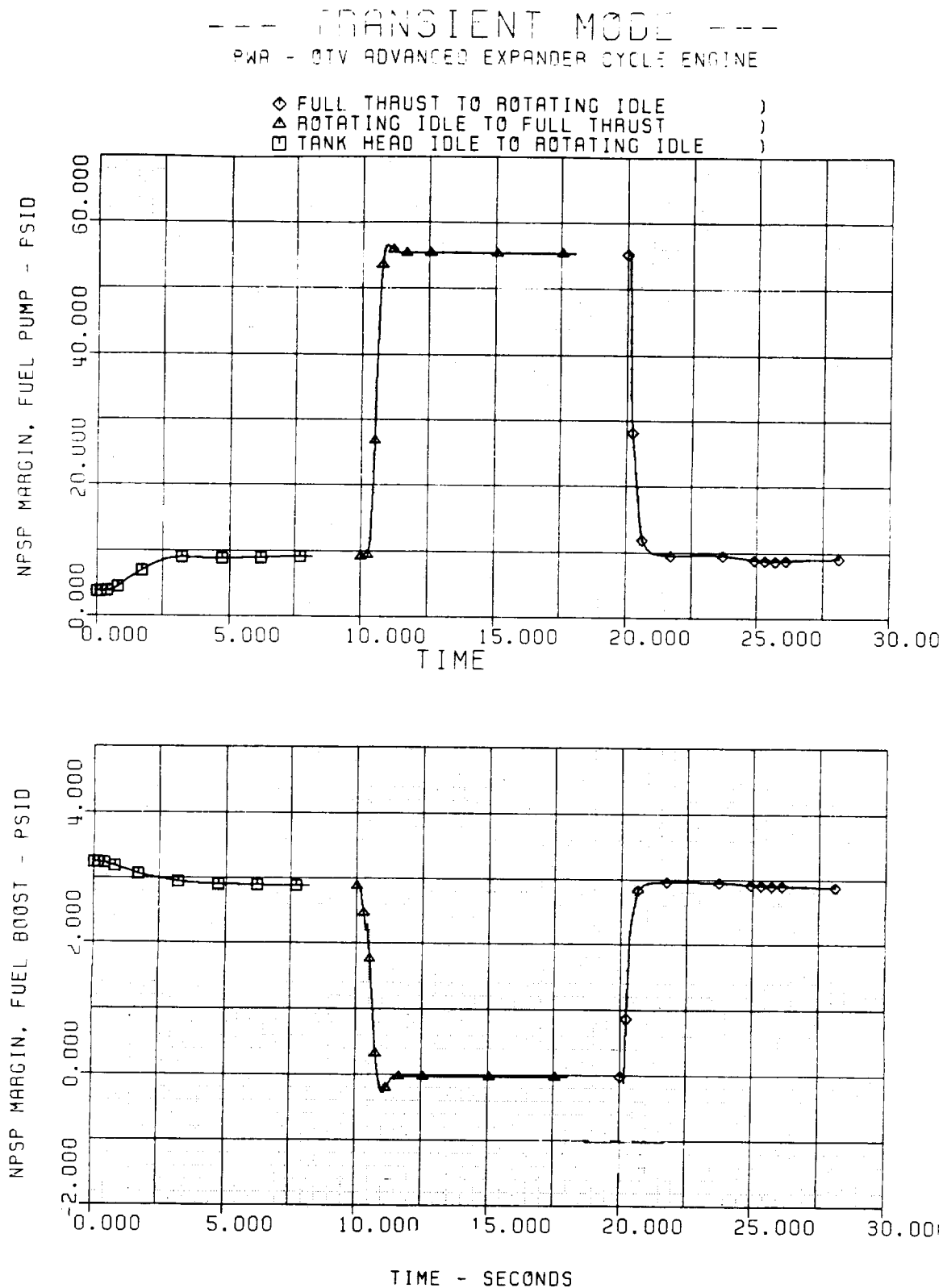


Figure 2-37. Fuel Pump Suction Characteristics During Transients

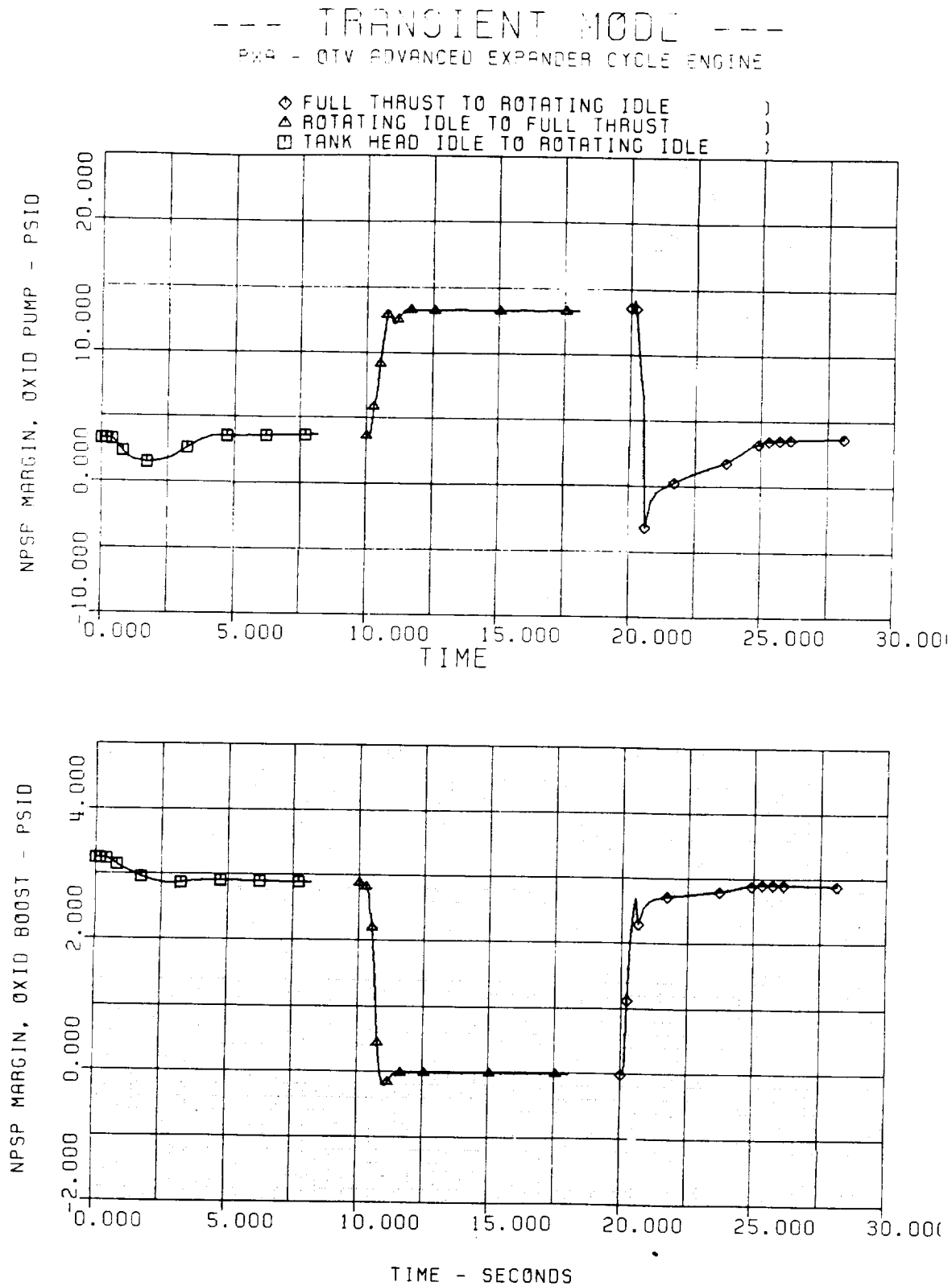


Figure 2-38. Oxidizer Pump Suction Characteristics During Transients

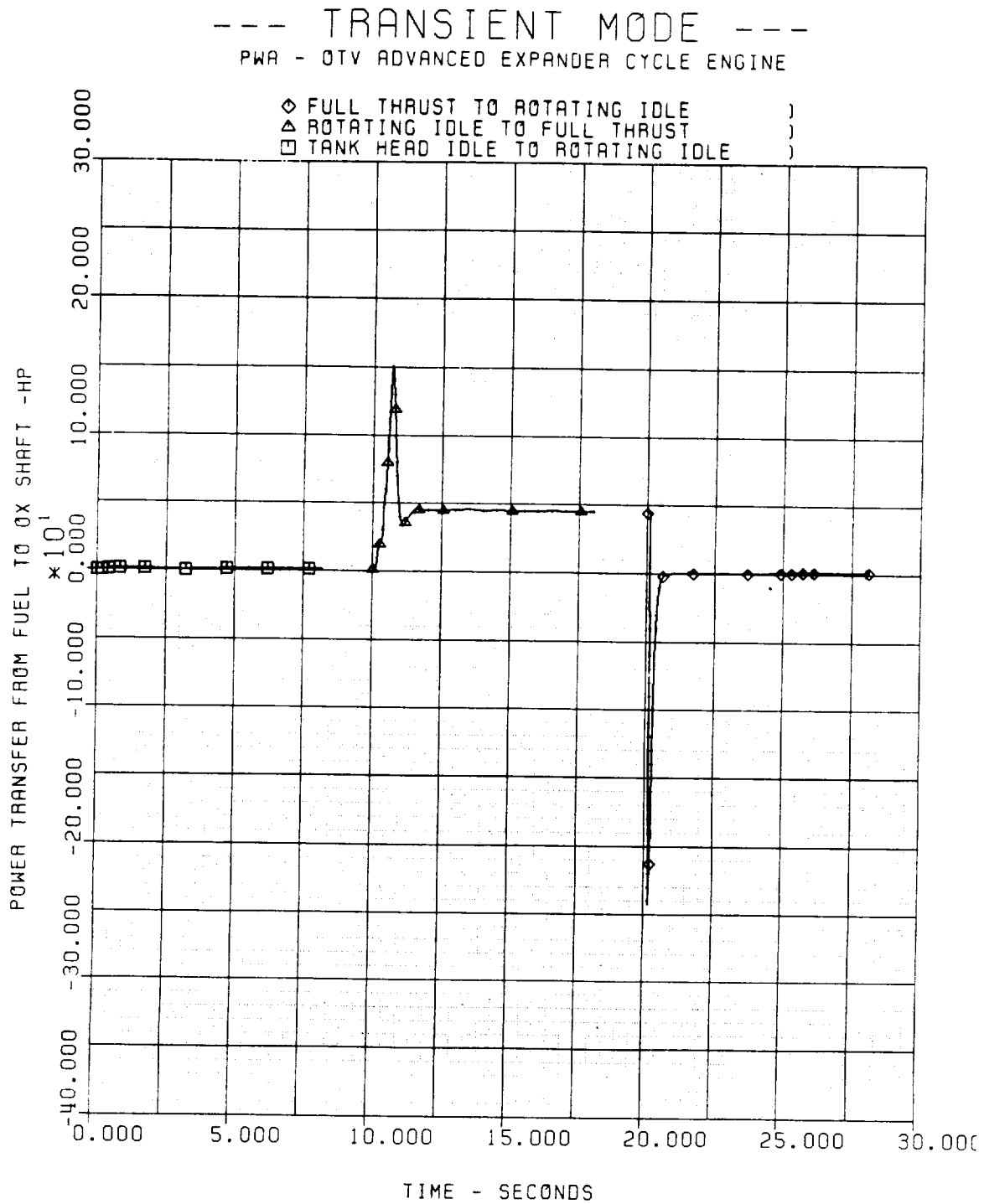


Figure 2-39. Power Transfer from Fuel Shaft to Oxidizer Shaft Via Idler Gear

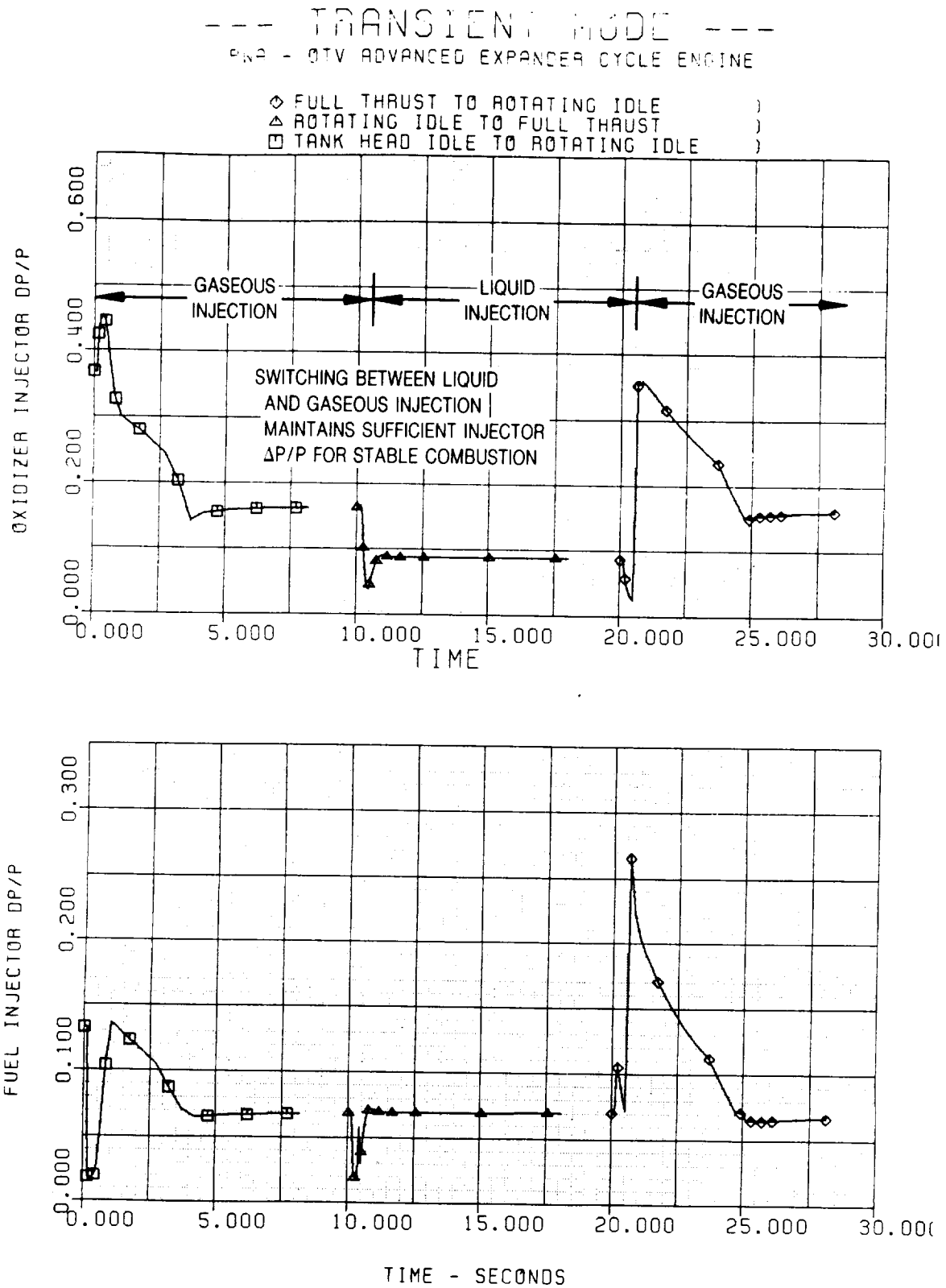


Figure 2-40. Injector Pressure Differentials Sufficient for Stable Combustion

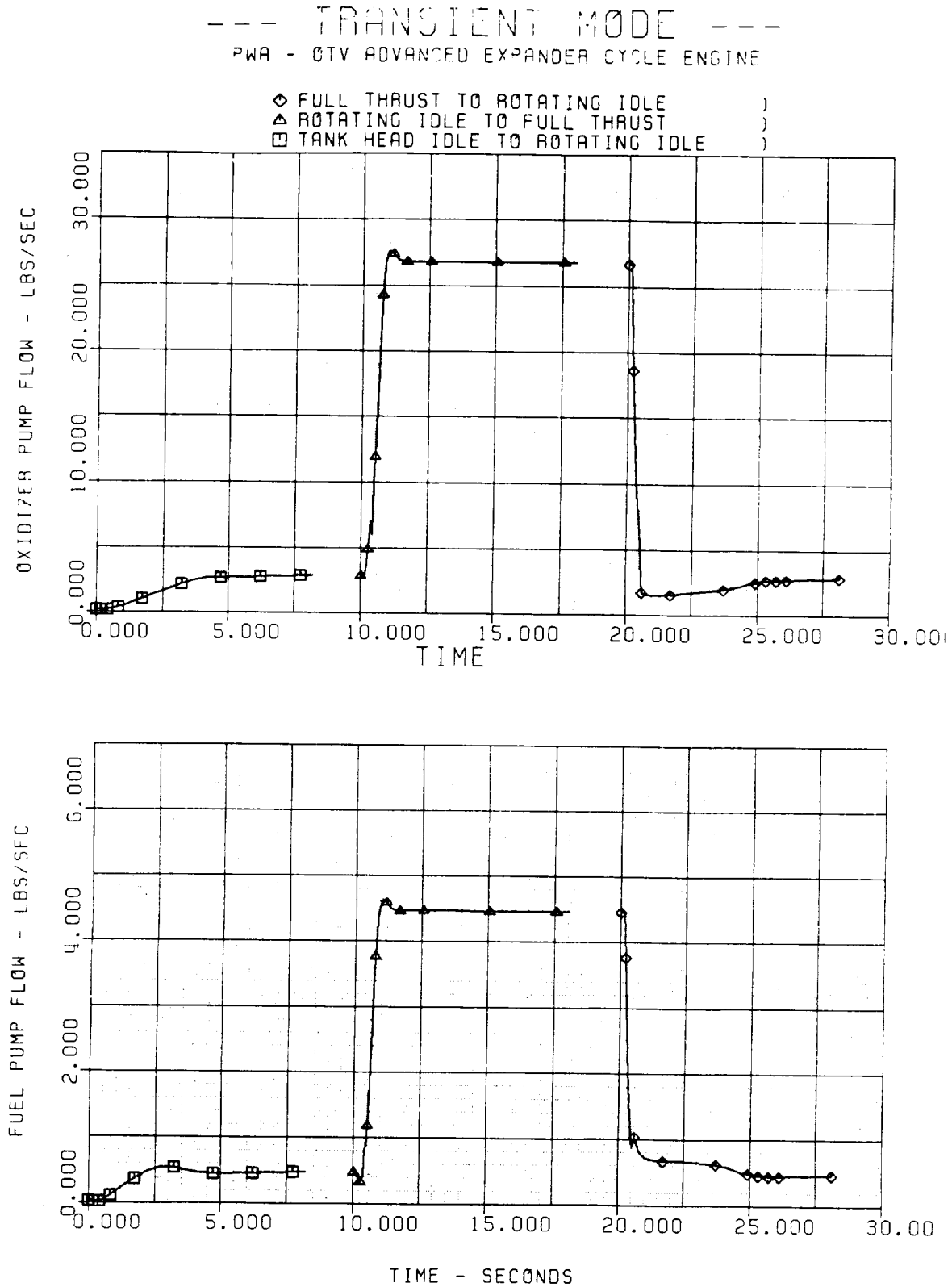


Figure 2-41. Pump Flows During Transients

--- TRANSIENT MODE ---
PWA - QTV ADVANCED EXPANDER CYCLE ENGINE

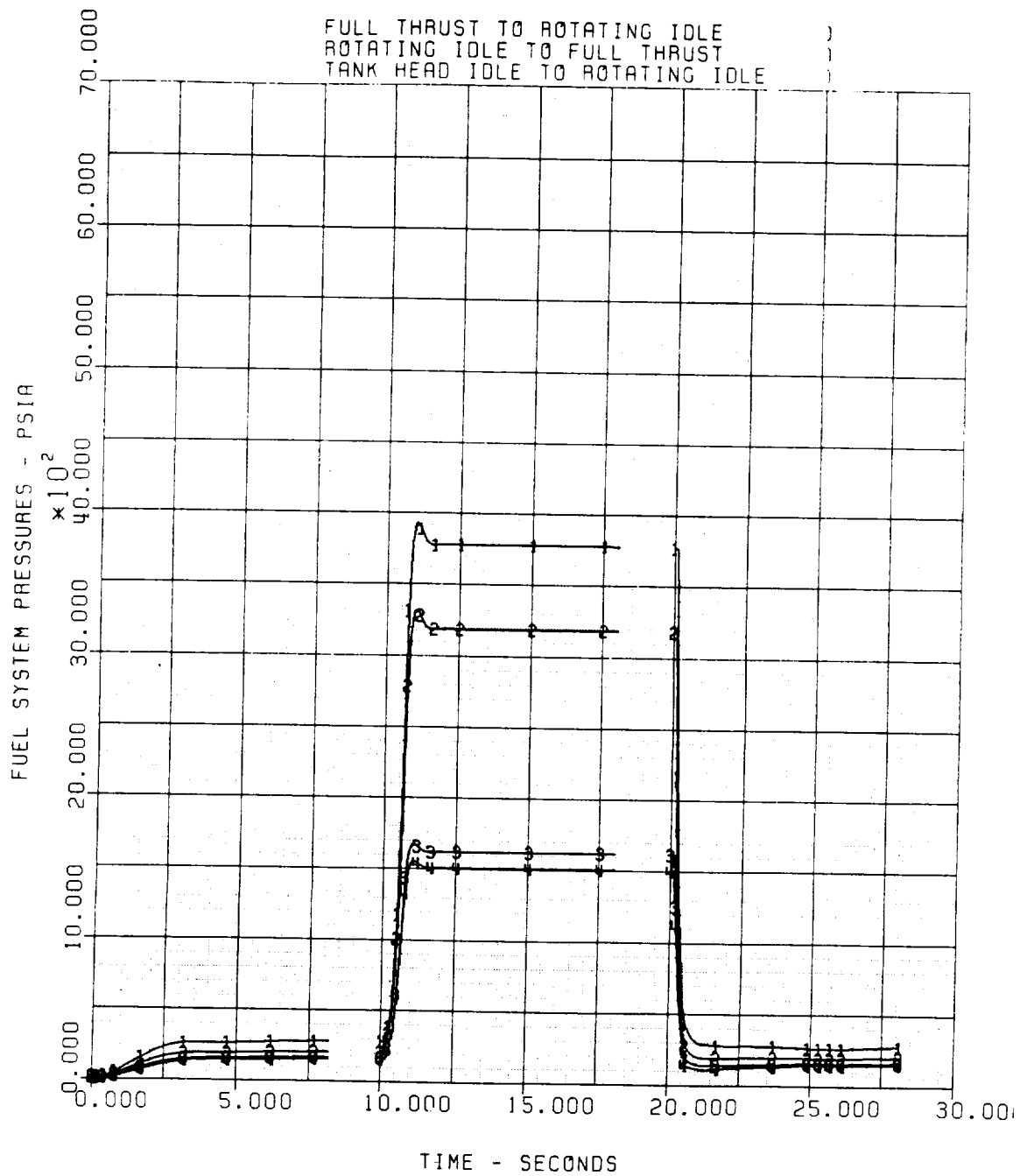


Figure 2-42. Fuel System Pressures During Transients

--- TRANSIENT MODE ---

PWA - QTV ADVANCED EXPANDER CYCLE ENGINE

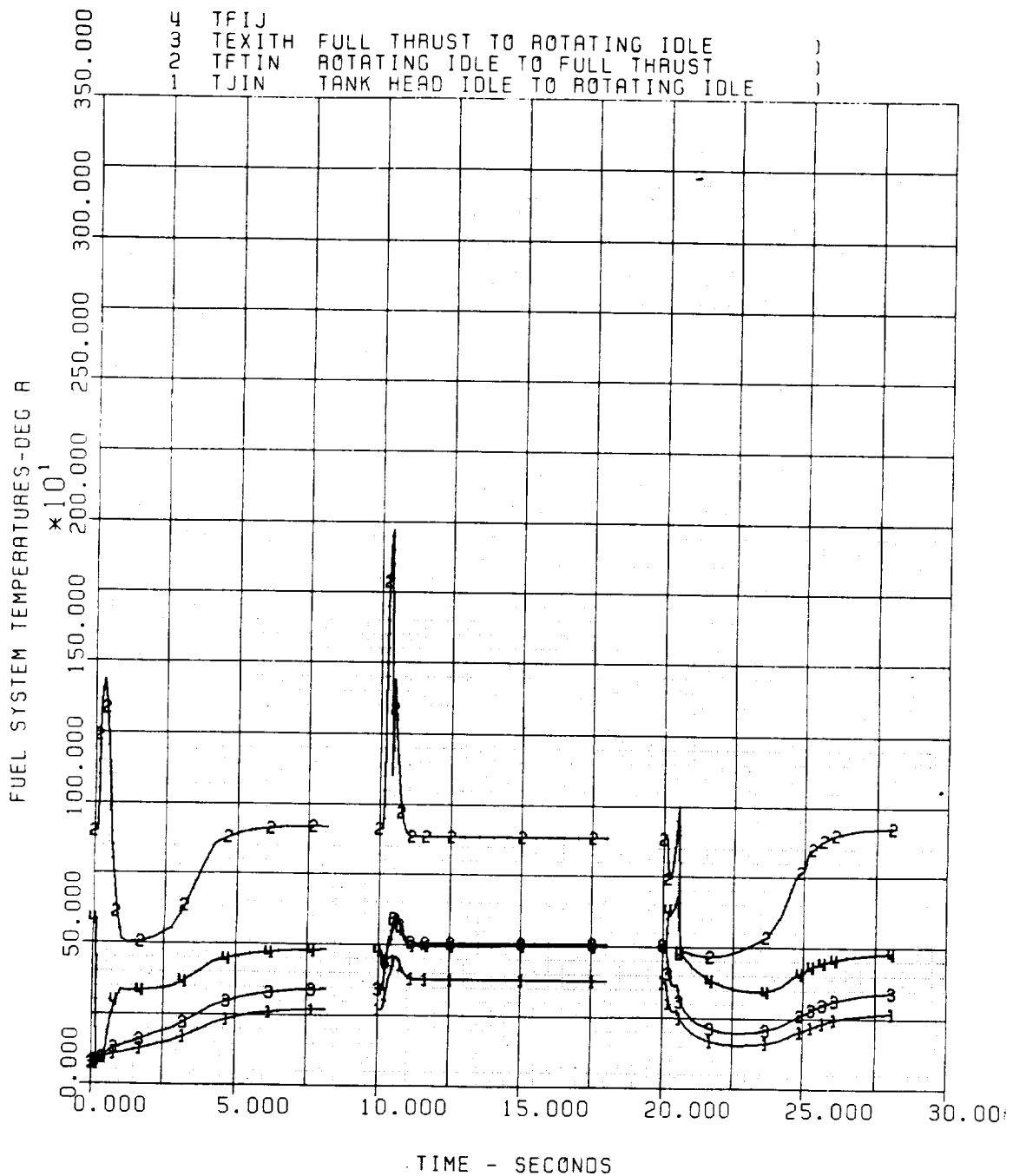


Figure 2-43. Fuel System Temperatures During Transients

--- TRANSIENT MODE ---

PWA - QTV ADVANCED EXPANDER CYCLE ENGINE

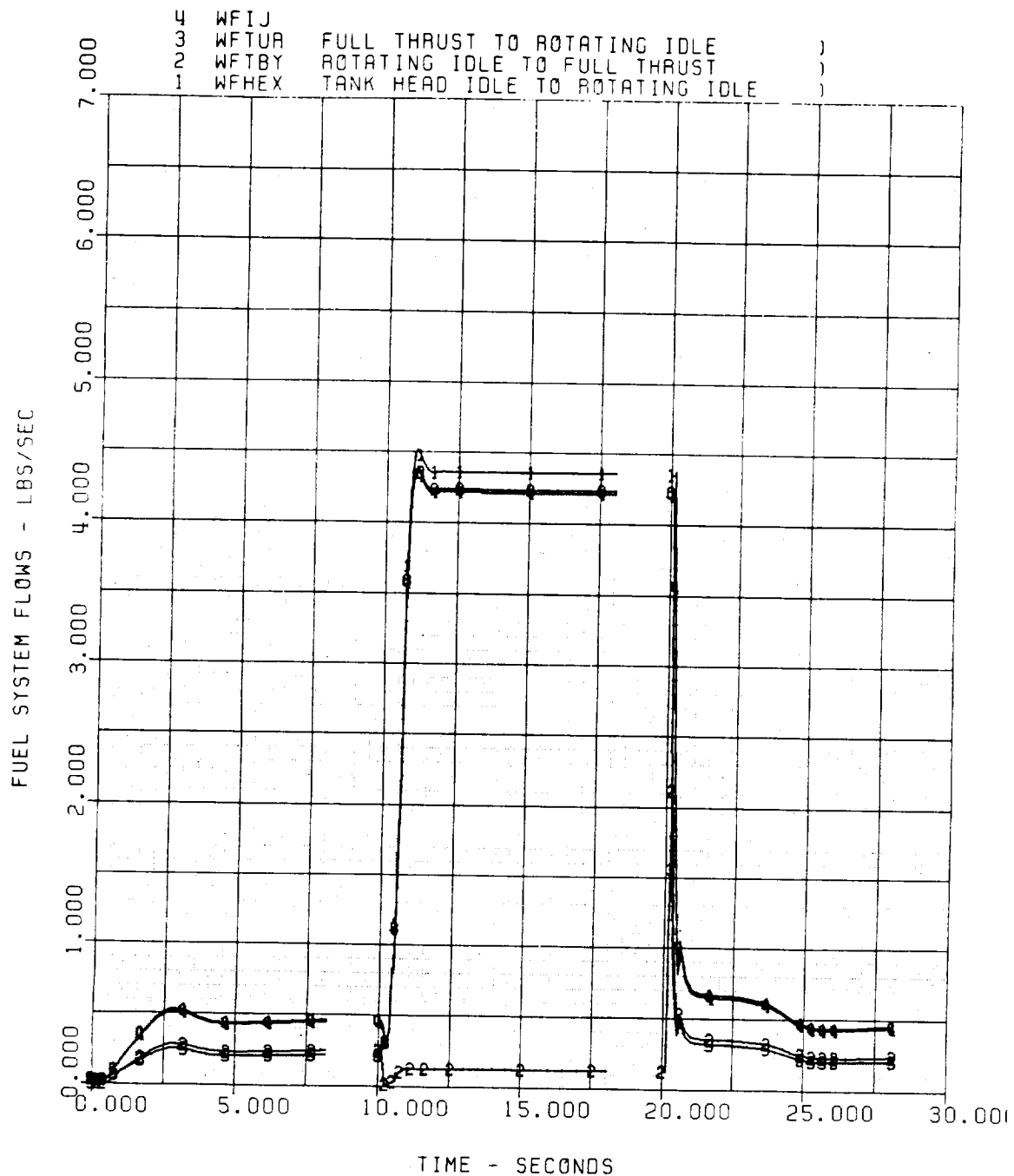


Figure 2-44. Fuel System Flows During Transients

--- TRANSIENT MODE ---

PWA - OTV ADVANCED EXPANDER CYCLE ENGINE

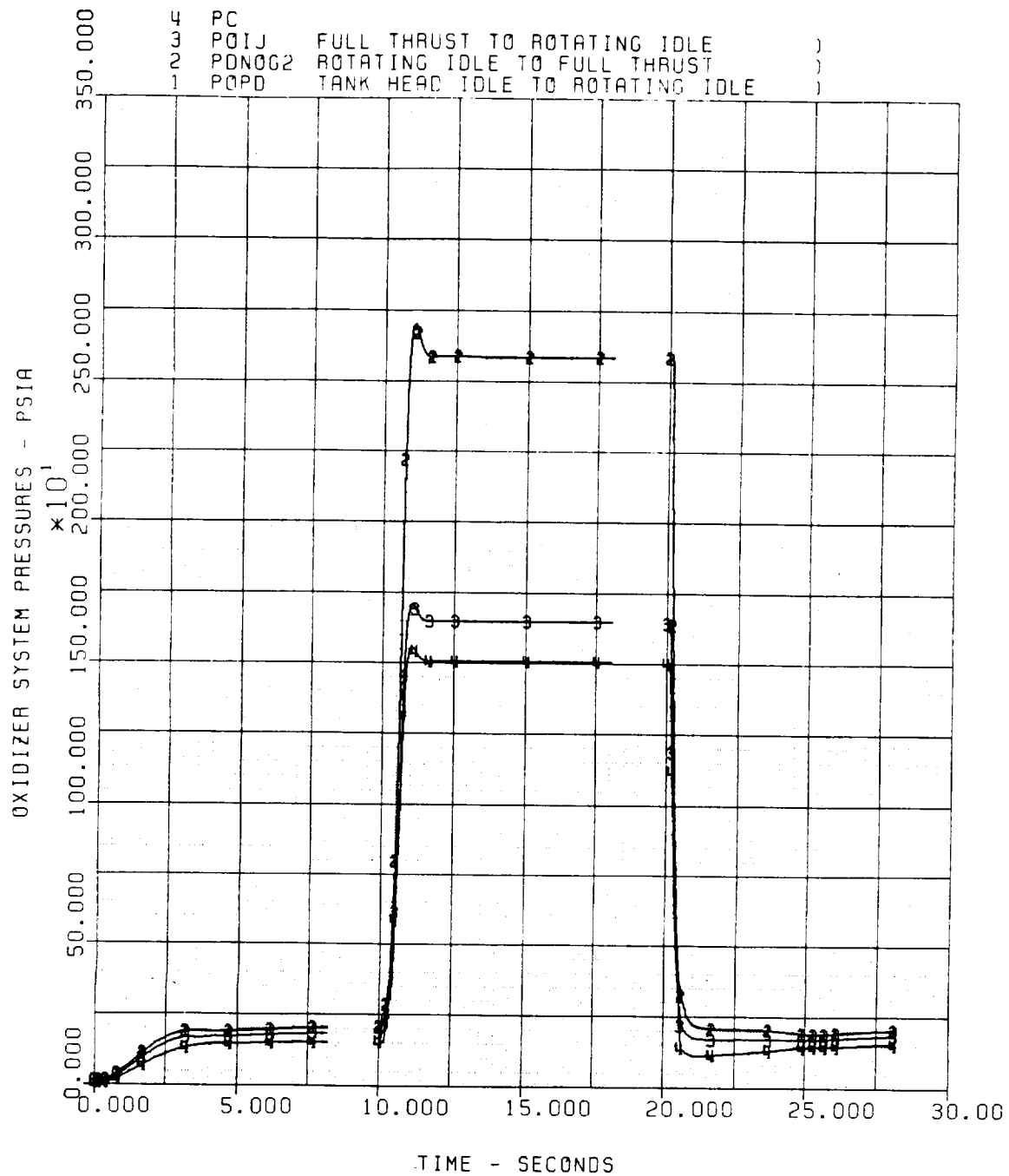


Figure 2-45. Oxidizer System Pressures During Transients

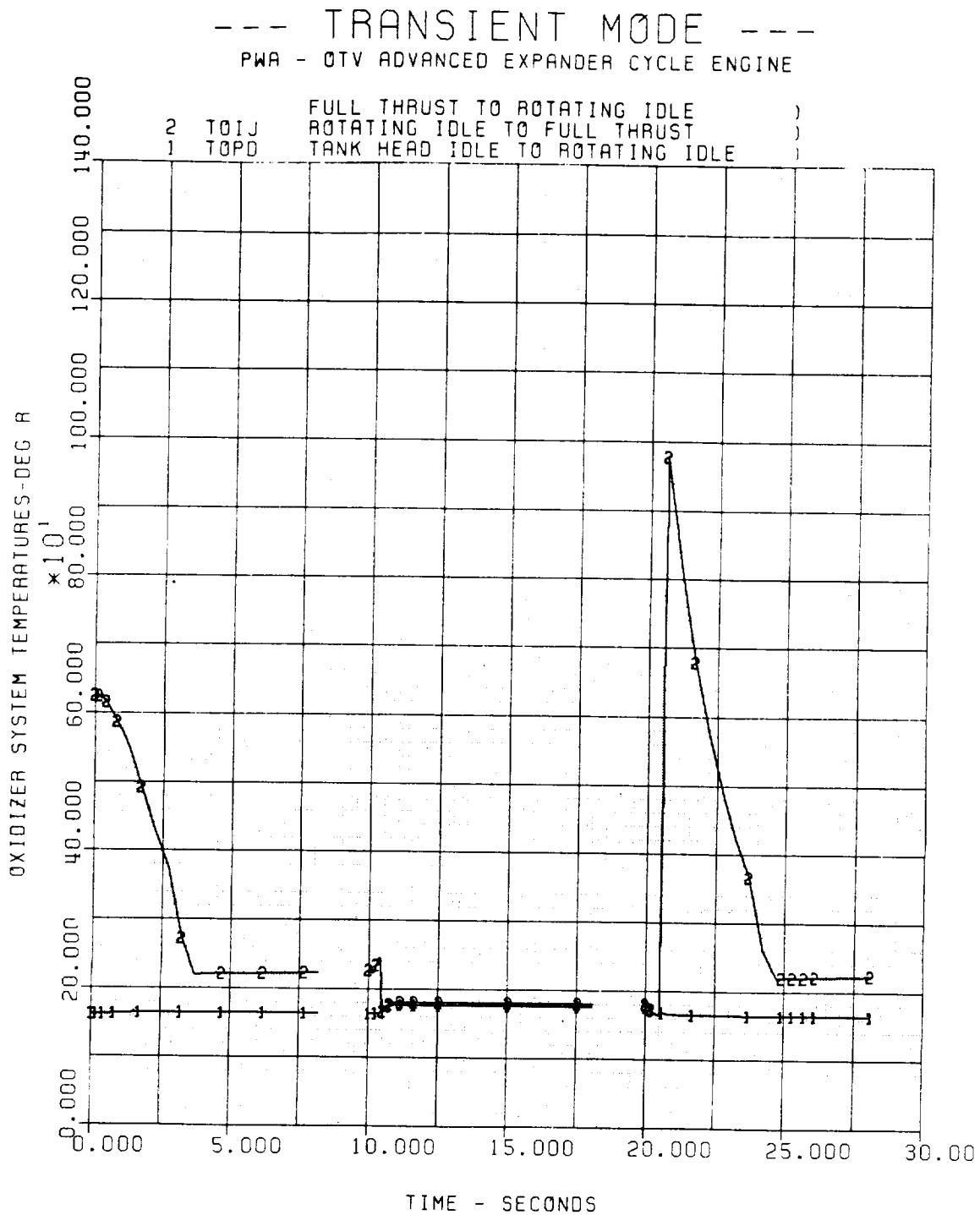


Figure 2-46. Oxidizer System Temperatures During Transients

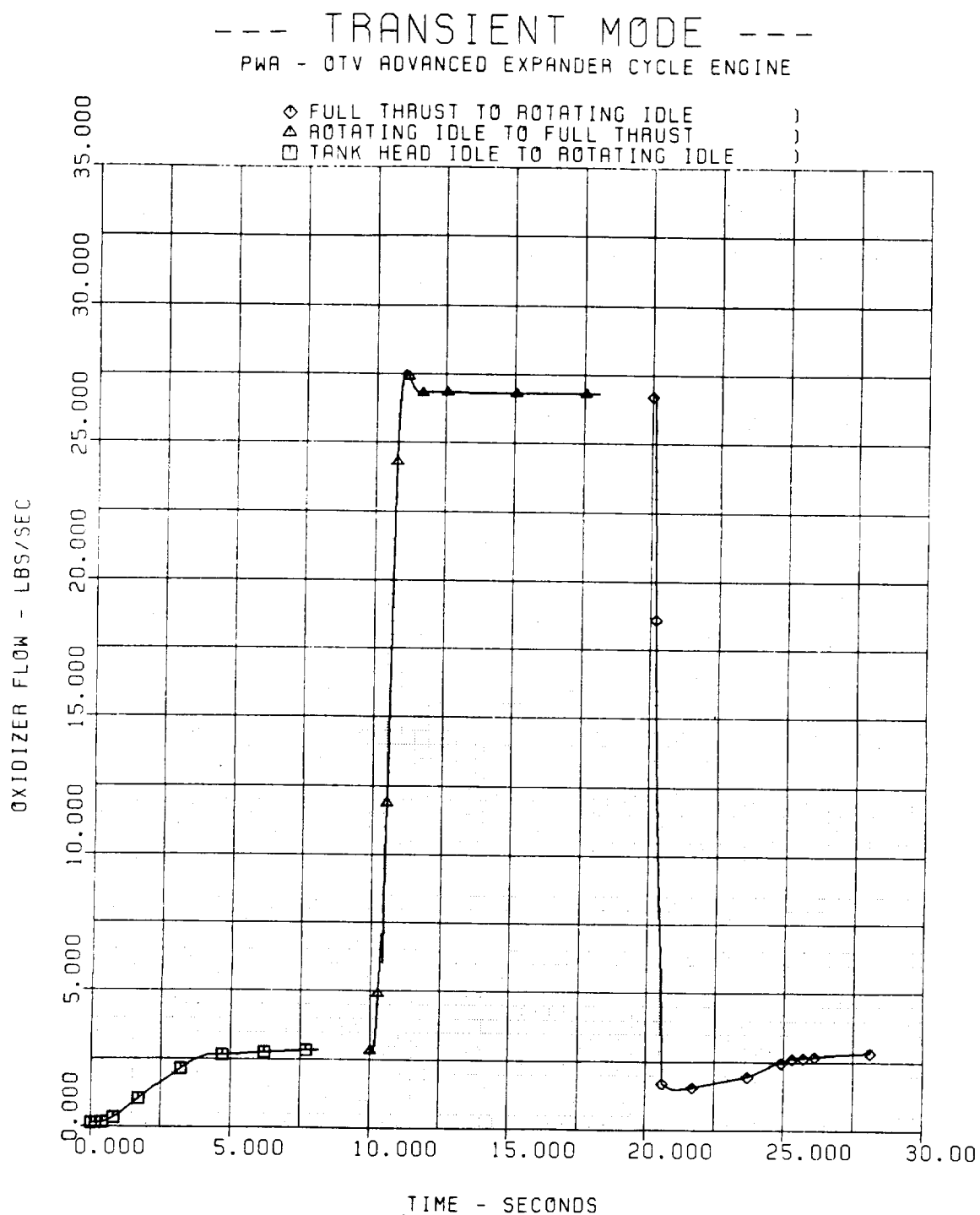


Figure 2-47. Oxidizer Flow During Transients

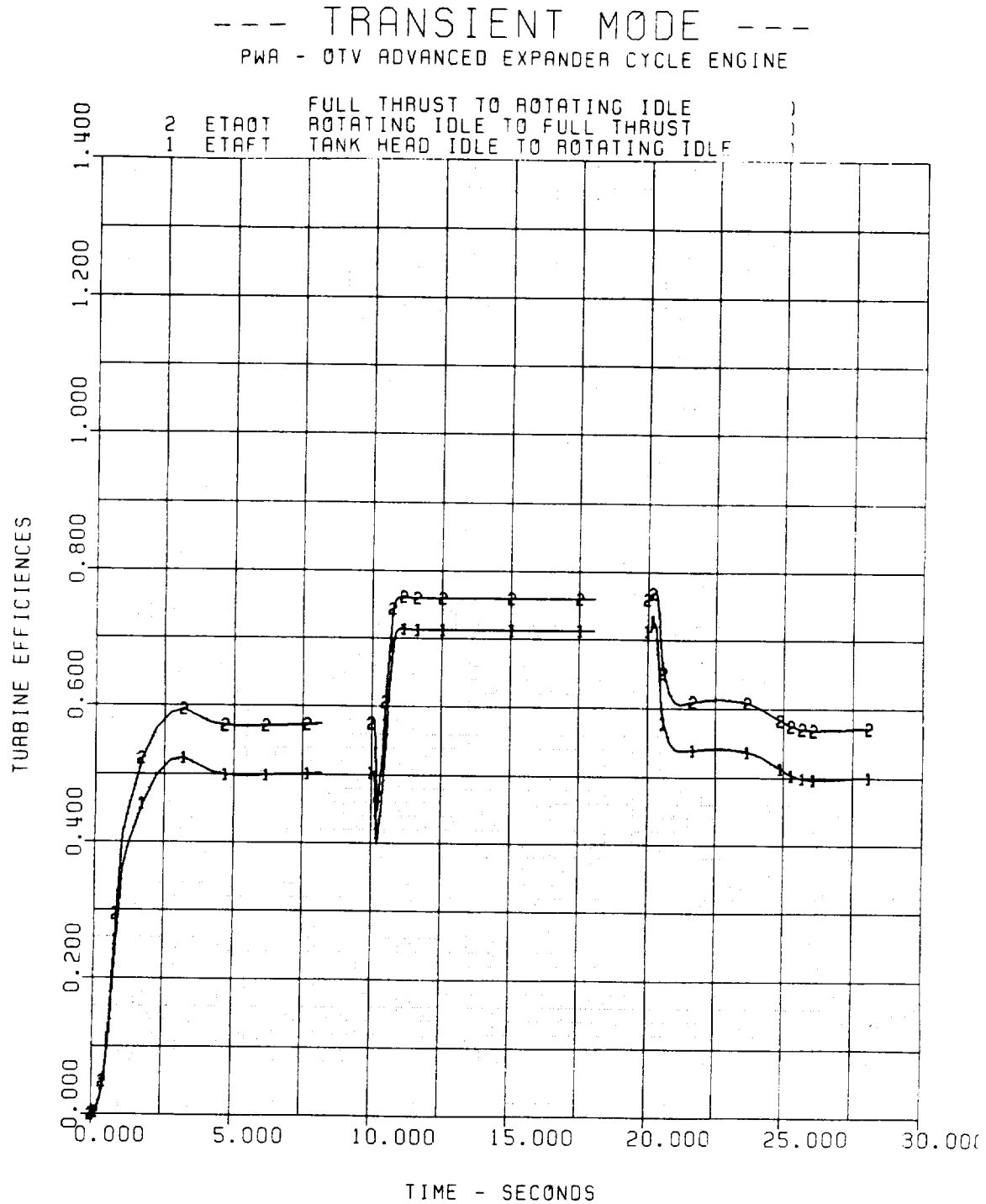


Figure 2-48. Turbine Efficiencies During Transients

--- TRANSIENT MODE ---

PWA - QTV ADVANCED EXPANDER CYCLE ENGINE

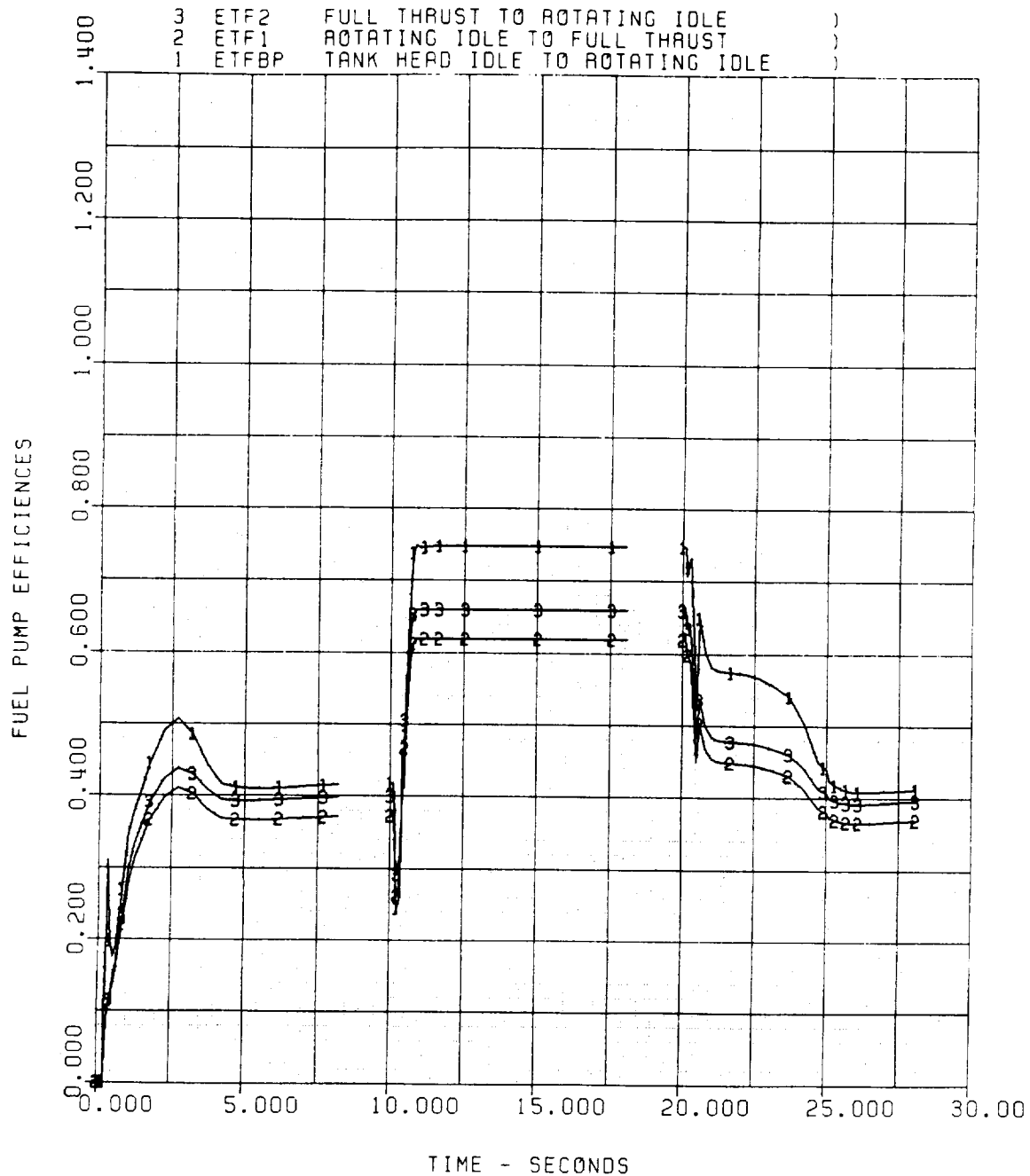


Figure 2-49. Fuel Pump Efficiencies During Transients

--- TRANSIENT MODE ---

PWA - OTV ADVANCED EXPANDER CYCLE ENGINE

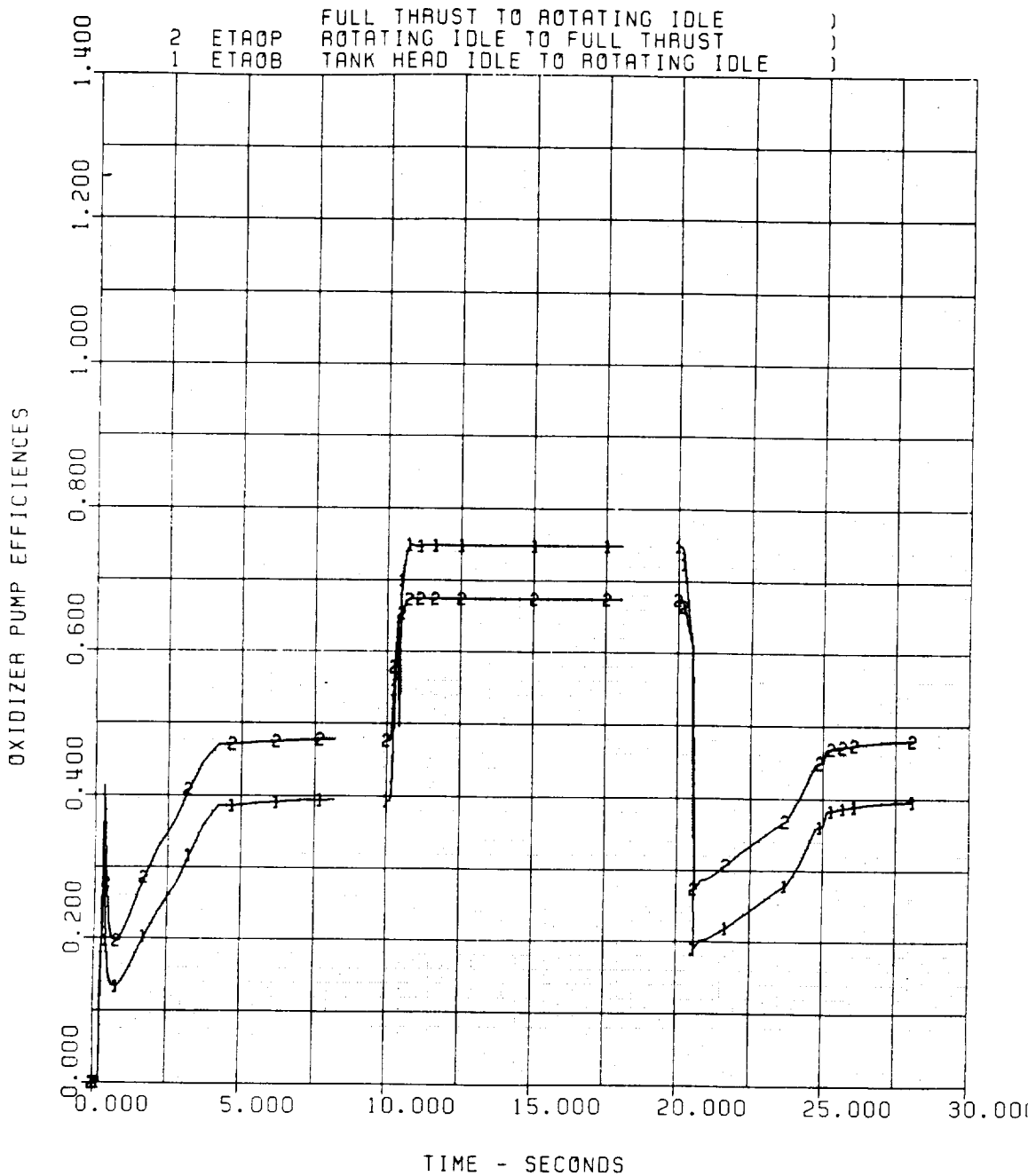


Figure 2-50. Oxidizer Pump Efficiencies During Transients

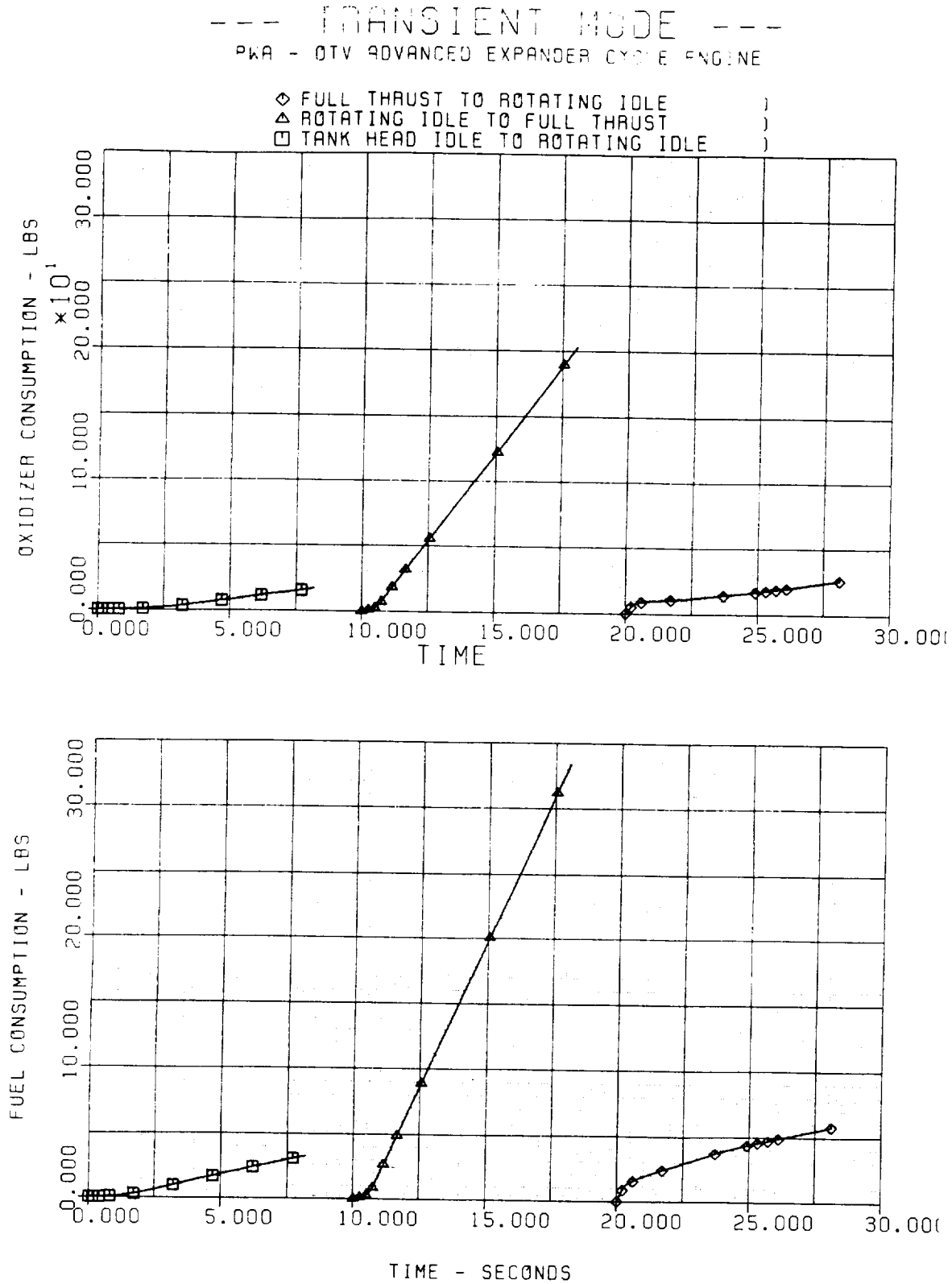


Figure 2-51. Propellant Consumption During Transients

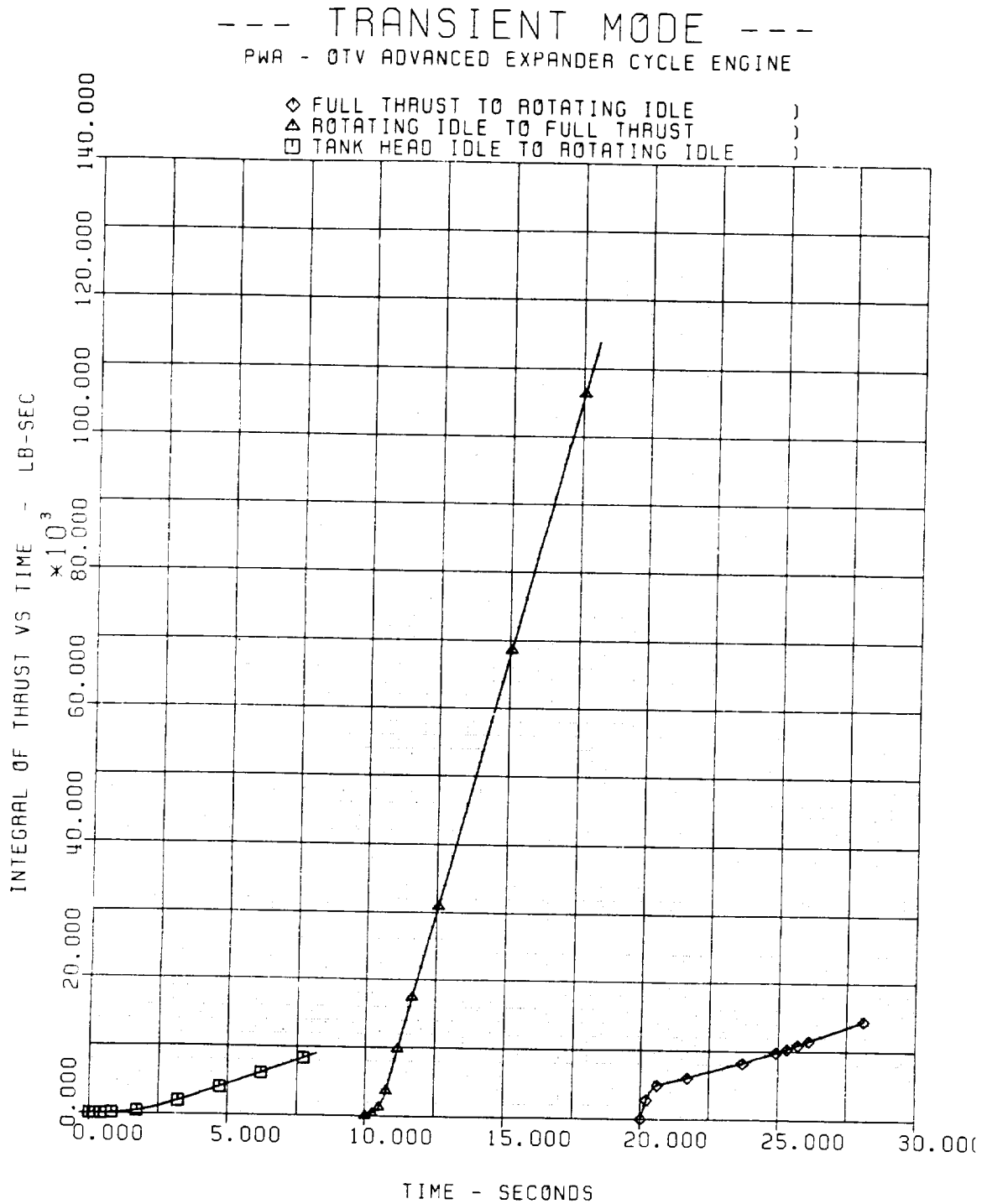


Figure 2-52. Transient Impulse (Integral of Thrust vs Time)

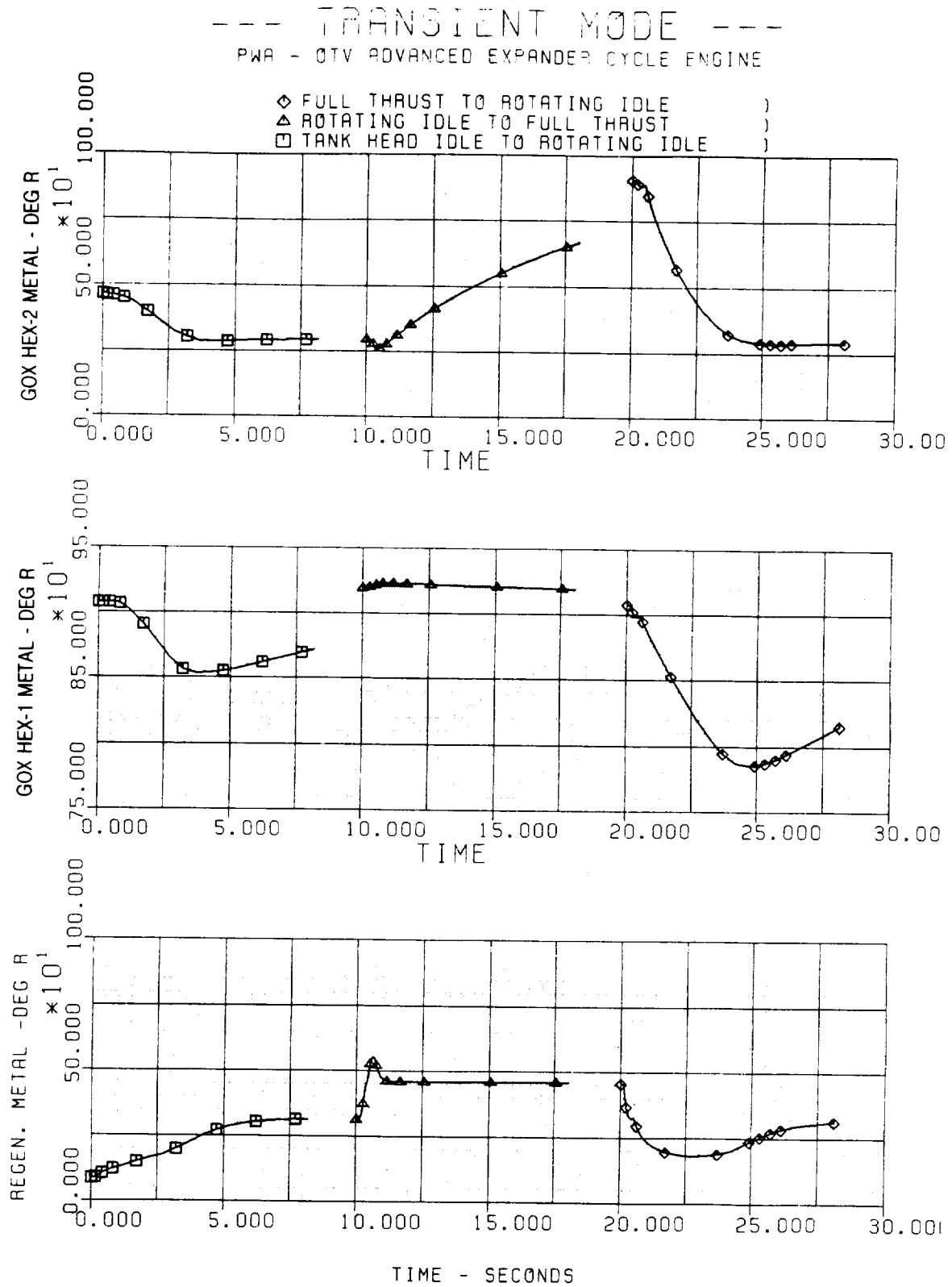


Figure 2-53. Heat Exchanger Transient Metal Temperatures

2.2.2.5 Full Thrust to Pumped Idle

For accurate shutdown impulse it was assumed that the engine would return to pumped idle prior to full engine shutdown.

The transition from full thrust to pumped idle is achieved by opening the bypass solenoid valve No. 2. The bypass valve area opens as the valve cavity fills. Speed will decrease rapidly with the associated loss in turbine flow. The gaseous oxidizer valve will open when its upstream pressure drops below 600 psia followed by closure of the oxidizer flow control valve when the oxidizer pump pressure rise drops below 465 psid (Figure 2-31C). The opening and closing of the two oxidizer valves directs the liquid oxygen through the oxidizer heat exchanger which changes it to a gas before it reaches the injector. The switch from liquid to gas is done to maintain sufficient injector velocity during low flow conditions to maintain stable combustion. These transient characteristics are shown between 20 and 28 sec shown in Figures 2-32 through 2-53.

The oxidizer solenoid valve is closed 5 sec following the command to return to pumped idle. If shutdown is imminent the oxidizer solenoid valve may remain opening allowing the shutdown signal to close it. However, if a steady-state pumped idle is required, the oxidizer solenoid valve should be closed anytime after the gaseous oxidizer valve opens (about 2 sec after the command is given to return to pumped idle). Figure 2-54 shows the influence on vehicle mixture ratio of closing or leaving open the oxidizer solenoid valve.

2.2.2.6 Shutdown

As previously stated, it was assumed that the engine would be shut down from either pumped idle or tank head idle. Shutdown is initiated by removing voltage from all solenoid valves causing the other valves to move to their fail safe positions. Both inlet shut-off valves close to eliminate further propellant consumption. A vent in the main fuel control valve opens to relieve pressure downstream of the fuel pumps. The fuel bleed valve, the turbine bypass valve (which is an integral part of the main fuel control valve) and the main fuel shut-off valve all close to starve the combustion chamber of fuel. The oxidizer control valve closes during the deceleration from full thrust when the oxidizer pump pressure rise drops below 465 psid. The gaseous oxidizer valve will open when power is removed from the solenoid. Oxidizer flow to the combustion chamber will continue until it is completely expelled downstream of the inlet shut-off valve. The fuel to the combustion chamber is depleted long before the oxidizer, causing an oxidizer rich flame-out.

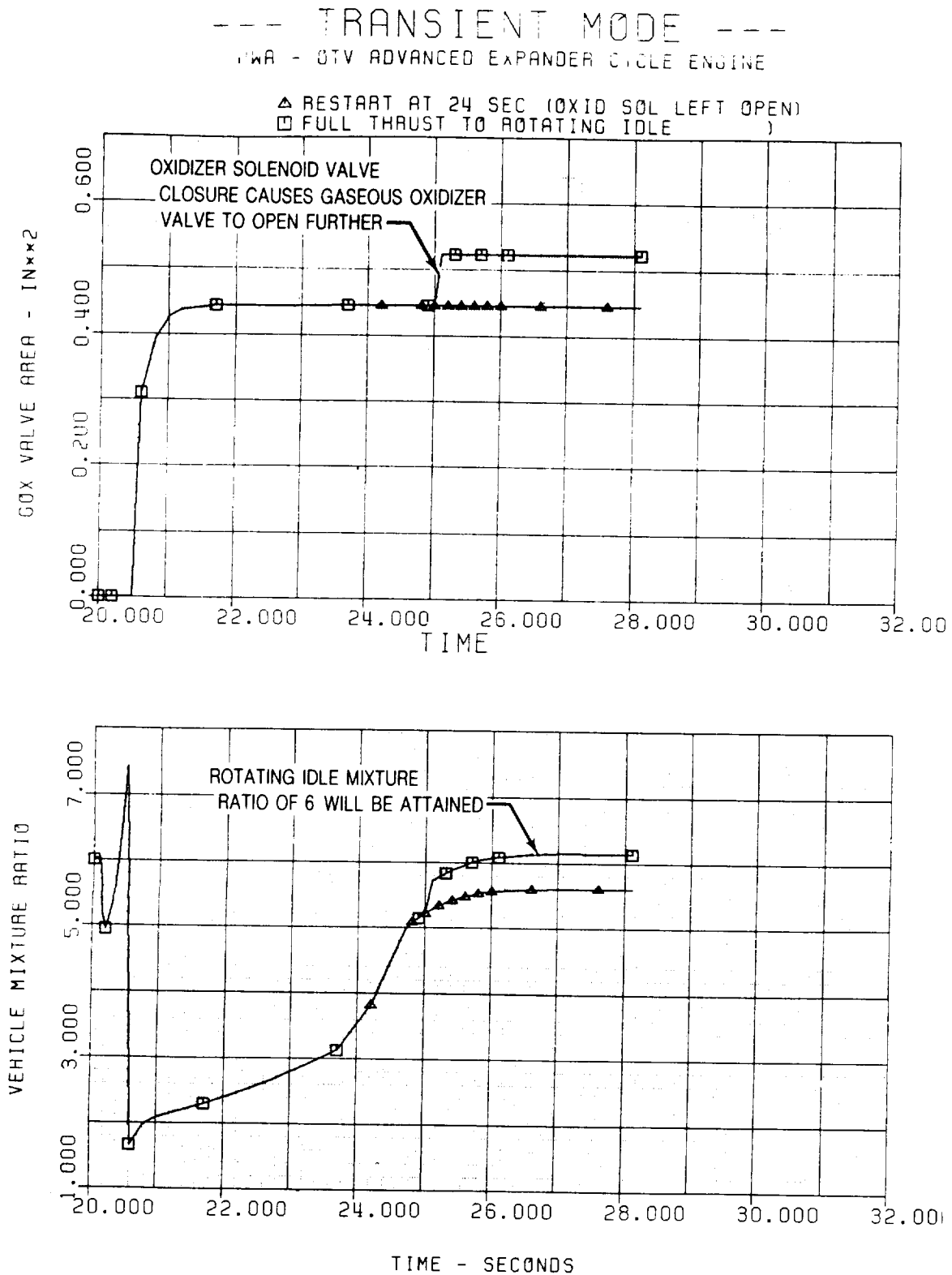


Figure 2-54. Influence of Closing the Oxidizer Solenoid Valve on Vehicle Mixture Ratio During Deceleration from Full Thrust to Pumped Idle

SECTION 3

MAJOR COMPONENT ANALYTICAL DESIGN

A detailed analytical design effort was conducted on the following major engine components: thrust chamber/nozzle assembly including the injector and ignitor, hydrogen regenerator GOX heat exchanger, and the fuel and oxidizer turbopumps. These components are discussed in the following paragraphs.

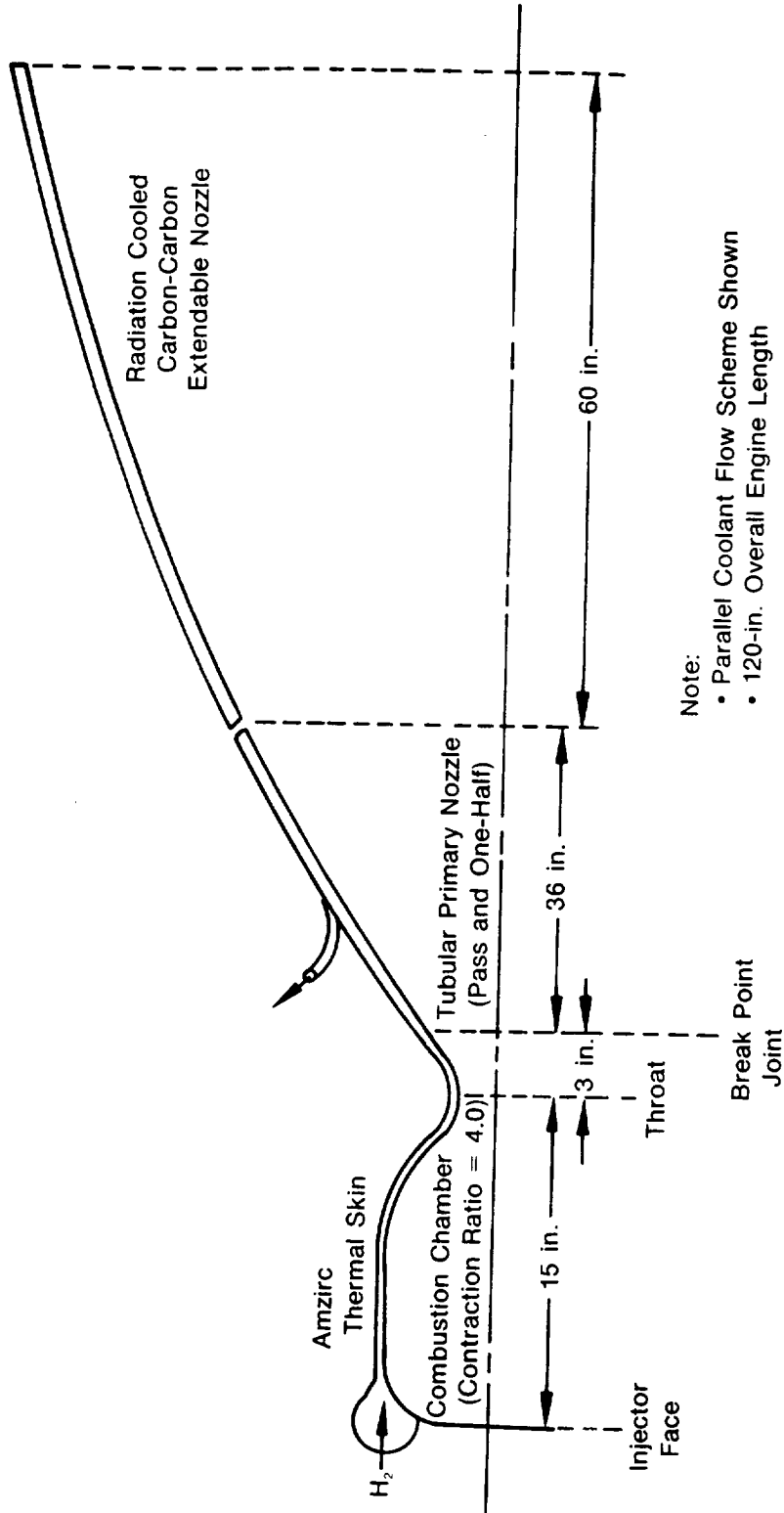
3.1 THRUST CHAMBER/NOZZLE ASSEMBLY DESIGN ANALYSIS

The thrust chamber and nozzle size and contours were initially determined during the parametric cycle performance studies and combustion system analysis performed under NASA Contract NAS8-33444. A chamber length of 15 in. and a chamber contraction ratio of 4 were selected as optimum for the advanced expander cycle engine. During this design study, a heat transfer analysis was conducted on the preliminary chamber design to ensure adequate cooling commensurate with cycle limitations. The design analysis of the thrust chamber and nozzle was performed at the engine off-design mixture ratio of 7.0 operating point because it provided the severest thermal conditions in the operating envelope. A schematic of the thrust chamber/nozzle assembly is presented in Figure 3-1. A maximum performance nozzle contour with an area ratio of 640:1 was chosen for the engine based on the length limitations and design point chamber pressure and mixture ratio. In addition, a radiation-cooled carbon-carbon composite secondary nozzle was selected over a conventional dump-cooled nozzle because of its lighter weight and favorable thermal characteristics.

3.1.1 Thrust Chamber Design Analysis

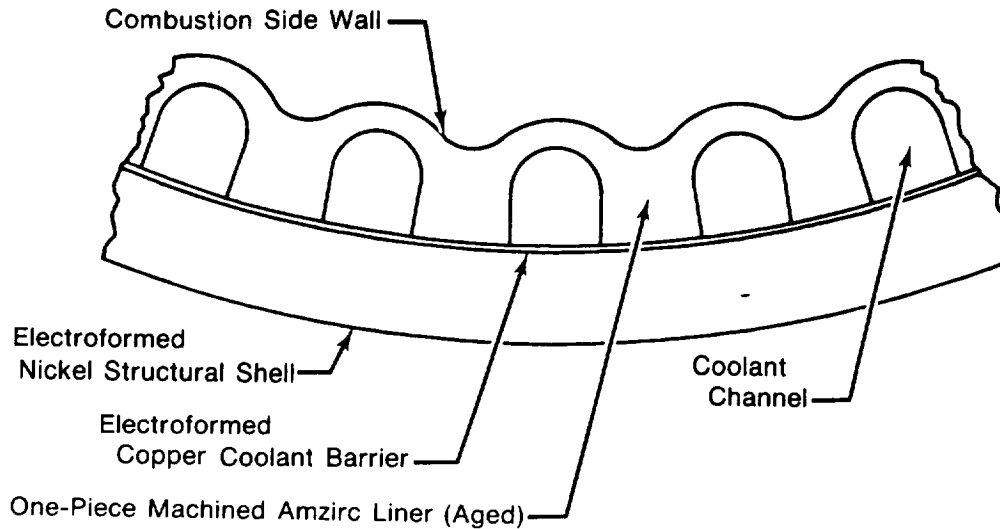
The advanced expander cycle combustion chamber, throat, and primary nozzle are of one piece, nontubular, regeneratively cooled construction, shown in Figure 3-2. The curved combustion side hot wall design was chosen over a flat hot wall design since it provided greater LCF life. The non-tubular thrust chamber liner design will be fabricated from the copper-zirconium alloy, aged AMZIRC. This alloy has improved thermal fatigue and strength properties over pure copper, but at a small loss in thermal conductivity. Axial cooling passages are milled in the AMZIRC thrust chamber liner OD and the passages are closed with electrodeposited copper. A shell of nickel is then electrodeposited over the copper to act as the strength-carrying member and outer wall. The non-tubular construction begins at the injector face and terminates downstream of the throat at an area ratio of approximately six, where the heat flux is low enough to allow the use of standard tubular construction. These slots vary in width and depth along their axial length to achieve the desired local coolant flow velocities.

P&WA/GPD — developed computer program D5160-90 was utilized to perform the heat transfer and pressure loss calculations; formulations were used that allowed the determination of the combustion-side and coolant-side convective environments from chamber geometries and engine operating conditions. The combustion gas environment was determined using the Mayer integral boundary layer analysis and enthalpy driving potential. The coolant gas environment was predicted by empirically determined correlations for hydrogen heat transfer coefficients modified to account for the effects of passage surface roughness (using the Dipprey and Sabersky method) and the effects of passage curvature. Constraints, used during the sizing of the coolant passage, are as follows: a maximum coolant Mach no. of 0.40 to limit the pressure loss through the passage and a maximum hot wall temperature of 1700°R to give 1200 cycles to failure for aged AMZIRC.



FD 212854

Figure 3-1. OTV Engine Thrust Chamber and Nozzle Schematic



FD 212855

Figure 3-2. Combustion Chamber Wall Detail

A contraction ratio of 4 was selected for the thrust chamber, based on previous parametric studies. The thermal analysis for the thrust chamber design was made at the off-design mixture ratio of 7 operating point, since it presented the severest conditions in the operating envelope. Parallel flow and counterflow cooling schemes were investigated for the chamber but the counterflow scheme was eliminated because of excessive pressure losses in the manifolding. Coolant passage geometry was defined and pressure and temperature characteristics were generated at mixture ratios of 6.0 and 7.0 for full thrust and at the pump idle and tank head idle design points. Table 3-1 presents these characteristics for the parallel flow configuration with a full thrust counterflow point at an O/F of 7 included for comparison. The optimized passage geometry selected and all pertinent parameters for the mixture ratio of 7.0 design point are shown in Figures 3-3 and 3-4.

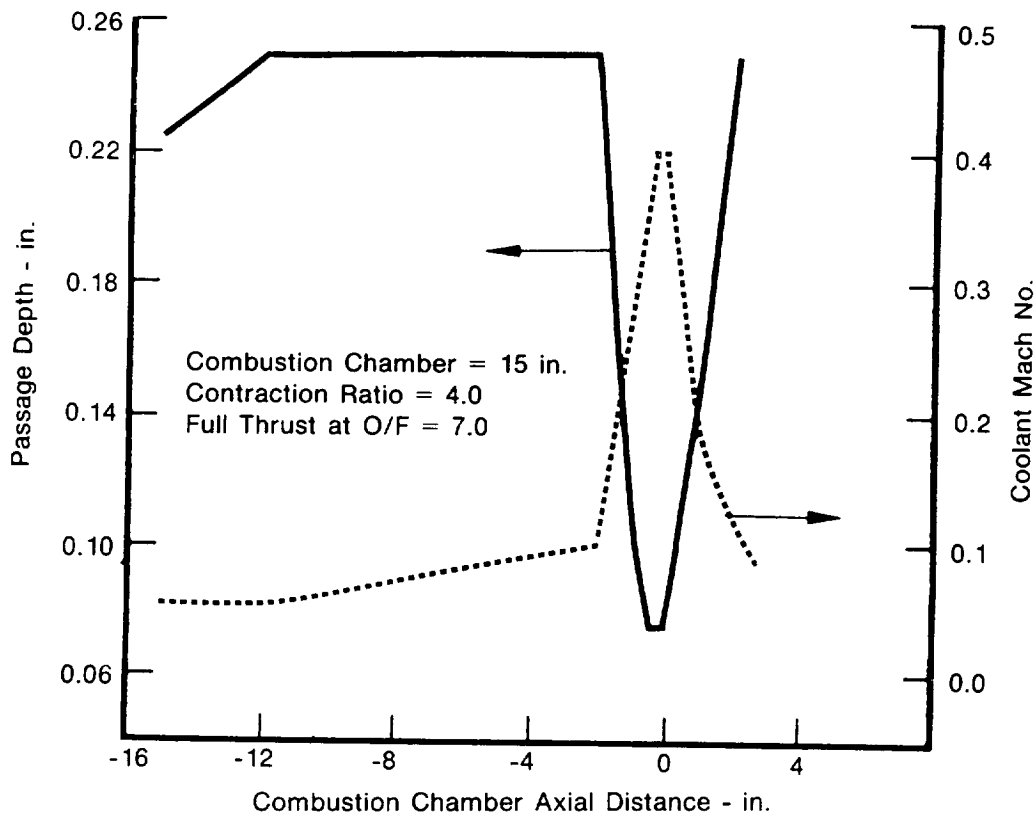
An LCF analysis of the thrust chamber was conducted using a MARC plastic finite element analysis that considered a complete upload/down load strain cycle, using the large displacement solution option. The OTV mission required 1200 cycles of life in the thrust chamber (300 cycles with a safety factor of 4). The performance requirements of the engine cycle point resulted in a 1759°R hot wall temperature and an 842°R cold wall temperature at the thrust chamber throat. Minimum life was found to occur at the throat and was calculated to be 760 cycles using ½ hard AMZIRC (zirconium copper) fatigue properties taken from NASA publication CR-121259. Decreasing the hot wall temperature by approximately 80°R would raise the minimum life to above the 1200 cycle goal. Analysis using limited LCF data on aged AMZIRC found in NASA publication TMX 73665 indicates that the predicted cycle life could be increased by more than a factor of 3 over ½ hard AMZIRC. It is recommended that additional material characterization and fatigue data be obtained for aged AMZIRC.

3.1.2 Tubular Primary Nozzle Design Analysis

The hydrogen coolant from the thrust chamber channels enters the inlet manifold (transition manifold) of the primary nozzle downstream of the throat and immediately flows into 180 single tapered tubes. The 180 tubes then taper until the primary nozzle circumference is correct to transfer over to a 360 double pass configuration. The coolant flow then passes through half the double pass tubes traveling toward the trailing edge of the primary nozzle where a turn-around manifold reverses the flow and returns it back up the nozzle in the other 180 tubes. Near the point where the double pass tubes begin (at $\epsilon=60$), the coolant is withdrawn as shown in Figure 3-5.

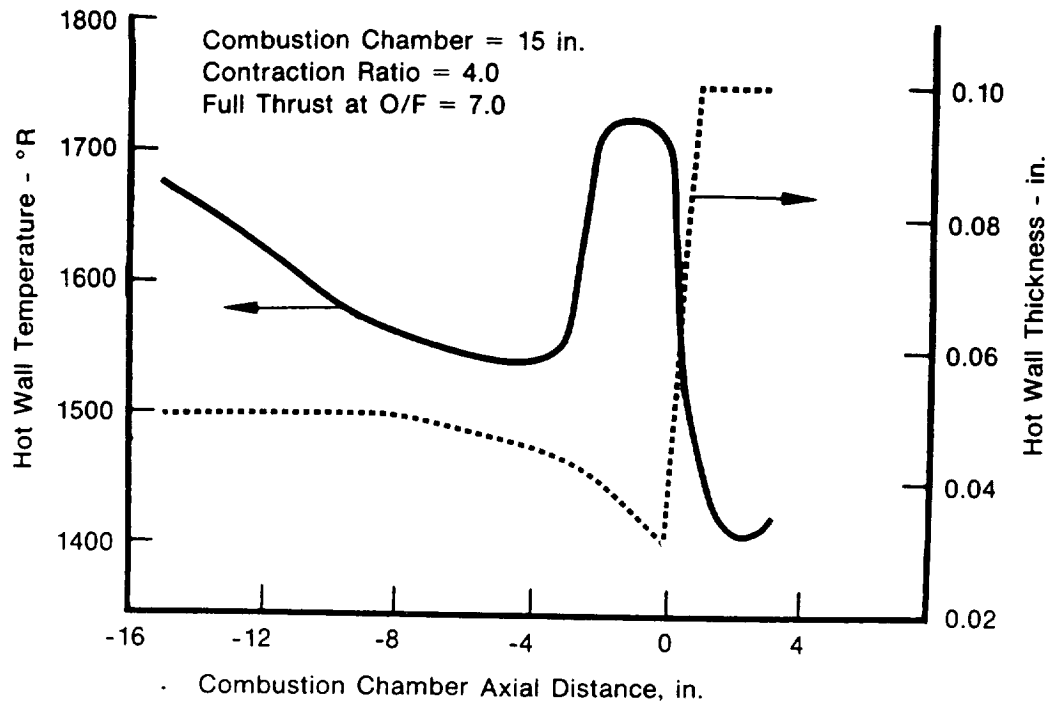
Table 3-1. Thrust Chamber and Primary Nozzle H_2 Coolant Conditions at Selected Design Points

| | | Parallel Flow | | | | |
|-----------------------------|---------------------------------|---------------|-----------|-----------|----------------|-----------------------|
| Design Point | | O/F = 7.0 | O/F = 6.0 | Pump Idle | Tank Head Idle | Counterflow O/F = 7.0 |
| Thrust Chamber Thermal Skin | $T_{in} - ^\circ R$ | 407 | 367 | 374 | 150 | 407 |
| | $P_{in} - psia$ | 4055 | 3859 | 304 | 16.2 | 4055 |
| | $T_{out} - ^\circ R$ | 845 | 738 | 876 | 543 | 844 |
| | $P_{out} - psia$ | 3673 | 3496 | 248 | 12.6 | 1561 |
| | $T_{hot\ wall\ max} - ^\circ R$ | 1710 | 1514 | 1160 | 603 | 1460 |
| Primary Nozzle | $T_{out} - ^\circ R$ | 990 | 874 | 1068 | 729 | — |
| | $P_{out} - psia$ | 3597 | 3425 | 233 | 11.3 | — |



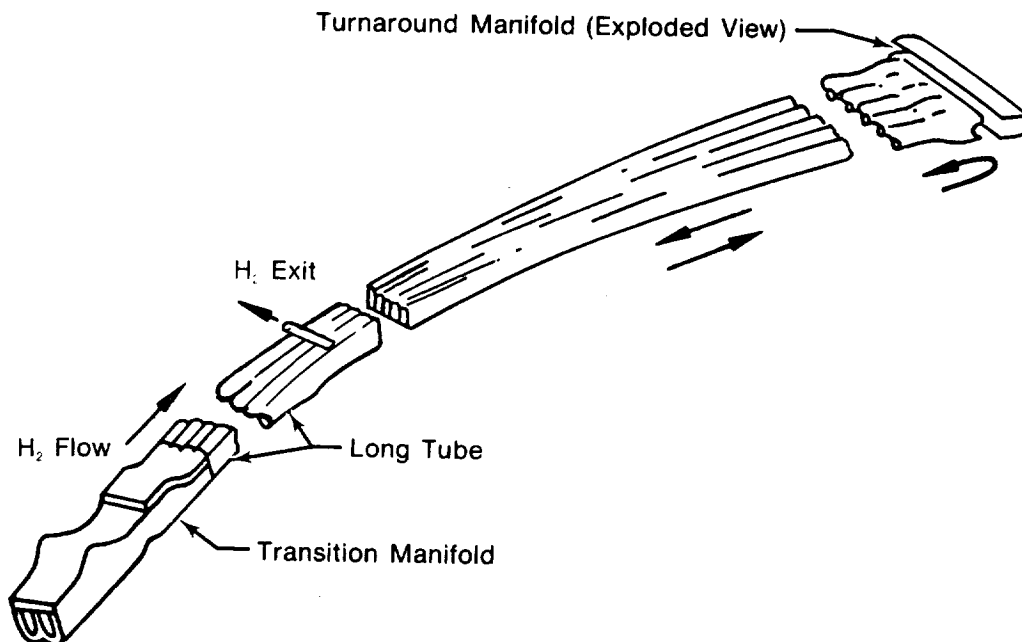
FD 212899

Figure 3-3. Combustion Chamber Coolant Passage Depth and Mach No.



FD 212856

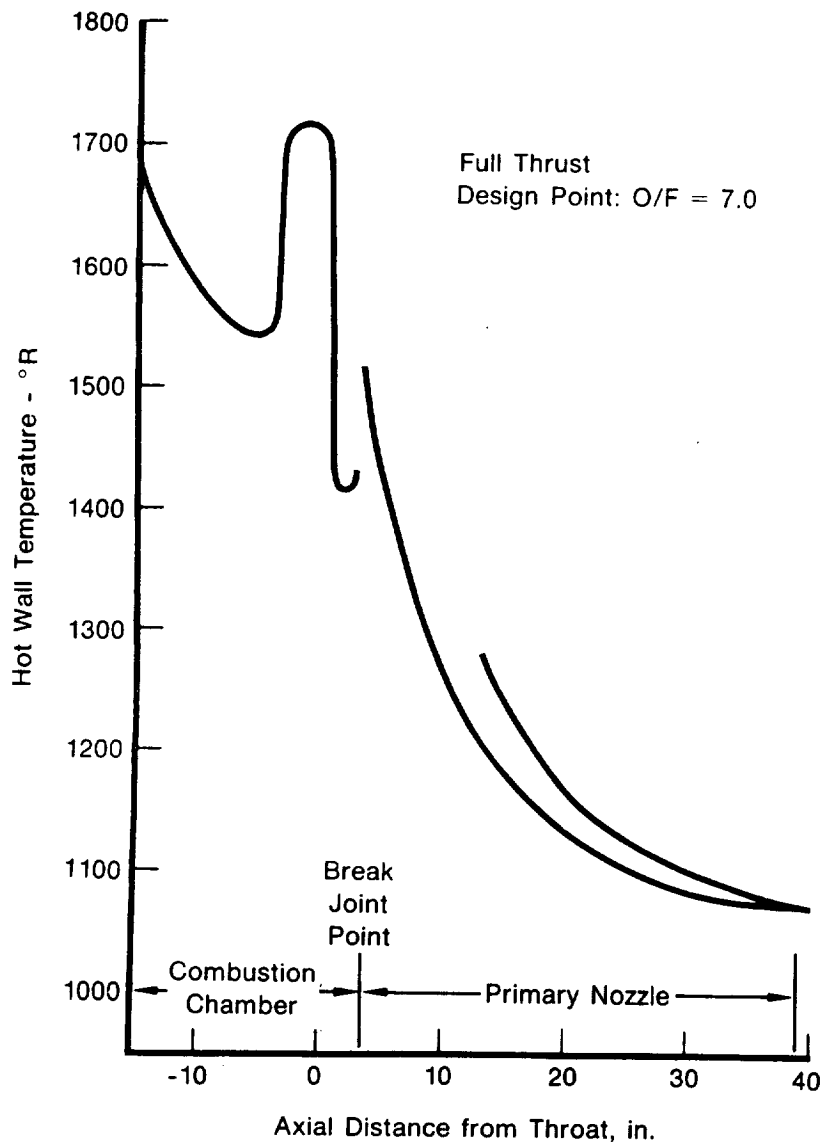
Figure 3-4. Combustion Chamber Hot Wall Temperature and Wall Thickness



FD 212857

Figure 3-5. Primary Nozzle Schematic

Using exit pressures and temperatures from the combustion chamber coolant analysis (which includes the transition manifold pressure loss) to define the initial flow conditions entering the primary nozzle, P&WA/GPD heat transfer computer program D5160-69, was used to predict metal and fluid criteria for the tubular nozzle. In this code, the wall temperatures are predicted based on a one-dimensional steady state heat balance analysis. Combustion gas and coolant gas environments were determined using the same analysis techniques described earlier for the thrust chamber. Table 3-1 contains fluid pressure loss and temperature increase characteristics for the primary nozzle for full thrust at mixture ratios of 6.0 and 7.0, a pumped idle point and a tank head idle point. Figure 3-6 presents the predicted hot wall metal temperature profile for the thrust chamber/tubular primary nozzle assembly at full thrust and a mixture ratio of 7.0.



FD 212858

Figure 3-6. OTV Engine Thrust Chamber and Primary Nozzle Hot Wall Metal Temperature Prediction

3.1.3 Carbon-Carbon Extendible Nozzle Design Analysis

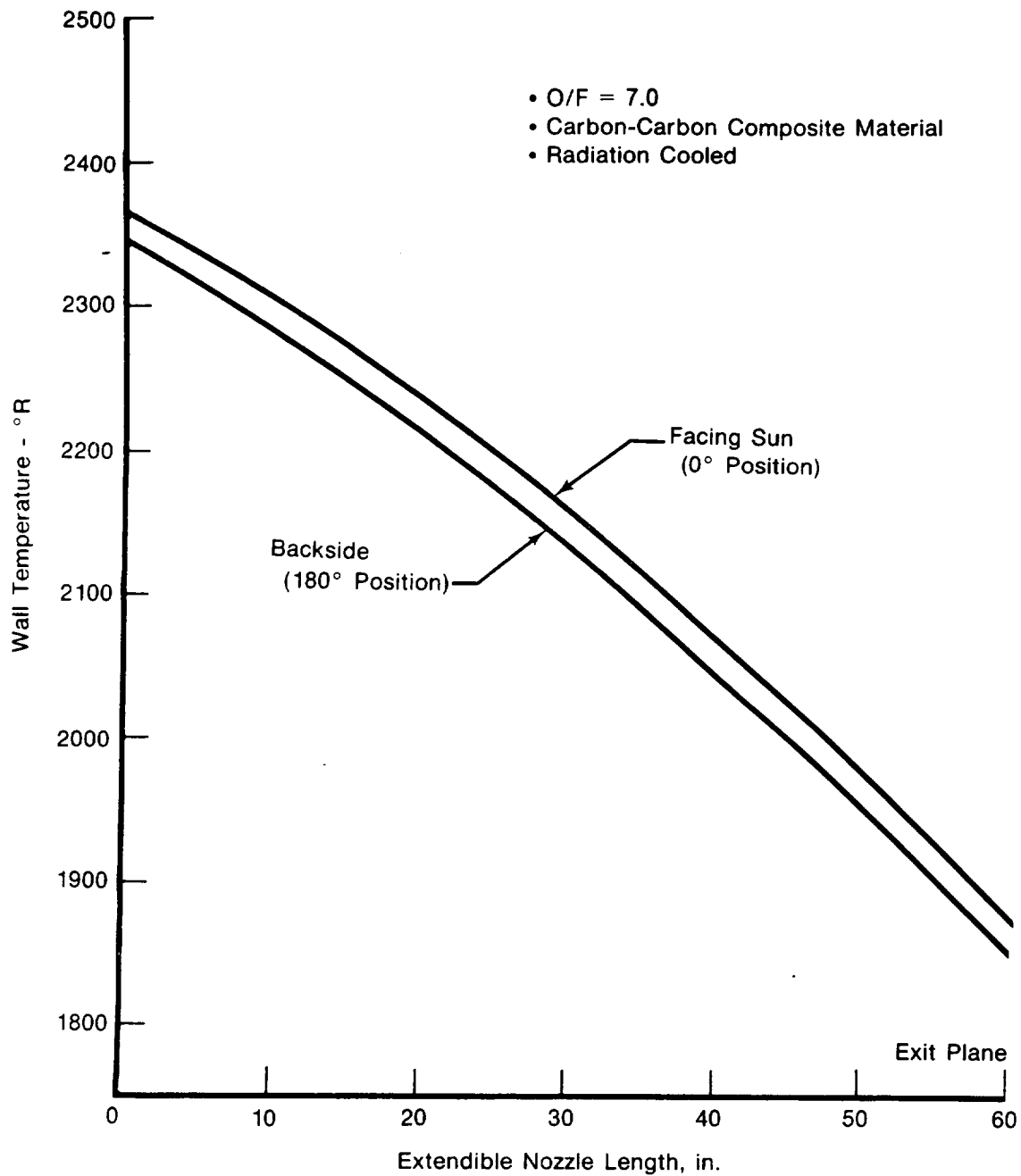
A radiation-cooled carbon-carbon extendible nozzle was selected for over a conventional dump-cooled metal alloy nozzle because of its light weight and favorable thermal characteristics. The thermal characteristics of the radiation-cooled secondary nozzle were defined at the severest thermal environment: full thrust and a mixture ratio of 7.0. A series of finger seals will be provided between the tubular primary nozzle and the nozzle extension. These seals will be purged with gearbox H₂ leakage which will then be used as a film cooling agent for the extendible nozzle. For the thermal analysis conducted during this preliminary design phase, film cooling effects of the primary nozzle/secondary nozzle seal coolant flow were not considered. However, maximum predicted nozzle temperatures were still less than 2400°R which is well within the allowable temperatures for carbon-carbon material. Wall temperature profile characteristics are shown for the secondary nozzle in Figure 3-7.

3.1.4 Injector Design Analysis

The injector was designed to provide efficient and stable combustion under all normal operating conditions. A combustion efficiency of 99.7% and a stability of less than $\pm 5\%$ chamber pressure oscillations were used as design goals during analysis. Figure 3-8 shows combustion efficiency as a function of injector element at the design point conditions. The injector contains 84 tangential entry swirl injection elements arranged in a uniform hexagonal pattern around a central torch igniter. Figure 3-9 presents the injector assembly as well as a cross section of one of the elements. The design for these elements is based on empirical correlations resulting from many years of P&WA experience with this type of element in rocket and laser development systems. The fuel is injected through an annulus around each oxidizer element, except that which is required for rigimesh cooling ($\approx 5\%$). The fuel orifice is full annular, a design preferred for uniform distribution. The annulus has extremely close tolerances, however, and since concentricity must be assured, it may be necessary to insert 3 tangs into the annulus to preserve that concentricity. The effective flow area of the annulus must remain the same and, to preserve as much fuel flow uniformity as possible, the tangs should be designed to present the minimum blockage.

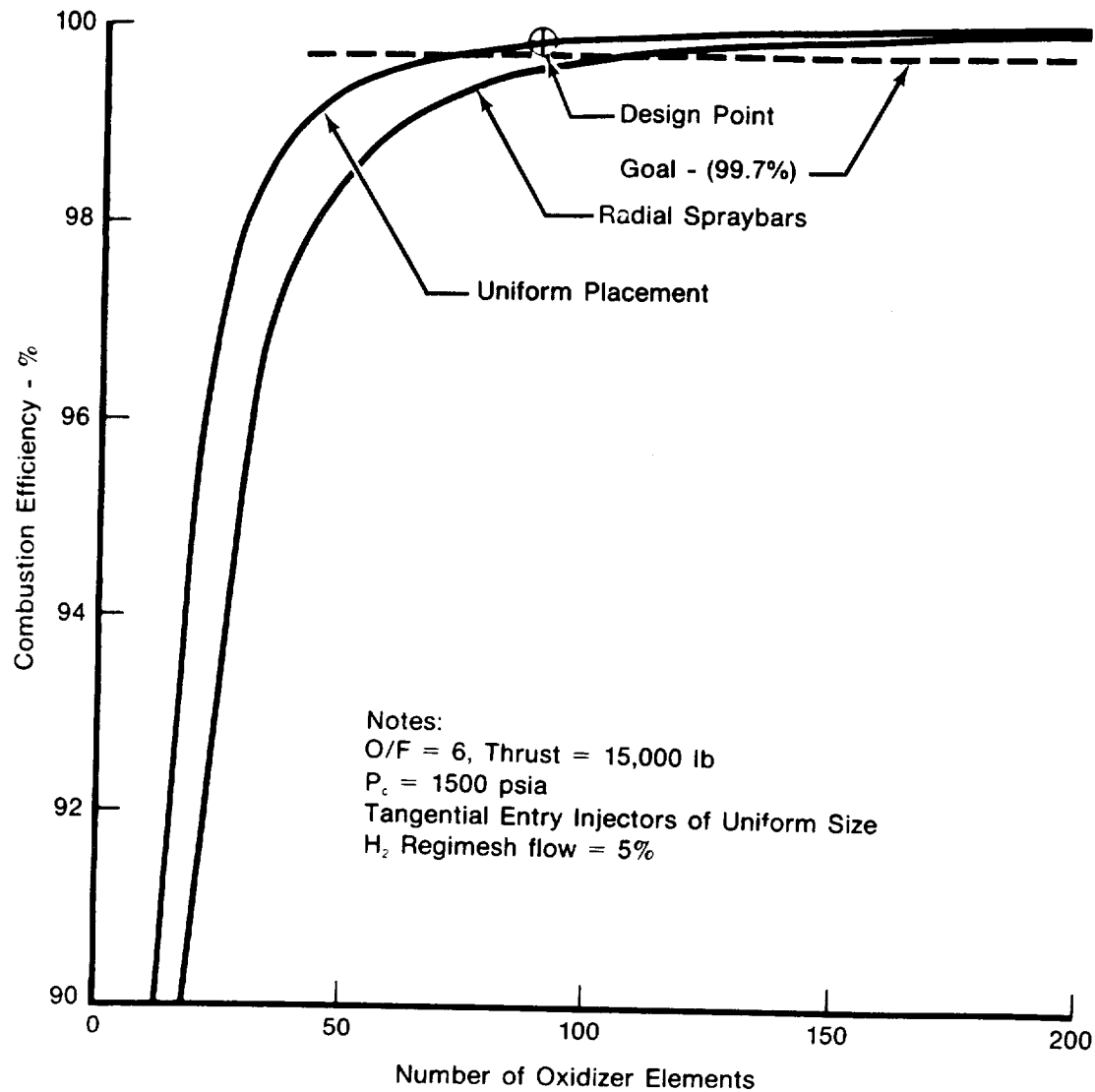
The outer oxidizer elements of the injector are scarfed at a 45 deg angle to prevent oxidizer impingement on the wall. The injector face is coned at a 5 deg angle to prevent an oxidizer spud failure from producing an oxidizer impingement on the wall. In addition, the coned configuration of the injector face has been shown, in previous programs, to contribute to the combustion stability of the chamber.

The rigimesh injector faceplate uses a 400 SCFM rated rigimesh material to produce a cooling flow of 5% of the hydrogen flow at the design point. Standoffs required to attach the rigimesh are cylindrical, with as small a diameter as feasible. They are located equidistant from the three closest oxidizer spuds and are uniformly distributed at equal radii. The fuel manifold has a 0.50 in height between the back of the rigimesh and the oxygen manifold. This separation is required to minimize static pressure drop between the outer and inner radii allowing optimum fuel flow uniformity.



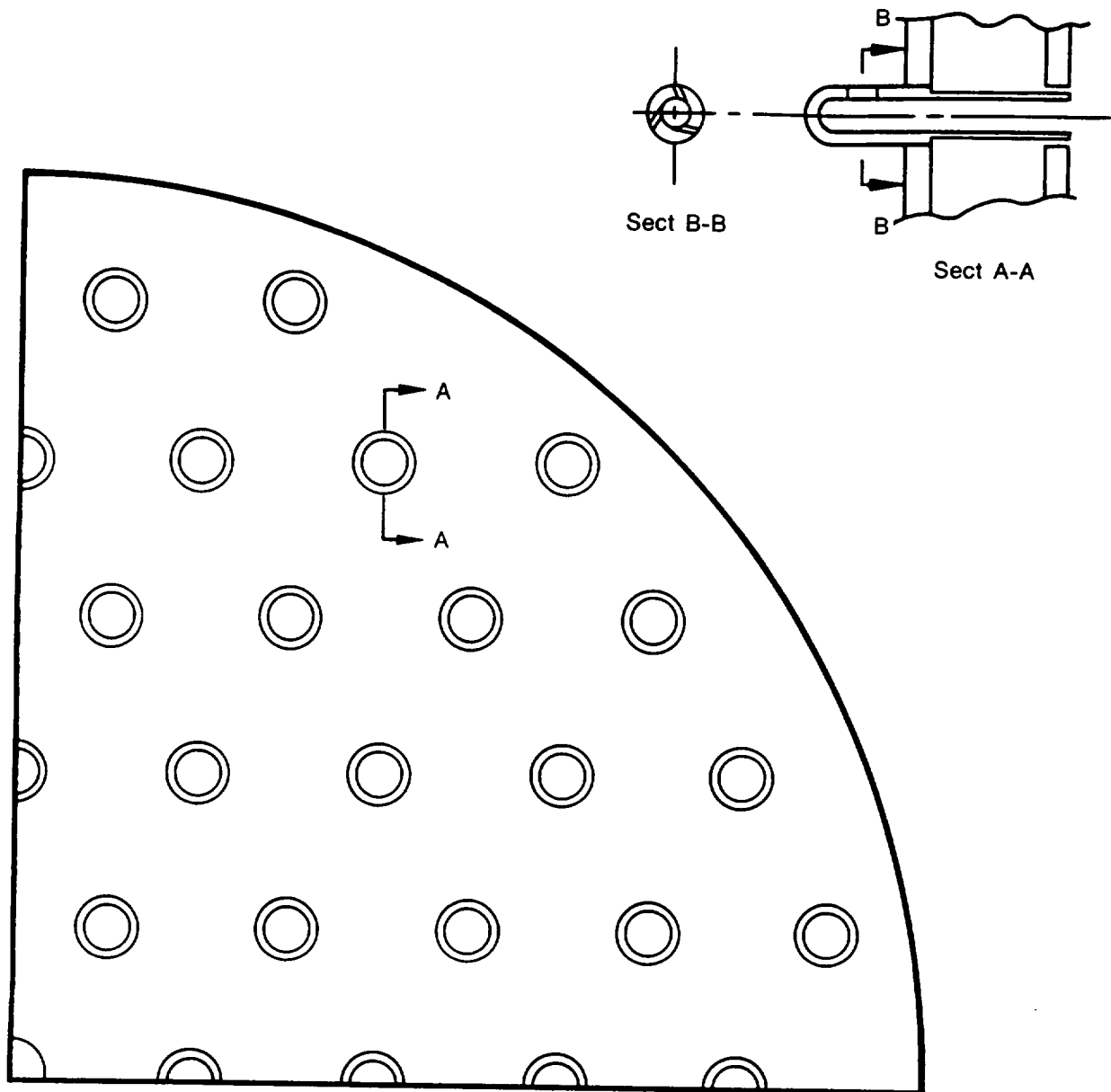
FD 212859

Figure 3-7. Extendable Nozzle Wall Temperature Prediction



FD 212860

Figure 3-8. Efficiency at Design Point as a Function of Injector Configuration



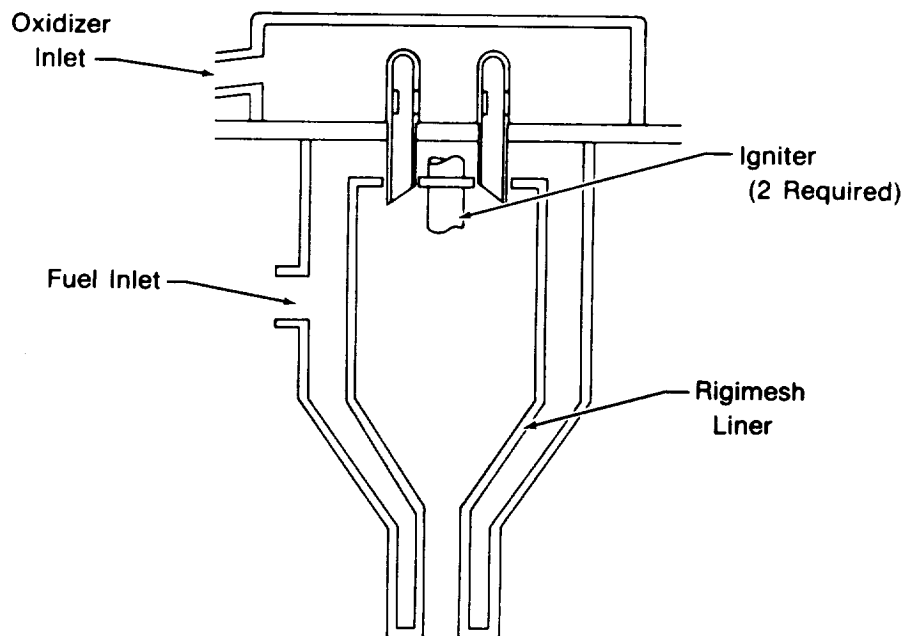
- 84 Injection Elements
- Tangential Oxidizer Entry
- Transpiration Cooled Injector Face

Figure 3-9. Advanced Expander Cycle Engine Injector Assembly

FD 212861

3.1.5 Torch Igniter Design Analysis

The igniter selected for the advanced expander cycle engine, shown in Figure 3-10, is a continuous torch igniter with the capability of a vacuum start and reliable multiple ignitions. The igniter is centrally located on the injector face and utilizes two tangential entry swirl injection elements. Two spark igniters are located in the same plane as the injectors. This arrangement will provide for rapid ignition while protecting the spark igniters during extended operation. The torch igniter liner is formed of hydrogen cooled rigimesh, similar to the one proposed for the P&WA Advanced Space Engine in 1973. The rigimesh liner will allow continuous operation with high durability as demonstrated in the RL10. The torch igniter is designed for continuous operation at an $O/F=4.0$. This mixture ratio will burn cooler than the engine mixture of 6.0 and enhance the igniter life. Additionally, the igniter will provide a continuous source of hot hydrogen to the chamber.



FD 197595

Figure 3-10. Igniter Assembly

3.2 HYDROGEN REGENERATOR DESIGN ANALYSIS

The function of the hydrogen regenerator is to increase the turbine inlet temperature by recovering heat downstream of the turbines and by using it to preheat the fuel prior to cooling the thrust chamber and primary nozzle. This provides a higher fluid temperature at the turbine inlet, increasing the available turbopump power. Because of the relatively low thermal effectiveness requirements ($\approx 40\%$) of the regenerator, a cross-flow configuration was selected to provide ease of manifolding. The regenerator is a milled channel design consisting of a stack of 0.050 in. thick aluminum plates with small passages machined in each plate. Hot and cold-side plates are alternated with the passages at right angles for a total of 61 hot and 60 cold plates. This design is lightweight, compact, easy to fabricate, and capable of withstanding the high hot-to cold-side differential pressure. Fluid and thermal analysis for the regenerator was carried out using a conventional effectiveness — number of transfer units (NTU) procedure. Figure 3-11 shows a sketch of the regenerator core arrangement and provides the design parameters and fluid condition at the design point.

FD 213627

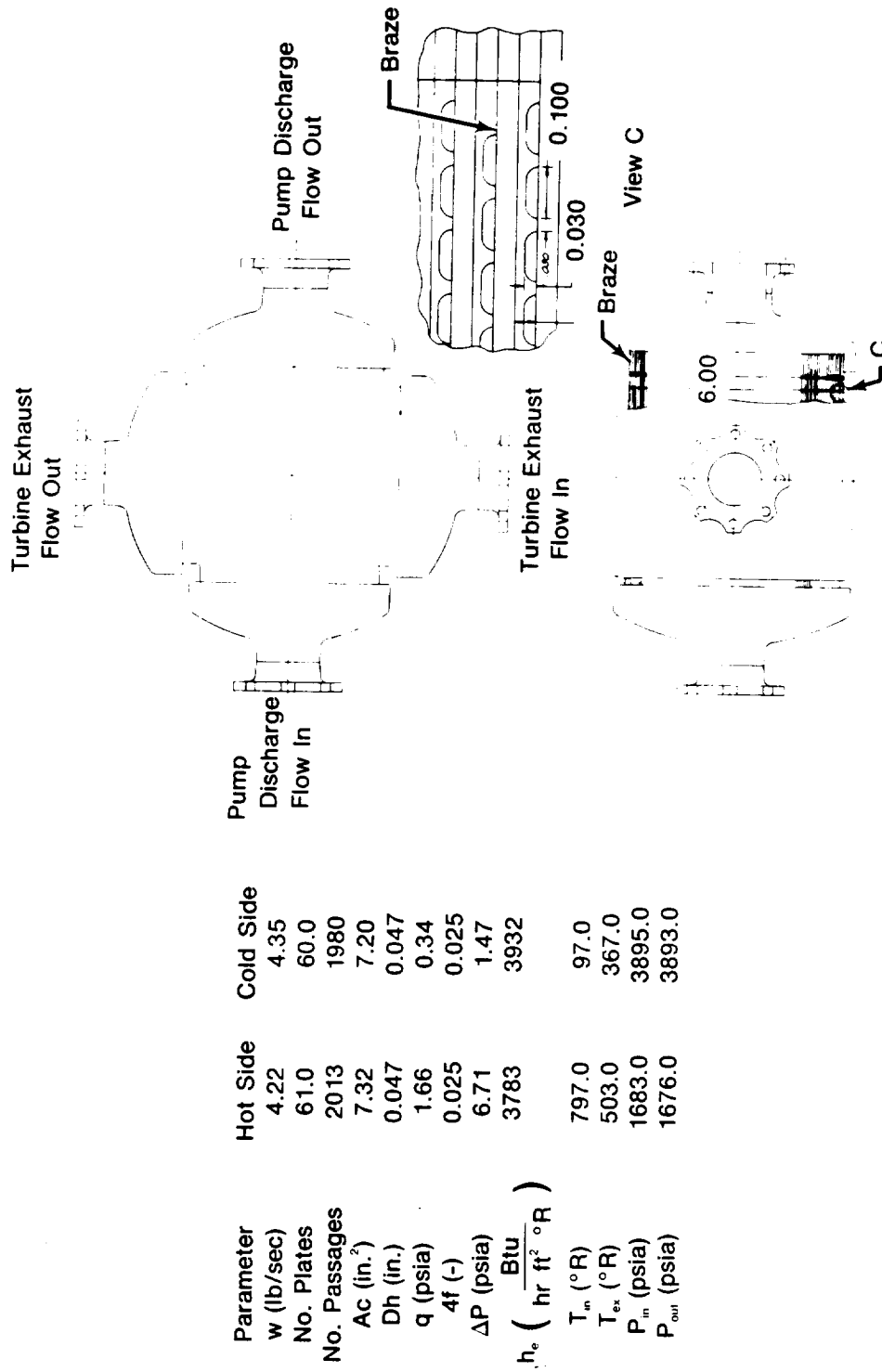


Figure 3-11. Single Pass Hydrogen Regenerator

3.3 GASEOUS OXYGEN HEAT EXCHANGERS

A GOX heat exchanger is required for the OTV engine to provide gaseous oxygen for propellant tank pressurization during full thrust and pumped idle operating modes and also to vaporize the engine oxidizer during tank head idle operation. However, studies indicate that a single compact heat exchanger could be subject to large, boiling-induced pressure and flow oscillations on the O_2 side at low mass qualities (less than 15%) which occur during the tank head idle mode.

This condition would result in unacceptable mixture ratio changes occurring in the main combustion chamber. The inclusion of a GOX vortex tube prevaporizer upstream of the GOX heat exchanger (O_2 side) is recommended specifically to eliminate such a problem.

The vortex tube prevaporizer concept is based on a unique application of state-of-the-art technology being studied for high-energy laser mirror and fusion target plate designs where high heat transfer rates and dynamically stable flow are critical requirements. The vaporization of liquid oxygen in zero "g" space environment is, furthermore, a logical application of the tangential entry, free vortex, swirl flow concept. The proposed design configuration of the vortex tube prevaporizer and tank head idle fluid parameters are shown in Figure 3-12 with the basic operation discussed in the following paragraphs.

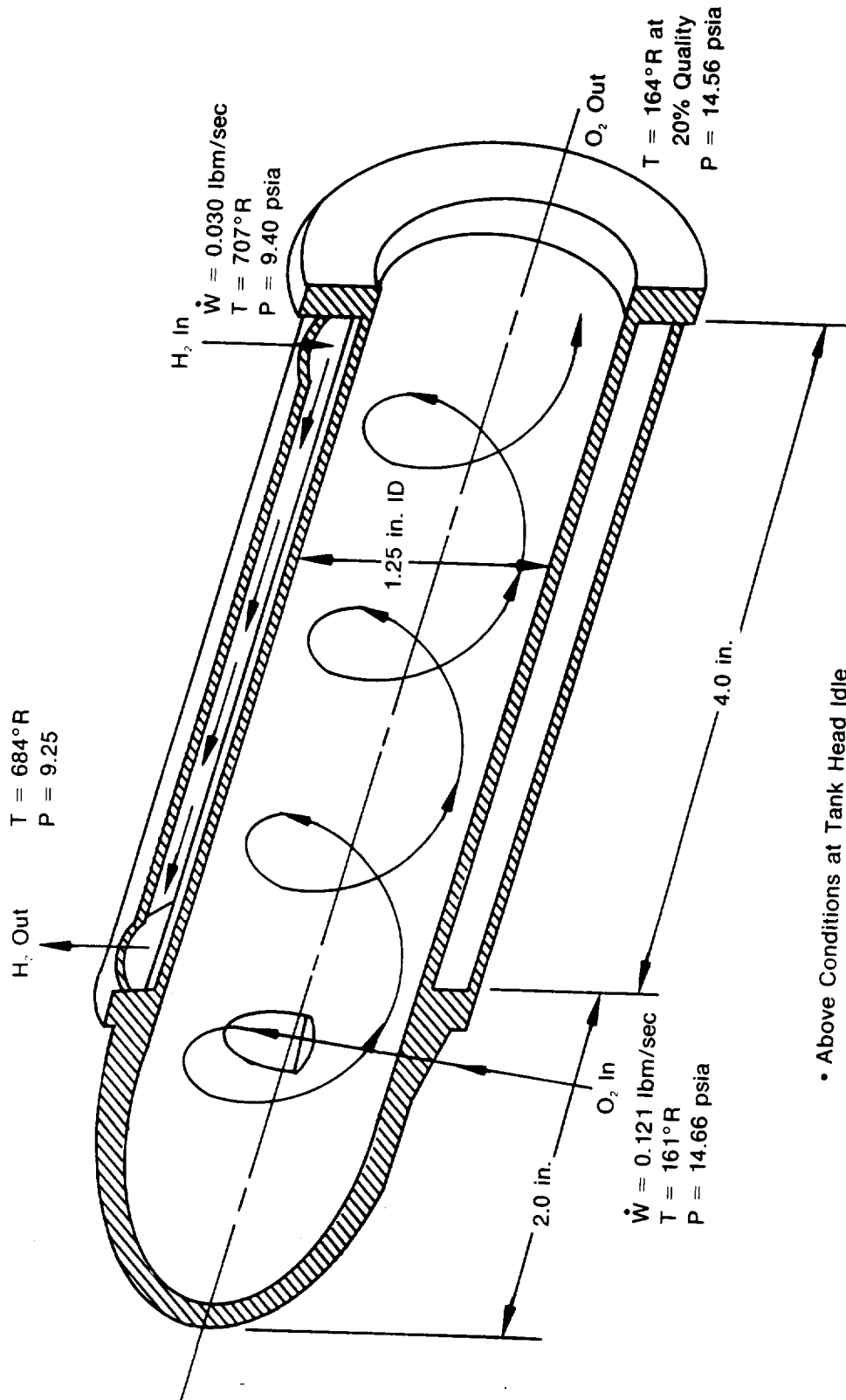
Saturated LOX is injected tangentially near the closed end of a large diameter pipe and is allowed to spiral in a helical path toward the open end. The vortex pattern thus produced suppresses the transition from nucleate boiling to film boiling and allows extremely high heat transfer rates to be achieved. The centrifugal forces generated by the swirling flow, force the liquid to the outer wall and allow the vapor to flow to the center of the tube. This action, in effect, separates the liquid and vapor phases so that boiling instabilities are not present. The liquid oxygen flowing along the wall is then allowed to stop its vortex flow pattern (by vanes or other antivortex devices) as it exits the prevaporizer, whereupon it "flashes" to tiny droplets and joins the vapor flow before entering the GOX heat exchanger. The heat source for LOX vaporization is the GH_2 flowing in a jacket that surrounds the vortex tube.

The GOX heat exchanger was sized for single phase gas conditions on both the hot-and cold-sides. The selected geometry was of a compact crossflow design utilizing a milled channeled construction. Figure 3-13 show a sketch of the GOX heat exchanger core arrangement and provides important geometric and fluid flow design. parameters at tank head idle and pumped idle.

3.4 TURBOPUMPS

3.4.1 Main Fuel Pump

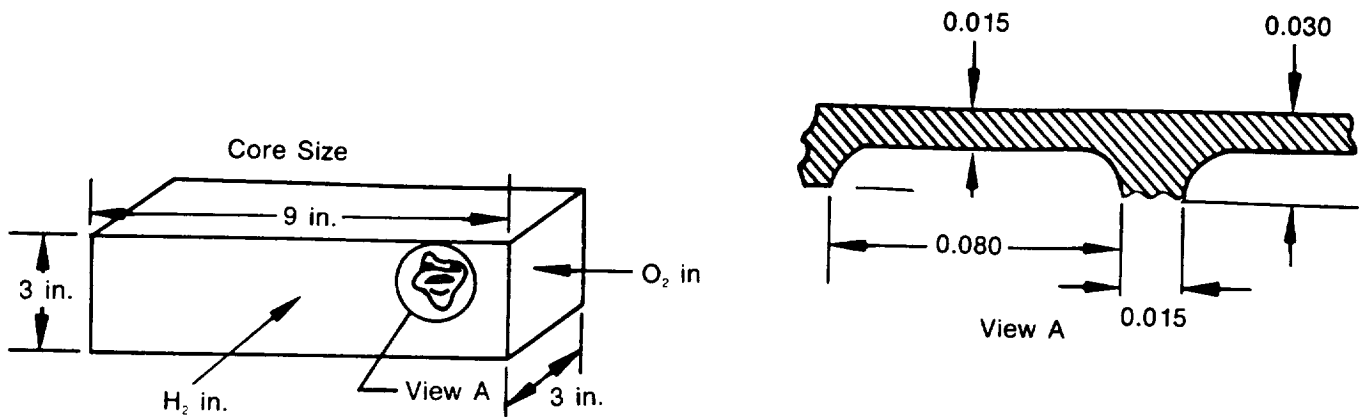
The OTV main fuel pump is a two-stage centrifugal turbopump design. The design constraints which were established for this pump include: (1) 2000 ft/sec tip speed limit for the bonded shrouded impellers with 25 deg back-swept blades, (2) 3×10^6 DN bearing limit and (3) 25% critical speed margin. Both two and three stage designs were assessed with regard to pertinent hydrodynamic and structural considerations prior to selecting the two stage configuration.



FD 212862

Figure 3-12. GO₂ Vortex Pre vaporizer

• Above Conditions at Tank Head Idle



Note: Sized for Gas Conditions Both Sides

| Parameter | Tank Head Idle | Pumped Idle |
|---------------------------------------|----------------|-------------|
| H ₂ W (lbm/sec) | 0.028 | 0.251 |
| O ₂ W (lbm/sec) | 0.128 | 2.783 |
| H ₂ T _{IN} (°R) | 882 | 940 |
| H ₂ T _{EX} (°R) | 637 | 641 |
| O ₂ T _{IN} (°R) | 162 | 164 |
| O ₂ T _{EX} (°R) | 612 | 218 |
| H ₂ P _{IN} (psia) | 9.46 | 165.1 |
| H ₂ P _{EX} (psia) | 9.39 | 164.7 |
| O ₂ P _{IN} (psia) | 15.60 | 205.4 |
| O ₂ P _{EX} (psia) | 15.53 | 193.6 |
| H ₂ ΔP (psia) | 0.07 | 0.4 |
| O ₂ ΔP (psia) | 0.07 | 11.8 |
| Q (Btu/sec) | 19.3 | 413 |

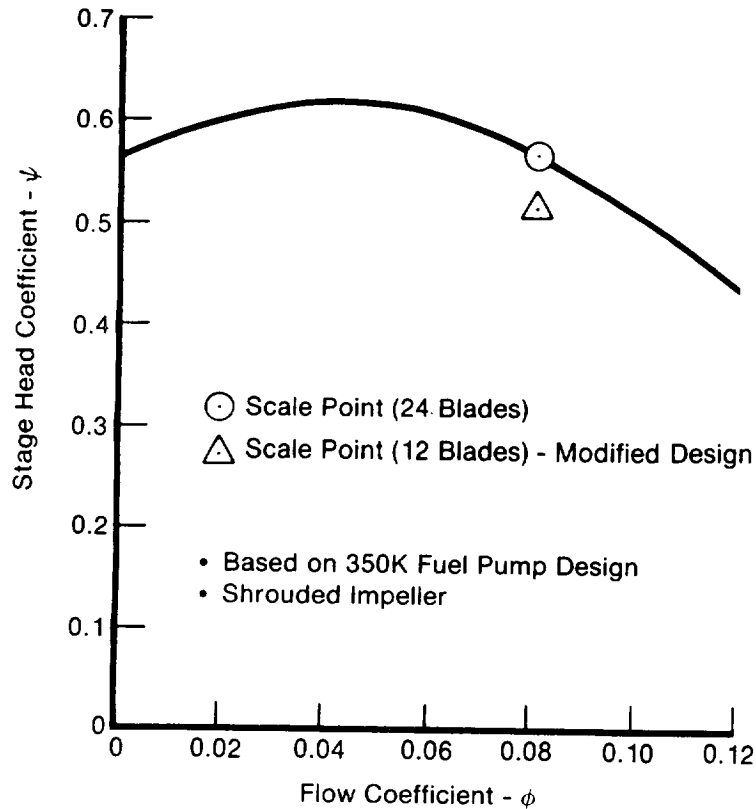
FD 212863

Figure 3-13. Gaseous Oxygen (GOX) Heat Exchanger

Preliminary sizing estimates showed that the pump would require a minimum bearing size of 20 mm. In the interest of attaining the highest possible specific speed and efficiency, the maximum allowable design rpm, based on the bearing DN limit, was established at 150,000 rpm. The shaft length was then sized to accommodate the two shrouded impellers plus inducer, two bearings, second stage volute inlet, thrust piston and the turbine rotor. This configuration just met the 25% critical speed margin requirement at the 150,000 design rpm. Both stages were designed for a resultant specific speed of 811.5 To obtain the necessary stage head-rise, a tip speed of 1960 fps, slightly less than the 2000 ft/sec tip speed limit with a 3-in. impeller diameter, was required.

In an effort to obtain higher efficiency through increased specific speed, a three-stage design was also considered during the design study. Analysis of the three-stage design showed that this configuration would not be capable of meeting the 25% critical speed margin requirement at the 150,000 design rpm due to the increased pump length. Only by decreasing the speed to a level lower than that necessary to yield the same specific speed as the two-stage pump, could the required critical speed margin be attained. As a result, the three-stage pump design, being also more complicated, difficult to manufacture and costly than a two-stage pump, was not given further consideration.

The impellers for the two-stage fuel pump were scaled from previously proven P&WA turbopump designs with shrouds added to control leakages. The first-stage impeller excluding the inducer, was scaled from the first-stage of the 350K fuel pump, a design which demonstrated 95% hydraulic efficiency with use of shrouds. As a modification for the OTV design, 12 splitter blades were removed due to the small size of the impeller, leaving 6 full blades and 6 long splitter blades. Analysis indicated that this would result in an 8.7% decrease in head coefficient, which was accounted for in the design as shown in Figure 3-14. The first-stage was scaled at a flow and head coefficient compatible with the desired specific speed. This results in only a slight loss of stage efficiency as indicated in Figure 3-15.



FD 212864

Figure 3-14. Fuel Pump 1st Stage Impeller Head Coefficient

The second-stage impeller was scaled from the high efficiency second-stage of the XLR-129 fuel pump in the same manner as the first-stage. Again, the 12 short splitter blades were removed, resulting in a 10.3% loss in head coefficient as shown in Figure 3-16, leaving 6 full blades and 6 long splitter blades. The second-stage was also scaled at a flow and head coefficient necessary to obtain the desired specific speed, resulting in a minor efficiency loss as indicated in Figure 3-17. Both the first and second-stage impellers provide a configuration with optimum specific diameter as shown in Figure 3-18.

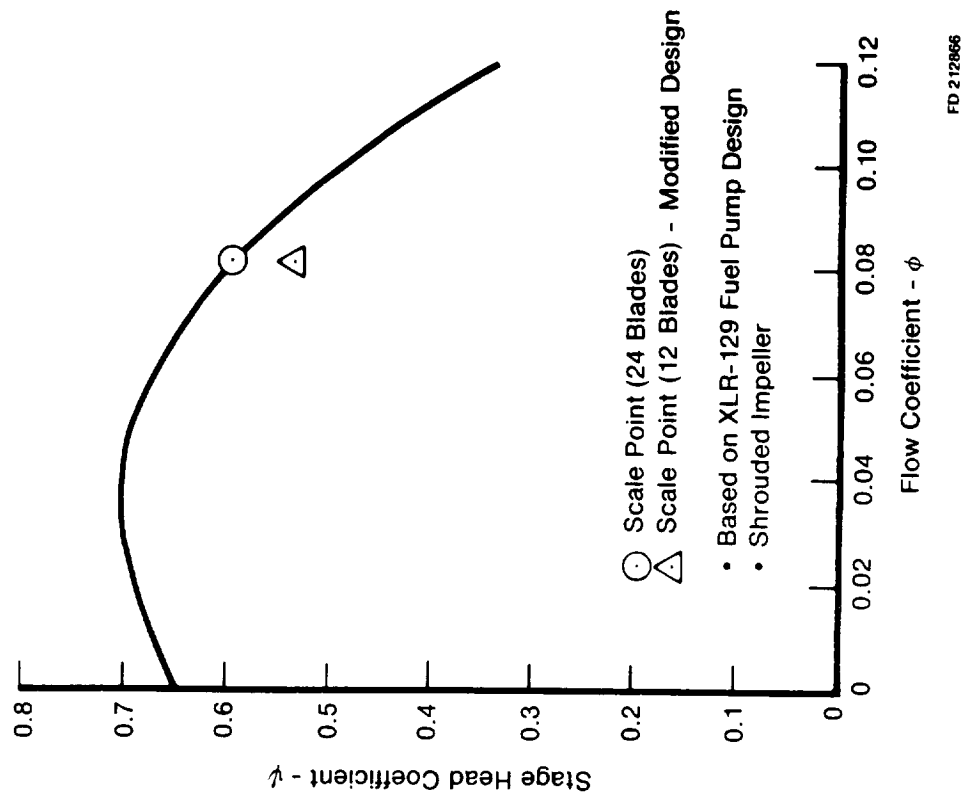


Figure 3-15. Fuel Pump 1st Stage Impeller Efficiency

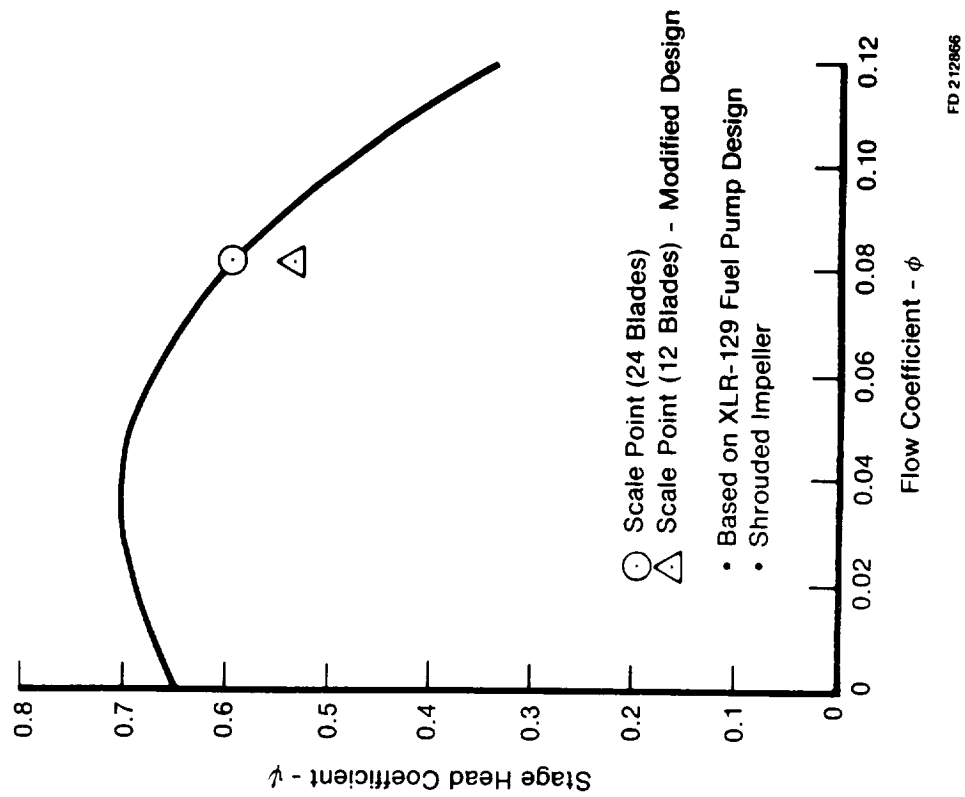
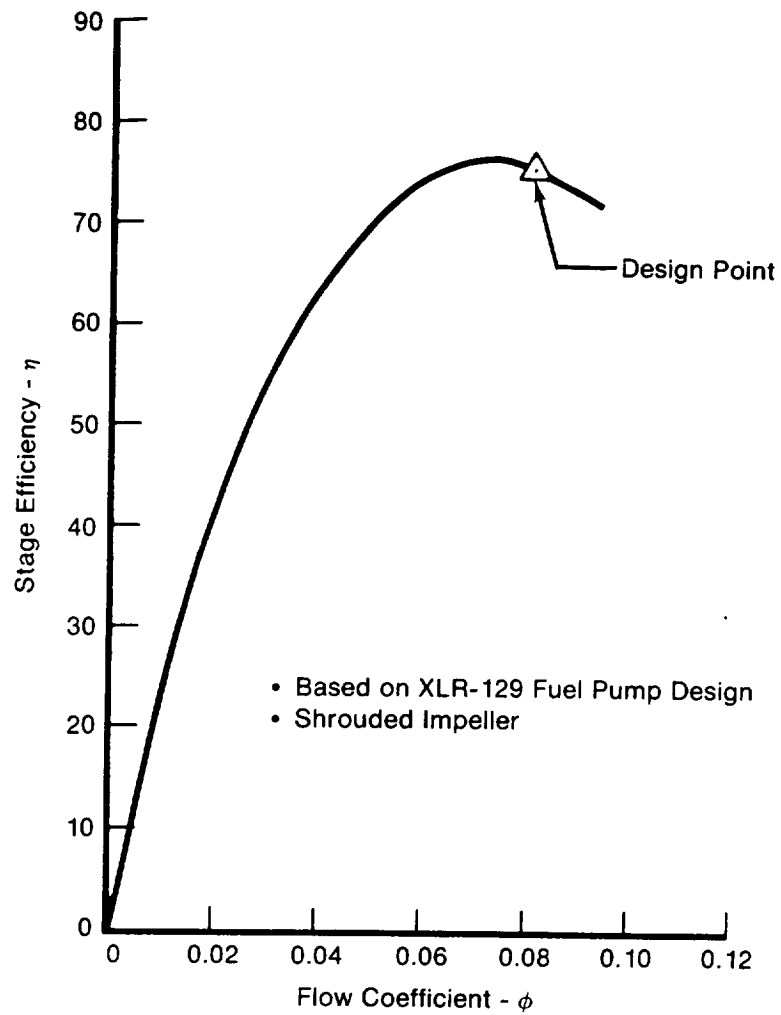
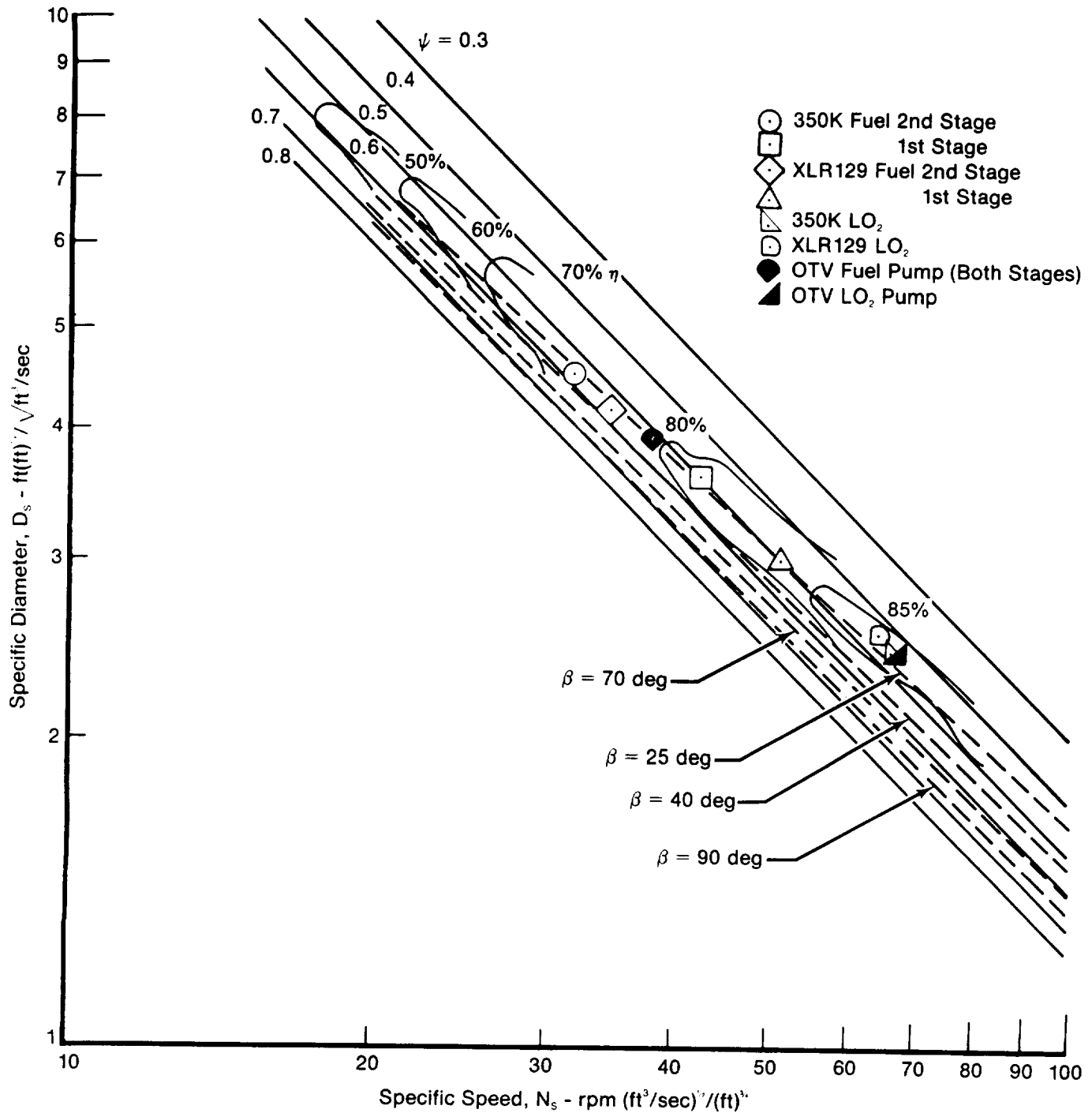


Figure 3-16. Fuel Pump 2nd Stage Impeller Head Coefficient



FD 212867

Figure 3-17. Fuel Pump 2nd Stage Impeller Efficiency



FD 212868

Figure 3-18. Pump Design Parameters Optimized from Test Data

Radial loads for each stage are found in Table 3-2 for the nominal design, off-design (O/F=7.0) and pumped idle point. The impellers employ stepped labyrinth seals on the front and back shrouds at approximately 2 in. seal diameter to minimize leakage recirculations. Each impeller discharges into a constant velocity, single discharge volute collector followed by a conical diffuser.

Table 3-2. OTV Impeller Radial Loads

| Pump Location | Pumped Idle | | | Nominal Design | | | Off Design | | |
|---------------------|------------------------|--------|----------------------|-------------------------|---------|----------------------|-------------------------|---------|----------------------|
| | O/F = 6.0 — 10% Thrust | | | O/F = 6.0 — 100% Thrust | | | O/F = 7.0 — 111% Thrust | | |
| | Q/N | | | Q/N | | | Q/N | | |
| | Q/N _{HEP} | N | F _T , No. | Q/N _{HEP} | N | F _T , No. | Q/N _{HEP} | N | F _T , No. |
| Main LOX Pump | 0.4 | 17,631 | 47.6 | 1.0 | 67,390 | 46.2 | 1.13 | 68,709 | 212.4 |
| Fuel Pump 1st-Stage | 0.4 | 39,244 | 47.1 | 1.0 | 150,000 | 61.7 | 0.97 | 152,932 | 98.2 |
| Fuel Pump 2nd-Stage | 0.4 | 39,244 | 27.4 | 1.0 | 150,000 | 71.6 | 0.97 | 152,932 | 88.9 |

The pump configuration includes an inducer on the first-stage impeller to provide the required suction capability compatible with the fuel boost pump discharge, and ensure cavitation-free performance of the impeller. Three helical blades and a solidity of 1.5 were employed in the design providing a suction specific speed capability of 29,200 at an inlet tip flow coefficient of 0.013 (Figure 3-19).

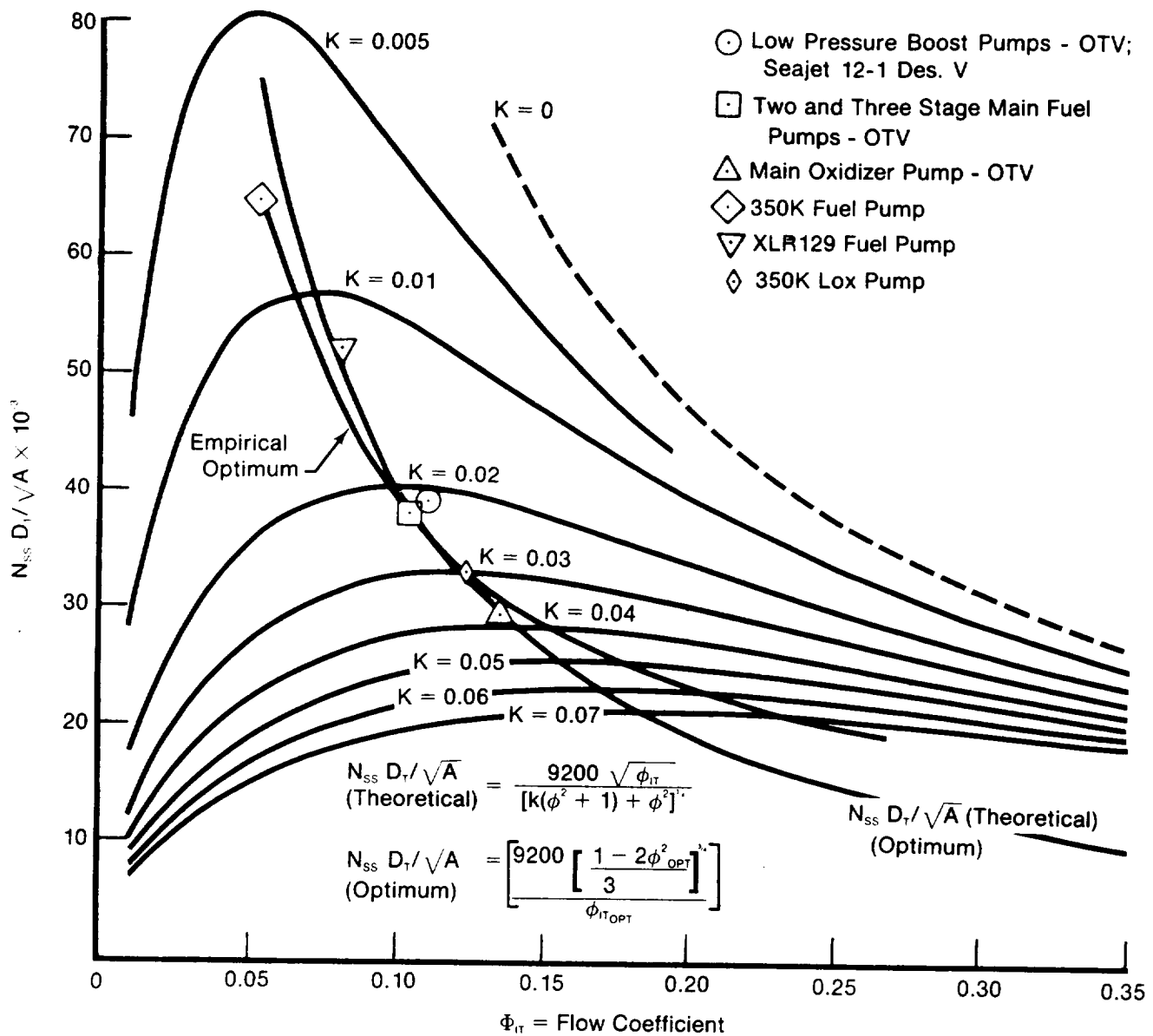
The overall pump efficiency has been estimated to be 64% establishing a shaft horse power requirement of 1571. To achieve this efficiency the design will require tight seal clearances in order to minimize leakage recirculations. At least 80% volumetric efficiency is required with preliminary estimates indicating that this can be obtained by holding all diametral seal clearances on the impellers to 0.004 in. Mechanical and hydrodynamic efficiencies were estimated at 94% and 85% respectively. Other pertinent design parameters are tabulated in Table 3-3. Figure 3-20 shows a preliminary configuration drawing of the OTV main fuel pump.

3.4.2 Main Oxidizer Pump

The OTV main oxidizer pump is a single-stage, shrouded centrifugal turbopump design. The configuration consists of a three bladed inducer with solidity of 2.0, a shrouded impeller with 6 full length blades plus 6 long splitters, a constant velocity, single discharge volute collector, and conical diffuser. The pump impeller, a 25 deg backswept design, and inducer, have been scaled from the P&WA SSME main LOX pump design modified by a slight extension in the impeller diameter to obtain the required head rise. Figure 3-18 shows that the adjusted impeller diameter provides an optimized specific diameter for the design point specific speed of 1431.

The inducer was designed for a suction specific speed capability of 23,000 as shown in Figure 3-19. The overall pump efficiency has been estimated at 67.4% establishing a shaft-horse power requirement of 375. As with the main fuel pump, the lab seal clearances will require close control to obtain the desired efficiency due to the small impeller size.

A list of pertinent design parameters is provided in Table 3-4 and radial loads in Table 3-2. A configuration sketch of the OTV main LOX pump and turbine drive is shown in Figure 3-21.



FD 212869

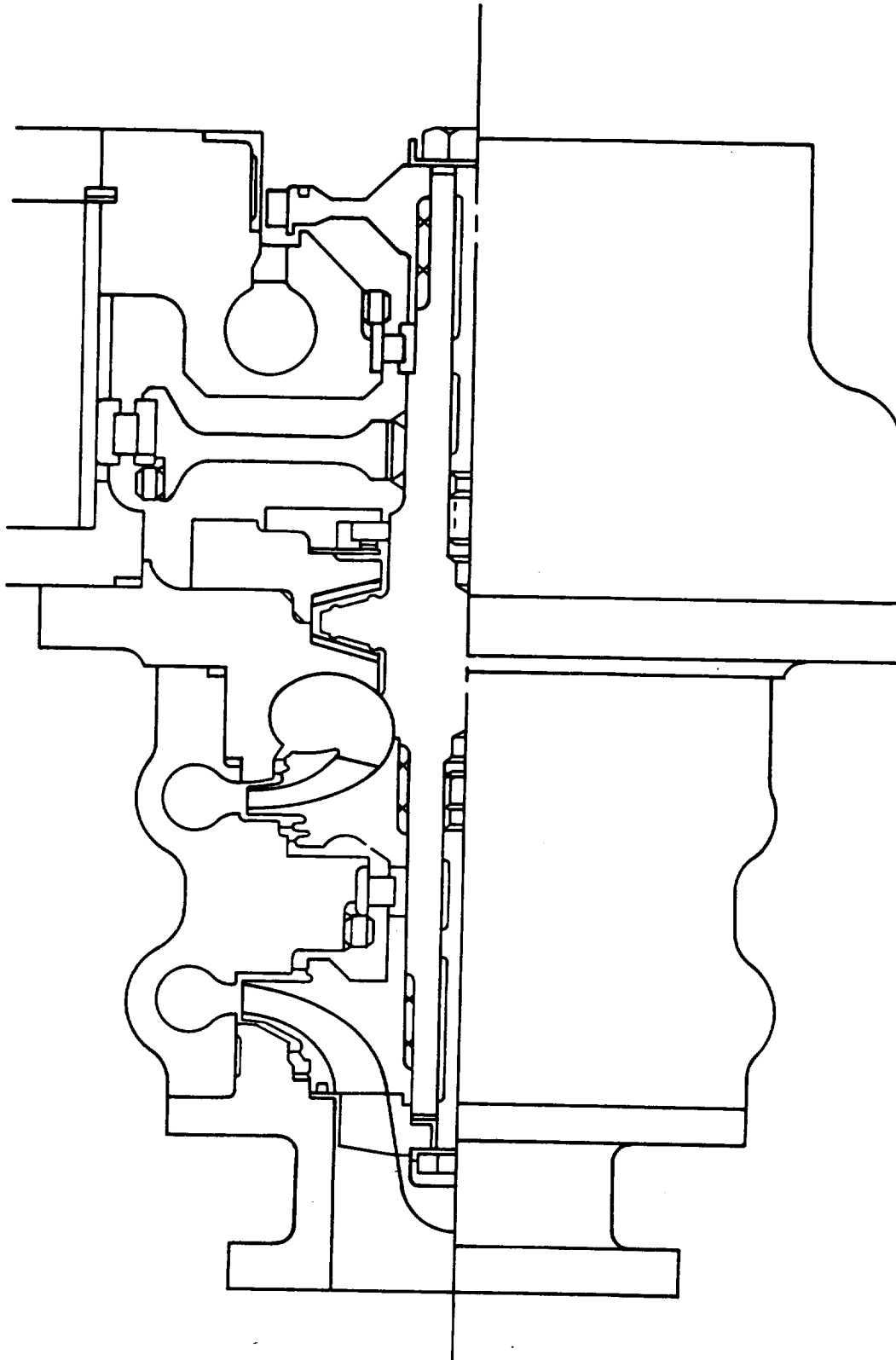
Figure 3-19. Theoretical Pump Suction Capability (N_{ss})

Table 3-3. OTV Main Fuel Pump Design

| | Parameter | Units | Value |
|----------------------|---|--|---------|
| Pump | Q | gpm | 452 |
| | N | rpm | 150,000 |
| | ΔH Pump Overall | ft | 124,022 |
| | W | lb/sec | 4.46 |
| | P _i Inlet | psia | 87.4 |
| | P _i Outlet | psia | 3905 |
| | P _{vapor} | psia | 16.5 |
| | T _i Inlet | °R | 37.2 |
| | ρ Inlet | lb/ft ³ | 4.432 |
| | η -Overall Efficiency | % | 64 |
| | SHP | hp | 1571 |
| | NPSH Inlet | ft | 2305 |
| | TSH | ft | 90 |
| Inducer | N _{ss} Capability | — | 29,200 |
| | ϕ_{IT} | — | 0.103 |
| | D _{1I} | in. | 1.694 |
| | D _{1H} | in. | 0.593 |
| | D _{2I} | in. | 1.694 |
| | D _{2H} | in. | 0.971 |
| | h Tip Axial Length | in. | 0.452 |
| | A ₁ | in. ² | 1.698 |
| | A ₂ | in. ² | 1.423 |
| | σ -Tip Solidity | — | 1.5 |
| First-Stage Impeller | Scale Factor | — | 0.2258 |
| | ΔH Rotor | ft | 66,894 |
| | ΔH Stage | ft | 62,011 |
| | N _s | $\frac{(\text{rpm})(\text{gpm})}{(\text{ft})^3}$ | 811.5 |
| | ψ_{2M} Rotor | — | 0.561 |
| | ψ_{2M} Stage | — | 0.520 |
| | ϕ_{2M} | — | 0.081 |
| | U _{2M} | ft/sec | 1959.8 |
| | D _{1T} | in. | 1.694 |
| | D _{1H} | in. | 0.971 |
| | D _{2T} , D _{2M} , D _{2H} | in. | 2.992 |
| | h Mean | in. | 0.613 |
| | A ₁ | in. ² | 1.229 |
| | A ₂ | in. ² | 0.914 |
| | b ₂ Exit Blade Height | in. | 0.108 |
| First-Stage Volute | α_2 | deg | 8.22 |
| | A _v | in. | 0.152 |
| | D _v | in. | 0.44 |
| | D | in. | 3.22 |
| First-Stage Diffuser | L | in. | 1.67 |
| | 2 θ | deg | 9.0 |

Table 3-3. OTV Main Fuel Pump Design (Continued)

| | Parameter | Units | Value |
|-----------------------|--------------------------|--|---------|
| Second-Stage Impeller | Scale Factor | — | 0.23254 |
| | ΔH Rotor | ft | 66,894 |
| | ΔH Stage | ft | 62,011 |
| | N_s | $\frac{(\text{rpm})(\text{gpm})}{(\text{ft})^3}$ | 811.5 |
| | ψ_{2M} Rotor | — | 0.576 |
| | ψ_{2M} Stage | — | 0.534 |
| | ϕ_{2M} | — | 0.082 |
| | U_{2M} | ft/sec | 1934.3 |
| | D_{1T} | in. | 1.628 |
| | D_{1H} | in. | 1.087 |
| | D_{2T}, D_{2M}, D_{2H} | in. | 2.953 |
| | h Mean | in. | 0.307 |
| | A_1 | in. ² | 0.822 |
| | A_2 | in. ² | 0.915 |
| | b_2 Exit Blade Height | in. | 0.110 |
| Second-Stage Volume | α_2 | deg | 8.1 |
| | A_3 | in. ² | 0.15 |
| | D_3 | in. | 0.437 |
| | D_4 | in. | 3.177 |
| Second-Stage Diffuser | L | in. | 1.66 |
| | 2θ | deg | 9 |

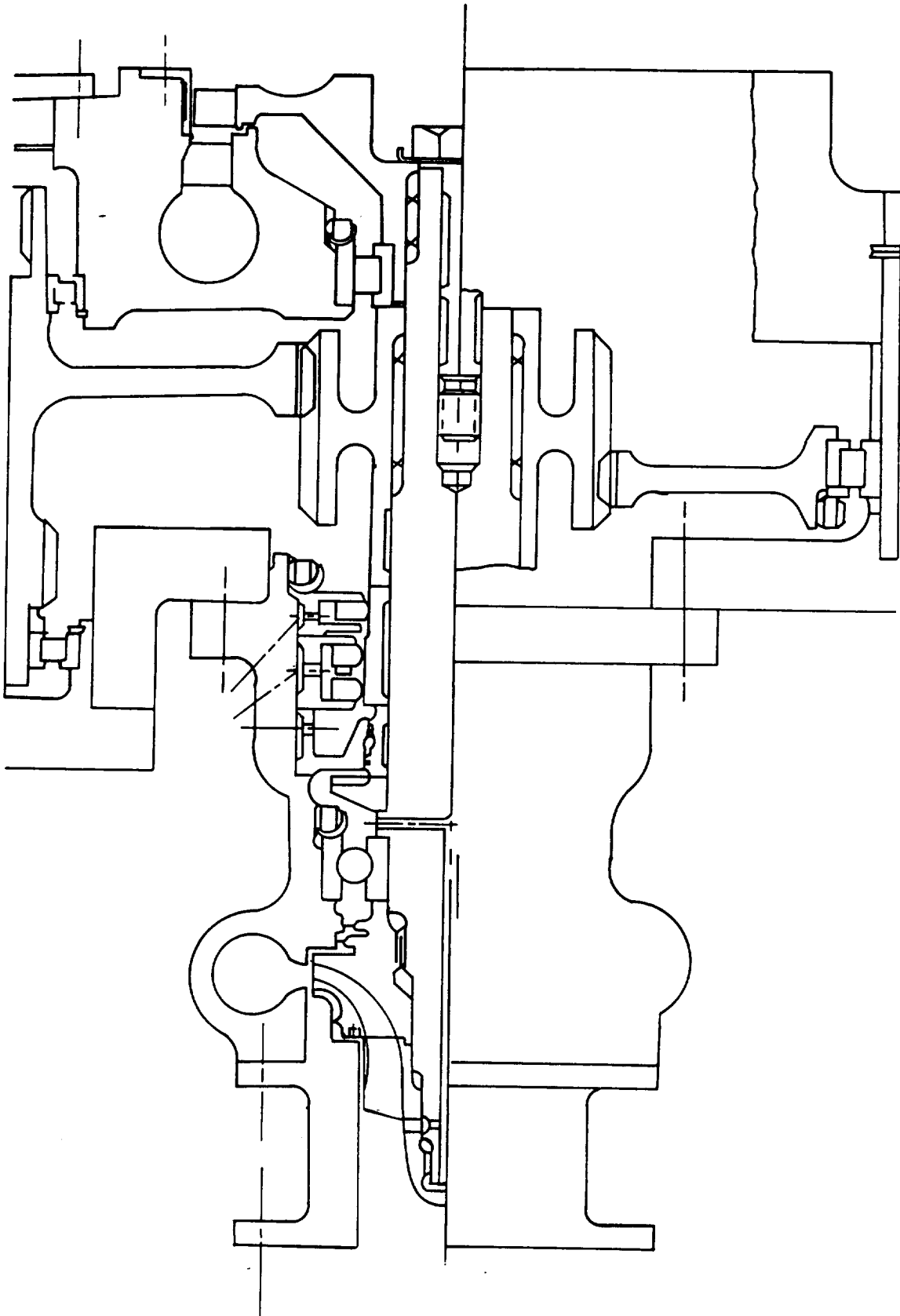


FD 212870

Figure 3-20. Main Fuel Pump

Table 3-4. OTV Main Oxidizer Pump Design

| | Parameter | Units | Value |
|----------|---|--------------------|---------|
| Pump | Q | gpm | 168.75 |
| | N | rpm | 67,390 |
| | ΔH Pump Overall | ft | 5,191.0 |
| | W | lb/sec | 26.76 |
| | P _i Inlet | psia | 94.2 |
| | P _i Outlet | psia | 2,660.8 |
| | P _{vapor} Inlet | psia | 16.0 |
| | T _i Inlet | °R | 164.0 |
| | ρ Inlet | lb/ft ³ | 71.2 |
| | η -Overall Efficiency | % | 67.4 |
| | SHP | hp | 375 |
| | NPSH Inlet | ft | 158 |
| | TSH | ft | 5 |
| Inducer | N _{ss} Capability | (rpm)(gpm) | 23,000 |
| | | (ft) | |
| | ϕ_{IT} | — | 0.133 |
| | D _{1I} | in. | 1.283 |
| | D _{1H} | in. | 0.562 |
| | D _{2I} | in. | 1.283 |
| | D _{2H} | in. | 0.729 |
| | h Tip Axial Hub Length | in. | 0.646 |
| | A ₁ | in. ² | 0.981 |
| | A ₂ | in. ² | 0.831 |
| | Scale Factor | — | 0.1757 |
| | σ -Tip Solidity | — | 2.0 |
| Impeller | Scale Factor | — | 0.1757 |
| | ΔH Rotor | ft | 5634.0 |
| | ΔH Stage | ft | 5191.0 |
| | N _s | (rpm)(gpm) | 1431 |
| | | (ft) | |
| | ψ_{2M} Rotor | — | 0.472 |
| | ψ_{2M} Stage | — | 0.435 |
| | ϕ_{2M} | — | 0.13 |
| | U _{2M} | ft/sec | 620.5 |
| | D _{1T} | in. | 1.283 |
| | D _{1H} | in. | 0.729 |
| | D _{2T} , D _{2M} , D _{2H} | in. | 2.11 |
| | h Mean | in. | 0.430 |
| Volute | A ₁ | in. ² | 0.788 |
| | A ₂ | in. ² | 0.687 |
| | b2 Exit Blade Height | in. | 0.115 |
| | α_2 | deg | 14.3 |
| | A _v | in. ² | 0.249 |
| Diffuser | D _v | in. | 0.282 |
| | D ₃ | in. | 2.374 |
| | L | in. | 2.14 |
| | 2 θ | deg | 9.0 |



FD 212871

Figure 3-21. Main Oxidizer Pump

3.4.3 Fuel Boost Pump

The fuel boost pump is an unshrouded axial flow, low speed inducer (LSI) type pump, designed for an inlet NPSH of 15 and 90 ft of TSH. The fuel LSI has been scaled from the P&WA Seajet 12-1V design to take advantage of its proven test performance. The design configuration employs three full length cambered blades and three splitter blades followed by a single discharge constant velocity volute collector with conical diffuser. The shaft is supported by a 10 mm roller bearing at the front end of the pump and by a 25 mm ball bearing at the back end.

The suction capability of 30,000 NSS for the fuel LSI design is shown in Figure 3-19 at its optimum design inlet tip flow coefficient of 0.11. Based on demonstrated Seajet 12-1V performance and collector loss calculations the overall efficiency of the fuel LSI has been estimated to be approximately 75%, with a resultant shaft horse power requirement of 25.3. Other pertinent design parameters are provided in Table 3-5. A preliminary sketch of the pump assembly is shown in Figure 3-22.

Table 3-5. OTV Fuel LSI Design

| | Parameter | Units | Value |
|----------|--------------------------|--|--------|
| | Q | gpm | 457.2 |
| | N | rpm | 46,021 |
| | ΔH Rotor | ft | 2,600 |
| | ΔH Overall | ft | 2,340 |
| | NPSH Inlet | ft | 15 |
| | TSH | ft | 90 |
| | N_s | $\frac{(\text{rpm})(\text{gpm})}{(\text{ft})}$ | 2,925 |
| | N_{ss} Capability | | 30,000 |
| | ψ_{2M} Rotor | — | 0.475 |
| | ψ_{2M} Overall | — | 0.428 |
| | ϕ_{1T} | | 0.11 |
| | ψ_{2M} | — | 0.197 |
| | P_1 Inlet | psia | 16.2 |
| | P_1 Outlet | psia | 87.4 |
| | W | lb/sec | 4.46 |
| | T Inlet | °R | 36.8 |
| | T Outlet | °R | 37.2 |
| | P_{vapor} Inlet | psia | 15.74 |
| | ρ Inlet | lb/ft ³ | 4.38 |
| | η Overall | % | 75 |
| | SHP | hp | 25.3 |
| | U_{2M} | ft/sec | 419.6 |
| | D_{1T} | in. | 2.217 |
| | D_{1H} | in. | 0.6435 |
| | D_{2T} | in. | 2.357 |
| | D_{2H} | in. | 1.780 |
| | h Hub Axial Length | in. | 1.645 |
| | σ -Tip Solidity | | 3.5 |
| | A_1 | in. ² | 3.414 |
| | A_2 | in. ² | 1.774 |
| | Scale Factor | — | 0.4284 |
| Volute | α_2 | deg | 22.5 |
| | A_v | in. | 0.68 |
| | D_v | in. | 0.93 |
| Diffuser | L | in. | 2.88 |
| | 2θ | deg | 10.0 |

FD 212872

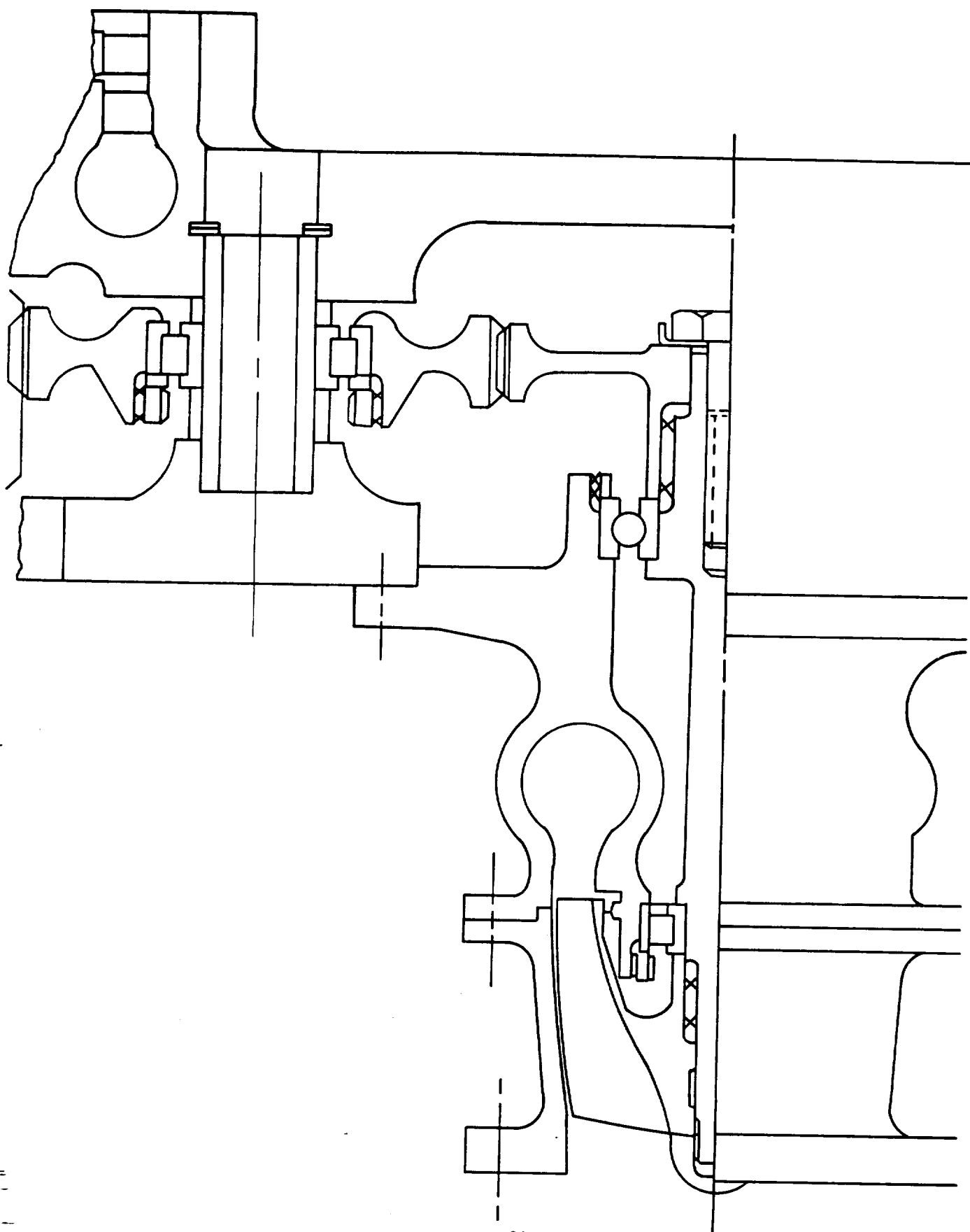


Figure 3-22. Fuel LSI Pump

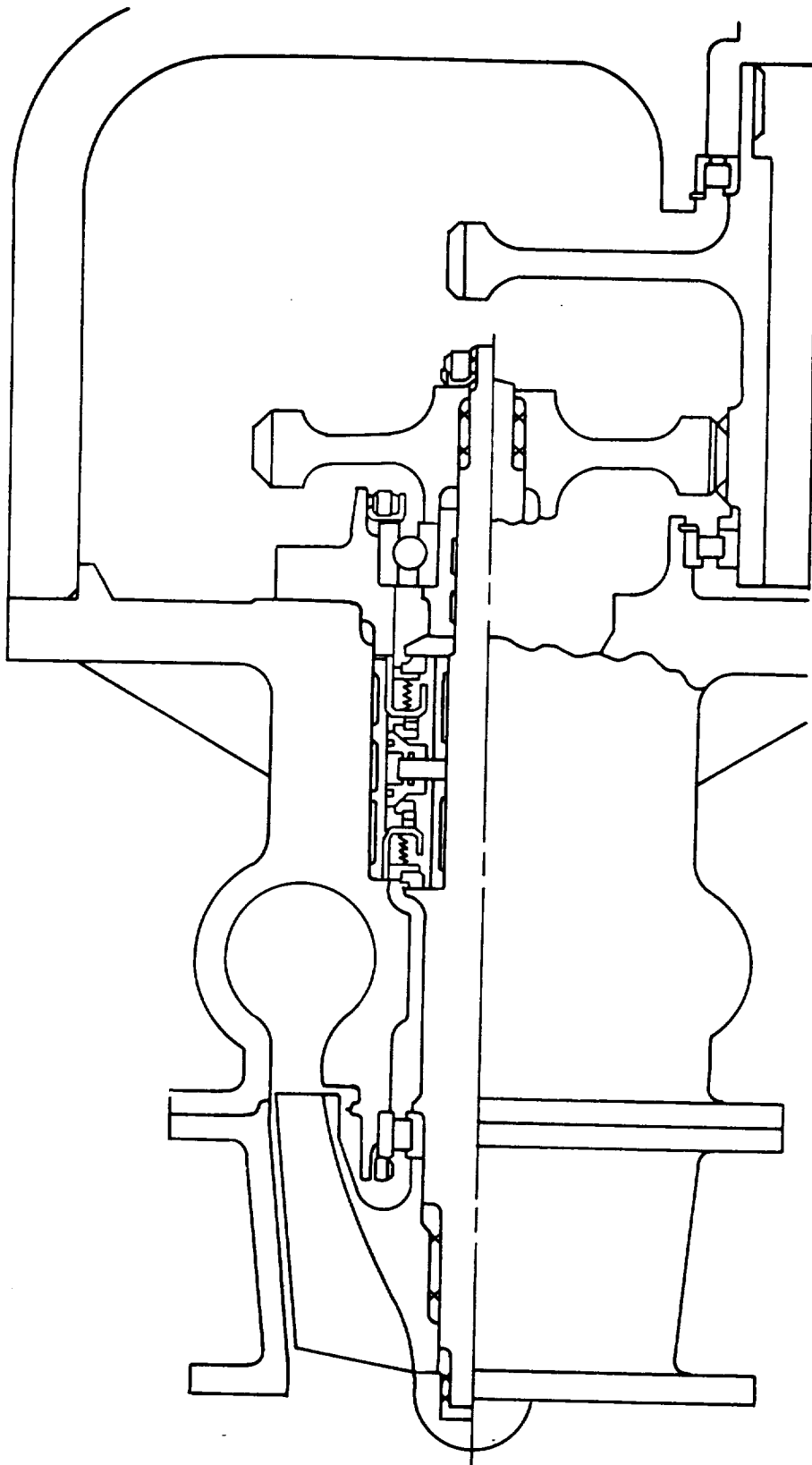
3.4.4 Oxidizer Boost Pump

The oxidizer boost pump (LOX LSI) is a scaled version of the fuel LSI since it also has been scaled from the Seajet 12-1V design to take full advantage of its proven test performance. The LOX LSI is a larger scale design than the fuel LSI to provide the required flowrate and headrise with 2 ft of inlet NPSH and 5 ft of TSH. The LOX LSI has the same configuration features as the fuel LSI, employing three full length cambered blades plus three cambered splitter blades, and a single discharge, constant velocity volute collector with conical diffuser. The shaft is supported by a 15 mm roller bearing at the front end of the pump and by a 25 mm ball bearing at the back end.

The 30,000 NSS suction capability of the LOX LSI is shown in Figure 3-19 at its optimum design inlet tip flow coefficient of 0.11. As with fuel LSI design, the overall pump efficiency was estimated to be approximately 75%, establishing a shaft horsepower requirement of 10.1 hp. Table 3-6 shows a listing of other pertinent design parameters for the LOX LSI. Preliminary sketch of the pump assembly is shown in Figure 3-23.

Table 3-6. OTV Oxidizer LSI Design

| | Parameter | Units | Value |
|----------|------------------------|--------------------|--------|
| | Q | gpm | 168.5 |
| | N | rpm | 9,946 |
| | ΔH Rotor | ft | 173.5 |
| | ΔH Overall | ft | 156.0 |
| | NPSH Inlet | ft | 2.0 |
| | TSH | ft | 5.0 |
| | N_s | (rpm)(gpm) (ft) | 2,925 |
| | N_{ss} Capability | (rpm)(gpm) (ft) | 30,000 |
| | ψ_{2M} Rotor | — | 0.475 |
| | ψ_{2M} Overall | — | 0.428 |
| | ϕ_{1T} | — | 0.11 |
| | ψ_{2M} | — | 0.197 |
| | P_1 Inlet | psia | 17.0 |
| | P_1 Outlet | psia | 94.2 |
| | W | lb/sec | 26.76 |
| | T Inlet | °R | 162.7 |
| | T Outlet | °R | 164.0 |
| | P_v Inlet | psia | 16.0 |
| | ρ Inlet | lb/ft ³ | 71.3 |
| | η Overall | % | 75 |
| | SHP | hp | 10.1 |
| | U_{2M} | ft/sec | 108.4 |
| | D_{1T} | in. | 2.650 |
| | D_{1H} | in. | 0.769 |
| | D_{2T} | in. | 2.817 |
| | D_{2H} | in. | 2.127 |
| | h Hub Axial Length | in. | 1.966 |
| | σ -Tip Solidity | — | 3.5 |
| | A_1 | in. ² | 4.874 |
| | A_2 | in. ² | 2.537 |
| | Scale Factor | — | 0.512 |
| Volute | α_2 | deg | 22.5 |
| | A_v | in. | 0.97 |
| | D_v | in. | 1.11 |
| Diffuser | L | in. | 3.45 |
| | 2θ | deg | 10.0 |

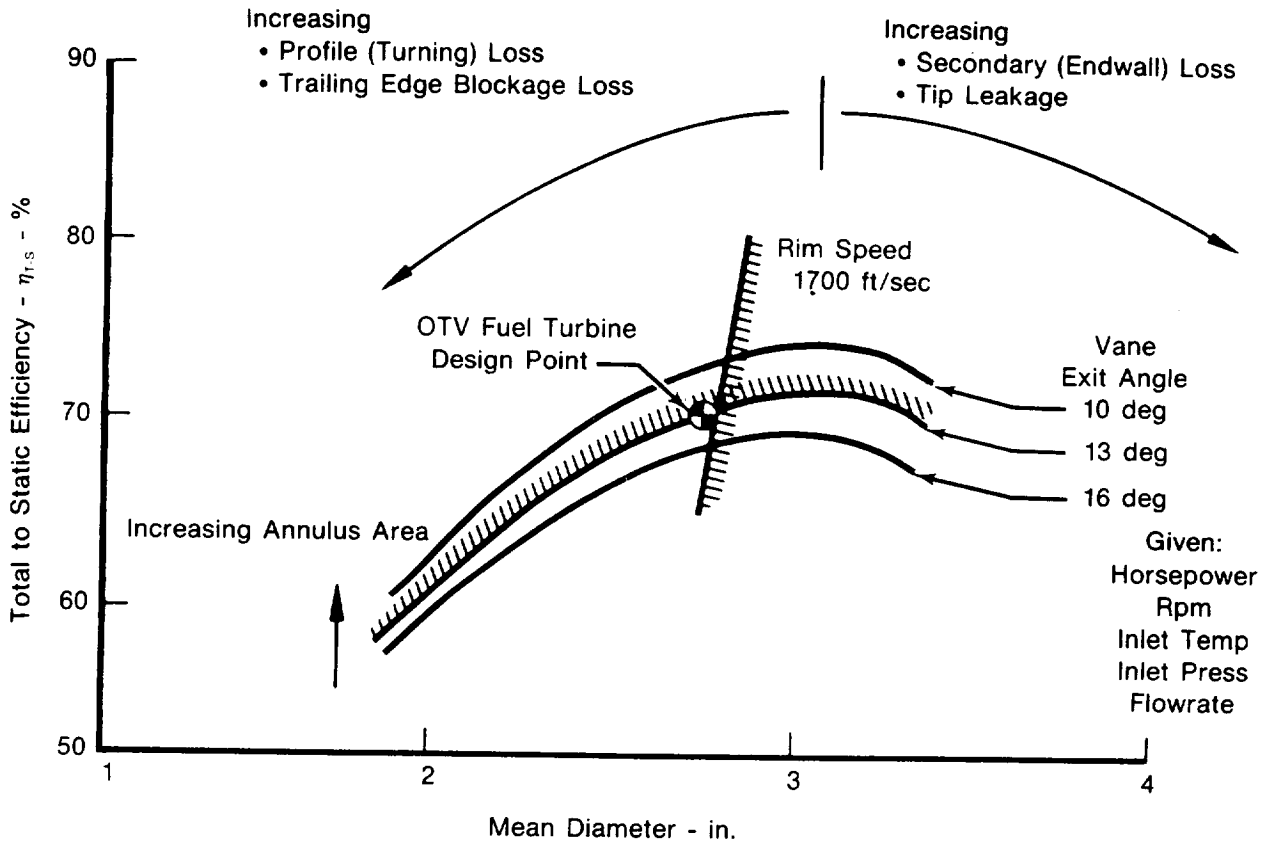


FD 212873

Figure 3-23. Oxidizer LSI Pump

3.4.5 Fuel Turbine

The fuel pump drive turbine is an axial flow, full admission, single stage design deriving its power from the expansion of the heated hydrogen propellant used to cool the thrust chamber/nozzle. A low reaction blade design was chosen to minimize axial thrust loads. A parametric study was used to size the turbine for maximum performance as shown in Figure 3-24. A maximum turbine rim speed of 1700 ft/sec was set as a limit, as being within but near the limits of design experience. This resulted in a turbine efficiency slightly below the maximum attainable, but the 1 to 2% increase in available efficiency was judged not worth the possible structural problems resulting from a higher rim speed.



FD 212874

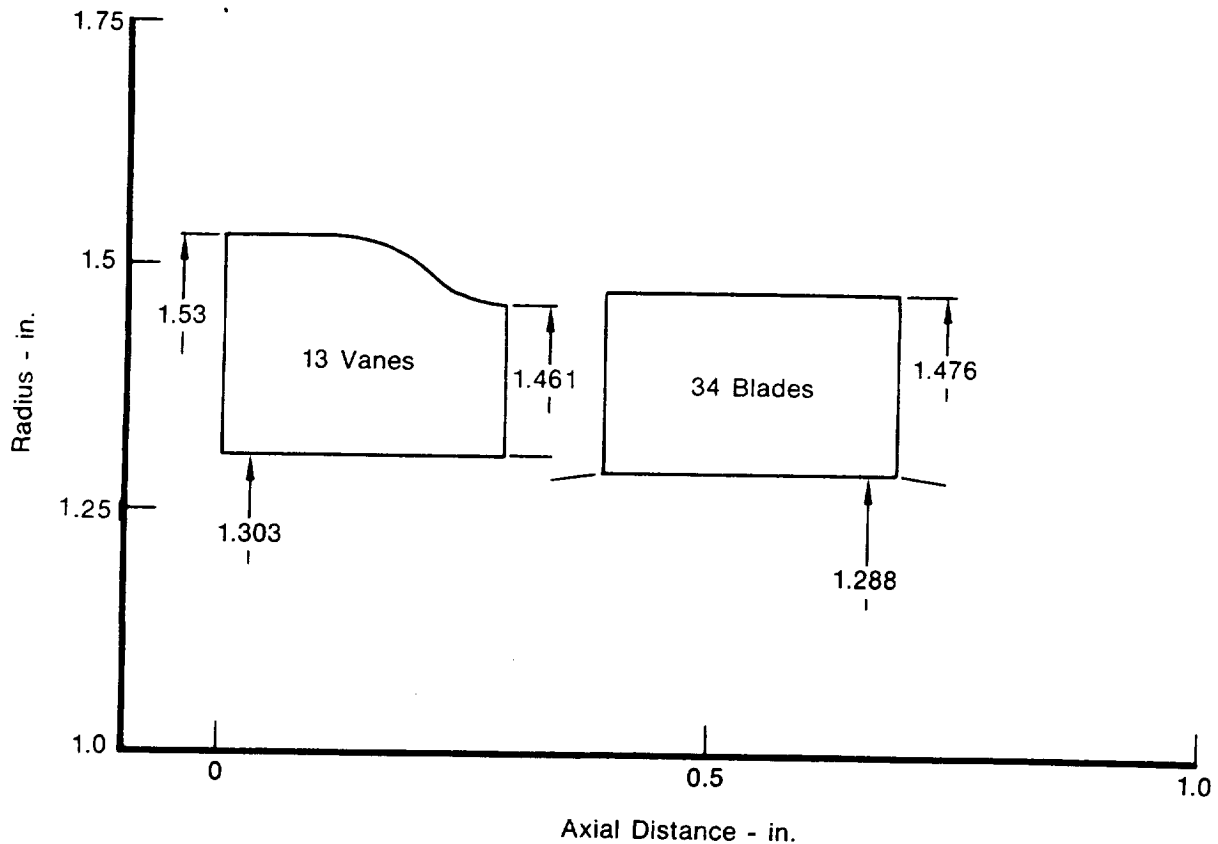
Figure 3-24. OTV Fuel Turbine Parametric Sizing Study

The fuel turbine develops 1630 hp at the design point with a total to static pressure ratio of 1.562 and an efficiency of 71.2%. The turbine design point is at 100% thrust and mixture ratio of 6.0. Table 3-7 presents the turbine design point operating conditions.

The fuel turbine elevation is shown in Figure 3-25. The axial chord lengths for the vanes and blades were set at 0.29 in. and 0.30 in., respectively. These were selected as being the smallest allowable to minimize aerodynamic losses of each airfoil. For a given height, small chords yield high aspect ratios, which in turn maintain low airfoil end losses. A blade radial tip clearance of 0.01 in. is required to achieve the design efficiency for the fuel turbine.

Table 3-7. Advanced Expander Cycle Engine Fuel
Turbine Operating Conditions at De-
sign Point

| | |
|------------------------|----------------------|
| Rotor Speed, rpm | 150,000 |
| Rim Velocity, ft/sec | 1,686 |
| Tip Velocity, ft/sec | 1,932 |
| Velocity Ratio | 0.449 |
| Flow Rate, lb/sec | 4.203 |
| Inlet Temperature, °R | 859 |
| Inlet Pressure, psia | 3,144 |
| Efficiency, % | 71.2 |
| Pressure Ratio | 1.565 |
| Power, hp | 1,628 |
| Reaction % | 13 |
| Tip Clearance, in. | 0.01 |
| Number Vanes | 13 |
| Number Blades | 34 |
| Vane Axial Chord, in. | 0.29 |
| Blade Axial Chord, in. | 0.30 |
| Vane Inlet Angle, deg | 90 |
| Blade Inlet Angle, deg | 26.3 |
| Vane Exit Angle, deg | 13.4 |
| Blade Exit Angle, deg | 17.8 |
| Mean Diameter, in. | 2.76 |
| AN | 304×10^{-6} |



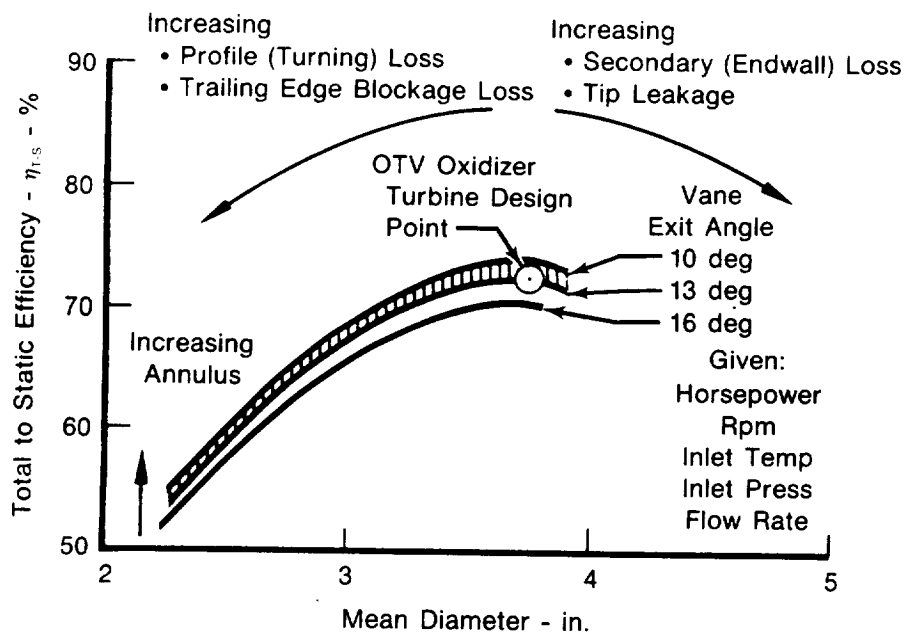
FD 212875

Figure 3-25. OTV Expander Cycle Fuel Turbine Elevation

3.4.6 Oxidizer Turbine

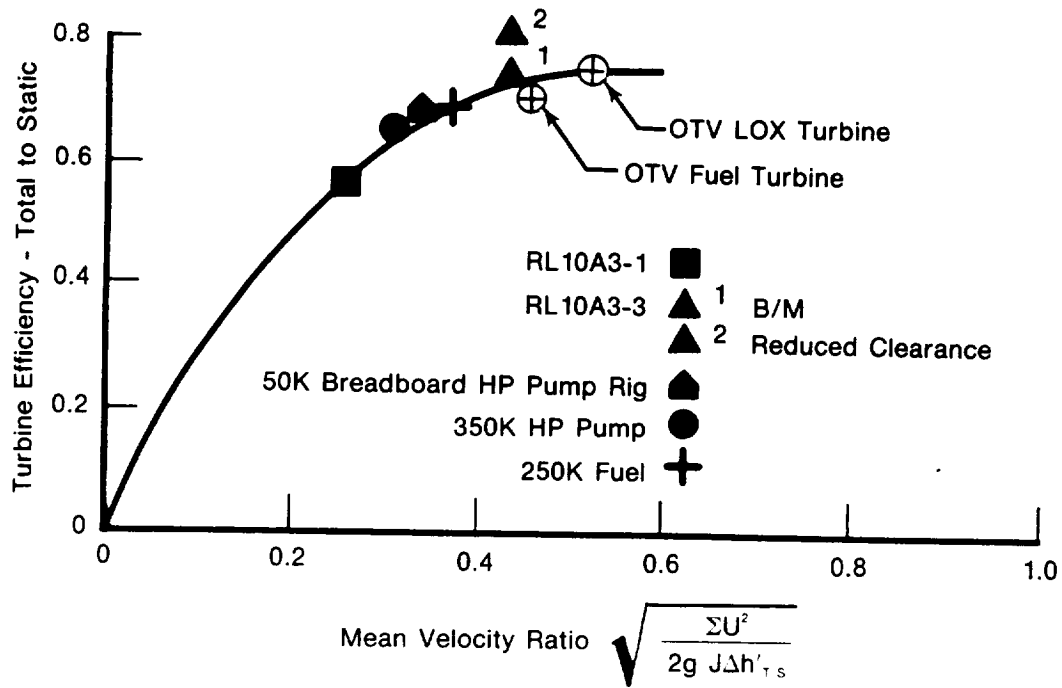
The oxidizer pump drive turbine is an axial flow, full admission, single stage design placed in series with the fuel turbine, therefore utilizing the same driving fluid. This turbine is also used to drive the fuel and oxidizer low speed inducers through a gearing system. As with the fuel turbine, a low reaction blade design was chosen to minimize axial thrust loads, and a parametric study was used to size the turbine for maximum performance as shown in Figure 3-26. However, unlike the fuel turbine, the oxidizer turbine, rim speed (1000ft/sec) was well below the chosen limit value of 1700 ft/sec allowing the maximum attainable efficiency to be achieved. A comparison of the Advanced Expander Cycle engine fuel and oxidizer turbine efficiencies with past P&WA designs is shown in Figure 3-27, indicating the design efficiencies are consistent with previously achieved levels.

Table 3-8 presents the oxidizer turbine design point operating conditions, and an elevation schematic is shown in Figure 3-28. The oxidizer turbine requires a blade radial tip clearance of 0.01 in. to achieve the design efficiency.



FD 212876

Figure 3-26. OTV Oxidizer Parametric Turbine Sizing Study

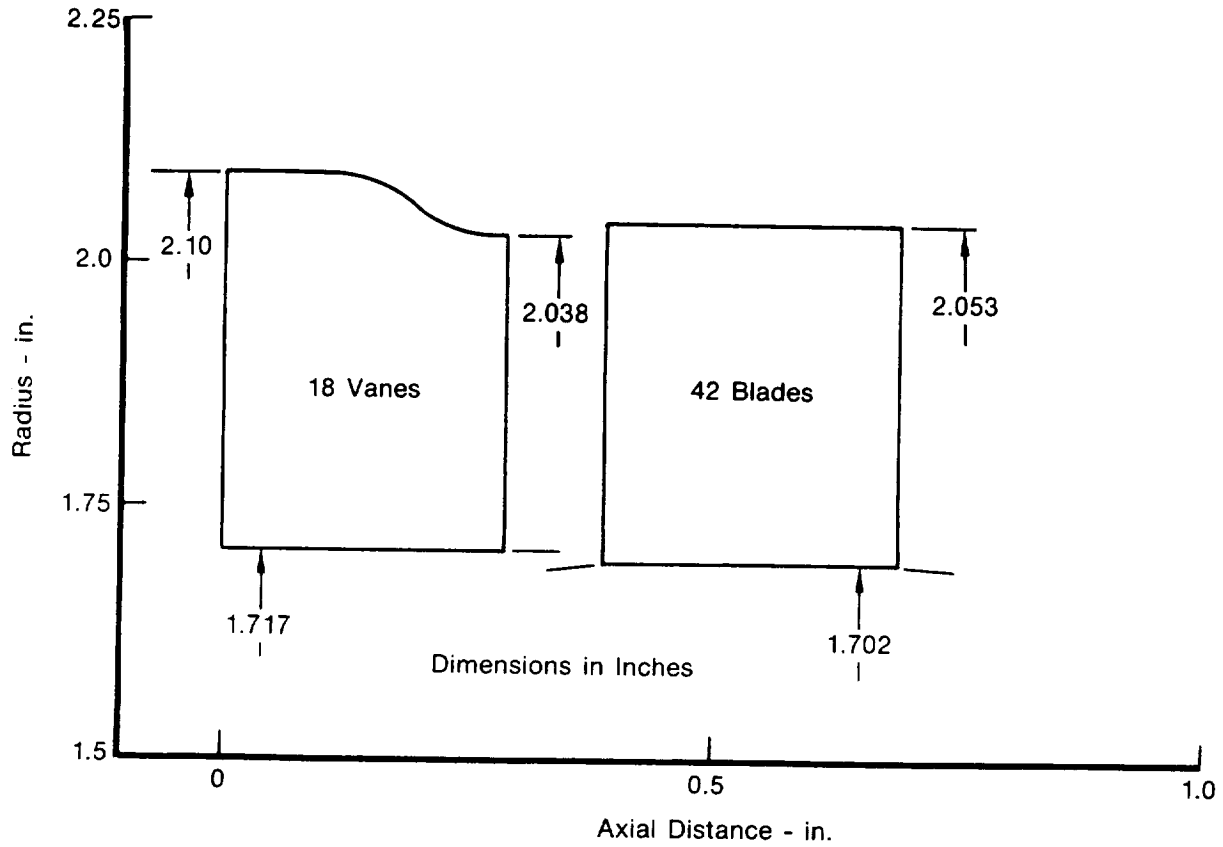


FD 212877

Figure 3-27. OTV Expander Cycle Oxidizer Turbine Elevation

Table 3-8. Advanced Expander Cycle Engine Oxidizer Turbine Operating Conditions at Design Point

| | |
|------------------------|-------------------|
| Rotor Speed, rpm | 66,000 |
| Rim Velocity, ft/sec | 1,001 |
| Tip Velocity, ft/sec | 1,207 |
| Velocity Ratio | |
| Flow Rate, lb/sec | 4.203 |
| Inlet Temperature, °R | 788 |
| Inlet Pressure, psia | 1,955 |
| Efficiency, % | 75.7 |
| Pressure Ratio | 1.103 |
| Power, hp | 359 |
| Reaction % | 19 |
| Tip Clearance, in. | 0.01 |
| Number Vanes | 18 |
| Number Blades | 42 |
| Vane Axial Chord, in. | 0.29 |
| Blade Axial Chord, in. | 0.30 |
| Vane Inlet Angle, deg | 75 |
| Blade Inlet Angle, deg | 30 |
| Vane Exit Angle, deg | 13 |
| Blade Exit Angle, deg | 18 |
| Mean Diameter, in. | 3.76 |
| AN ² | 169×10^8 |



FD 212878

Figure 3-28. Oxidizer Turbine Elevation

SECTION 4

COMPONENT MECHANICAL DESIGN

4.1 THRUST CHAMBER/NOZZLE ASSEMBLY

The performance requirements set down for the Advanced Expander Cycle engine calls for an advanced technology thrust chamber/nozzle assembly design to ensure combustion efficiency and stability during steady-state and transient operation. The results of performance, heat transfer, and structural assessments were culminated in a mechanical design layout, where the analytical studies were traded against fabrication, component geometry, and weight requirements. The thrust chamber/nozzle assembly consists of four major components: 1) the injector, 2) The nontubular, regeneratively-cooled thrust chamber, 3) the tubular regeneratively-cooled nozzle, and 4) the radiation-cooled carbon-carbon extendible nozzle. A layout of the thrust chamber/nozzle assembly is presented in Figure 4-1 and a mechanical description of each component follows.

4.1.1 Injector

The propellant injector is schematically depicted in Figure 4-2 . The function of the propellant injector is to atomize the oxidizer and thoroughly mix fuel and oxidizer to provide the correct conditions necessary for efficient combustion. The propellant injector consists of multiple injection elements arranged in a hexagonal pattern around a central torch igniter, each element consisting of an oxidizer tube and a concentric fuel orifice. Liquid oxygen enters the injector through the oxidizer injector manifold, flows into the injector cavity and out oxidizer orifices into the combustion chamber. The oxidizer is admitted to the injector element through three tangential slots swirling the oxidizer flow and promoting mixing with hydrogen flow at the end of the element. The outer oxidizer elements of the injector are scarfed at a 45 deg angle to prevent oxidizer impingement on the wall.

Gasous hydrogen enters the peripheral fuel injector manifold and flows into the injector cavity. The fuel cavity has a 0.5 in. height between the back of the injector faceplate and oxidizer cavity to minimize static pressure drop across the cavity, providing fuel flow uniformity. Most of the hydrogen flows out through the annular orifices around each oxidizer element. The full annular design of the fuel orifices is preferred for uniform distribution. It has extremely close tolerances and, since concentricity must be maintained, it may be necessary to insert 3 tangs into the annulus to preserve that concentricity. Approximately 5% of the fuel flow passes out into the combustion chamber through a porous-weld, steel-mesh plate (Rigimesh). This flow provides transpiration cooling of the injector face during engine operation.

Immediate contact between oxidizer and fuel is made at each element as the propellants leave the injector face and enter the combustion chamber. This configuration is designed to provide thorough combustion, high combustion efficiency, and high specific impulse.

Thrust chamber ignition is provided by a torch igniter system as shown in Figure 4-3. The igniter is centrally located in the injector face. A metered flow of hydrogen and oxygen is mixed in an igniter chamber, ignited by a spark, and passed into the combustion chamber to ignite the main propellants. Increased reliability is accomplished by providing dual exciters and spark igniters and, with continuous operation, by eliminating the need for igniter propellant shutoff valves. The dual spark and exciter configuration provides a fail-safe energy source and designing the igniter to operate at rated thrust with oxidizer and fuel igniter flows eliminates the possibility of igniter damage due to valve leakage.

FD 213618

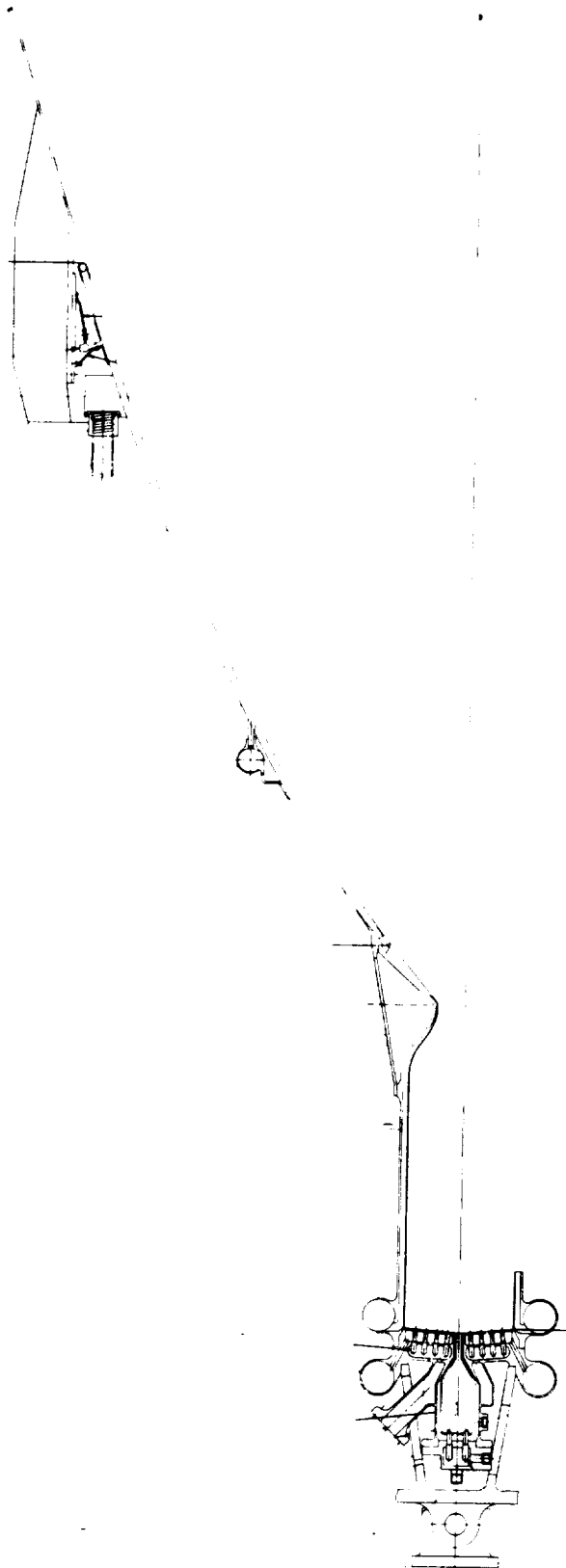
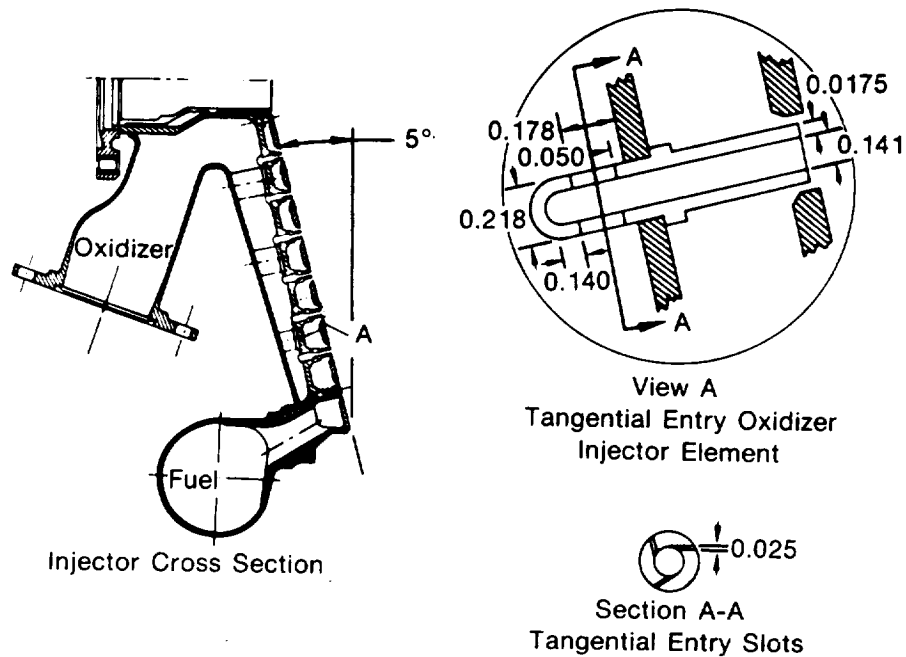
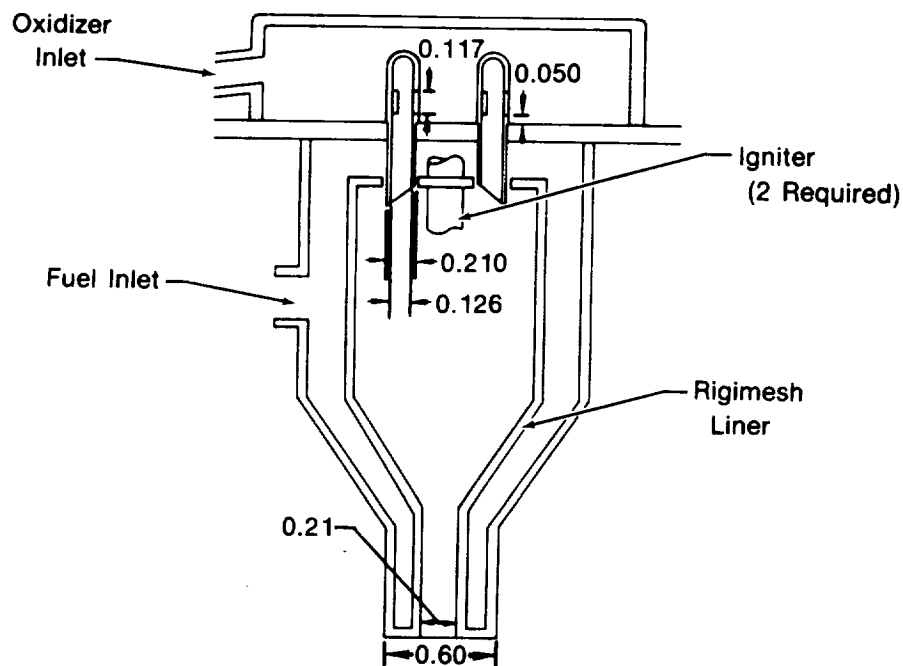


Figure 4-1. Thrust Chamber/Injector/Nozzle Assembly



FD 212879
810505
bet-752

Figure 4-2. Advanced Expander Cycle Engine Injector



FD 212880

Figure 4-3. Advanced Expander Cycle Engine Igniter Assembly

The fuel and oxidizer is ignited by a spark exciter assembly which provides a minimum of 20 sparks/sec at an energy level of 0.1 joules. The total oxidizer flow is injected into the igniter through two tangential entry swirl elements located at the upper end of the igniter chamber. Fuel flow is split; part of the flow is delivered to a concentric slot surrounding each oxidizer injector element and the remainder is used for igniter barrel cooling, flowing through a rigimesh liner. The burned propellants are discharged into the main chamber through the igniter injector sleeve.

4.1.2 Thrust Chamber

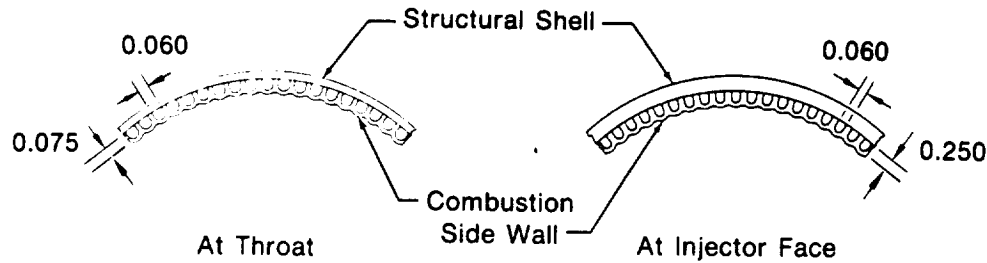
The thrust chamber has a one-piece copper alloy liner. The heat fluxes experienced by the chamber are high and require the use of a high thermal conductivity material such as copper. The thermal fatigue properties of pure copper can be improved with only a slight reduction in conductivity by alloying with small amounts of other metals. The alloy selected for this design was AMZIRC, an oxygen-free copper alloy containing 0.15% zirconium. The AMZIRC is obtained as a forging and cold-worked by spinning to rough shape on a mandrel to increase strength. After spinning, the ID surface is final machined and 80 coolant channels are machined or EDM in the OD. The passages are filled with an electrically conductive wax and a thin copper layer is electrodeposited on top. A nickel outer shell is electroformed over the milled liner to provide structural integrity to the cooling passages. The thin copper layer acts as a protective barrier between the hydrogen coolant and the nickel shell to alleviate possible property-reducing hydrogen embrittlement of the nickel. Finally, the wax is removed, leaving the chamber with cooling passages.

Thrust chamber low-cycle fatigue (LCF) life is a major consideration in the selection of an engine operating point. The LCF of the regeneratively cooled thrust chamber results from the large thermal strains that are introduced between the heated inner wall of the chamber and the cooler outer structural wall. The problem of evaluating thrust chamber LCF life capability has been approached by: 1) identifying the critical locations in the thrust chamber for analysis, 2) determining the LCF life capability at those locations, and 3) making modifications to the chamber geometry and/or engine operation to ensure that the life requirements have been met.

A LCF analysis of the thrust chamber showed that the minimum life occurs at the throat and was calculated to be 190 cycles using $\frac{1}{2}$ hard AMZIRC fatigue properties. The OTV mission requirement is 1200 cycles (300 cycles with a safety factor of 4). The analysis made used a square passage geometry for the coolant channels. A domed passage geometry, shown in Figure 4-4, was then considered as a means of reducing the pressure bending stresses and increasing the flexibility to lower thermal stresses. The calculated life for the improved configuration analyzed was 760 cycles. Incremental load data from a MARC plastic finite element analysis indicates that lowering the hot-wall temperature by approximately 80 deg would result in 1200 cycles life with $\frac{1}{2}$ hard AMZIRC. Based on limited LCF data available, using aged AMZIRC instead of $\frac{1}{2}$ hard AMZIRC could increase the predicted life by more than a factor of 3 (\approx 2500 cycles).

4.1.3 Tubular Nozzle

The tubular regeneratively-cooled nozzle is identical in concept to the tubular nozzle used on the RL10 production engine. It consists of a pass-and-a-half heat exchanger made up of 180 long and 180 short tubes extending from the end of the nontubular section at $\epsilon = 6$ to the start of the radiation-cooled nozzle at $\epsilon = 210$. The tube split, required to accommodate the change in circumference while providing tube cross sections consistent with cooling requirements and fabrication limitations, is at an area ratio of 60:1. Flow is from the transition manifold at $\epsilon = 6$, parallel to the combustion gases through the long tubes, to a turnaround manifold at $\epsilon = 210$, and then through the short tubes, counterflow, to the exit manifold at $\epsilon = 60$.



Chamber Diameter 5.06 in.

Throat Diameter 2.53 in.

Axial Length 15.00 in.

- 80 milled cooling passage slots vary in depth along axial length
- Electro-formed outer wall provides structural shell

FD 212881

Figure 4-4. Combustion Chamber Assembly

Alloy PWA 770 (347SST) was selected as the tube material. Both full-length and short tubes are furnace brazed together to form a seal and are structurally supported by stiffener bands to carry the chamber hoop loads and minimize the effect of any flow-induced vibration. To establish band locations, tubes are treated analytically as beams subjected to thermal stress by the hot-cold wall temperature differential and from nozzle static wall temperature differential and bending stress from nozzle static wall pressure; longitudinal loads due to thrust, maneuver loads, and gimbaling acceleration are also considered. Bands are placed to establish beam lengths, which limit tube stresses to a level below the material yield strength at a factor of safety of 1.1.

4.1.4 Nozzle Extension

The nozzle extension is radiation cooled, and made of a lightweight carbon-carbon composite. This composite is capable of withstanding high temperatures and is currently being developed for gas turbine engine components such as augmentor cases and nozzle flaps.

The nozzle extension actuation system (Figure 4-5) is identical to the one used for Category IV Derivative Engine. The extendible nozzle is translated by means of a jackscrew actuation system. The translating structure consists of three ballscrew jackshafts which are attached on the rear of the primary nozzle by individual drive gearbox and bearing assemblies, and are supported at their forward end by an adjustable link. The ballscrew shaft is supported on antifriction bearings at both the front and rear locations. These ball bearings, which take axial and radial loads, are housed in a spherical ball joint that compensates for shaft misalignment as great as 2 deg.

The nozzle drive/synchronization system consists of two electric motors and three interconnecting flexible cables which transmit motor torque to three gear transmissions which drive the ballscrew shafts. A locking mechanism at the base of one ballscrew assembly locks the nozzle in either the extended or retracted position. The lock is a springloaded normally locked mechanism.

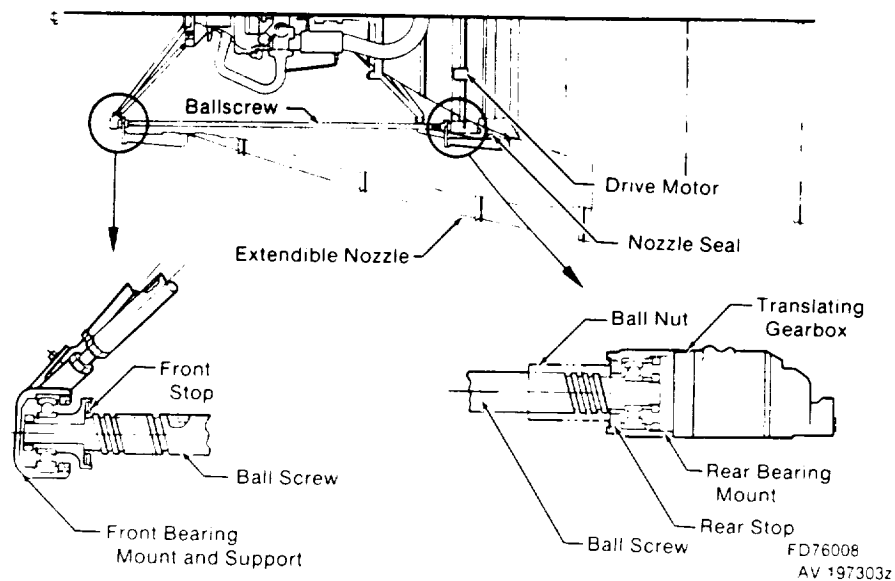


Figure 4-5. Nozzle Translation System

A spline is added to the cable at the lock location so that engaging the spline stops the travel. The engagement is ensured by dual helical springs loading the spline locks. When electric power is supplied to the drive motor, the electric solenoids within the lock are energized and movement of the solenoid rotates the cam, and depresses the cam follower and springs within the lock mechanism. This disengages the spline lock and allows the drive shaft to rotate. The fixed spline lock is always the first to engage and it moves with the shaft pulling the floating spline into the locked position. Rotation torque is taken out by the spline lock pivot pin. The redundant lock solenoids are actuated during nozzle translation only.

The nozzle is attached to the translating mechanism at three equally spaced points through a nozzle attachment bracket to the ballscrew. The nozzle attachment bracket consists of a split circular ring and two piece yoke. The ballnut gimbal attachment bracket provides 2 degrees of freedom to prevent transferring bending loads from the nozzle attachment bracket to the ballnut.

The extendible nozzle seal is cooled by the turbopump gearbox hydrogen. The ballscrew rods may be made from carbon-carbon composite.

4.2 HEAT EXCHANGERS

The heat exchangers (gaseous oxygen and hydrogen regenerator) are composed of plates with grooves etched on one side, stacked and brazed together with manifolds brazed on each of the ends. The heat exchanger plates alternately contain hydrogen and oxygen, in a cross flow configuration. Both hydrogen and oxygen plates in the GOX HEX and the hot and cold hydrogen plates in the hydrogen regenerator, are the same except for the direction in which the fluid passages (grooves) are etched. The core of the heat exchanger is based on laser mirror heat exchanger designs. The heat exchangers are made of aluminum (manifolds and core) to minimize weight. However, development of an aluminum braze that would not plug the fluid passages is required.

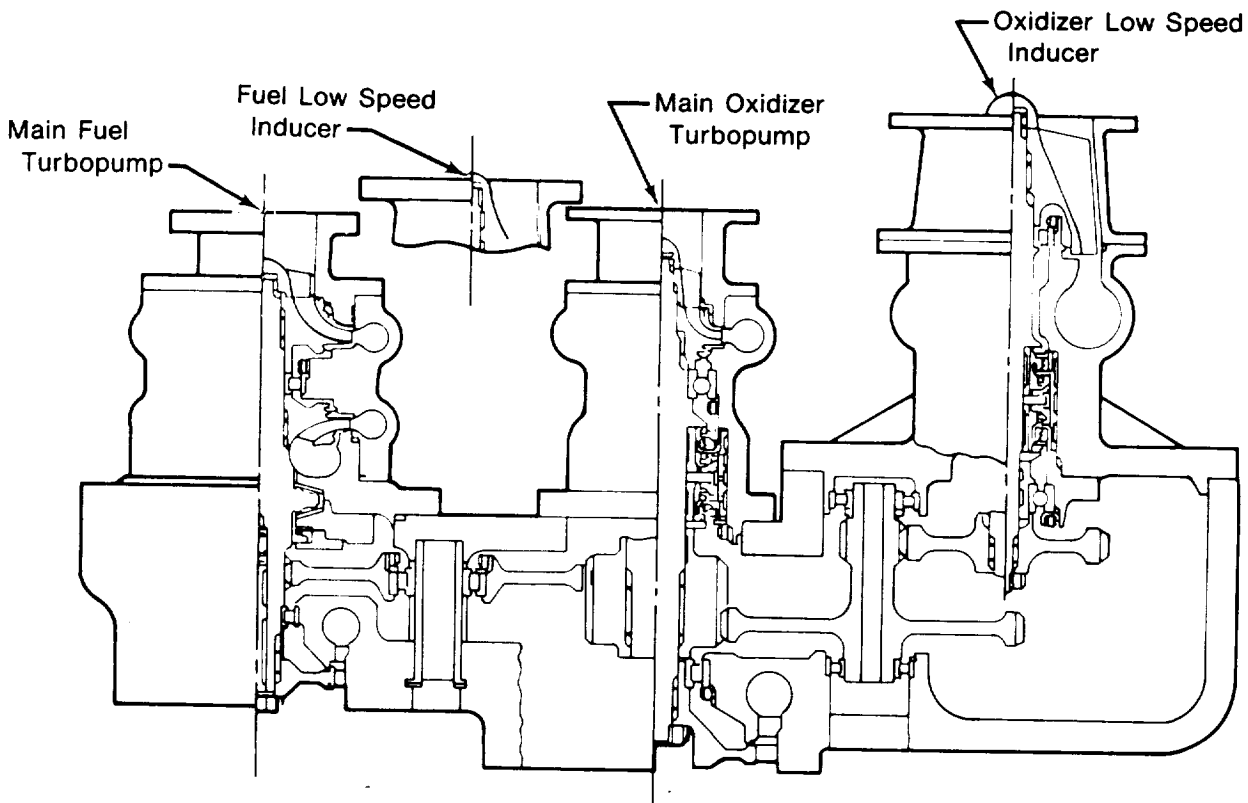
The GOX heat exchanger manifold required internal structural reinforcing webs due to the high internal and long unsupported manifold span on the hydrogen side. An additional oxygen outlet was incorporated into the HEX to provide gaseous oxygen for tank pressurization. The tank pressurization outlet is to have its own dedicated portion of the heat exchanger within the GOX HEX in order to provide the required state of oxygen for tank pressurization. However, the heat exchanger layout does not reflect this because this additional outlet was not known to be required until the design of the HEX was completed and the schedule did not permit a redesign.

A vortex prevaporizer was designed and placed upstream, on the oxygen side of the GOX heat exchanger. The design is of a concentric tube configuration with LOX entering the inner tube tangentially. An outer jacket of hot hydrogen gas heats the liquid oxygen. The light oxygen gas goes to the center of the tube, while the heavy liquid remains at the OD due to the centrifugal force. Radial fins at the inner tubes exit changes the tangential flow into an axial flow direction. This configuration provides a gradual phase change of oxygen from the liquid to approximately 20% quality condition to prevent instability problems.

4.3 TURBOPUMPS

4.3.1 Mechanical Description

The fuel and oxidizer main pumps and low speed inducers comprise the turbopump assembly (Figure 4-6). The pumps are driven by two single stage turbines, a turbine on both main pump shafts. The low speed inducers are gear driven off the oxidizer pump shaft. A synchronizing gear has been included between the fuel and oxidizer main pump shafts to simplify the control system.



FD 212882

Figure 4-6. Turbopump Assembly

The fuel pump is a two-stage centrifugal design driven by a single stage turbine. The impellers, arranged back-to-back, are made of titanium and have diffusion bonded shrouds. The impellers and turbine disk are splined onto the shaft which transmits the torque. The pump housing is made of AMS 4215 aluminum (casting). The housing contains the two circumferential volute diffusers, each having a single conical discharge. The shaft is supported by two 20mm roller bearings, one located between the two impellers and the other one immediately forward of the turbine disk. The bearings are hydrogen cooled and the aft bearing may be jetted with hydrogen if additional cooling is required. A bearing DN of 3.0×10^6 is obtained with the fuel pump speed of 150,000 rpm. A bearing DN of 2.64×10^6 was run in the XLR 129 fuel pump. Some development is required to design and manufacture a roller bearing that is reliable at this operational parameter. Tiebolts fore and aft on shaft maintain a preload on the impellers, bearings and turbine. A double acting thrust piston has been incorporated onto the shaft to restrain the shaft thrust load. The piston is fed 2nd-stage impeller discharge pressure to each side. The resultant thrust is in the forward direction thereby allowing the aft piston pressure feed to be channeled back to the 2nd-stage inlet. The thrust piston lands rub against leaded bronze inserts in the pump housing. This piston configuration is similar to the one used in the XLR-129 fuel pump. A controlled gap carbon circumferential seal is used to prevent the thrust piston, high-pressure hydrogen, from entering the gearbox cavity. The pump has the capability of being high speed balanced as an assembly by the insertion of cylindrical weights into holes predrilled on the forward side of the impeller shroud and the aft side of the turbine disk.

The oxidizer pump incorporates several of the same features as the fuel pump (assembly balancing capability, single-stage turbine, volute diffuser). The single stage shrouded centrifugal design is driven by a single-stage hydrogen turbine. The shaft axial thrust load (200 lb) is restrained by a 25 mm ball bearing located just aft of the impeller. A 25 mm roller bearing is located on the aft portion of the shaft. The ball bearing is cooled by LOX while the aft roller bearing is cooled by hydrogen. A controlled gap, multiple vented cavity arrangement was used to prevent mixing of the hydrogen and oxygen.

Both fuel and oxidizer low speed inducers are axial flow with three blades and three splitters. The inducers have an axial volute diffuser with a single discharge. The inducers are gear driven off the oxidizer pump shaft. A roller bearing has been placed under the inducer and a ball bearing just forward of the gear. The inducers are made of AMS 5362 SST. The oxidizer low speed inducer contains the basic seal design as the RL10 LOX pump.

The hydrogen flow to the two turbines is arranged in series, with the fuel pump turbine being upstream of the oxidizer turbine. The turbopump gears are encased in a one piece aluminum casting gearbox. The one piece gearbox minimizes gear misalignment by allowing the bearing races and mounting surfaces to be matched with a minimum of overall tolerances. The synchronizing gear and oxidizer-pump-to-fuel-low-speed-inducer idler gear have a single roller bearing to minimize misalignment. The gear teeth will be dry film lubricated with PWA 550. Spur gears, made of AMS 6265, are used exclusively with a diametral pitch of 18 and pitch line velocity of 39,300 ft per min. The gear train is lightly loaded and therefore can operate successfully at this high pitch line velocity.

The gears are cooled by the gaseous hydrogen that flows through the gearbox and is then used to cool the seal for the extendable nozzle. If it is determined that additional cooling is required, liquid hydrogen can be jetted onto the teeth. A Hertz stress of 100,000 psi has been used to determine the gear teeth configurations. A reduction idler gear was needed between the oxidizer pump and oxidizer LSI to reduce the speed from 67,390 rpm to 9950 rpm. A list of the selected turbopump materials is presented in Table 4-1.

Table 4-1. Turbopump Materials

| | | |
|---------------------|---|---|
| Impeller (Hydrogen) | — | Titanium (A-110) AMS 4924 |
| Impeller (Oxygen) | — | Nickel Alloy (Inco 718) PWA 1010 |
| Low Speed Inducers | — | Stainless Steel AMS 5362 |
| Shafts | — | Nickel Alloy (Inco X-750) AMS 5667 |
| Turbine Disks | — | GATORIZED [®] nickel alloy (IN-100) PWA 1073 |
| Housings | — | Aluminum (C355) AMS 4215 |
| Gears | — | Carburizing Steel AMS 6265 |
| Bearings | — | Stainless Steel AMS 5630 |

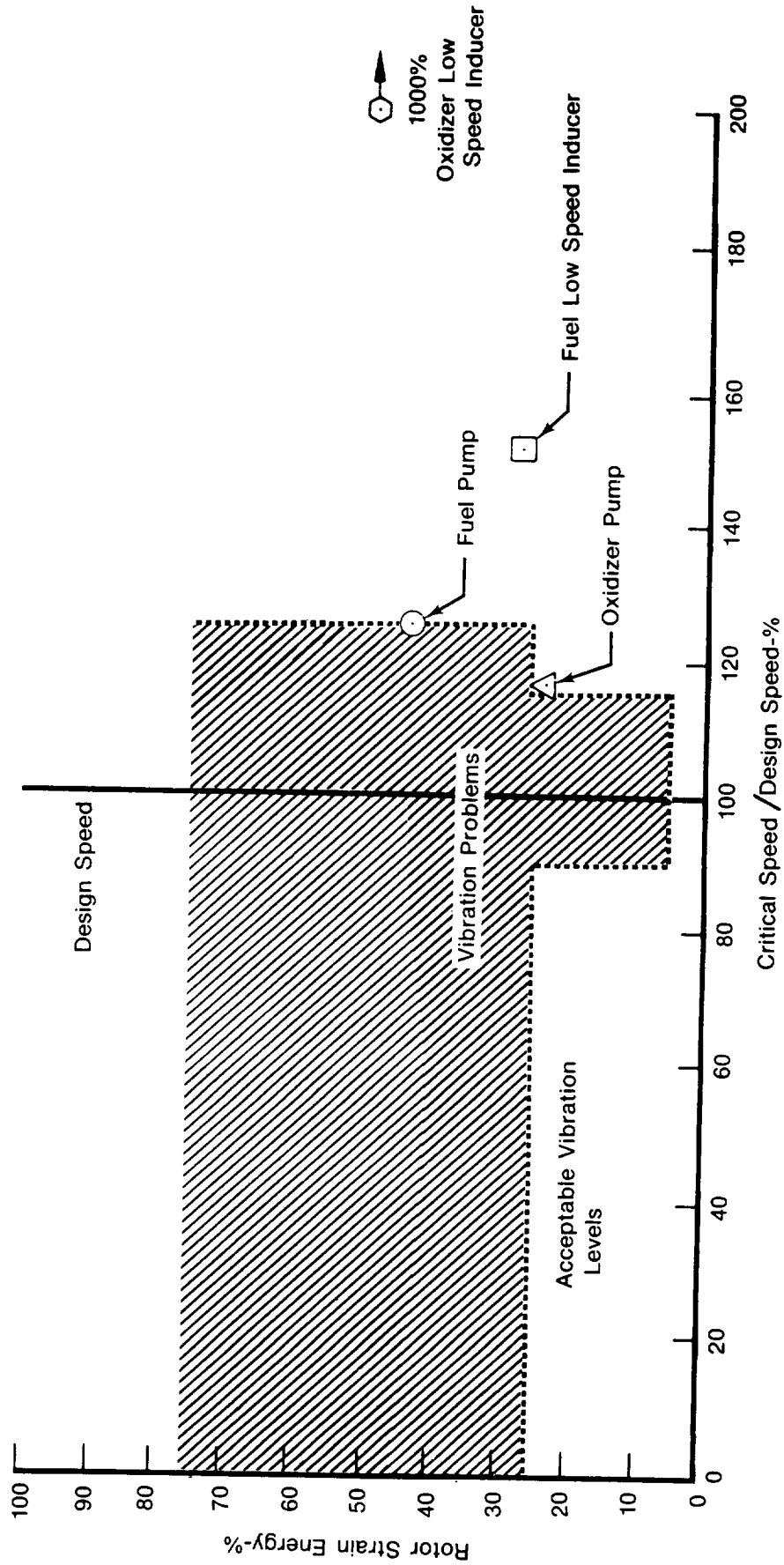
4.3.2 Critical Speed and Bearing Loads

The performance goals of the OTV program necessitate state-of-the-art components. The resulting turbomachinery contains lightweight, high speed rotors. Table 4-2 summarizes the various pump rotor weights and maximum operating speeds. Rotor dynamics analyses of the main fuel pump, main oxidizer pump, fuel low speed inducer, and oxidizer low speed inducer predict acceptable margins over the maximum operating speeds as shown in Figure 4-7. For this design, acceptable critical speed margins were defined as a 15% margin over maximum operating speed for modes with less than 25% rotor strain energy and a 25% margin over maximum operating speed for modes with more than 25% rotor strain energy. These criteria require careful rotor design and multiplane balancing during final pump design.

The turbopump ball and roller bearings were evaluated using Jones II Bearing Analysis Deck (A926). A life factor of one (1X) was used for both ball and roller bearings. The 100 hr design life includes a 10% reliability factor used for cryogenic applications. The dynamic bearing loads (Figures 4-8 and 4-9) were calculated by assuming unbalances equal to the weight of the impellers and turbine disks offset 0.001 in. from the rotor centerline, with phase relationships that produce the maximum bearing load. The analysis revealed that the ball and roller bearings for the fuel LSI pump, oxidizer pump, and oxidizer LSI pump will reach 100-hr life if the bearings have the geometry indicated in Figures 4-10 through 4-15. Table 4-3 summarizes the maximum loads allowable to obtain the 100-hr fatigue life at the condition noted. The fuel pump roller bearings will not reach a life of 100 hrs unless silicon nitride elements are used instead of steel elements. The use and manufacture of silicon nitride roller bearings was demonstrated during a high speed roller bearing test program conducted at Orenda Ltd. in 1973. Table 4-4 exemplifies the centrifugal force effect of steel and silicon nitride on the fatigue life of a bearing at 3×10^6 DN. A bore reduction to 18 mm from 20 mm would provide the 100 hr fatigue life for the silicon nitride roller bearings at 150,000 rpm for the fuel pump roller bearings. Decreasing the pump speed to 147,000 rpm will provide the required 100 hr fatigue life for 20 mm bearings. Since the design point operating speed of the fuel turbopump is 147,000 rpm the life requirement was met although with no excessive margin.

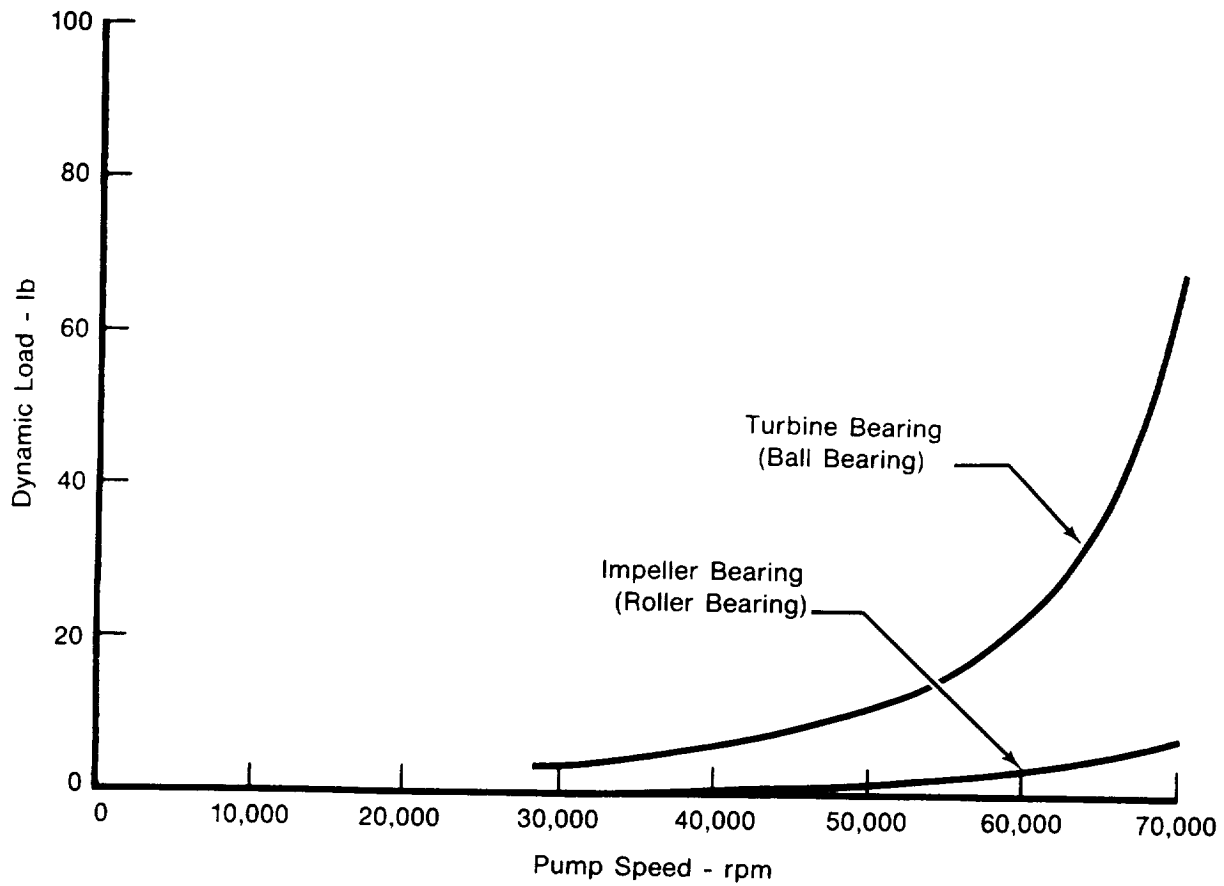
Table 4-2. Turbomachinery Rotor Weights and Operating Speeds

| Pump | Rotor Weight lb | Maximum Operating Speed (rpm) |
|----------------------------|--------------------|----------------------------------|
| Main Fuel Pump | 2.24 | 150,000 |
| Main Oxidizer Pump | 2.98 | 67,390 |
| Fuel Low Speed Induc | 1.90 | 46,021 |
| Oxidizer Low Speed Inducer | 2.16 | 8,850 |



FD 212883

Figure 4-7. OTV Pumps Critical Speed Analysis



FD 212884

Figure 4-8. Oxidizer Pump Dynamic Bearing Loads

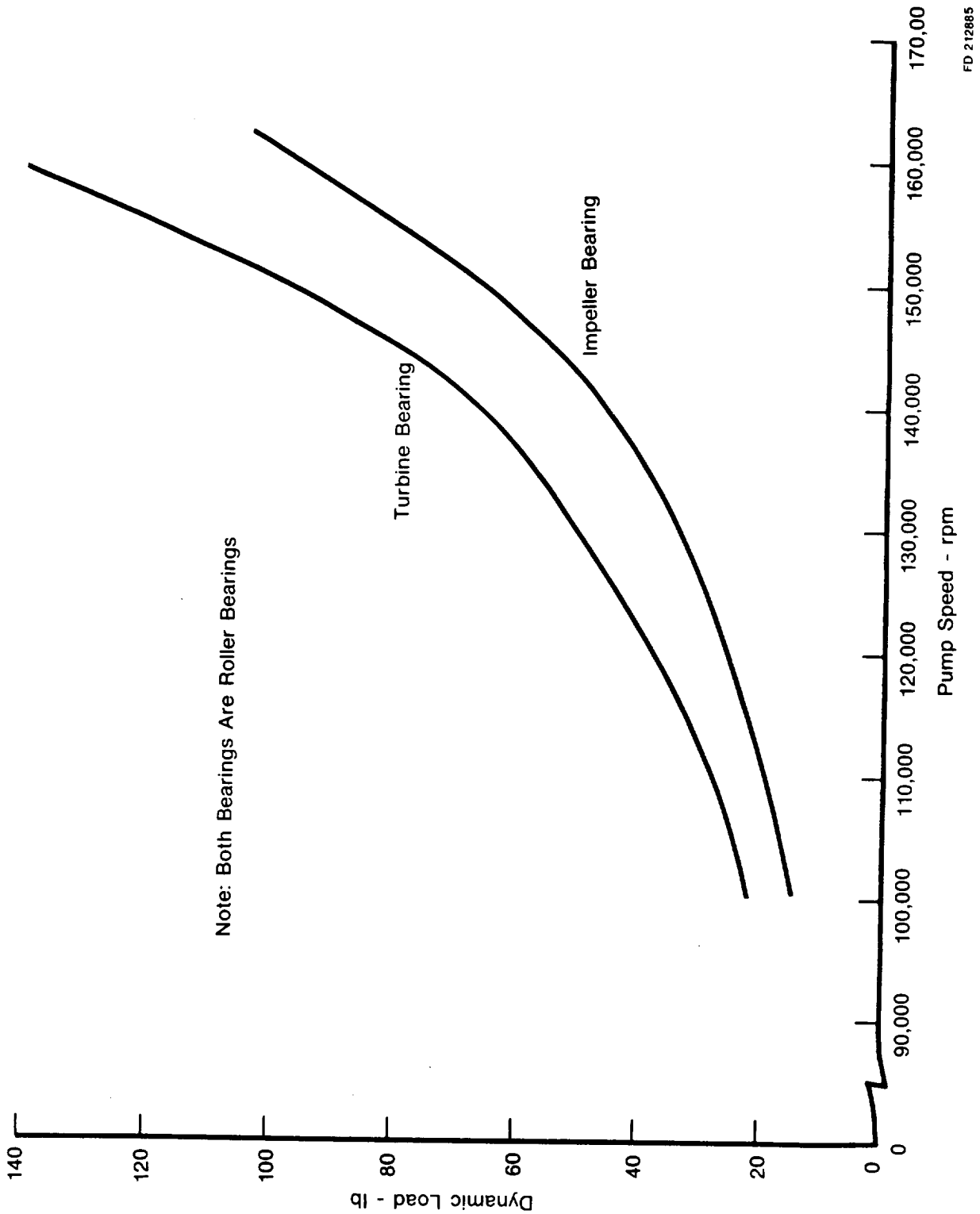
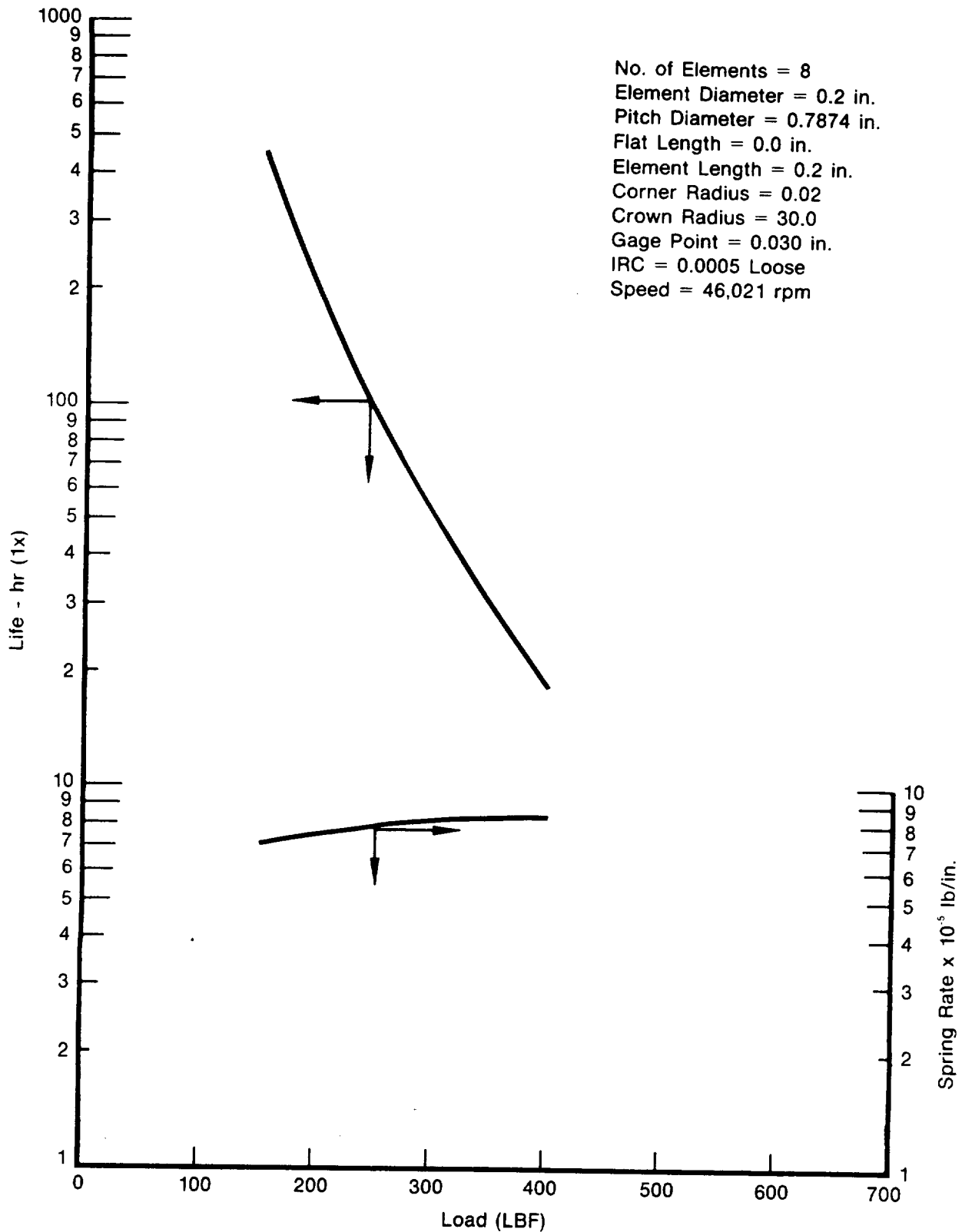
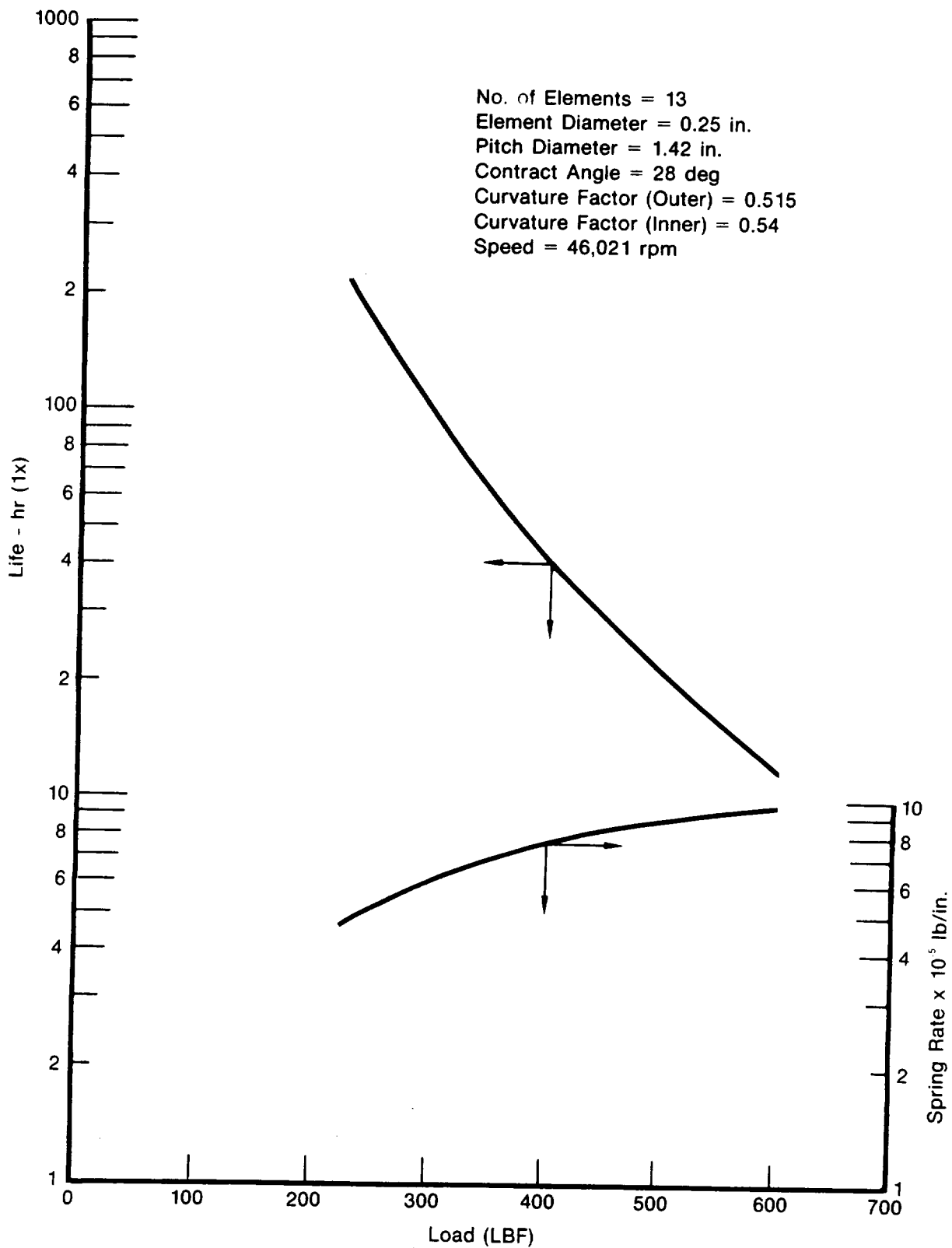


Figure 4-9. OTV Fuel Pump Dynamic Bearing Loads



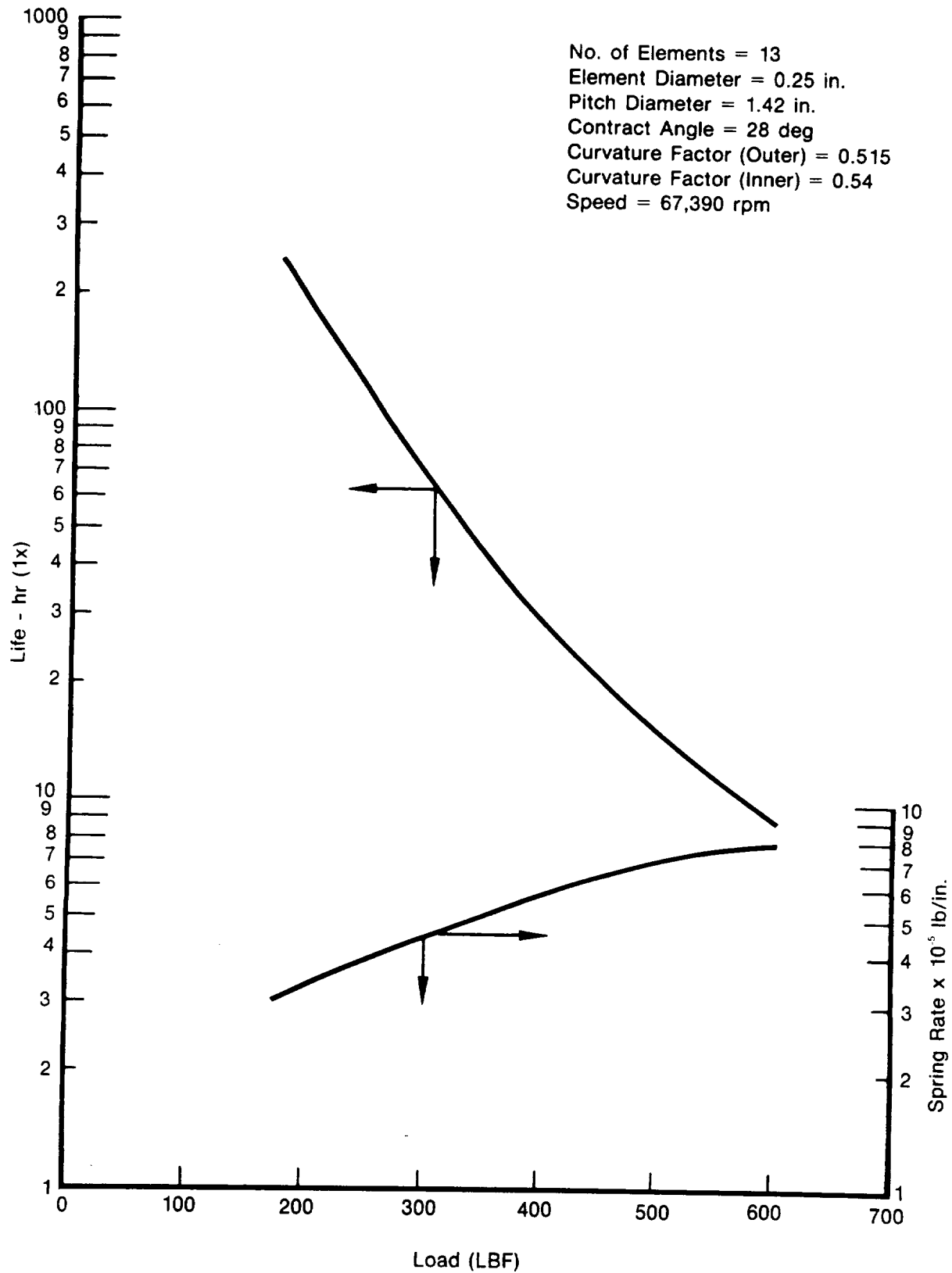
FD 212886

Figure 4-10. Fuel LSI Roller Bearing Characteristics



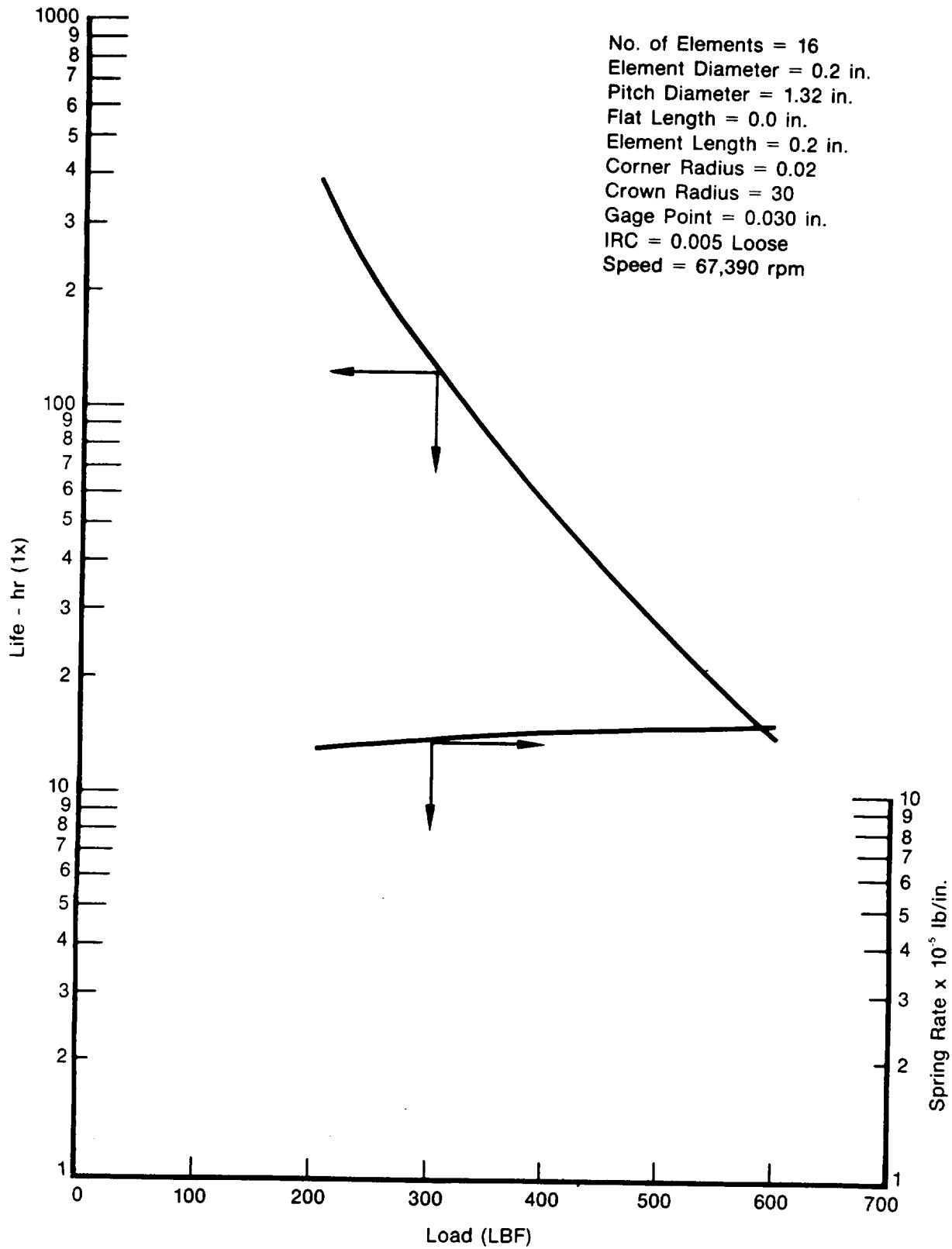
FD 212887

Figure 4-11. Fuel LSI Ball Bearing Characteristics



FD 212888

Figure 4-12. LOX Pump Ball Bearing Characteristics



FD 212889

Figure 4-13. LOX Pump Roller Bearing Characteristics

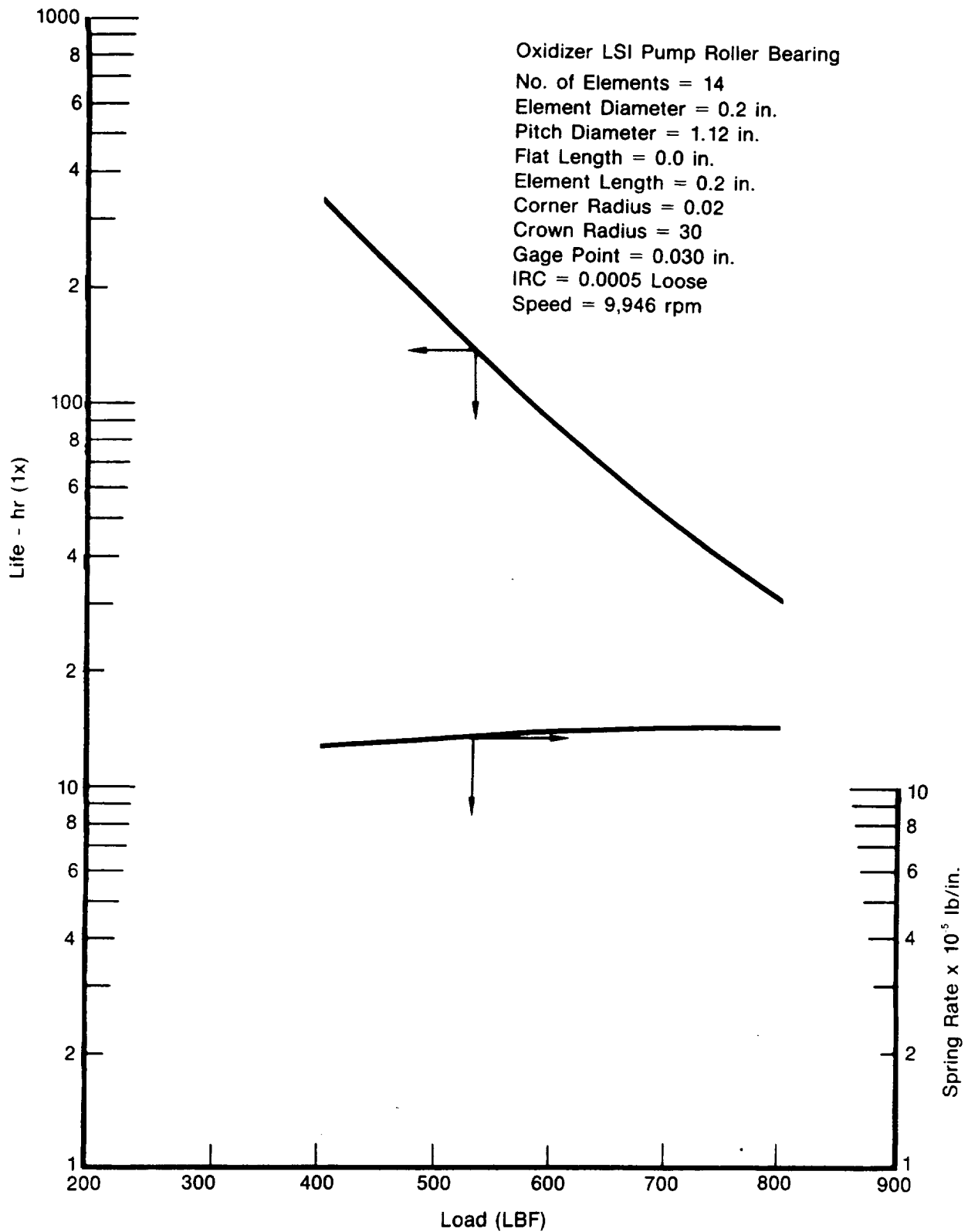
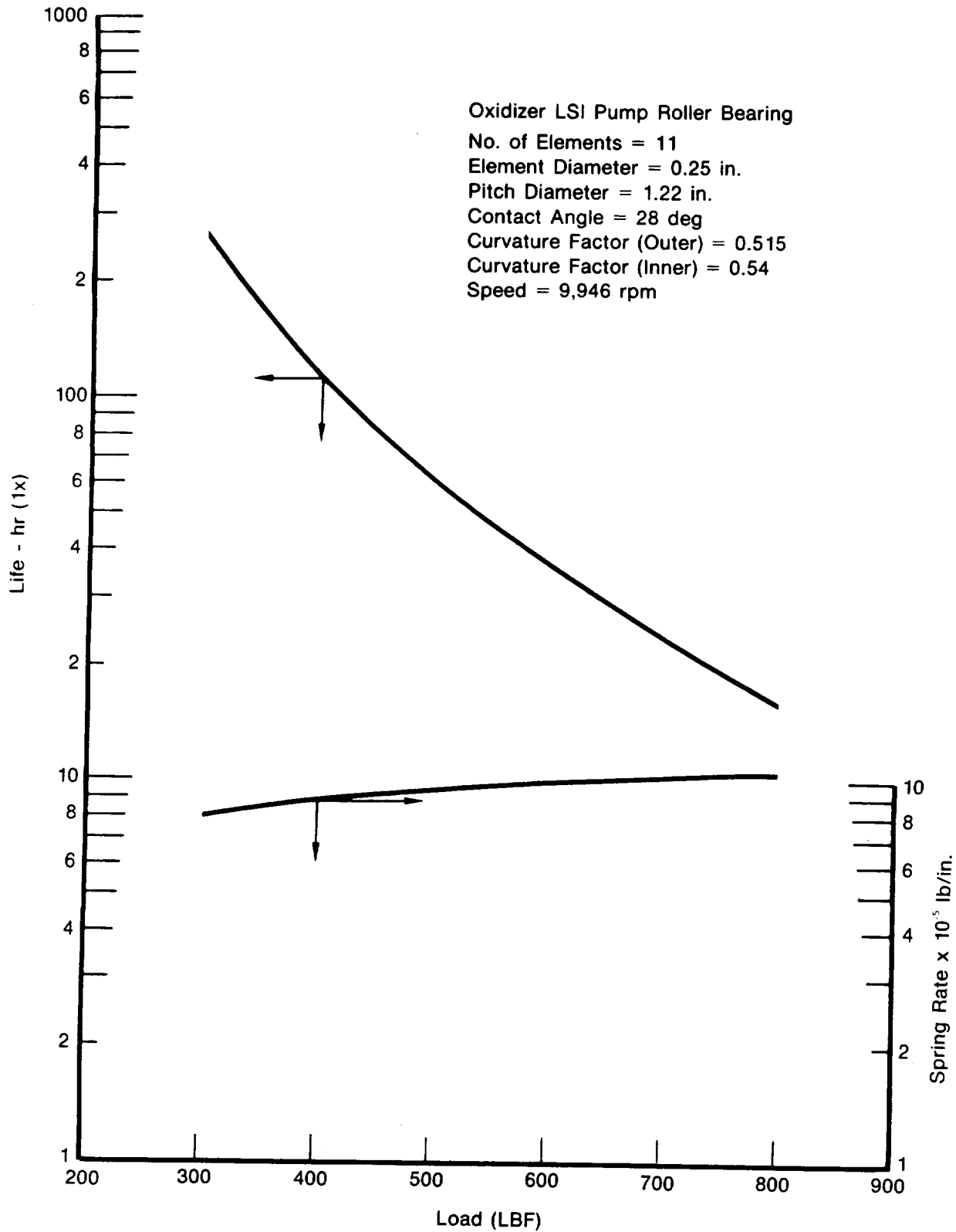


Figure 4-14. LOX LSI Roller Bearing Characteristics

FD 212890



FD 212891

Figure 4-15. LOX LSI Ball Bearing Characteristics

Table 4-3. Bearings Summary — Conditions Resulting in 100 hr Fatigue Life

| Pump | Bearing Type And Position | Bore Size (MM) | Speed | Max Load (lbf) | Springrate (lb/in.) | Life (hr) |
|--------------------------------------|------------------------------|-------------------|-------------------------------------|-------------------|------------------------|--------------|
| Fuel Low Speed Inducer (LSI) Pump | Roller (Front) | 12 | 0.55×10^6 DN 46,021 rpm | 245 Radial | 780,000 | 100 |
| Fuel LSI Pump | Ball (Rear) | 25 | 1.15×10^6 DN 46,021 rpm | 295 Thrust | 610,000 | 100 |
| Oxidizer Pump | Ball (Front) | 25 | 1.68×10^6 DN 67,390 rpm | 255 Thrust | 400,000 | 100 |
| Oxidizer Pump | Roller (Rear) | 25 | 1.68×10^6 DN 67,390 rpm | 325 Radial | 1,400,000 | 100 |
| Oxidizer LSI Pump | Roller (Front) | 20 | 0.2×10^6 DN 9946 rpm | 580 Radial | 1,400,000 | 100 |
| Oxidizer LSI Pump | Ball (Rear) | 20 | 0.2×10^6 DN 9946 rpm | 415 Thrust | 880,000 | 100 |

Table 4-4. Comparison of the Centrifugal Effect of Steel and Si_3N_4 Elements on Bearing Life at 3.0×10^6 DN

| Bearing Type and Position | Bore Size (MM) | Speed | Load (lbf) | Life (hr) |
|---|-------------------|-------------------------------------|---------------|--------------|
| Roller (Front) Steel Elements | 20 | 3.0×10^6 DN 150,000 rpm | 103 | 45 |
| Roller (Front)* Si_3N_4 Elements | 20 | 3.0×10^6 DN 150,000 rpm | 103 | 93 |
| Roller (Rear) Steel Elements | 20 | 3.0×10^6 DN 150,000 rpm | 116 | 43 |
| Roller (Rear)* Si_3N_4 Elements | 20 | 3.0×10^6 DN 150,000 rpm | 116 | 81 |

*A bore reduction from 20 mm to 18 mm was required to obtain 100 hr fatigue life. This results in 2.7×10^6 DN at 150,000 rpm.

4.4 ENGINE CONTROL VALVES

The location of the Advanced Expander Cycle Engine valves are shown in Figure 4-16. Several of these valves are similar to the ones used in the RL10 engine, (ie., the propellant inlet shut-off valves, main fuel shut-off valve, and the solenoid valves).

The propellant pressurization valves (Figure 4-17) are spring loaded, normally closed, line pressure actuated, two-position poppet valves that supply propellants for fuel and oxidizer tank pressurization. These valves limit but do not regulate the tank pressurization flowrate. When the differential between line pressure and an internal cavity vented to pump inlet pressure increases to a predetermined value, the total force acting on the poppet overcomes the spring load and the valve opens fully.

FD 208394B

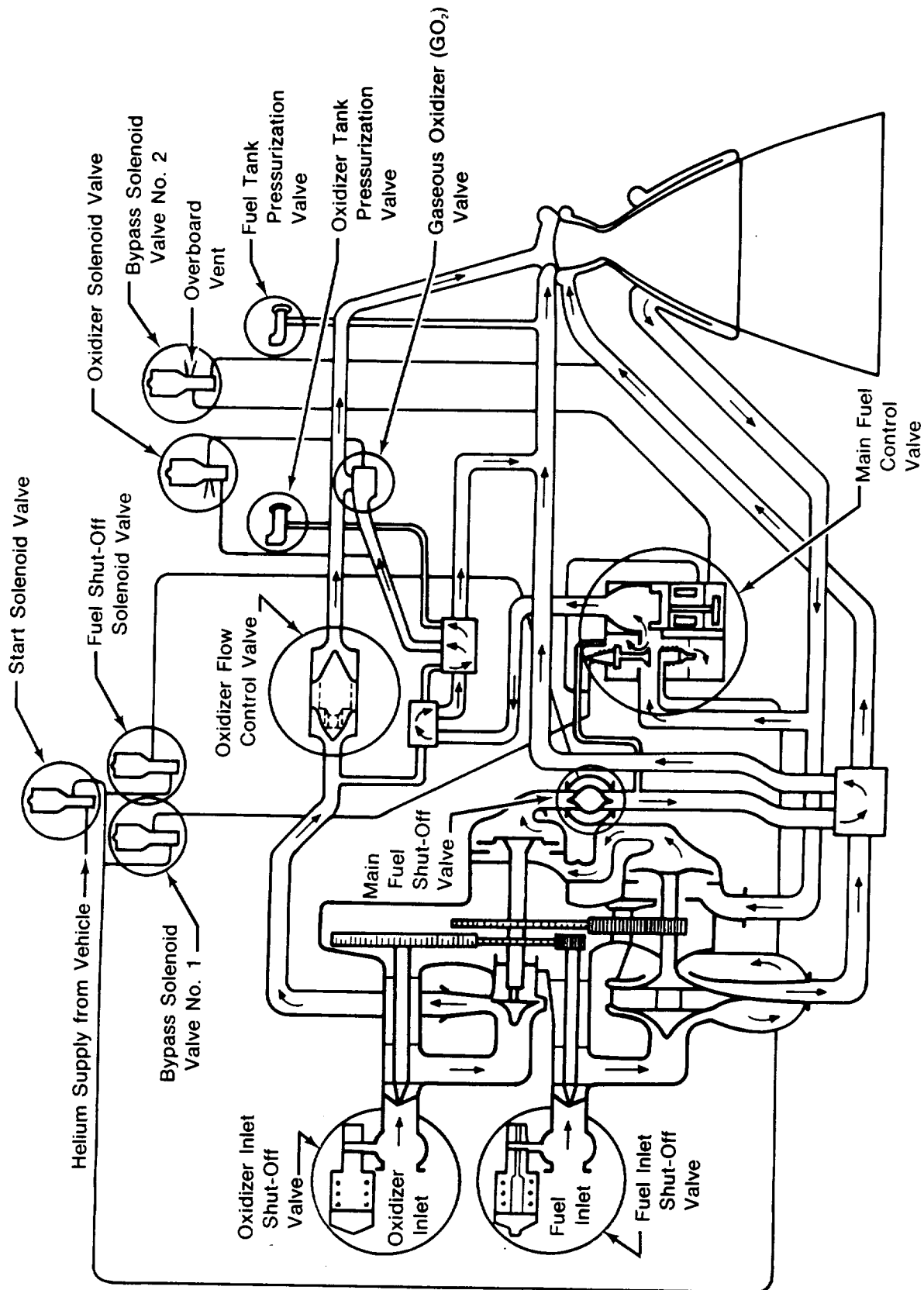
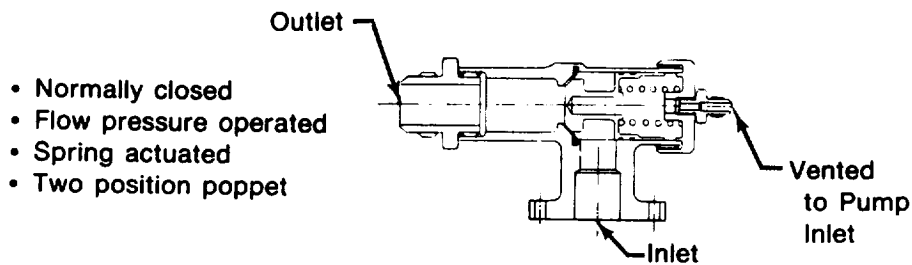


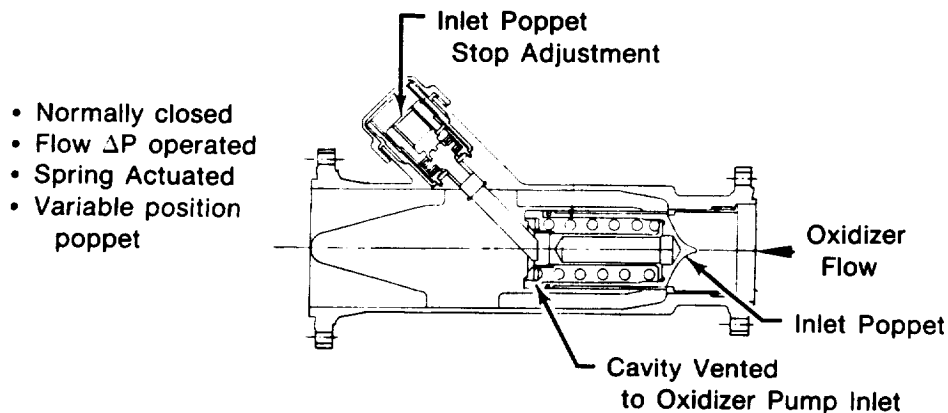
Figure 4-16. Engine Valve Location Schematic



FD 212892

Figure 4-17. Fuel and Oxidizer Propellant Pressurization Valves

The oxidizer flow control valve (Figure 4-18) is a spring-loaded, normally closed, line pressure actuated valve. It is similar to the one used on the RL10 except that the propellant utilization portion has been eliminated for the OTV engine. It is configured to provide ground trim of full thrust propellant mixture ratio. The valve contains a spring-loaded poppet valve used to meter oxidizer flow during full thrust and regulate flow during the engine transient to full thrust. The poppet valve is spring-loaded closed and opens as a function of the pressure differential between valve inlet pressure and a pressure within the valve cavity which has been vented to pump inlet pressure. During tank head idle and pumped idle operation, the poppet is closed and liquid oxidizer is not allowed to enter the injector. When the engine accelerates from pumped idle to full thrust operation, the main poppet valve is also opened as a function of the differential pressure between valve inlet and pump inlet pressure. The bypass and main poppet valves both remain open during full thrust operation and the combined areas meter the required oxidizer flow. The full open position of the main poppet valve can be ground trimmed by a threaded mechanical stop to ground adjust engine mixture ratio.



FD 212893

Figure 4-18. Oxidizer Flow Control Valve

The propellant inlet shut-off valves (Figure 4-19) are spring loaded, normally closed, helium operated, two position ball valves that provide a seal between the vehicle propellant tank and the engine pumps. Both valves are located just upstream of their respective pump inlets and are of the same respective diameter as the fuel and oxidizer pump inlets. The valves are actuated by helium operating on a piston bellows assembly. The linear motion of the actuator is translated by rack and pinion into a rotary motion at the ball valve. Ball sealing is accomplished with dual pressure loaded fluorocarbon rub seals. The valves incorporate a vented cavity between the dual seals such that any leakage past the closed valve is vented overboard.

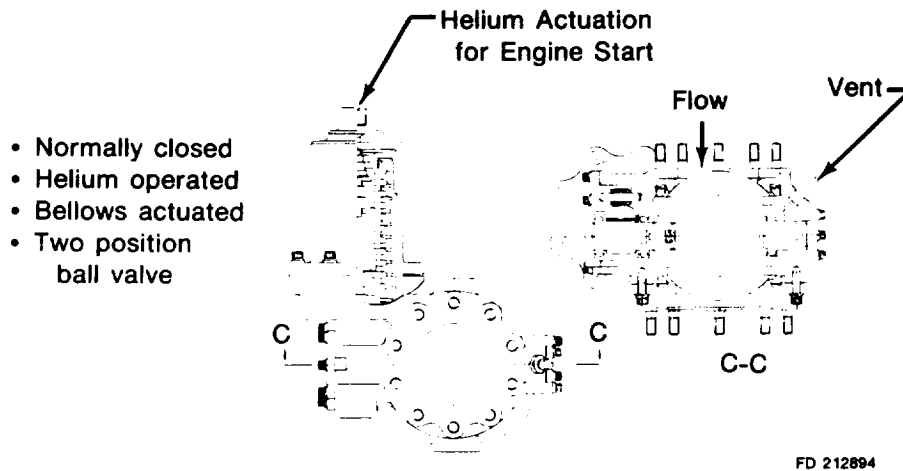


Figure 4-19. Fuel and Oxidizer Propellant Inlet Shut-Off Valves

The main fuel shut-off valve (Figure 4-20) is a helium operated, two position, normally closed annular gate valve. The valve serves to prevent the flow of fuel through the fuel pump turbine during tank head idle operation and provides a rapid cutoff of fuel flow to the combustion chamber at engine shutdown. The shutoff gate is opened by helium pressurization of a bellows assembly to allow the flow of fuel through the turbine at the operating modes above tank head idle. The compressed shut off valve spring returns the gate to its normally closed position when helium pressure is vented at engine shutdown. Sealing is accomplished by the sealing of the spherical surface of the gate seal ring.

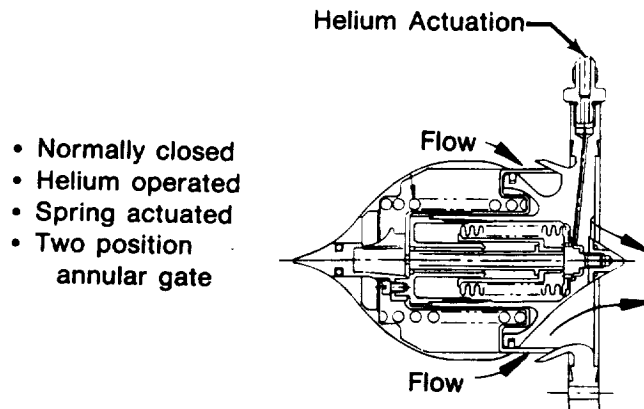
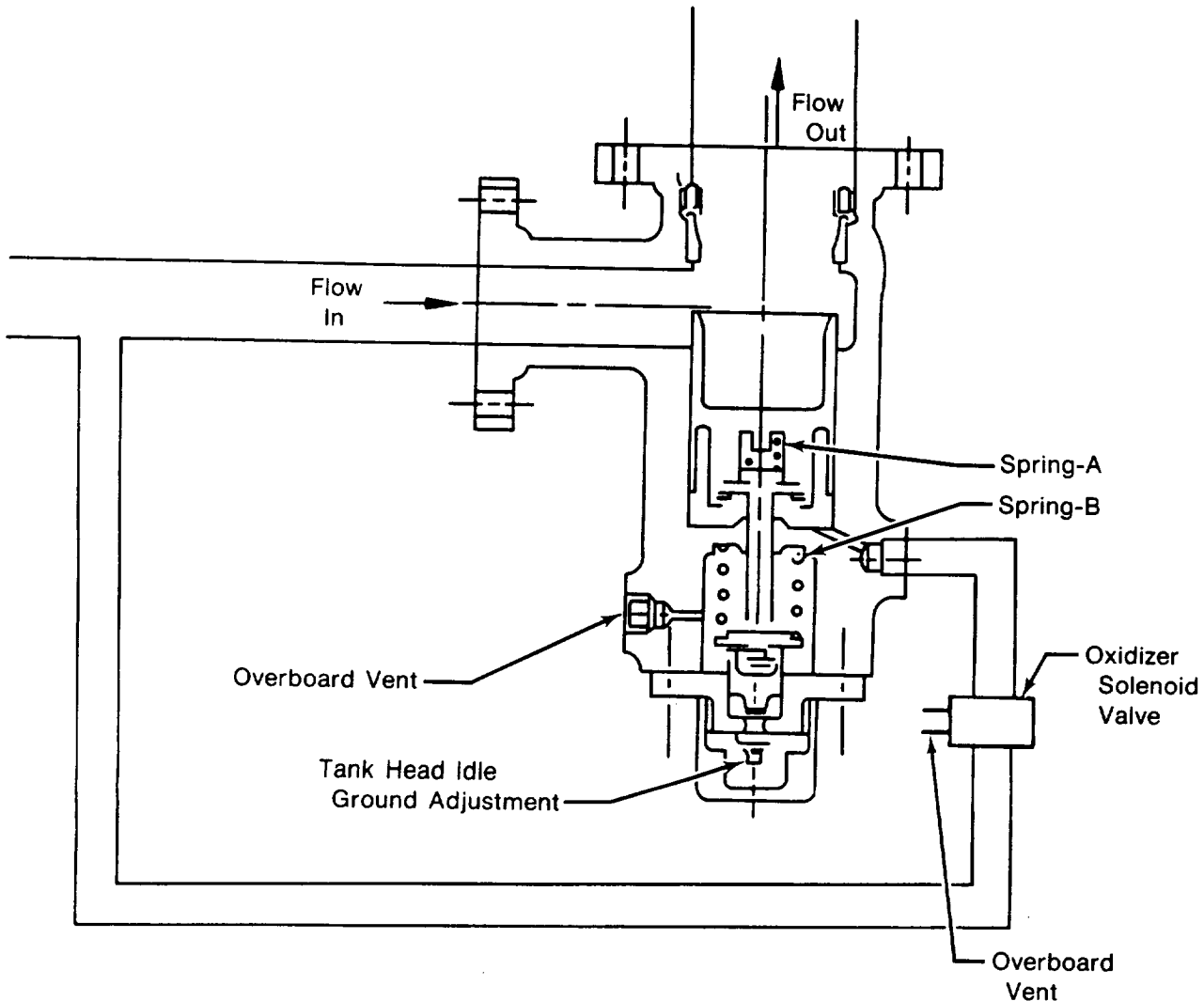


Figure 4-20. Main Fuel Shut-Off Valve

The gaseous oxidizer valve (Figure 4-21) is a spring loaded, normally open, pressure actuated sleeve valve located between the GOX heat exchanger and the injector. This valve meters gaseous oxygen flow during tank head and pumped idle operation and regulates oxygen flow during the transient to pumped idle. In the tank head idle mode, the valve is normally partially opened to a predetermined position to meet the required oxidizer flow. The sleeve valve is opened fully during the pumped idle mode by the increase in oxidizer line pressure acting on the face of the sleeve which compresses the spring within the sleeve/piston assembly. During the full thrust operation the valve is closed, actuated by the oxidizer pump discharge pressure acting on the piston of the sleeve/piston assembly.



1. Tank Head Idle Setting (as drawn). Solenoid valve is closed. Valve flow path pressure insufficient to compress spring-A.
2. Pumped Idle Setting. Solenoid valve is closed. Valve flow path pressure sufficient to compress spring-A (valve opens farther than shown).
3. Transient from Pumped Idle to Full Thrust. Solenoid valve opens. As valve pressure increases, valve closes. (Function of spring-B spring rate.) Valve is fully closed above thrust levels of about 30% of rated thrust.

FD 212896

Figure 4-21. Gaseous Oxidizer Valve

The main fuel control valve (Figure 4-22) provides the control functions of turbine bypass flow for thrust regulation, ventage of fuel at shutdown, and provides fuel flow to hydrogen regenerator during tank head idle operation. The thrust control portion of the valve is a normally closed, helium and hydrogen pressure actuated, three position sleeve bypass valve used to control engine thrust by regulation of turbine power. Control of engine thrust is provided at full thrust by a ground adjusted needle valve which allows approximately 4% hydrogen flow to bypass the closed sleeve valve and therefore bypass the turbines. It should be noted that a continuous feedback of chamber pressure vs bypass flow as used in the RL10, has not been incorporated into this engine design. It was determined that thrust variance without this feedback system was acceptable for the OTV application. The valve is also pressure actuated to allow the setting of two discrete areas for metering turbine bypass hydrogen flow during tank head and pumped idle operation. During tank head idle operation, the valve is actuated to full open position by helium pressure action on the concentric (annular) piston assembly. During pumped idle operation the valve is actuated to an intermediate area by gaseous hydrogen acting on a secondary concentric piston as the annular helium piston is vented. Holes are provided through the valve's sleeve face to maintain hydrogen pressure on both sides of the face, in order to reduce the spring load required to move the valve from the full open to the intermediate position.

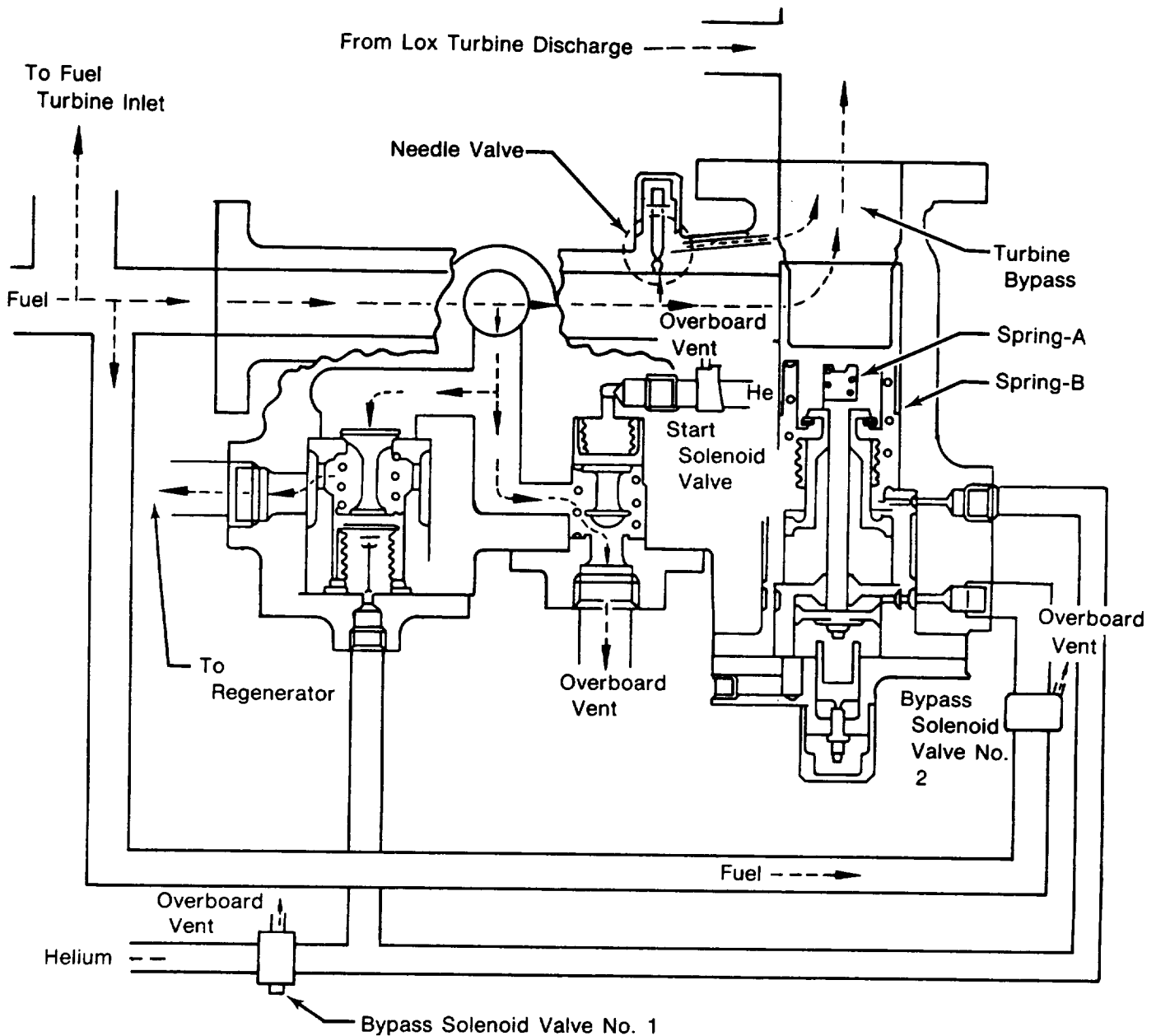
The fuel vent portion of the main fuel control is a pressure operated, two-position poppet valve that is spring loaded open to provide pressure relief of the fuel system lines during engine shutdown. The valve is maintained in the closed position during all three active modes of engine operation. At the start signal, helium pressure actuates the valve assembly, moving the valve to close the overboard vent port. At shutdown, when helium pressure is removed, the vent port opens fully relieving fuel pressure in the fuel system lines.

The hydrogen regenerator flow portion of the main fuel control is a pressure operated, two-position, poppet valve that is spring loaded, normally closed. At the start (SOV1) signal for tank head idle operation, helium pressure actuates the valve assembly, moving the poppet to the full open position thereby providing hydrogen flow to the hydrogen regenerator. The valve is maintained in the closed position for the pumped idle and full thrust modes of engine operation.

The solenoid valves (Figure 4-23) are solenoid actuated, direct acting, 3-way valves with double-ended poppets that supply helium, hydrogen or oxygen actuation pressure to the various propellant valves. The five solenoid valves used in the OTV engine are identical in design and function. The start solenoid valve controls the actuator helium supply to the fuel shut-off valve. Bypass solenoid valve No. 1 controls the actuator helium supply to the turbine bypass valve and hydrogen regenerator flow valve, both on the main fuel control, for tank head idle operation. Bypass solenoid valve No. 2 controls the actuator hydrogen supply to the turbine bypass valve for pumped idle operation. The oxidizer solenoid valve controls the actuator oxidizer supply to the gaseous oxidizer valve, for full thrust operation.

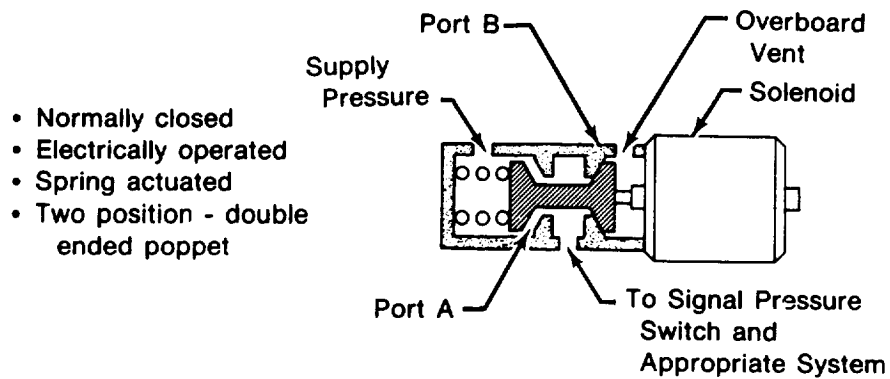
4.5 ENGINE WEIGHT

The estimated weights of the various Advanced Expander Cycle engine components are shown in Table 4-5.



| | |
|----------------|---|
| Off | All solenoid valves Closed. Valve in positions shown. Turbine bypass through needle valve only. No flow to the regenerator. Overboard vent valve open. (Fail safe position) |
| Tank Head Idle | Bypass solenoid valve No. 1 open, No. 2 closed. Start solenoid valve open. Turbine bypass open (springs A and B compressed). Flow to regenerator. Overboard vent valve closed. |
| Pumped Idle | Bypass solenoid valve No. 1 closed, No. 2 open. Start solenoid valve open. Turbine bypass is a function of valve inlet pressure and spring-B (spring-A is not compressed). No flow to regenerator. Overboard vent valve closed. |
| Full Thrust | Bypass solenoid valves No. 1 and No. 2 closed. Start solenoid valve open. Turbine bypass through needle valve only. No flow to regenerator. Overboard vent valve closed. |

Figure 4-22. Main Fuel Valve



FD 212898

Figure 4-23. Solenoid Valves

Table 4-5. Estimated Weights — Advanced Expander Cycle Engine Components

| Item | Material | Weight, lb |
|----------------------------|---|------------|
| Primary Nozzle Assy | | |
| Cooling Tubes | 347 SST | 31.0 |
| Thrust Chamber | 347 SST, N-155 RigiMesh, Amzirc | 58.1 |
| Primary to Secondary Seal | 347 SST | 12.0 |
| Secondary Nozzle Assy | | |
| Nozzle shell | Uncoated Carbon/Carbon | 60.2 |
| Nozzle Supports | Uncoated Carbon/Carbon | 8.8 |
| Screw Jacks and Actuation | | |
| Screw Jacks | Uncoated Carbon/Carbon | 7.7 |
| Bearings & Housings | 347 SST | 6.9 |
| Gear Drive & Drive Motor | 347 SST | 5.9 |
| Gimbal Mount | Al Alloy | 4.0 |
| Turbo Pump Assy | Al Alloy, 347 SST, 17-7 PH, A-286, Titanium | 60.7 |
| Heat Exchangers | | |
| H ₂ Regenerator | Aluminum Alloy | 32.8 |
| Vortex Prevaporizer | | 5.2 |
| GOX Heat Exchanger | | 16.3 |
| Control Valves | Al Alloy, 347 SST, 17-7 PH, A-286 | 54.0 |
| Plumbing & Misc | 347 SST | 63.0 |
| Total | | 426.6 |

SECTION 5

CONCLUSIONS AND RECOMMENDATIONS

5.1 GENERAL

This study program has shown that an expander cycle engine can be designed which will provide very high performance for an OTV application. In order to proceed with confidence into a full-scale development program for such an engine, it is recommended that the following areas be addressed in future technology programs.

5.2 TURBOMACHINERY

5.2.1 Bearings

The 3.0×10^6 DN value used in this study for the fuel pump roller bearings is essentially at the limit of the state of the art. To attain higher pump speeds (and thereby increase pump efficiency) without incurring critical speed problems, other approaches in bearing concepts (such as improved roller element and case materials and hydrostatic journals) may be required. Rig testing is recommended for any concept prior to commitment in a development program.

5.2.2 Seals

The critical seal area for an engine of this type is the oxidizer pump seal package. While this engine design uses a controlled gap arrangement, it is believed that a high velocity rubbing bellows seal could be used provided that the oxidizer pump is properly balanced. If achievable, such a design would provide less leakage and thus better performance. A program to optimize controlled gap seal configurations is also recommended.

5.2.3 Gears

The gear design of this engine uses a spur configuration. To improve load carrying capability which decreases wear (and thereby increases engine life) a helical gear, because of its increased contact area, might be considered. Improved coatings and/or case treatment for both spur and helical gears should be investigated. Since very little data is available on the characteristics of hydrogen-cooled gears, a technology program involving rig testing is recommended.

5.3 THRUST CHAMBERS

The design of the advanced expander cycle engine's thrust chamber, using aged or $\frac{1}{2}$ hard AMZIRC, appears to be adequate to meet the engine life requirements. However, the manufacturing of the convoluted wall design, while believed to be within the current state of the art, has not been demonstrated on hardware of this size. Also, progress made with electrodeposited coatings (e.g., ZrO_2) in recent years indicates a potential benefit for chamber LCF and for thermal enhancement. A subscale rig test technology program is recommended in this area.

5.4 MATERIALS

5.4.1 Characterization

There are a great many new materials which are being brought into use in various aerospace applications to improve durability. Unfortunately, few of these materials have been sufficiently characterized under the conditions imposed by the OTV engine design (e.g., hydrogen environment, cryogenic temperatures). Therefore, it is recommended that technology programs to investigate promising materials are studied. This effort should follow through sufficiently to provide potential users, a "design practice" requirements document so that a designer can utilize the new material as easily as current material.

5.5 PERFORMANCE

It is probable that the OTV will depend on a very high area ratio nozzle to obtain the maximum possible specific impulse. To date, there has been very limited test data of hydrogen/oxygen combustion systems with high area ratio nozzles ($\gamma > 175:1$) and none greater than 400:1. Since the test data was shown to disagree with the accepted JANNAF computer prediction of specific impulse by as much as 1.3% and since the OTV engine may well use nozzle area ratio of $> 600:1$ the performance of such a nozzle should be verified. A technology demonstration is therefore recommended.